Applied Reactor Technology

Henryk Anglart

Applied Reactor Technology

Preface

The main goal of this textbook is to give an introduction to nuclear engineering and reactor technology for students of energy engineering and engineering sciences as well as for professionals working in the nuclear field. The basic aspects of nuclear reactor engineering are presented with focus on how to perform analysis and design of nuclear systems.

ICON KEY
 Note Corner
 Examples
 Computer Program
 More Reading

The textbook is organized into seven chapters devoted to the description of nuclear power plants, to the nuclear reactor theory and analysis, as well as to the environmental and economical aspects of the nuclear power. Parts in the book of special interest are designed with icons, as indicated in the table above. "Note Corner" contains additional information, not directly related to the topics covered by the book. All examples are marked with the pen icon. Special icons are used to mark sections containing computer programs and suggestions for additional reading.

The first chapter of the textbook is concerned with various introductory topics in nuclear reactor physics. This includes a description of the atomic structure as well as various nuclear reactions and their cross sections. Neutron transport, distributions and life cycles are described using the one-group diffusion approximation only. The intention is to provide an introduction to several important issues in nuclear reactor physics avoiding at the same time the full complexity of the underlying theory. Additional literature is suggested to those readers who are interested in a more detailed theoretical background. The second chapter contains description of nuclear power plants, including their schematics, major components, as well as the principles of operation. The rudimentary reactor theory is addressed in chapter three. That chapter contains such topics as the neutron diffusion and neutron distributions in critical stationary reactors. It also includes descriptions of the time-dependent reactor behavior due to such processes as the fuel burnup, the reactivity insertions and changes of the concentration of reactor poisons. The principles of thermal-hydraulic analyses are presented in chapter four, whereas chapter five contains a discussion of topics related to the mechanics of structures and to the selection of materials in nuclear applications. The principles of reactor design are outlined in chapter six. Finally, in chapter seven a short presentation of the environmental and economic issues of nuclear power is given.

Table of Contents

Chapter 1

1 Introduction

Nunclear engineering has a relatively short history. The first nuclear reactor was brought to operation on December 2, 1942 at the University of Chicago, by a group of researches led by Enrico Fermi. However, the history of nuclear energy probably started in year 1895, when Wilhelm Röntgen discovered X-rays. In December 1938 Otto Hahn and Fritz Strassman found traces of barium in a uranium sample bombarded with neutrons. Lise Meitner and her nephew Otto Robert Frisch correctly interpreted the phenomenon as the nuclear fission. Next year, Hans Halban, Frederic Joliot-Curie and Lew Kowarski demonstrated that fission can cause a chain reaction and they took a first patent on the production of energy. The first nuclear power plants became operational in 1954. Fifty years later nuclear power produced about 16% of the world's electricity from 442 commercial reactors in 31 countries. At present (2011) the nuclear industry experiences its renaissance after a decade or so of slowing down in the wakes of two major accidents that occurred in Three-Mile Island and Chernobyl nuclear power plants.

As an introduction to this textbook, the present Chapter describes the fundamentals of nuclear energy and explains its principles. The topics which are discussed include the atomic structure of the matter, the origin of the binding energy in nuclei and the ways in which that energy can be released.

1.1 Basics of Atomic and Nuclear Physics

1.1.1 Atomic Structure

Each atom consists of a positively charged **nucleus** surrounded by negatively charged electrons. The atomic nucleus consists of two kinds of fundamental particles called nucleons: namely a positively charged **proton** and an electrically neutral **neutron**. Mass of a single proton is equal to 1.007277 **atomic mass units** (abbreviated as u), where 1 u is exactly one-twelfth of the mass of the ^{12}C atom, equal to $1.661 \cdot 10^{-27}$ kg. Mass of a single neutron is equal to 1.008665 u and mass of a single electron is 0.000548 u. The radius of a nucleus is approximately equal to 10^{-15} m and the radius of an atom is about 10^{-10} m.

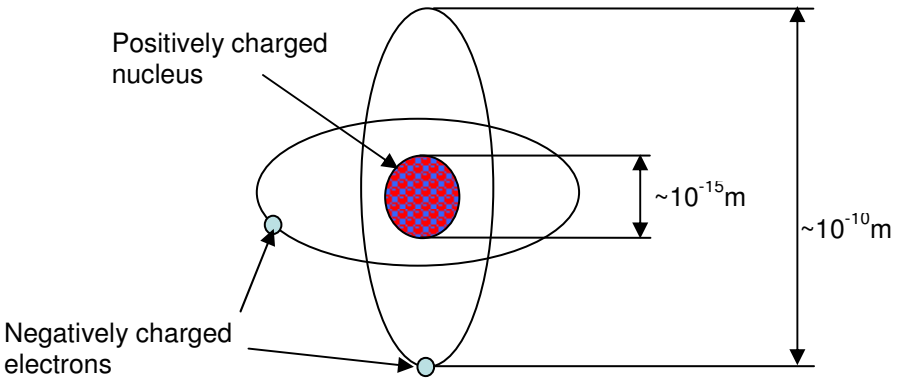

FIGURE 1-1: Typical structure and dimensions of atoms.

The number of protons in the atomic nucleus of a given element is called the **atomic number** of the element and is represented by the letter *Z*. The total number of nucleons in an atomic nucleus is called the **mass number** of the element and is denoted with the letter *A*.

Neutrons, discovered by Chadwick in 1932, are particles of particular interest in nuclear reactor physics since they are causing fission reactions of uranium nuclei and facilitate a sustained chain reaction. Both these reactions will be discussed later in a more detail. Neutrons are unstable particles with mean life-time equal to 1013 s. They undergo the beta decay according to the following scheme,

(1-1) $$n \rightarrow p + e^{-} + \tilde{\nu}_e + \text{energy}\ .$$

Here p is the proton, e^- is the electron and $\tilde{\nu}_e$ is the electronic antineutrino.

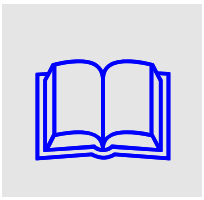

MORE READING: Atomic structure and other topics from atomic and nuclear physics are presented here in a very simplified form just to serve the purpose of the textbook. However, for readers that are interested in more thorough treatment of the subject it is recommended to consult any modern book in physics, e.g. Kenneth S. Krane, *Modern Physics*, John Wiley & Sons. Inc., 1996.

1.1.2 Isotopes

Many elements have nuclei with the same number of protons (same atomic number Z) but different numbers of neutrons. Such atoms have the same chemical properties but different nuclear properties and are called **isotopes**. The most important in nuclear engineering are the isotopes of uranium: ^{233}U, ^{235}U and ^{238}U. Only the two last isotopes exist in nature in significant quantities. Natural uranium contains 0.72% of ^{235}U and 99.274% of ^{238}U.

A particular isotope of a given element is identified by including the mass number *A* and the atomic number *Z* with the name of the element: ${}^{A}_{Z}X$. For example, the

common isotope of oxygen, which has the mass number 16, is represented as ${}^{16}_{8}O$. Often the atomic number is dropped and the isotope is denoted as ${}^{16}O$.

1.1.3 Nuclear Binding Energy

The atomic nuclei stability results from a balance between two kinds of forces acting between nucleons. First, there are attractive forces of approximately equal magnitude among the nucleons, i.e., protons attract other protons and neutrons as well as neutrons attract other neutrons and protons. These characteristic intranuclear forces are operative on a very short distance on the order of 10^{-15} m only. In addition to the short-range, attractive forces, there are the conventional, coulomb repulsive forces between the positively charged protons, which are capable of acting over relatively large distances.

The direct determination of nuclear masses, by means of spectrograph and in other ways, has shown that the actual mass is always less than the sum of the masses of the constituent nucleons. The difference, called the **mass defect**, which is related to the energy binding the nucleons, can be determined as follows:

Total mass of protons = $Z \cdot m_p$

Total mass of electrons = $Z \cdot m_e$

Total mass of neutrons = $(A-Z) \cdot m_n$

If the measured mass of the atom is M, the mass defect ΔM is found as,

(1-2) $$\Delta M = Z \cdot (m_p + m_e) + (A-Z) \cdot m_n - M .$$

Based on the concept of equivalence of mass and energy, the mass defect is a measure of the energy which would be released if the individual Z protons and (A-Z) neutrons combined to form a nucleus (neglecting electron contribution, which is small). The energy equivalent of the mass effect is called the **binding energy** of the nucleus. The Einstein equation for the energy equivalent E of a particle moving with a speed v is as follows,

(1-3) $$E = \frac{m_0 c^2}{\sqrt{1 - v^2/c^2}} = mc^2 .$$

Here m_0 is the rest mass of the particle (i.e. its mass at $v \approx 0$), c is the speed of light and m is the effective (or relativistic) mass of the moving particle.

The speeds of particles of interest in nuclear reactors are almost invariably small in comparison with the speed of light and Eq. (1-3) can be written as,

(1-4) $$E = mc^2$$

where E is the energy change equivalent to a change m in the conventional mass in a particular process.

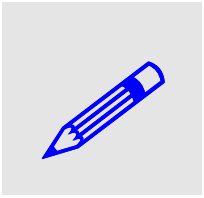

EXAMPLE 1-1. Calculate the energy equivalent to a conventional mass equal to 1u.
SOLUTION: Since c = 2.998 • 10^8 m/s and u = 1.661 • 10^{-27} kg then E = 1.661 • 10^{-27} x (2.998 • 10^8)^2 kg m^2/s^2 = 1.492 • 10^{-10} J.
EXAMPLE 1-2. Calculate the energy as in EXAMPLE 1-1 using MeV as units.
SOLUTION: One **electron volt** (1 eV) is the energy acquired by a unit charge which has been accelerated through a potential of 1 volt. The electronic (unit) charge is 1.602 • 10-19 coulomb hence 1 eV is equivalent to 1.602 • 10-19 J and 1 MeV = 1.602 • 10-13 J. Finally, E = 1.492 • 10-10 / 1.602 • 10-13 MeV = 931.3 MeV.

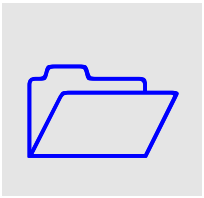

NOTE CORNER:

Unit of mass - atomic mass unit:	1 u = 1.661 • 10^{-27} kg
Unit of energy - electron volt:	1 eV = 1.602 • 10^{-19} J
Conversion:	1 u is equivalent to 931.3 MeV energy

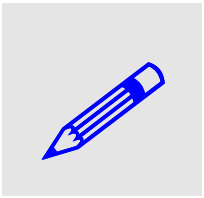

EXAMPLE 1-3. Calculate the mass defect and the binding energy for a nucleus of an isotope of tin ^{120}Sn (atomic mass M = 119.9022 u) and for an isotope of uranium ^{235}U (atomic mass M = 235.0439).
SOLUTION: Using Eq. (1-2) and knowing that A = 120 and Z = 50 for tin and correspondingly A = 235 and Z = 92 for uranium, one gets:
$\Delta M = 50 \cdot 1.007825 + 70 \cdot 1.008665 - 119.9022 = 1.0956\ \text{u} = 1020.3323\ \text{MeV}$ for tin and correspondingly
$\Delta M = 92 \cdot 1.007825 + 143 \cdot 1.008665 - 235.0439 = 1.915095\ \text{u} = 1783.528\ \text{MeV}$ It is interesting to calculate the binding energy per nucleon in each of the nuclei. For tin one gets $e_B = E_B/A$ = 1020.3323/120 = 8.502769 MeV and for uranium e_B = 1783.528/235 = 7.589481 MeV.

EXAMPLE 1-3 highlights one of the most interesting aspects of the nature. It shows that the binding energy per nucleon in nuclei of various atoms differ from each other. In fact, if the calculations performed in EXAMPLE 1-3 are repeated for all elements existing in the nature, a diagram – as shown in FIGURE 1-2 – is obtained. Sometimes this diagram is referred to as the "most important diagram in the Universe". And in fact, it is difficult to overestimate the importance of that curve.

Assume that one uranium nucleus breaks up into two lighter nuclei. For the time being it assumed that this is possible (this process is called **nuclear fission** and later on it will be discussed how it can be done). From EXAMPLE 1-3 it is clear that the total binding energy for uranium nucleus is ~235 x 7.59 = 1783.7 MeV. Total binding energy of fission products (assuming that both have approximately the same e_B as obtained for tin) 235 x 8.5 = 1997.5 MeV. The difference is equal to 213.8 MeV and this is the energy that will be released after fission of a single ^{235}U nucleus.

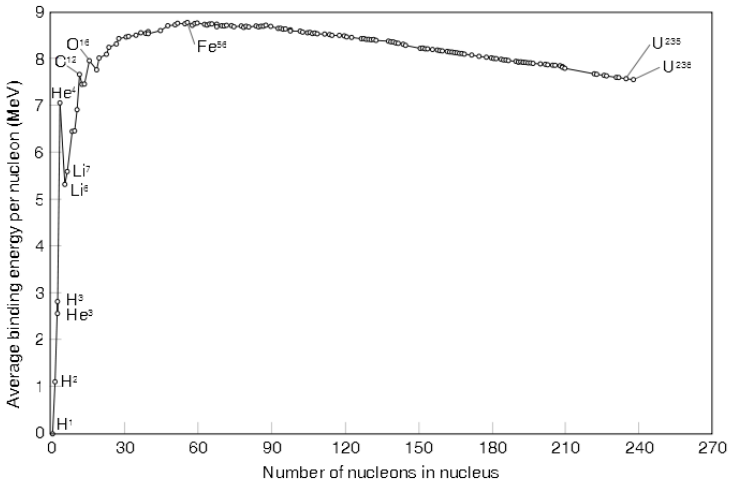

FIGURE 1-2: Variation of binding energy per nucleon with mass number (from Wikimedia Commons).

The total binding energy can be calculated from a semi-empirical equation,

$$E = 15.75A - 94.8\frac{\left(A/2 - Z\right)^2}{A} - 17.8A^{2/3} - 0.71Z^2A^{-1/3} + 34\delta A^{-3/4}, \tag{1-5}$$

where δ accounts for a particular stability of the even-even nuclei, for which $\delta = 1$ and instability of the odd-odd nuclei, for which $\delta = -1$. This equation is very useful since it approximates the binding energy for over 300 stable and non-stable nuclei, but it is applicable for nuclei with large mass numbers only.

1.2 Radioactivity

Isotopes of heavy elements, starting with the atomic number $Z = 84$ (polonium) through $Z = 92$ (uranium) exist in nature, but they are unstable and exhibit the phenomenon of radioactivity. In addition the elements with $Z = 81$ (thallium), $Z = 82$ (lead) and $Z = 83$ (bismuth) exist in nature largely as stable isotopes, but also to some extend as radioactive species.

1.2.1 Radioactive Decay

Radioactive nuclide emits a characteristic particle (alpha or beta) or radiation (gamma) and is therefore transformed into a different nucleus, which may or may not be also radioactive.

Nuclides with high mass numbers emit either positively charged **alpha particles** (equivalent to helium nuclei and consist of two protons and two neutrons) or negatively charged **beta particles** (ordinary electrons).

In many cases (but not always) radioactive decay is associated with an emission of **gamma rays**, in addition to an alpha or beta particle. Gamma rays are electromagnetic radiations with high energy, essentially identical with **x-rays**. The difference between the two is that gamma rays originate from an atomic nucleus and x-rays are produced from processes outside of the nucleus.

The radioactive decay of nuclei has a stochastic character and the probability of decay is typically described by the **decay constant** λ. Thus, if N is the number of the particular radioactive nuclei present at any time t, the number of nuclei ΔN that will decay during a period of time Δt is determined as,

(1-6) $$\Delta N = -\lambda N \Delta t ,$$

which gives the following differential equation for N,

(1-7) $$\frac{dN}{dt} = -\lambda N .$$

Integration of Eq. (1-7) yields,

(1-8) $$N = N_0 e^{-\lambda t} ,$$

where N_0 is the number of radioactive nuclei at time $t = 0$.

The reciprocal of the decay constant is called the **mean life of the radioactive species** (t_m), thus,

(1-9) $$t_m = \frac{1}{\lambda} .$$

The most widely used method for representing the rate of radioactive decay is by means of the **half-life of the radioactive species**. It is defined as the time required for the number of radioactive nuclei of a given kind to decay to half its initial value. If N is set equal to $N_0/2$ in Eq. (1-8), the corresponding half-life time $t_{1/2}$ is given by,

(1-10) $$\ln \frac{1}{2} = -\lambda t_{1/2} \Rightarrow t_{1/2} = \ln 2 \cdot \frac{1}{\lambda} = \ln 2 \cdot t_m .$$

The half-life is thus inversely proportional to the decay constant or directly proportional to the mean life.

The half-lives of a number of substances of interest in the nuclear energy field are given in TABLE 1.1.

TABLE 1.1. Radioactive elements.

Naturally occurring			Artificial		
Species	Activity	Half-Life	Species	Activity	Half-Life
Thorium-232	Alpha	$1.4 \cdot 10^{10}$ yr	Thorium-233	Beta	22.2 min
Uranium-238	Alpha	$4.47 \cdot 10^{9}$ yr	Protactinium-233	Beta	27.0 days
Uranium-235	Alpha	$7.04 \cdot 10^{8}$ yr	Uranium-233	Alpha	$1.58 \cdot 10^{5}$ yr

			Uranium-239	Beta	23.5 min
			Neptunium-239	Beta	2.35 days
			Plutonium-239	Alpha	$2.44 \cdot 10^4$ yr

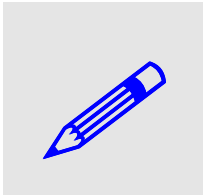

EXAMPLE 1-4. Calculate the decay constant, mean life and half-life of a radioactive isotope which radioactivity after 100 days is reduced 1.07 times. SOLUTION: Equation (1-8) can be transformed as follows: $\lambda = \ln(N_0/N)/t \cdot$ Substituting $N_0/N = 1.07$ and $t = 100 \cdot 24 \cdot 3600 = 8.64 \cdot 10^6\ s$ yields $\lambda = 7.83 \cdot 10^{-9}\ s^{-1}$. The mean life is found from Eq. (1-9) as $t_m = 1/\lambda \approx 4.05$ years and the half-life from Eq. (1-10) $t_{1/2} = \ln 2 \cdot t_m \approx 2.81$ years.

NOTE CORNER: Radioactive isotopes are useful to evaluate age of earth and age of various object created during earth history. In fact, since radioactive isotopes still exist in nature, it can be concluded that the age of earth is finite. Since the isotopes are not created now, it is reasonable to assume that at the moment of their creation the conditions existing in nature were different. For instance, it is reasonable to assume that at the moment of creation of uranium, both U-238 and U-235 were created in the same amount. Knowing their present relative abundance (U-238/U-235 = 138.5) and half-lives, the time of the creation of uranium (and probably the earth) can be found as: $N_8/N_5 = N_0 e^{-\lambda_8 t}/N_0 e^{-\lambda_5 t} = e^{(\lambda_5 - \lambda_8)t} = 138.5$. Substituting decay constants of U-235 and U-238 from TABLE 1.1, the age of earth is obtained as $t \approx 5 \cdot 10^9$ years. In archeology the age of objects is determined by evaluation of the content of the radioactive isotope C-14. Comparing the content of C-14 at present time with the estimated content at the time of creation of the object gives an indication of the object's age. For example, if in a piece of wood the content of C-14 corresponds to 60% of the content in the freshly cut tree, its age can be found as $t = -\ln(0.6)/\lambda = t_{1/2} \cdot \ln(1.667)/\ln 2 \approx 4000$ years (assuming $t_{1/2} = 5400$ years for C-14)

1.2.2 Radioactivity Units

A sample which decays with 1 disintegration per second is defined to have an activity of 1 **becquerel** (1 Bq). An old unit 1 **curie** (1 Ci) is equivalent to an activity of 1 gram of radium-226. Thus activity of 1 Ci is equivalent to 3.7 10^{10} Bq.

Other related units of radioactivity are reflecting the influence of the radioactivity on human body. First such unit was **roentgen**, which is defined as the quantity of gamma or x-ray radiation that can produce negative charge of 2.58 10^{-4} coulomb in 1 kg of dry air.

One **rad** (*r*adiation *a*bsorbed *d*ose) is defined as the amount of radiation that leads to the deposition of 10^{-2} J energy per kilogram of the absorbing material. This unit is applicable to all kinds of ionizing radiation. For x-rays and gamma rays of average energy of about 1 MeV, an exposure of one roentgen results in the deposition of 0.96 10^{-2} J /kg of soft body tissue. In other words the exposure in roentgens and the absorbed dose in soft tissue in rads are roughly equal numerically.

The SI unit of absorbed dose is 1 **gray** (Gy) defined as the absorption of 1 J of energy per kilogram of material, that is 1 Gy = 100 rad.

The biological effects of ionizing radiation depend not only on the amount of energy absorbed but also on other factors. The effect of a given dose is expressed in terms of

the dose equivalent for which the unit is **rem** (*r*adiation *e*quivalent in *m*en). If D is the absorbed dose in rads, the dose equivalent (DE) in rems is defined by,

$$DE(rems) = D(rads) \times QF \times MF$$

where QF is the quality factor for the given radiation and MF represents other factors. Both these factors depend on the kind of radiation and the volume of body tissue within which various radiations deposit their energy. In SI units the above equation defines the dose equivalent in **Siverts** (Sv) with reference to absorbed dose in grays. Thus, 1 Sv is equivalent to 100 rems.

1.3 Neutron Reactions

As already mentioned, neutrons play a very important role in nuclear reactor operations and their interactions with matter must be studied in details.

Reaction of neutron with nuclei fall into two broad classes: scattering and absorption. In scattering reactions, the final result is an exchange of energy between the colliding particles, and neutron remains free after the interaction. In absorption, however, neutron is retained by the nucleus and new particles are formed. Further details of neutron reactions are given below.

Neutrons can be obtained by the action of alpha particles on some light elements, e.g. beryllium, boron or lithium. The reaction can be represented as,

(1-11) $$^{9}_{4}Be + ^{4}_{2}He \rightarrow ^{12}_{6}C + ^{1}_{0}n\,.$$

The reaction can be written in a short form as ^{9}Be(α,n)^{12}C indicating that a ^{9}Be nucleus, called the **target nucleus**, interacts with an incident alpha particle (α); a neutron (n) is ejected and a ^{12}C nucleus, referred to as the **recoil nucleus**, remains. As alpha-particle emitters are used polonium-210, radium-226, plutonium-239 and americium-341.

1.3.1 Cross Sections for Neutron Reactions

To quantify the probability of a certain reaction of a neutron with matter it is convenient to utilize the concept of cross-sections. The **cross-section** of a target nucleus for any given reaction is thus a measure of the probability of a particular neutron-nucleus interaction and is a property of the nucleus and of the energy of the incident neutron.

Suppose a uniform, parallel beam of I monoenergetic neutrons per m^2 impinges perpendicularly, for a given time, on a thin layer δx m in thickness, of a target material containing N atoms per m^3, so that $N\delta x$ is the number of target nuclei per m^2, see FIGURE 1-3.

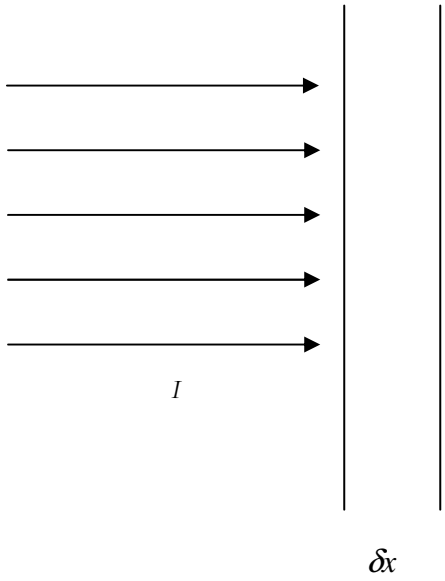

FIGURE 1-3: Beam of neutrons impinging a target material.

Let N_R be the number of individual reactions occurring per m^2. The nuclear cross section σ for a specified reaction is then defined as the averaged number of reactions occurring per target nucleus per incident neutron in the beam, thus,

(1-12) $$\sigma = \frac{N_R}{(N\delta x)I}\, m^2 / \text{nucleus}\,.$$

Because nuclear cross sections are frequently in the range of 10^{-26} to 10^{-30} m^2 per nucleus, it has been the practice to express them in terms of a unit of 10^{-28} m^2 per nucleus, called a **barn** (abbreviated by the letter b).

Equation (1-12) can be rearranged as follows,

(1-13) $$(N\delta x)\sigma = \frac{N_R}{I}\,.$$

The right-hand-side of Eq. (1-13) represents the fraction of the incident neutrons which succeed in reacting with the target nuclei. Thus $(N\delta x)\sigma$ may be regarded as the fraction of the surface capable of undergoing the given reaction. In other words of 1 m^2 of target surface $(N\delta x)\sigma$ m^2 is effective. Since 1 m^2 of the surface contains $(N\delta x)$ nuclei, the quantity σ m^2 is the effective area per single nucleus for the given reaction.

The cross section σ for a given reaction applies to a single nucleus and is frequently called the **microscopic cross section**. Since N is the number of target nuclei per m^3, the product $N\sigma$ represents the total cross section of the nuclei per m^3. Thus, the **macroscopic cross section** Σ is introduced as,

(1-14) $$\Sigma = N\sigma \text{ m}^{-1}\,.$$

If a target material is an element of atomic weight A, 1 mole has a mass of 10^{-3} A kg and contains the **Avogadro number** ($N_A = 6.02 \cdot 10^{23}$) of atoms. If the element density is ρ kg/m^3, the number of atoms per m^3 N is given as,

$$N = \frac{10^3 \rho N_A}{A}. \tag{1-15}$$

The macroscopic cross section can now be calculated as,

$$\Sigma = \frac{10^3 \rho N_A}{A} \sigma. \tag{1-16}$$

For a compound of molecular weight M and density ρ kg/m^3, the number N_i of atoms of the i_{th} kind per m^3 is given by the following equation (modified Eq. (1-15)),

$$N_i = \frac{10^3 \rho N_A}{M} \nu_i, \tag{1-17}$$

where ν_i is the number of atoms of the kind i in a molecule of the compound. The macroscopic cross section for this element in the given target material is then,

$$\Sigma_i = N_i \sigma_i = \frac{10^3 \rho N_A}{M} \nu_i \sigma_i. \tag{1-18}$$

Here σ_i is the corresponding microscopic cross section. For the compound, the macroscopic cross section is expressed as,

$$\Sigma = N_1\sigma_1 + N_2\sigma_2 + \cdots + N_i\sigma_i + \cdots = \frac{10^3 \rho N_A}{M}\left(\nu_1\sigma_1 + \nu_2\sigma_2 + \cdots\right). \tag{1-19}$$

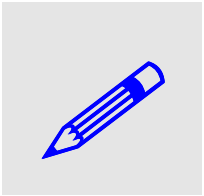

EXAMPLE 1-5. The microscopic cross section for the capture of thermal neutrons by hydrogen is 0.33 b and for oxygen $2 \cdot 10^{-4}$ b. Calculate the macroscopic capture cross section of the water molecule for thermal neutrons. SOLUTION: The molecular weight M of water is 18 and the density is 1000 kg/m^3. The molecule contains 2 atoms of hydrogen and 1 of oxygen. Equation (1-19) yields, $\Sigma_{H_2O} = \frac{10^3 1000 N_A}{18}\left(2 \cdot 0.33 + 1 \cdot 2 \cdot 10^{-4}\right) \cdot 10^{-28} \approx 2.2$ m^{-1}

As a rough approximation, the potential scattering cross section for neutrons of intermediate energy may be found as,

$$\sigma_s \approx 4\pi R^2, \tag{1-20}$$

where R is the radius of the nucleus.

At high neutron energies (higher than few MeV) the total cross section (e.g. for various reactions together) approaches the **geometrical cross section of the nucleus**,

(1-21) $$\sigma_t \approx \sigma_{absorption+inelastic\ scattering} + \sigma_{elastic\ scattering} \approx \pi R^2 + \pi R^2 = 2\pi R^2 .$$

It has been found that the radii of atomic nuclei (except those with very low mass number) may be approximated with the following expression,

(1-22) $$R \approx 1.3 \cdot 10^{-15} A^{1/3} \text{ m},$$

where A is the mass number of the nucleus. The total microscopic cross section is given by,

(1-23) $$\sigma_t \approx 0.11 A^{1/3} \text{ b}.$$

In general, the total microscopic cross section is equal to a sum of the scattering (both elastic and inelastic) and absorption cross sections,

(1-24) $$\sigma_t = \sigma_s + \sigma_a .$$

The microscopic cross section for absorption is further classified into several categories, as discussed below.

1.3.2 Neutron Absorption

It is convenient to distinguish between absorption of slow neutrons and of fast neutrons. There are four main kinds of slow-neutron reactions: these involve capture of the neutron by the target followed by either:

1. The emission of gamma radiation – or the radiative capture- (n,γ)
2. The ejection of an alpha particle (n,α)
3. The ejection of a proton (n,p)
4. Fission (n,f)

Total cross section for absorption is thus as follows,

(1-25) $$\sigma_a = \sigma_\gamma + \sigma_{n,\alpha} + \sigma_{n,p} + \sigma_f + \cdots$$

One of the most important reactions in nuclear engineering is the nuclear fission, which is described in a more detail in the following subsections.

1.3.3 Nuclear Fission

Relatively few reactions of fast neutrons with atomic nuclei other then scattering and fission, are important for the study of nuclear reactors. There are many such fast-neutron reactions, but their probabilities are so small that they have little effect on reactor operation.

Fission is caused by the absorption of neutron by a certain nuclei of high atomic number. When fission takes place the nucleus breaks up into two lighter nuclei: fission fragments.

Only three nuclides, having sufficient stability to permit storage over a long period of time, namely uranium-233, uranium-235 and plutonium-239, are fissionable by neutrons of all energies. Of these nuclides, only uranium-235 occurs in nature. The other two are produced artificially from thorium-232 and uranium-238, respectively.

In addition to the nuclides that are fissionable by neutrons of all energies, there are some that require fast neutrons to cause fission. Thorium-232 and uranium-238 are fissionable for neutrons with energy higher than 1 MeV. In distinction, uranium-233, uranium-235 and plutonium-239, which will undergo fission with neutrons of any energy, are referred to as **fissile nuclides**.

Since thorium-232 and uranium-238 can be converted into the fissile species, they are also called **fertile nuclides**.

The amount of energy released when a nucleus undergoes fission can be calculated from the net decrease in mass (mass defect) and utilizing the Einstein's mass-energy relationship. The total mean energy released per a single fission of uranium-235 nuclei is circa 200 MeV. Most of this energy is in a form of a kinetic energy of fission fragments (84%). The rest is in a form of radiation.

The fission cross sections of the fissile nuclides, uranium-233, uranium-235, and plutonium-239, depend on neutron energy. At low neutron energies there is $1/v$ region (that is, the cross section is inversely proportional to neutron speed) followed by resonance region with many well defined resonance peaks, where cross section get a large values. At energies higher than a few keV the fission cross section decreases with increasing neutron energy. FIGURE 1-4 shows uranium-235 cross section.

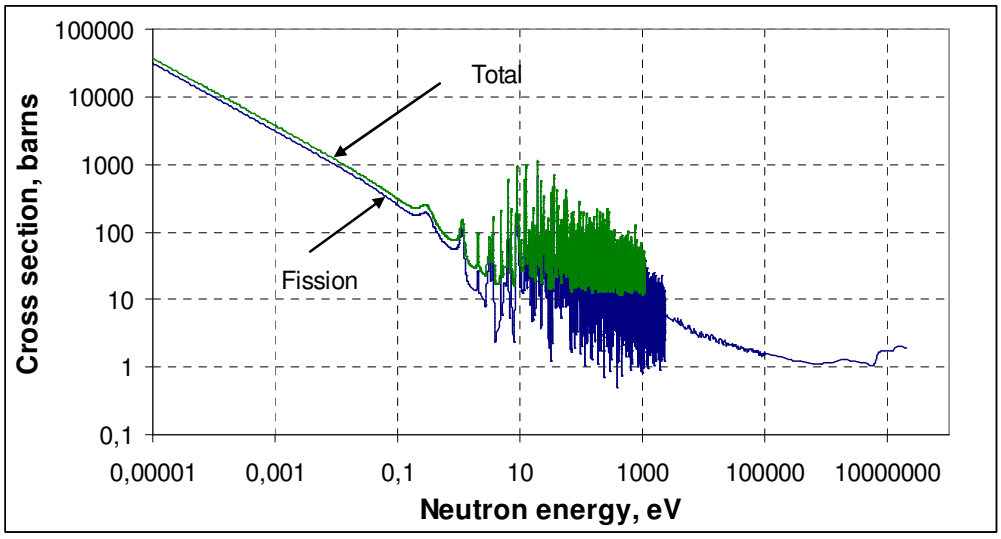

FIGURE 1-4: Total and fission cross section of uranium-235 as a function of neutron energy.

1.3.4 Prompt and Delayed Neutrons

The neutrons released in fission can be divided into two categories: **prompt neutrons** and **delayed neutrons**. More than 99% of neutrons are released within 10^{-14} s and are the prompt neutrons. The delayed neutrons continue to be emitted from the fission

fragments during several minutes after the fission, but their intensity fall rapidly with the time.

The average number of neutrons liberated in a fission is designed ν and it varies for different fissile materials and it also depends on the neutron energy. For uranium-235 $\nu = 2.42$ (for thermal neutrons) and $\nu = 2.51$ (for fast neutrons).

All prompt neutrons released after fission do not have the same energy. Typical **energy spectrum of prompt neutrons** is shown in FIGURE 1-5.

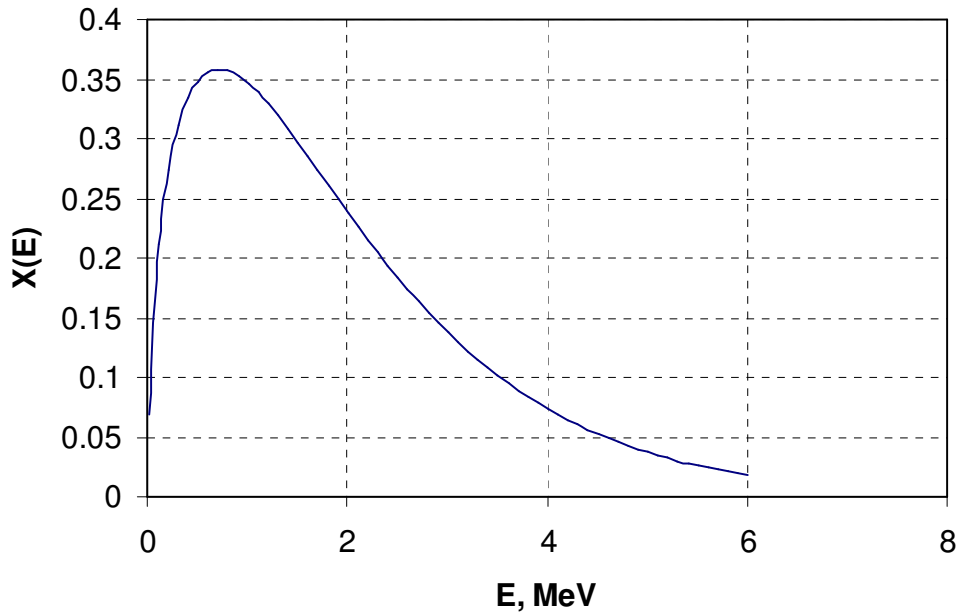

FIGURE 1-5: Energy spectrum of prompt neutrons, Eq. (1-26).

As can be seen, most neutrons have energies between 1 and 2 MeV, but there are also neutrons with energies in excess of 10 MeV. The energy spectrum of prompt neutrons is well approximated with the following function,

(1-26) $$\mathrm{X}(E) = 0.453 e^{-1.036E} \sinh\sqrt{2.29E}\,,$$

where E is the neutron energy expressed in MeV and $\mathrm{X}(E)dE$ is the fraction of prompt neutrons with energies between E and $E+dE$.

Even though less then 1% of neutrons belong to the delayed group of neutrons, they are very important for the operation of nuclear reactors. It has been established that the delayed neutrons can be divided into six groups, each characterized by a definite exponential decay rate (with associated a specific half-life with each group).

The delayed neutrons arise from a beta decay of fission products, when the "daughter" is produced in an excited state with sufficient energy to emit a neutron. The characteristic half-life of the delayed neutron is determined by the parent, or precursor,

of the actual neutron emitter. This topic will be discussed in more detail in sections devoted to the nuclear reactor kinetics.

1.3.5 Slowing Down of Neutrons

After fission, neutrons move chaotically in all directions with speed up to 50000 km/s. Neutrons can not move a longer time with such high speeds. Due to collisions with nuclei the speed goes successively down. This process is called scattering. After a short period of time the velocity of neutrons goes down to the equilibrium velocity, which in temperature equal to 20 C is 2200 m/s.

Neutron scattering can be either elastic or inelastic. Classical laws of dynamics are used to describe the elastic scattering process. Consider a collision of a neutron moving with velocity V_1 and a stationary nucleus with mass number A.

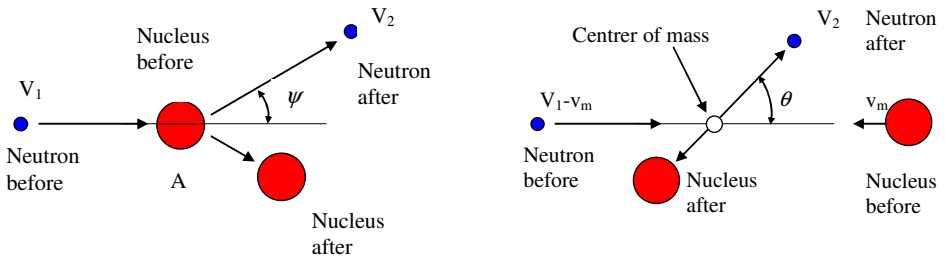

FIGURE 1-6: Scattering of a neutron in laboratory (to the left) and center-of-mass (to the right) systems.

It can be shown that after collision, the minimum value of energy that neutron can be reduced to is αE_1, where E_1 is the neutron energy before the collision, and,

$$\alpha = \left(\frac{A-1}{A+1}\right)^2 . \tag{1-27}$$

The maximum energy of neutron after collision is E_1 (neutron doesn't loose any energy).

The **average cosine of the scattering angle** ψ in the laboratory system describes the preferred direction of the neutron after collision and is often used in the analyses of neutron slowing down. It can be calculated as follows,

$$\overline{\cos\psi} \equiv \bar{\mu}_0 = \frac{\int_0^{4\pi} \cos\psi d\Omega}{\int_0^{4\pi} d\Omega} = \frac{2\pi\int_0^{4\pi} \cos\psi \sin\theta d\theta}{2\pi\int_0^{4\pi} \sin\theta d\theta} = \frac{2}{3A}, \tag{1-28}$$

since, as can be shown,

$$\cos\psi = \frac{A\cos\theta + 1}{\sqrt{A^2 + 2A\cos\theta + 1}} . \tag{1-29}$$

EXAMPLE 1-6. Calculate the minimum energy that a neutron with energy 1 MeV can be reduced to after collision with (a) nucleus of hydrogen and (b) nucleus of carbon. SOLUTION: For hydrogen A = 1 and $\alpha = 0$. For carbon A = 12 and $\alpha = 0.716$. Thus, the neutron can be stationary after the collision with the hydrogen nucleus, and can be reduced to energy E = 716 keV after collision with the carbon nucleus.

A useful quantity in the study of the slowing down of neutrons is the average value of the decrease in the natural logarithm of the neutron energy per collision, or the **average logarithmic energy decrement** per collision. This is the average of all collisions of $\ln E_1 - \ln E_2 = \ln(E_1/E_2)$, where E_1 is the energy of the neutron before and E_2 is that after collision,

$$\xi \equiv \overline{\ln \frac{E_1}{E_2}} = \frac{\int_{-1}^{1} \ln \frac{E_1}{E_2} d(\cos\theta)}{d(\cos\theta)}. \tag{1-30}$$

Here θ is a collision angle in the centre-of-mass system. Integration means averaging over all possible collision angles.

Analyzing energy change in scattering, the ratio E_1/E_2 can be expressed in terms of mass number A and the cosine of the collision angle $\cos\theta$. Substituting this to the equation above yields,

$$\xi = 1 + \frac{(A-1)^2}{2A} \ln \frac{A-1}{A+1}. \tag{1-31}$$

If the moderator is not a single element but a compound containing different nuclei, the effective or **mean-weighted logarithmic energy decrement** is given by,

$$\overline{\xi} = \frac{\nu_1 \sigma_{s1} \xi_1 + \nu_2 \sigma_{s2} \xi_2 + \ldots + \nu_n \sigma_{sn} \xi_n}{\nu_1 \sigma_{s1} + \nu_2 \sigma_{s2} + \ldots + \nu_n \sigma_{sn}}. \tag{1-32}$$

where n is the number of different nuclei in the compound and ν_i is the number of nuclei of i-th type in the compound. For example, for water (H_2O) it yields,

$$\overline{\xi}_{H_2O} = \frac{2\sigma_{s(H)} \xi_H + \sigma_{s(O)} \xi_{(O)}}{2\sigma_{s(H)} + \sigma_{s(O)}}. \tag{1-33}$$

An interesting application of the logarithmic energy decrement per collision is to compute the average number of collisions necessary to thermalize a fission neutron. It can be shown that this number is given as,

$$N_C = \frac{14.4}{\xi}. \tag{1-34}$$

The **moderating power** or **slowing down power** of a material is defined as,

(1-35 $M_P = \xi\Sigma_s$.

The moderating power is not sufficient to describe how good a given material is as a moderator, since one also wishes the moderator to be a week absorber of neutrons. A better figure of merit is thus the following expression, called the **moderating ratio**,

(1-36) $M_R = \dfrac{\xi\Sigma_s}{\Sigma_a}$.

REFERENCES

[1-1] Krane, K.S. *Modern Physics*, John Wiley & Sons. Inc., 1996

[1-2] Duderstadt, J.J. and Hamilton, L.J., *Nuclear Reactor Analysis*, John Wiley & Sons, 1976

[1-3] Glasstone, S. and Sesonske, A., *Nuclear Reactor Engineering*, Van Nostrand Reinhold Compant, 1981, ISBN 0-442-20057-9.

[1-4] Stacey, W.M., *Nuclear Reactor Physics*, Wiley-VCH, 2004

EXERCISES

EXERCISE 1-1: Disregarding uranium-234, the natural uranium may be taken to be a homogeneous mixture of 99.28 %w (weight percent) of uranium-238 and 0.72 %w of uranium-235. The density of natural uranium metal is 19.0 10^3 kg m^{-3}. Determine the total macroscopic and microscopic absorption cross sections of this material. The microscopic absorption cross sections for uranium-238 and uranium-235 are 2.7 b and 681 b, respectively. *Hint*: first find mass of uranium-235 and uranium-238 per unit volume of mixture and then number of nuclei per cubic meter of both isotopes.

EXERCISE 1-2: Calculate the moderating power and the moderating ratio for H_2O (density 1000 kg/m^3) and carbon (density 1600 kg/m^3). The macroscopic cross sections are as follows:

Isotope	σ_a , [b]	σ_s , [b]
Hydrogen	0.332	38
Oxygen	2.7 10^{-4}	3.76
Carbon	3.4 10^{-3}	4.75

EXERCISE 1-3: A neutron with energy 1 MeV scatters elastically with nucleus of ^{12}C. The scattering angle in the centre of mass system is 60°. Find the energy of the neutron and the scattering angle in the laboratory system. What can be the minimum energy of the neutron after collision? *Ans.* E = 0.929MeV, $\theta = 56°$, E_{min} = 0.716 MeV.

EXERCISE 1-4: Assuming that in each collision with the nucleus of ^{12}C neutron loses the maximum possible energy, calculate the number of collisions after which the neutron energy drops down from 1MeV to 0.025 eV. *Ans*: 52.

EXERCISE 1-5: Calculate the average cosine of the scattering angle in the laboratory system for ^{12}C and ^{238}U. *Ans:* 0.0555 and 0.028, resp.

Chapter

2

2 Nuclear Power Plants

Nuclear Power Plants (NPP) are complex systems that transform the fission energy into electricity on a commercial scale. The complexity of plants stems from the fact that they have to be both efficient and safe, which requires that several parallel systems are provided. The central part of a nuclear power plant consists of a system that ensures a continuous transport of the fission heat energy out of the nuclear reactor core. Such system is called the primary system.

Equally important are so-called secondary systems, whose main goal is to transform the thermal energy released from the primary system into electricity (or any other final form of energy that is required). If the system is based on the steam thermodynamic cycle, it consists of steam lines, turbine sets with generators, condensers, regeneration heat exchangers and pumps. In some cases gas turbines are used and the systems then in addition contain compressors, generators and heat exchangers.

Occasionally the primary and the secondary systems are connected through an additional intermediate system. This feature is characteristic for sodium-cooled reactor, where an intermediate sodium loop is used to prevent an accidental leakage of radioactive material from the primary to the secondary system.

If steam is used as the carrier of the thermal energy, the system is called the Nuclear Steam Supply System (NSSS). Such systems are typical for nuclear power plants which are using steam turbines to convert the thermal energy into the kinetic energy.

In addition to the above-mentioned process systems, NPPs contain various safety and auxiliary systems which are vital for over-all performance and reliability of the plants. The schematics and principles of operation of such systems are described in the first section of this chapter. In the following section the focus is on nuclear reactors and their components. Finally, the last section contains an introduction to plant analysis using computer simulations.

2.1 Plant Components and Systems

In this section the major systems that exist in NPPs are discussed. To focus the attention, systems typical to pressurized and boiling water reactors are chosen.

2.1.1 Primary System

The primary system (called also the primary loop) of a nuclear power plant with PWR is schematically shown in FIGURE 2-1. The main components of the system are as follows:

- reactor pressure vessel

- pressurizer
- steam generator
- main circulation pipe
- hot leg (piping connecting the outlet nozzle of the reactor pressure vessel with the steam generator)
- cold leg (piping connecting the steam generator with the inlet nozzle of the reactor pressure vessel)

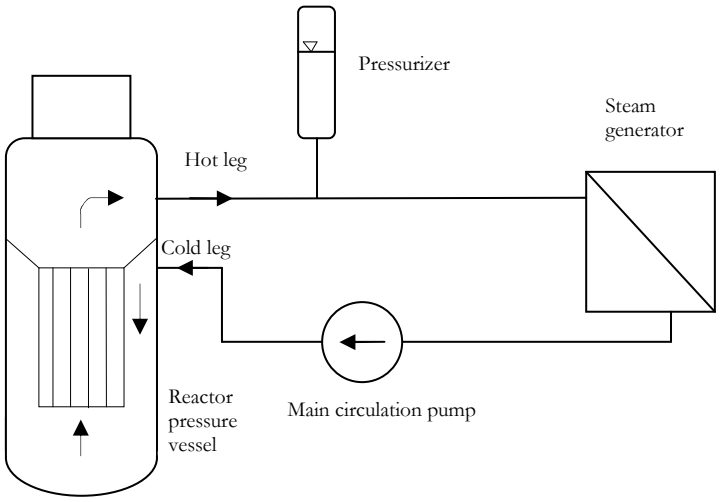

FIGURE 2-1: Primary system of a nuclear power plant with PWR.

Due to a limited power of main circulation pumps, the primary systems of PWRs consist of several parallel loops. In French PWRs with 910 MWe power there are three loops, whereas in American reactors with power in range 1100÷1300 MWe there are 2, 3 or 4 parallel loops. In multi-loop systems the pressurizer is present only in one of the loops.

Typical parameters of the primary loop of PWR with 900 MWe power are given in TABLE 2.1.

TABLE 2.1. Typical parameters of a primary system of PWR with 900 MWe power.

Parameter	**Value**
Reactor rated thermal power	**2785 MW**
Coolant mass flow rate	**13245 kg/s**
Coolant volume at rated power	**263.2 m^3**
Reactor Pressure Vessel (RPV) rated pressure	**15.5 MPa**
RPV pressure drop	**0.234 MPa**

RPV coolant inlet temperature	**286.0 °C**
RPV coolant outlet temperature	**323.2 °C**
Number of circulation loops	**3**
Steam Generator (SG) inlet coolant temperature	**323.2 °C**
SG outlet coolant temperature	**286.0 °C**
SG inlet coolant pressure	**15.5 MPa**
SG coolant pressure drop	**0.236 MPa**
SG total heat transfer area	**4751 m^2**
Inside diameter of hot leg	**736 mm**
Inside diameter of cold leg	**698 mm**
Main Circulation Pump (MCP) speed	**1485 rpm**
MCP developed head	**91 m**
MCP rated flow rate	**21250 m^3/h**
MCP electrical power at cold condition	**7200 kW**
MCP electrical power at hot conditions	**5400 kW**

Nuclear power plants with BWRs are single-loop systems, in which NSSS and the turbine sets are combined into a single circulation loop. Typical schematic of such loop is shown in FIGURE 2-2.

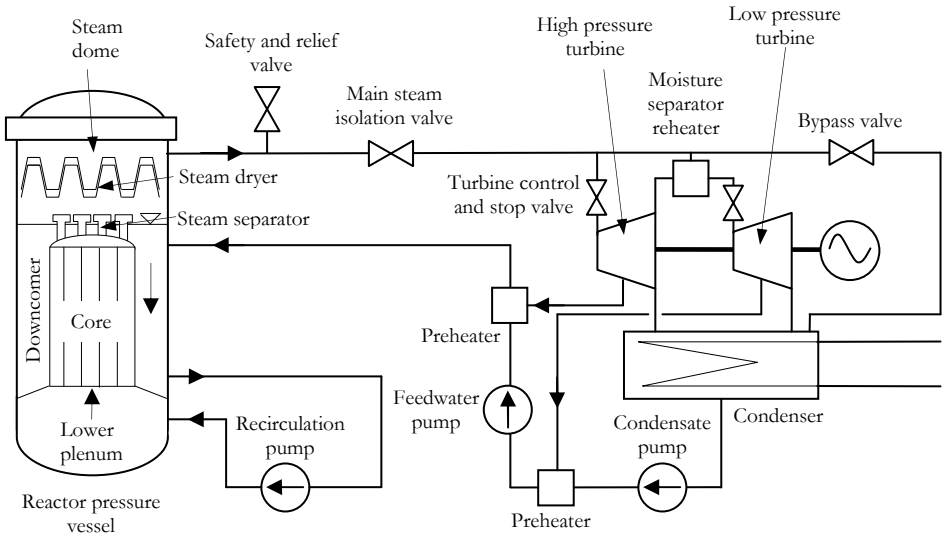

FIGURE 2-2: Schematic of a BWR system.

Typical process parameters for BWR system are given in TABLE 2.2.

TABLE 2.2. Typical process parameters in BWR system.

Parameter	Value
Reactor thermal power	**3020 MWt**
Generator output (electrical)	**1100 MWe**
Steam pressure in reactor dome	**7 MPa**
Steam pressure at inlet to HP turbine	**6 MPa**
Steam pressure at inlet to LP turbine	**0.8 MPa**
Pressure in condenser	**4 kPa**
Fraction of steam flow from reactor to HP turbine	**91%**
Fraction of steam flow to MSR	**9%**
Fraction of steam flow to high-pressure preheaters	**15%**
Fraction of steam flow to low-pressure preheaters	**11%**
Fraction of steam flow to condenser	**54%**
Water/steam temperature in upper plenum	**286 °C**
Feedwater temperature at inlet to RPV	**215 °C**
Feedwater temperature at inlet to feedwater pump	**170 °C**
Feedwater temperature at outlet from condensate pump	**30 °C**
Cooling water temperature at condenser inlet	**7 °C (mean)**

2.1.2 Secondary System

The secondary system of a nuclear power plant with the PWR is shown in FIGURE 2-3. The main parts of the system are as follows:

- steam lines
- turbine set
- moisture-separator reheater
- condenser
- preheaters

- condensate and feedwater pumps
- feedwater piping

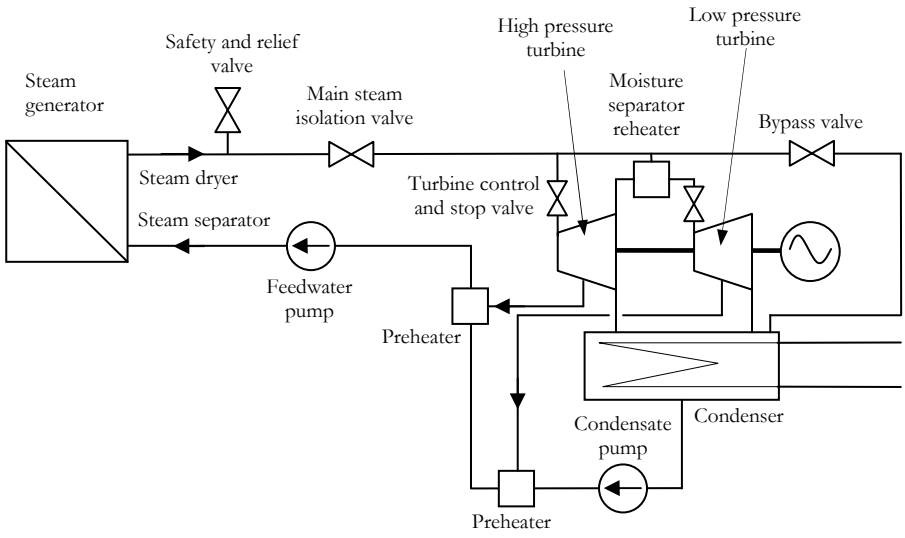

FIGURE 2-3: Secondary system in PWR nuclear power plant.

2.1.3 Auxiliary Systems Connected to the Primary System

The following systems are connected to the primary system,

- chemical and volume control system
- safety injection system
- residual heat removal system
- containment spray system

Other nuclear auxiliary systems,

- component cooling system
- reactor cavity and spent fuel pit cooling system
- auxiliary feedwater system.

2.1.4 Plant Auxiliary Systems

Main auxiliary systems are as follows,

- ventilation and air-conditioning system
- compressed air system
- fire protection system

2.1.5 Safety Systems

The major safety system is the **Emergency Core Cooling System** (ECCS). It usually consists of several subsystems as listed below.

ECCS in PWRs

ECCS in PWRs consists of the following subsystems:

- High-Pressure Injection System (HPIS)
- Low-Pressure Injection System (LPIS)
- Accumulators

ECCS in BWRs

ECCS in BWRs consists of:

- High-Pressure Core-spray System (HPCS)
- Low-Pressure Core-spray System (LPCS)
- Low-Pressure Injection System (LPIS)

2.2 Nuclear Reactors

Nuclear reactors are designed to transform heat released from nuclear fissions into enthalpy of a working fluid, which serves as a coolant of the nuclear fuel. The heat generated in the nuclear fuel would cause its damage and melting if not proper cooling was provided. Thus one of the most important safety aspects of nuclear reactors is to provide sufficient cooling of nuclear fuel under all possible circumstances. In some reactors it is enough to submerge nuclear fuel in a pool of liquid (or a compartment of gaseous) coolant, which provides sufficient cooling due to natural convection heat transfer. Such reactors are called to have passive cooling systems. Such systems are very advantageous from the safety point of view and are considered in future designs of nuclear reactors. The difficulty of such designs stems from the fact that the systems are prone to thermal-hydraulic instabilities.

In the majority of current power reactors a forced convection and boiling heat transfer is employed to retrieve the heat from the fuel elements. The systems are optimized to produce electricity by means of the Rankine cycle, in the similar manner as it is done in conventional power plants. The principles of operation, as well as basic classification of various reactor types are described in the following sections.

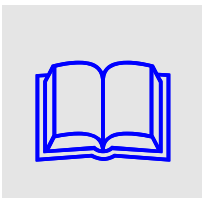

A recommended source of additional information and of the knowledge base on nuclear reactors is the web site supported by IAEA (www.iaea.org/inisnkm/nkm/aws/reactors.html).

2.2.1 Principles of Operation

The principle of operation of a thermal nuclear reactor is shown in FIGURE 2-4. In fact, the first nuclear reactor was created by the Nature some 2 billion years ago[2-2], not by scientists and engineers. Uranium-235 will sustain a chain reaction using normal water as neutron moderator and reflector. Such conditions can occur if uranium with 3% enrichment will be surrounded or penetrated by water. Due to neutron moderation by water, self-sustain chain reaction will occur. The released heat will cause water evaporation, effectively reducing the neutron moderation, and thus the power obtained from the process is self-controlled. Current reactors are utilizing the same principle, where self-sustained chain reaction is controlled by either inherent mechanisms (such as the above-mentioned water evaporation effect) or by deliberately designed systems that are controlling the distribution and level of the neutron flux in the reactor core.

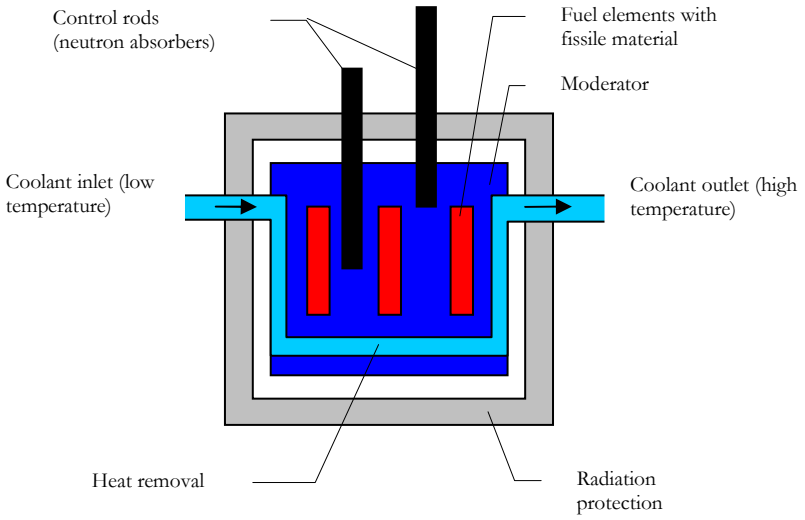

FIGURE 2-4: Principle of operation of a thermal nuclear reactor.

2.2.2 Reactor Types

There are numerous reactor types that have been either constructed or developed conceptually since the beginning of the nuclear era. The classification of reactors can be performed using various criteria, such as the type of nuclear fission reaction, type of coolant or type of moderator. The commonly used classification is given below.

Classification by type of nuclear reaction

- **Thermal reactors** are such reactors that use slow (thermal) neutrons in self-sustained chain reaction.

- **Fast reactors** are such reactors that use fast neutrons (typically average neutron energies higher than 100 keV) in self-sustained chain reaction.

Classification by moderator material

- **Water-moderated reactors** are divided into two different types:

  - **Light Water Reactors** (LWR) which are using ordinary water (H_2O) as the moderator.

  - **Heavy Water Reactors**, which are using heavy water (D_2O) as the moderator.

- **Graphite-moderated reactors** are using graphite as the moderating material. Such reactors need additional working fluid as a coolant. They can be further divided into the following types:

  - **Gas-cooled reactors** (for example Magnox and Advanced Gas-cooled Reactor – AGR)

  - Water-cooled reactors (for example Chernobyl-type reactor RBMK)

  - **High Temperature Gas-cooled Reactors** (HTGR), such as developed in the past AVR, Peach Bottom and Fort St. Vrain, or currently under development, Pebble Bed Reactor and Prismatic Fuel Reactor.

- **Light-element moderated Reactors** are such reactors where either lithium or beryllium is used as the moderator material. Two types of such reactors are considered:

  - Molten Salt Reactor (MSR) – in which light element (either lithium or beryllium) is used in combination with the fuel dissolved in the molten fluoride salt coolant.

  - Liquid-metal cooled reactors – in which BeO can be used as moderator and mixture of lead and bismuth serves as coolant.

- **Organically Moderated Reactors**, in which either biphenyl or terphenyl is used as the moderating material.

Classification by coolant

Water-cooled reactors are divided into two types: **Pressurized Water Reactors** (PWR), which use pressurized water (single-phase water typically at 15.5 MPa pressure) as coolant and **Boiling Water Reactors** (BWR), which use boiling water (two-phase mixture typically at 7 MPa pressure) .

- **Liquid-metal cooled reactors** use liquid metals, such as sodium, NaK (an alloy of sodium and potassium), lead, lead-bismuth eutectic, or (in earlier stages of development), mercury, as coolant.

- **Gas-cooled reactors** employ helium, nitrogen or carbon dioxide (CO_2) as coolant.

Classification by generation

Since early 1950s the reactor designs have been improved on the regular basis, bringing about various generations of reactors. A typical evolution of reactor generation from Generation-I through Generation-IV is shown in FIGURE 2-5.

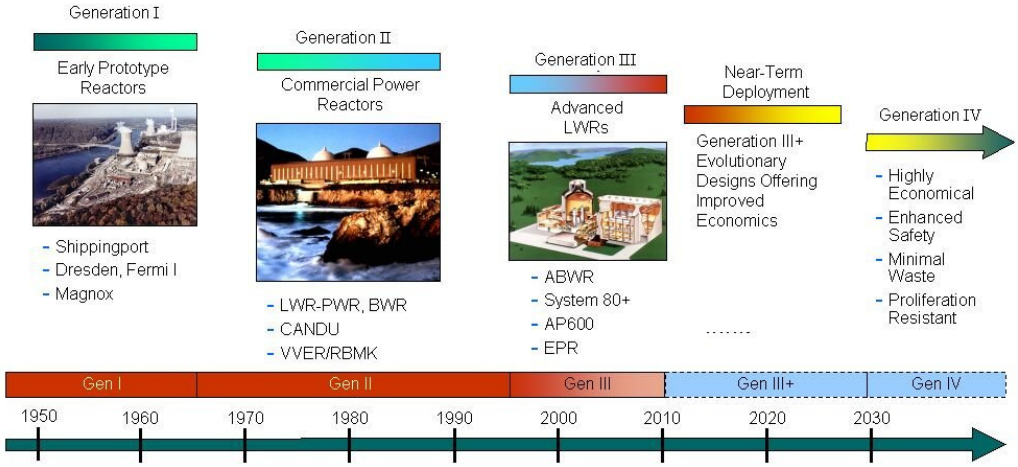

FIGURE 2-5: Evolution of reactor generations (from Wikimedia Commons).

2.2.3 Selected Current Technologies

Not all types of reactors mentioned in the previous section have received commercial maturity. Actually, most of the currently existing power reactors belong to the LWR category (in 2005 there were 214 PWRs, 53 WWERs and 90 BWRs out of 443 reactors in total). Full list of currently operating nuclear reactor types is given in TABLE 2.3. Some of the most popular reactor designs are described in more detail below.

TABLE 2.3 Reactor types (as of 31 Dec. 2005, source IAEA)

Type Code	Full Name	Opera-tional	Construction/ shutdown
ABWR	Advanced Boiling Light-Water-Cooled and Moderated Reactor	4	2/0
AGR	Advanced Gas-Cooled, Graphite-Moderated Reactor	14	0/1
BWR	Boiling Light-Water-Cooled and Moderated Reactor	90	0/20
FBR	Fast Breeder Reactor	3	1/6
GCR	Gas-Cooled Graphite-Moderated Reactor	8	0/29
HTGR	High-Temperature Gas-Cooled,	0	0/4

	Graphite-Moderated Reactor		
HWGCR	Heavy-Water-Moderated, Gas-Cooled Reactor	0	0/3
HWLWR	Heavy-Water-Moderated, Boiling Light-Water-Cooled	0	0/2
LWGR	Light-Water-Cooled, Graphite-Moderated Reactor	16	1/8
PHWR	Pressurized Heavy-Water-Moderated and Cooled Reactor	41	7/9
PWR	Pressurized Light-Water-Moderated and Cooled Reactor	214	4
WWER	Water Cooled Water Moderated Power Reactor	53	12
SGHWR	Steam-Generating Heavy-Water Reactor		
Total		**443**	**27/110**

Pressurized Water Reactor (PWR)

A schematic of a nuclear power plant with the **pressurized water-cooled reactor** is shown in FIGURE 2-6. The plant contains two circulation loops: the primary and the secondary one. The primary circulation loop, in which single-phase water is circulated between the reactor pressure vessel and the steam generator, is located inside a sealed containment. The secondary loop circulates steam, which is generated in the steam generator to the turbine.

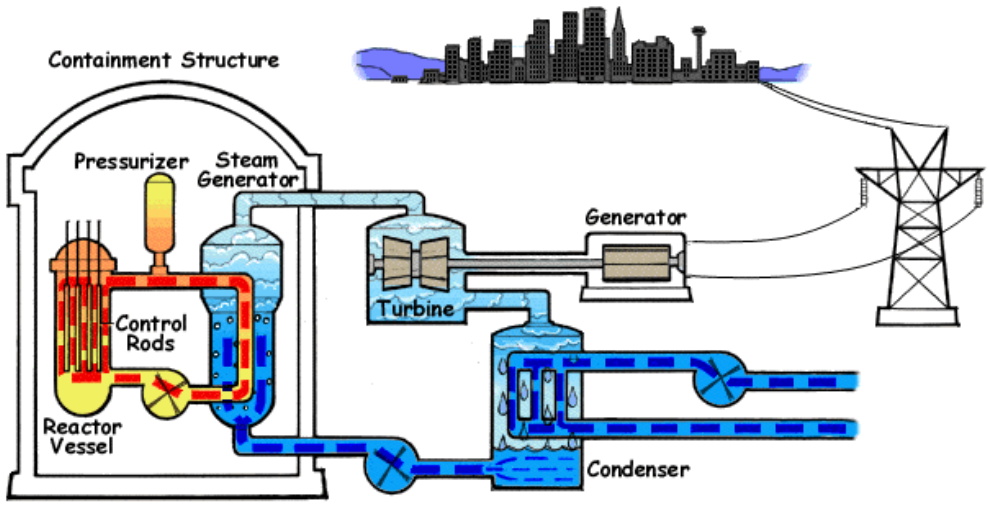

FIGURE 2-6: PWR nuclear power plant (from Wikimedia Commons).

Boiling Water Reactor (BWR)

A nuclear power plant with the **boiling water reactor** is schematically shown in FIGURE 2-7. The major difference between BWR and PWR is the direct generation of steam in the pressure vessel of BWR, which removes the need for steam generators and for the existence of two separate circulation loops. This particular feature greatly simplifies the over-all plant structure and allows for reduction of the containment size, which is much smaller for BWRs than for PWRs.

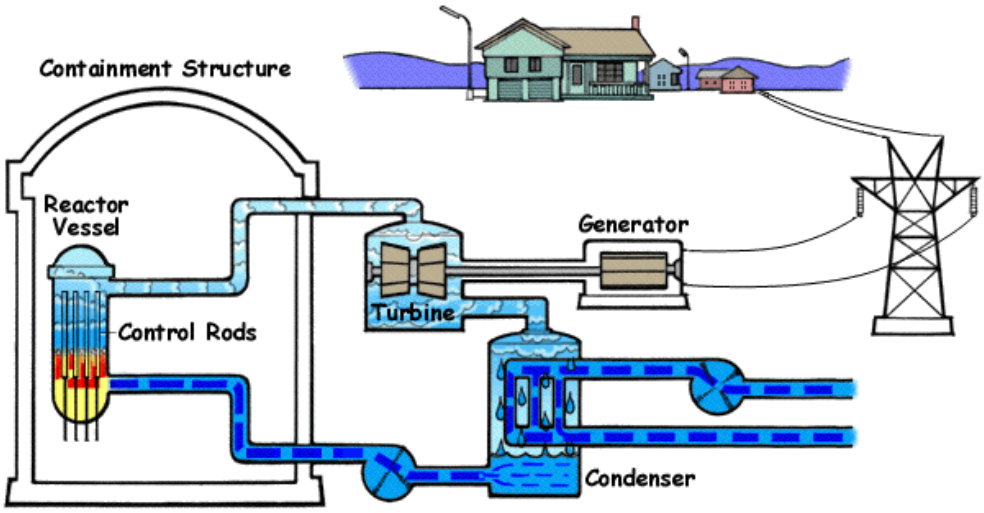

FIGURE 2-7: BWR nuclear power plant (from Wikimedia Commons).

Pressurized Heavy Water Reactor (PHWR)

The advantage of using heavy water (D_2O) as the moderator stems from the fact that, thanks to lower absorption of neutrons in D_2O as compared to H_2O, the natural uranium may be used as the nuclear fuel. Due to that the nuclear fuel is cheaper since the uranium enrichment in U-235 is not needed. This advantage is partly removed by the higher costs of the heavy water, which must be obtained in an artificial way.

An example of **PHWR** is the **CANDU** (CANada Deuterium Uranium) reactor, which uses the heavy water as both moderator and coolant, even though the two are completely separated. A schematic of the CANDU reactor is shown in FIGURE 2-8. This reactor can also operate with light water coolant. Due to higher neutron absorption in such systems, the uranium fuel must be slightly enriched.

High Power Channel Reactor (RBMK)

RBMK (shown in FIGURE 2-9) is an acronym for the Russian *Reaktor Bolshoy Moshchnosti Kanalniy* (High-Power Channel Type Reactor). This type of reactor employs light water as the coolant and graphite as the moderator. The reactor core consists of vertical pressure tubes running through the moderator. Fuel is low-enriched uranium oxide made up into 3.65 m long fuel assemblies. Since the moderator is solid, it is not expelled from the reactor core with increasing temperature. Since the water coolant is boiling, the reduction in neutron absorption causes a large positive void coefficient. Due to this feature the system is inherently unsafe, as it was exposed during the Chernobyl disaster.

This type of reactor was designed and built in the former Soviet Union. Currently all units (from 1 to 6) in Chernobyl, Ukraine, are shutdown. Still one unit (Ignalina-2, with total power of 1500 MWe) is operational in Lithuania. Several units (4 in Kursk, 4 in Sosnovy Bor, 80 km to the west from St Petersburg; and 3 in Smolensk) are operational in Russia.

Since the Chernobyl disaster this reactor type underwent a number of updates, including a new control-rod design, increased number of control rods and increased enrichment of uranium fro 2 to 2.4%.

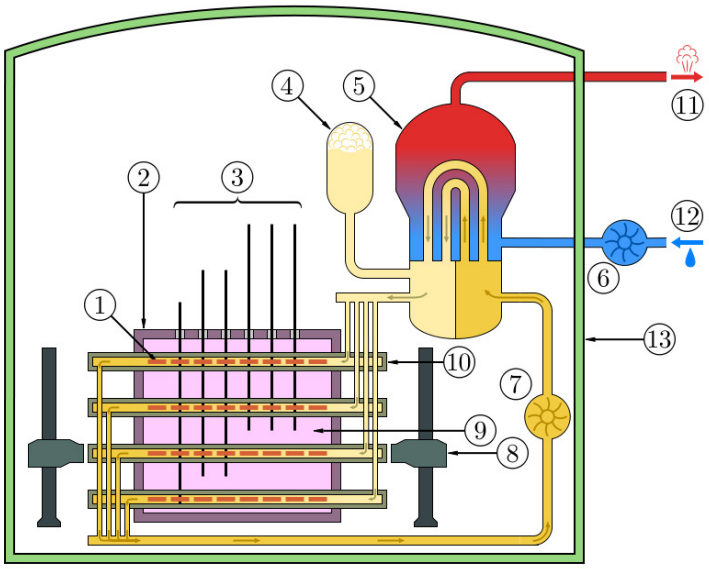

FIGURE 2-8: Canadian Heavy Water Reactor, CANDU (from Wikimedia Commons): 1- Fuel bundle, 2 – Calandria, 3 – Adjuster rods, 4 – Heavy water pressure reservoir, 5 – Steam generator, 6 – Light water pump, 7 – Heavy water pump, 8 – Fueling machines, 9 – Heavy water moderator, 10 – Pressure tube, 11 – Steam to steam turbine, 12 – cold water from condenser, 13 – containment.

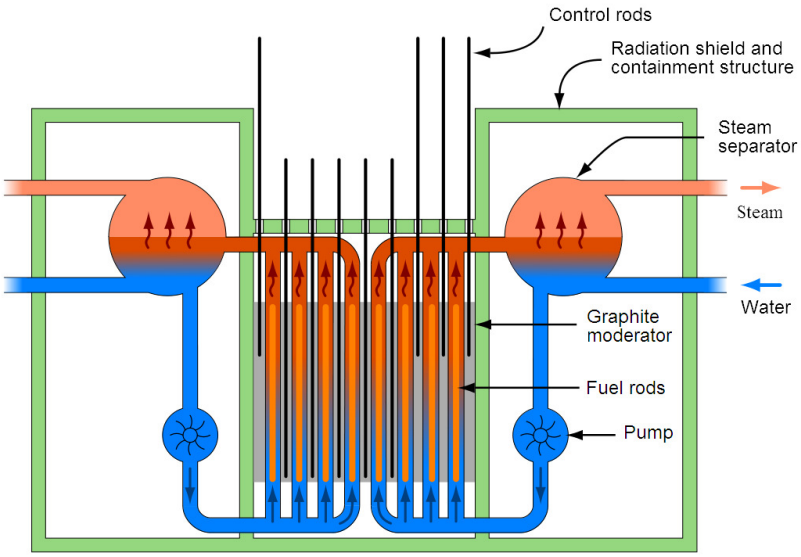

FIGURE 2-9: High Power Channel Reactor, RBMK (from Wikimedia Commons).

Advanced Gas Cooled Reactor (AGR)

Advanced Gas-Cooled Reactors (AGRs) have been developed in United Kingdom as a second generation of nuclear reactors following the Magnox nuclear power reactor. On the commercial scale the reactors became operational in 1976 and the estimated closure dates for 7 units in UK vary from 2014 to 2023. A schematic of AGR is shown in FIGURE 2-10.

AGRs have high thermal efficiency (up to 41%; to be compared with modern PWRs, which have the efficiency of 34%) thanks to the high temperature of the CO_2 coolant at the core exit (typically 913 K, or 640 °C and pressure 4 MPa). The benefit of the high efficiency is however hampered by relatively low fuel burnup ratio. Additional disadvantage of AGR is that its size must be much larger as compared to PWR of the same power output.

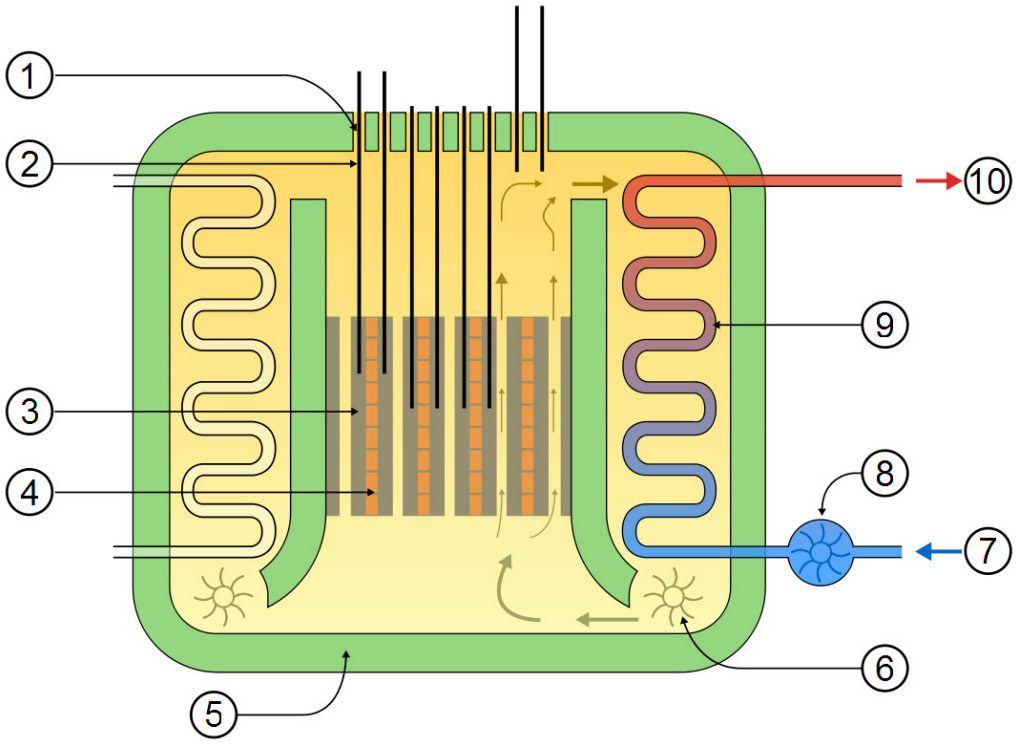

FIGURE 2-10: Advanced Gas-cooled Reactor, AGR: 1 – Charge tubes, 2 – Control rods, 3 – Graphite moderator, 4 – Fuel assembly, 5 – Concrete pressure vessel and radiation shielding, 6 – Gas circulator, 7 – Water, 8 – Water pump, 9 – Heat exchanger, 10 – Steam (from Wikimedia Commons).

Liquid Metal Fast Breeder Reactor (LMFBR)

There are two types of the **LMFBR**:

- loop type, in which coolant is circulated through the reactor core and an intermediate heat exchanger

- pool type (shown in FIGURE 2-11), in which the core and the intermediate exchangers are submerged in the liquid metal coolant, which is contained in a pool

The primary goal of the development of LMFBR is to improve the utilization of natural resources of uranium and to breed fuel by transmuting U-238 into Pu-239, Pu-240 and Pu-242, which all are fissile materials.

The major difficulty in the development of LMFBRs lies in the transferring heat from the liquid metal to other heat carriers (typically water and steam) that can be directly used in turbines the generate mechanical energy. In addition LMFBR is quite costly and is economically motivated when fuel prices are high (which has not been the case in the past decades).

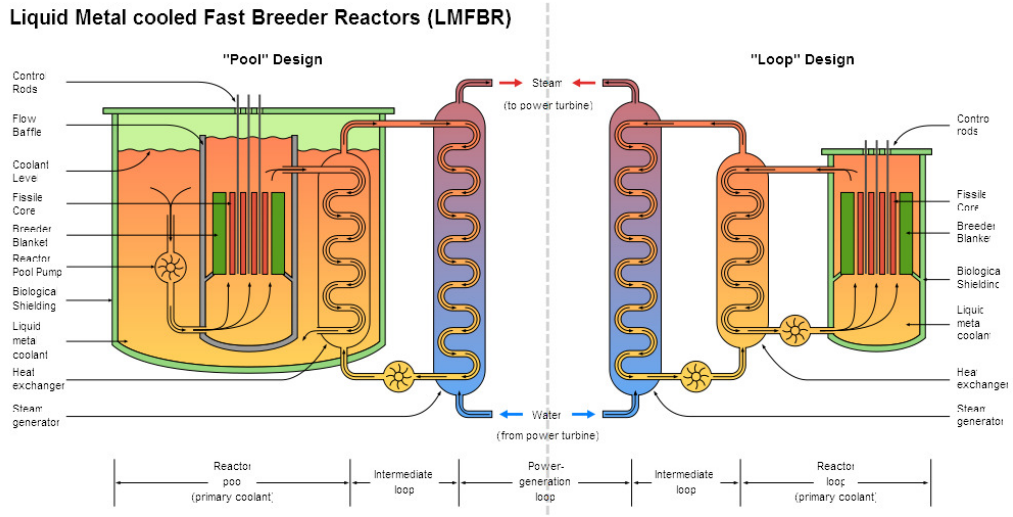

FIGURE 2-11: Liquid Metal cooled Fast Breeder Reactor, LMFBR: pool design to the left; loop design to the right (from Wikimedia Commons).

High Temperature Gas Cooled Reactor (HTGR)

The specific feature of the **HRGR** is the ability to operate at high temperatures, up to 1123 K (850 °C) for the pebble bed reactor and 998 K (725 °C) for the General Atomic's design. Due to the high temperatures, the over-all thermal efficiency of HTGR nuclear power plants is very high and comparable to the efficiencies of modern fossil-fuel plants. In addition, the high-temperature heat generated by HTGRs can be used in various heat-demanding industrial processes, such as steel manufacture, the conversion of coal into liquid and gaseous fuels and the steam cracking to produce hydrogen. Even though currently there are no such reactors under operation or construction, they have several important advantages and in various forms are considered as technological options within Generation-IV International Forum research.

A knowledge base for HTGR is supported by IAEA web site (www.iaea.org/inisnkm/nkm/aws/htgr/).

Several engineering designs of HTGRs have been proposed. Two of them are of particular interest:

- HTGR designed by General Atomic Co (USA)
- **Pebble Bed Modular Reactor** PBMR (Germany and South Africa)

The core of the HTGR (see FIGURE 2-12) consists of stacks of hexagonal graphite prisms with holes for fuel rods, for coolant (helium) flow and, if any, boron carbide control rods. The fuel rods are made of graphite containing coated particles (0.6÷0.9 mm in size) of highly enriched uranium and thorium dioxides. The oxide fuel is sometimes replaced with the carbide fuel. The coolant is not in contact with fuel elements and the heat is conducted through the graphite prisms. Thanks to the negative temperature coefficient and virtually no void coefficient (helium is virtually transparent to neutrons) the reactor possesses good inherent safety features.

PBMR was invented and build in Germany, where the first demonstration reactor (AVR in Jülich; see FIGURE 2-13) operated from 1967 to 1988. The fuel is similar to that used in HTGR, but fuel elements are in a shape of spheres with 60 mm diameter. The spheres are coated with pyrolytic carbon (or sometimes with silicon carbon). Thus a single fuel ball constitutes a "mini-reactor" containing fuel material, moderator and cladding. The fuel balls can be added and removed from a reactor on the continuous basis. A very important feature of PBMR is that it is inherently safe. In absence of cooling the reactor goes into idle stage (the power is reduced to high negative temperature coefficient of reactivity) and the remaining heat is removed by natural convection. The power will increase only when cooling is provided.

There is some criticism of the HTGR design, including the following concerns:

- hazards due to high content of potentially combustible graphite,
- lack of containments in some designs,
- relatively low experience with building HTGRs compared to LWRs,
- greater volume of the radioactive wastes,
- potential for jammed pebble damage (it occurred in AVR in 1986, partly contribution to discontinuation of the PBMR development),
- potential for contamination of the cooling circuit with metallic fission products (Sr-90, Cs-137),
- inaccurate temperature prediction in the core (in AVR the core temperature was underestimated with about 200 K).

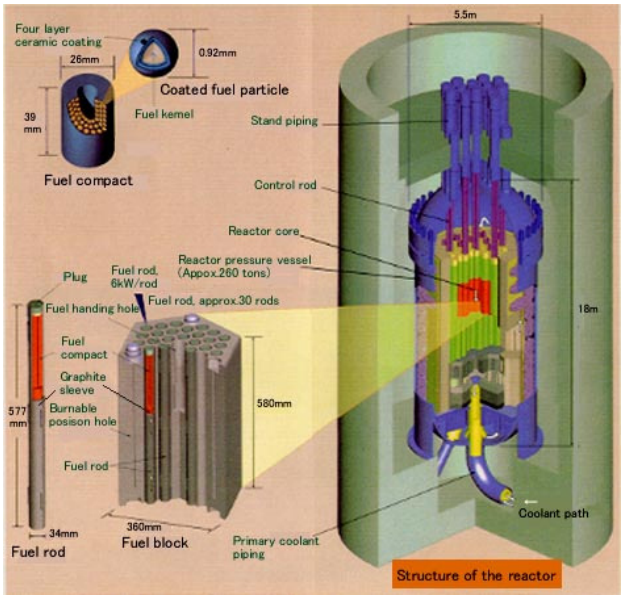

FIGURE 2-12: HTGR reactor and fuel (www.nukeworker.com).

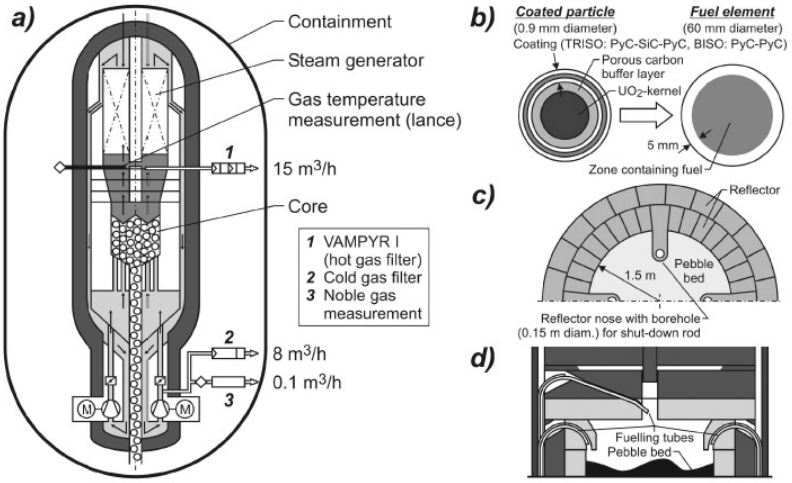

FIGURE 2-13: Schematics of the AVR; a) reactor, b) fuel, c-d) fueling facility (R. Moormann, Jül 4275).

2.3 Nuclear Reactor Components

Nuclear reactor contains the fuel material, which generates heat. The generated heat must be removed from the fuel material in an efficient manner to prevent the fuel melting. Due to that a nuclear reactor has a quite complex internal structure and contains several sub-systems. The most important ones are the reactor pressure vessel, the fuel assemblies and the control rods. These systems are discussed in a more detail in the following sections.

2.3.1 Reactor Pressure Vessel

Tepical reactor pressure vessels are shown in FIGURE 2-14.

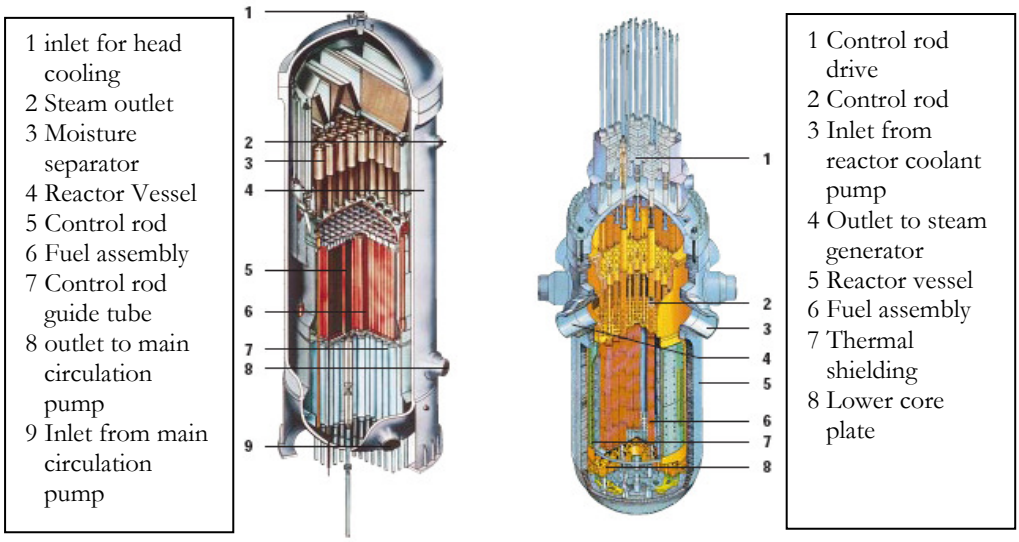

FIGURE 2-14: Reactor pressure vessels for BWRs (left) and PWRs (right).

The primary function of the **Reactor Pressure Vessel** (RPV) is to contain the core and the auxiliary systems, such as core support plates, shroud and internal pumps (if any) inside a sealed and pressurized volume. Due to their large volumes and thick walls, RPVs are made of thick bended steel plates that are welded together. The preferred material is a special fine-grained low alloy ferritic steel, well suited for welding. The inside is lined with austenitic steel cladding to protect against corrosion. Typical pressure vessel of PWR (with the power in the range of 1300 MWe) is 12÷13 m high, has the internal diameter about 5 m and the wall thickness about 20÷30 cm. The vessel is designed for a pressure of 17.5 MPa and the temperature of 623 K (350 °C).

The pressure vessels in BWRs have large dimensions, however, since the operating pressure is lower, the wall thickness can be kept in the range of 15÷20 cm.

The internals of the reactor pressure vessel must withstand the loads which are created during reactor operation and resulting from coolant flow and temperature gradients. Additional loads that are taken into account include vibrations caused by earthquakes and flow-structure interactions. The internals are made of hyper-quenched austenitic stainless steel. The main components of the PWR pressure vessel are as follows:

- the lower core support structure which consists of,
    - the core barrel (a cylinder surrounding the core)
    - the thermal shield, made of four pads attached to the outside of the core barrel by screws
    - the lower core plate, supporting the core
    - the baffle assembly inside the core barrel, which limits the bypass flow of the core
    - the secondary core support with the instrumentation port columns;

- the upper core support structure which consists of,
    - the upper support plate located directly on the fuel assemblies
    - the control rod guide tubes and the thermocouple columns
    - the guide tube support held in place by the vessel head, which contributes to support the core barrel
    - the support columns for connection between the upper support plate and the guide tube support

Some of the vessel internals are removable and replaceable for example to allow for refueling or for reactor vessel inspection.

2.3.2 Reactor Core and Fuel Assemblies

Reactor core consists of a number of **fuel assemblies** fixed in the pressure vessel between the lower and the upper core support plates. Fuel assemblies typical for PWRs and BWRs are shown in FIGURE 2-15.

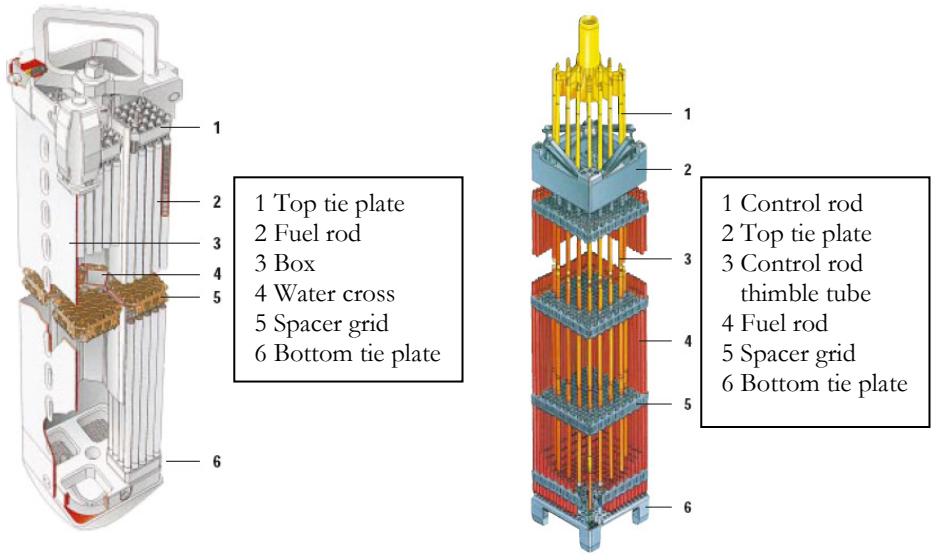

FIGURE 2-15: Typical fuel assemblies used in BWRs (left) and PWRs (right).

2.3.3 Control Rods

Control rods are movable elements that can be inserted into or withdrawn from a reactor to change the reactivity. They are manufactured from materials that are strong absorbers of neutrons. These are usually special alloys, for example 80 % silver, 15% indium and 5% cadmium. Generally, the material selected should have a good absorption cross section for neutrons and have a long lifetime as an absorber (not burn out rapidly).

The ability of a control rod to absorb neutrons can be adjusted during manufacture. A control rod that is referred to as a **black absorber** absorbs essentially all incident neutrons. A **grey absorber** absorbs only a part of them. While it takes more grey rods than black rods for a given reactivity effect, the grey rods are often preferred because they cause smaller depressions in the neutron flux and power in the vicinity of the rod.

This leads to a flatter neutron flux profile and more even power distribution in the core.

If grey rods are desired, the amount of material with a high absorption cross section that is loaded in the rod is limited. Material with a very high absorption cross section may not be desired for use in a control rod, because it will burn out rapidly due to its high absorption cross section. The same amount of reactivity worth can be achieved by manufacturing the control rod from material with a slightly lower cross section and by loading more of the material. This also results in a rod that does not burn out as rapidly.

Another factor in control rod material selection is that materials that resonantly absorb neutrons are often preferred to those that merely have high thermal neutron absorption cross sections. Resonance neutron absorbers absorb neutrons in the epithermal energy range. The path length traveled by the epithermal neutrons in a reactor is greater than the path length traveled by thermal neutrons. Therefore, a resonance absorber absorbs neutrons that have their last collision farther (on the average) from the control rod than a thermal absorber. This has the effect of making the area of influence around a resonance absorber larger than around a thermal absorber and is useful in maintaining a flatter flux profile.

There are several ways to classify the types of control rods. One classification method is by the purpose of the control rods. Three purposes of control rods are as follows,

1. **Shim rods** - used for coarse control and/or to remove reactivity in relatively large amounts

2. **Regulating rods** - used for fine adjustments and to maintain desired power or temperature

3. **Safety rods** - provide a means for very fast shutdown in the event of an unsafe condition. Addition of a large amount of negative reactivity by rapidly inserting the safety rods is referred to as a "scram" or "trip"

Not all reactors have different control rods to serve the purposes mentioned above. Depending upon the type of reactor and the controls necessary, it is possible to use dual-purpose or even triple-purpose rods. For example, consider a set of control rods that can insert enough reactivity to be used as shim rods. If the same rods can be operated at slow speeds, they will function as regulating rods. Additionally, these same rods can be designed for rapid insertion, or scram. These rods serve a triple function yet meet other specifications such as precise control, range of control, and efficiency. Examples of control rod designs for PWR and BWR are shown in FIGURE 2-16.

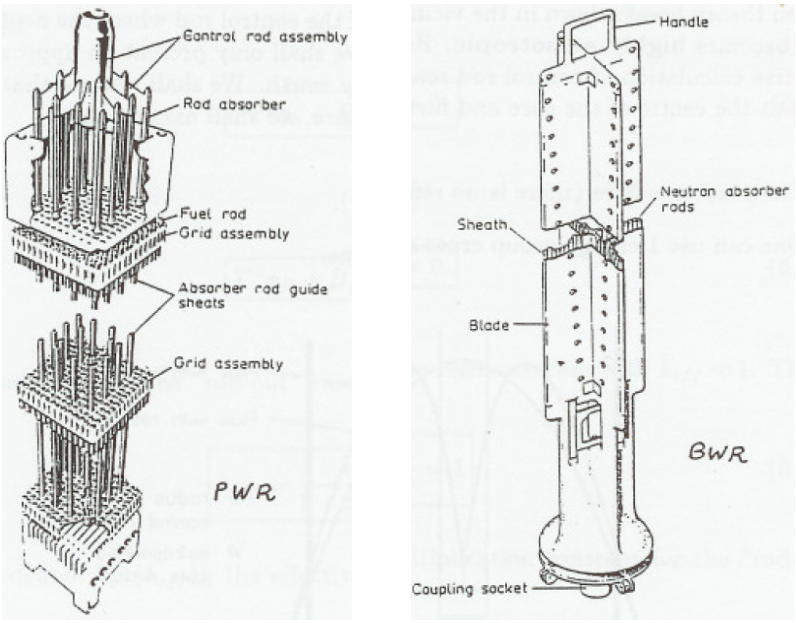

FIGURE 2-16: PWR and BWR control rods.

An important issue is to determine the change of reactivity caused by an insertion of control rods into a nuclear reactor. Since control rods are strong absorbers of neutrons, the neutron flux is strongly affected in their neighborhood and the neutron transport equation has to be solved. Clearly, the diffusion approximation is not able to replace fully the results obtained from the transport equations, but due to its relative simplicity it can be used to demonstrate some qualitative results.

2.4 Plant Operation

During the lifetime of a nuclear power plants it is necessary to start-up and stop the plant operation at various occasions. The typical procedures, which are followed in such situations, are described in this chapter.

2.4.1 Plant Startup to Full Power

The power of BWR during startup is controlled with the control rods and with changing the recirculation flow of coolant through the reactor core. With main circulation pumps kept at low speed (typically at 300 rpm), the control rods are withdrawn to the level that the reactor becomes critical. After that, further withdrawal of control rods causes release of power, which is initially used to warm up the reactor. The warming process after the reactor revision or refueling (when it was previously cooled down) may take up to 24 hours. After that time the reactor is brought to the hot standby condition, in which the pressure in the reactor is about 6.5 MPa, but the steam is not passed to turbines, since the main steam isolation valves and the steam dump valves are closed.

The first stage of increasing the reactor power from the hot standby to about 65% of the full power is achieved by further withdrawing the control rods. At that stage the recirculation flow through the reactor core increases from the natural-circulation level (roughly about 3000 kg/s for a 1000 MWe reactor) to about 4000 kg/s at power level of 65-70%. With increasing power the steam is directed to the steam lines, which are initially warmed up using a dedicated system. Main steam isolation valves open when the steam lines are warmed up and the steam is directed to the condenser through the

dump valve, to keep constant pressure in the reactor equal to 7 MPa. The turbine is started when the power is at about 30% level. At that stage the turbine is put in-phase with the external grid and rotates at 1500 rpm (50 Hz). After that the reactor power is increased steadily to 65-70% power.

In the meantime, the feed water system is operating, first at low-load mode and then in the high-load mode. After passing 40% power, the feedwater system operates at full capacity.

Power is increased from 65-70% to 100% in steps every 4 hours with magnitude of 2.5%. The reason for such a low paste of the power increase is to protect the fuel against excessive temperature-induced deformations which might result in so-called Pellet-Clad Interactions (PCI).

After reaching 100% of the power, the control rods need to be withdrawn additionally to compensate for the reactivity lost due to xenon build up. The xenon reactivity loss saturate to approximately 2.6% after 40-50 hours. Total time required for the reactor startup after refueling is about 3 to 4 days.

2.4.2 Plant Shutdown

The plant is shutdown to perform planned revisions and refueling of the nuclear reactor. The fission process is stopped by insertion of control rods into the reactor core. The reactor power, however, does not immediately drop to zero; instead it initially is at the level that corresponds to the β- and γ-radiation emitted from the fissions products. After reactor shutdown, the accumulated fission products continue to decay and generate heat within nuclear fuel elements. This heat is removed from the reactor using the Residual Heat Removal System (RHRS). In addition, before removing the reactor upper head, the reactor pressure vessel is cooled down by a dedicated spray system. After few hours the temperature in the reactor pressure vessel drops below the level that allows its opening.

2.5 Plant Analysis

The purpose of plant analysis is to optimize the plant operation under rated conditions and to predict the plant behavior under anticipated transient conditions. The major aspects of plant analyses are presented in the sub-sections below.

2.5.1 Steady State Conditions

The plant analysis at steady-state conditions can be performed at various power levels. The most important analysis is that performed at the rated conditions, since the plant is supposed to operate at such conditions at the most of its lifetime. The purpose of such analysis is to predict the plant efficiency and the safety margins. Often the steady-state analysis is performed at off-rated conditions, such as plant operation at the fraction of the rated power. The reason for such analyses is to predict the safety margins and over-all plant behavior, rather than plant efficiency, since plant is not expected to operate at such conditions for a long time.

2.5.2 Transient Conditions

Even though nuclear power plants are expected to operate at steady-state conditions during most of their lifetime, they have to be designed in such a way that safety will not be compromised under various anticipated transient conditions. Some of the transient

conditions are expected to occur during the normal and upset plant operation. To this category belong:

- heat up and cool down of the nuclear steam supply system
- load variation with prescribed steps (typically 5 to 10% of the rated power)
- house loading
- refueling
- turbine trip
- inactive loop start up
- loss of electrical power
- partial loss of reactor coolant flow
- reactor trip
- inadvertent reactor coolant pressure decrease
- control rod cluster drop

In addition to above-mentioned normal and upset conditions, various less frequent emergency conditions have to be analyzed. The following situations are considered:

- small reactor coolant pipe break
- small steam pipe break
- total loss of reactor coolant flow
- total loss of steam flow

Finally, highly improbable but severe faulted conditions are analyzed:

- reactor coolant pipe break (loss-of-coolant accident – LOCA)
- steam pipe break
- feedwater pipe break
- reactor coolant pump rotor locking
- control rod cluster ejection
- steam generator tube break

2.5.3 Computer Simulation of Nuclear Power Plants

Nuclear power plants are simulated with specialized computer codes, which employ the lumped-parameter approach. In this approach particular components are approximated with one or several computational volumes. The codes are particularly suited for analyses of whole systems and are often termed as system codes. Examples of such codes are TRACE, RELAP, CATHARE and ATHLET. The system codes typically require a very extensive description of input data, containing usually the following main groups:

- options (e.g. steady-state vs. transient, etc)
- nodalization (description of computational volumes and their connections)
- trip signals (usually used for actions of the control system and for the description of boundary conditions)
- initial conditions
- expected output data format and volume

Proper preparation of the input decks to the system codes is very time consuming and requires extensive system knowledge and experience with code simulations. Usually system code developers provide user guides, which should be carefully addressed by potential code users prior starting any simulation. An important part of the input deck preparation consists of the nodalization of the system. A rule of a thumb is that the particular nodes should follow the structure of the system under consideration and that the nodes should be well balanced in size. For example one should avoid placing a very large node in the direct vicinity to a very small node. An example of a nodalization of the BWR pressure vessel is shown in FIGURE 2-17.

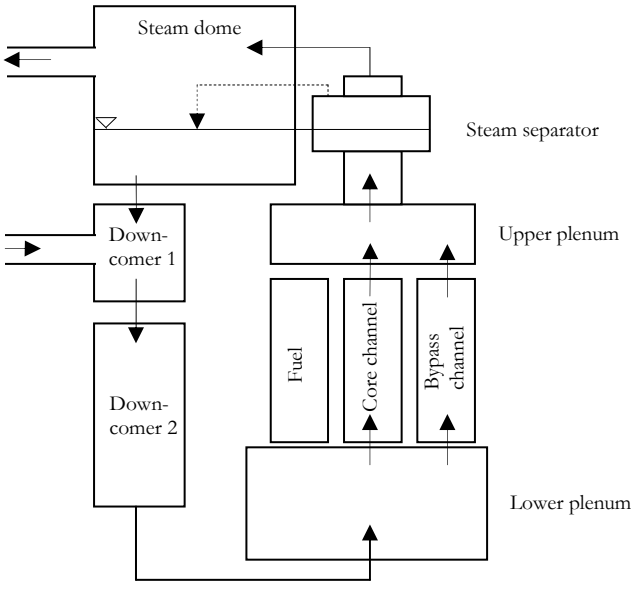

FIGURE 2-17: Example of nodalization of BWR pressure vessel.

Plant simulation training can be obtained through an IAEA initiative on the development of plant simulators for educational purposes, with a goal to provide insight and understanding of the general design and operational characteristics of various power reactor systems (www.iaea.org/NuclearPower/Education/Simulators/). Currently simulators for the following systems are provided:

- Advanced PWR
- Advanced BWR
- 2-loop PWR
- CANDU-9
- ACR-700
- WWER-1000

Since 1997 user workshops have been organized to facilitate the exchange of information and experience on using the plant simulators.

REFERENCES

[2-1] IAEA Nuclear Reactors Knowledge Base, www.iaea.org/inisnkm/nkm/aws/reactors.html

[2-2] New Scientest, Oklo reactor and fine-structure value, June 30, 2004, http://www.newscientist.com/article/dn6092

[2-3] Glasstone, S. and Sesonske, A., *Nuclear Reactor Engineering*, Van Nostrand Reinhold Compant, 1981, ISBN 0-442-20057-9.

[2-4] IAEA Knowledge Base for HTGR, www.iaea.org/inisnkm/nkm/aws/htgr/

[2-5] Moormann, R., A safety re-evaluation of the AVR pebble bed reactor operation and its consequences for future HTR concepts, Forschungszentrum Jülich, report 4275, ISSN 0944-2952.

[2-6] IAEA Collection of PC-based Simulators for Education, www.iaea.org/NuclearPower/Education/Simulators/

EXERCISES

EXERCISE 2-1: Taking typical PWR data given in TABLE 2.1 estimate the pumping power needed to ensure coolant flow through the reactor core. Compare with the total pump power given in the Table.

EXERCISE 2-2: Estimate the heat transfer coefficient in the steam generator using data from TABLE 2.1.

EXERCISE 2-3: For a BWR plant with parameters given in TABLE 2.2 derive the expression for the over-all plant efficiency. Plot the process in the T-s diagram.

Chapter

3

3 Nuclear Reactor Theory

The knowledge of neutron distribution in the reactor core is very important for prediction of its over-all features like, power level and power distribution. In general, exact description of positions and velocities of all neutrons is neither possible nor necessary. Even though the general form of equations are known (integro-differential Boltzmann equations), their simplified form known as diffusion theory approximation is employed. Further, it can be assumed that all neutrons have the same speed – which leads to the 1-group diffusion theory approximation. This kind of approximation leads to a quite crude model, nevertheless due to its simplicity it can be used for first-step analyses of nuclear reactors. As a most straightforward continuation, one can consider multi-group diffusion theory from which two-group approximation (where only fast and slow or thermal neutrons are considered) gained a considerable popularity and is often employed for practical analysis of nuclear reactors.

3.1 Neutron Diffusion

3.1.1 Neutron Flux and Current

Let n be a number of neutrons per unit volume and v the mean velocity of neutrons. The **neutron flux** is defined as follows,

(3-1) $$\phi = n \cdot v \quad [\text{neutron/m}^3 \times \text{m/s} = \text{neutron/(m}^2\text{s)}].$$

Inspecting units of neutron flux it can be concluded that nv is the number of neutrons falling on 1 m^2 of target material per second. Since σ [m^2] is the effective area per single nucleus for a given reaction and neutron energy, then Σ [m^{-1}] is the effective area of all the nuclei per m^3 of target and the product Σnv gives the number of interactions between neutrons and nuclei per m^3 of target material and per unit time. In particular, if Σ_f is the macroscopic cross section for fission with monoenergetic neutrons with velocity v, the product $\Sigma_f nv$ gives the rate of fissions per unit volume and unit time. Knowing the energy released per fission, the product determines the spatial power density distribution in material. Thus in general,

$$\text{Rate of neutron interactions} = \Sigma nv \ \text{interactions/m}^3 \cdot \text{s}$$

The **neutron current density** J_n in n direction is defined as a number of neutrons that cross a unit surface area dA in the n direction per unit time. The number of neutrons crossing the area dA per unit time is thus equal to $J_n\, dA$.

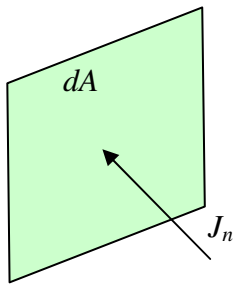

FIGURE 3-1: Neutron current.

3.1.2 Fick's Law

Neutron concentration is not uniform in a nuclear reactor, even though it would be most desirable to have this kind of distribution in many practical situations. In the same manner as for other species it is observed that neutrons will move from regions of high concentration to regions with low concentration due to a process known as diffusion. According to the **Fick's law of diffusion**, the neutron will flow from high to low concentration region with a rate proportional to the spatial gradient of concentration. Using the neutron flux ϕ as a measure of the neutron concentration, the Fick's law states that

(3-2) $$\mathbf{J} = -D\nabla\phi\,.$$

Here D is the **neutron diffusion coefficient**, $\nabla\phi$ is the gradient vector of the neutron flux and $\mathbf{J}$ is the vector of neutron current density.

It can be shown by a rigorous analysis that the neutron diffusion coefficient is given as,

(3-3) $$D = \frac{1}{3[\Sigma_t - \bar{\mu}_0\Sigma_s]} = \frac{1}{3\Sigma_{tr}},$$

where

(3-4) $$\Sigma_{tr} = \Sigma_t - \bar{\mu}_0\Sigma_s\,,$$

is the macroscopic **transport cross section**, Σ_t is the total macroscopic cross section, Σ_s is the macroscopic scattering cross section and $\bar{\mu}_0$ is the average value of the cosine of the scattering angle of neutrons ($\bar{\mu}_0 = 2/(3A)$, where A is the atomic mass number of the scattering material). The reciprocal of the macroscopic transport cross section is called the **transport mean free path** λ_{tr}; thus,

(3-5) $$\lambda_{tr} = \frac{1}{\Sigma_{tr}} = \frac{1}{\Sigma_t - \bar{\mu}_0\Sigma_s}\,.$$

For weakly absorbing materials Σ_a is small and Σ_t may be replaced with Σ_s; hence,

(3-6) $$\lambda_{tr} = \frac{1}{\Sigma_s(1-\bar{\mu}_0)} = \frac{\lambda_s}{(1-\bar{\mu}_0)},$$

where $\lambda_s = \Sigma_s^{-1}$ is the **scattering mean free path**.

3.1.3 Neutron Balance Equation

Balance equation for neutrons is derived in a same way as it is done for any conserved property. Consider an arbitrary volume V filled with neutrons. The balance equation can be expressed as,

{Time rate of change of neutrons in the volume V} =
{the net rate at which neutrons flow in – or out – of V across its surface A (leakage)} +
{rate at which neutrons are produced in volume V}
+ {rate at which neutrons are destroyed (absorbed) in volume V}.

The time rate of change of neutrons in the volume V is given by the following integral,

(3-7) $$\int_V \frac{\partial n}{\partial t} dV .$$

The rate of production of neutrons will be designed by the symbol $S(\mathbf{r},t)$, representing the production of neutrons per unit volume at location $\mathbf{r}$ and at time t.

The rate of absorption of neutrons in volume V is given as,

(3-8) $$\int_V \Sigma_a \phi dV .$$

Finally, the rate of neutron leakage from volume V is given as,

(3-9) $$\int_A \mathbf{J}\cdot\mathbf{n}dA = -\int_A D\nabla\phi\cdot\mathbf{n}dA = -\int_V D\nabla^2\phi dV ,$$

where in the last equation the Fick's law and the Gauss theorem have been employed.

Thus, the 1-group time dependent **neutron diffusion equation** (since an arbitrary volume is considered, integration over the volume is dropped) can be written as,

(3-10) $$\frac{\partial n}{\partial t} = \frac{1}{v}\frac{\partial \phi}{\partial t} = D\nabla^2\phi - \Sigma_a\phi + S .$$

The steady-state neutron diffusion equation is obtained by allowing the time derivative on the left-hand-side to be equal to zero,

(3-11) $$D\nabla^2\phi - \Sigma_a\phi + S = 0 .$$

Equation (3-11) is known as the Helmholtz equation and is very familiar type of equation in mathematical physics. It can be further transformed as follows,

(3-12) $$\nabla^2\phi - \frac{1}{L^2}\phi = -\frac{S}{D},$$

where

(3-13) $$L \equiv \sqrt{D/\Sigma_a},$$

is, by definition, the **neutron diffusion length**. It can be shown that L is a measure of how far a neutron will diffuse from a source before it is absorbed.

To solve the neutron diffusion equation, proper initial and boundary conditions must be specified. As an initial condition (essential for Eq. (3-10)), it is enough to know the flux distribution at the initial time,

(3-14) $$\phi(\mathbf{r},0) = \phi_0(\mathbf{r}).$$

At a boundary between two media A and B the neutron flux will be the same,

(3-15) $$\phi_A\big|_b = \phi_B\big|_b,$$

and the neutron current will be continuous,

(3-16) $$-D_A\left(\frac{d\varphi_A}{dx}\right)\Big|_b = -D_B\left(\frac{d\varphi_B}{dx}\right)\Big|_b.$$

At a boundary between a diffusion medium and vacuum a special condition is applied. At such boundary the neutron flux gradient is such that the linear extrapolation would lead to the flux vanishing at a certain distance beyond the boundary, see FIGURE 3-2.

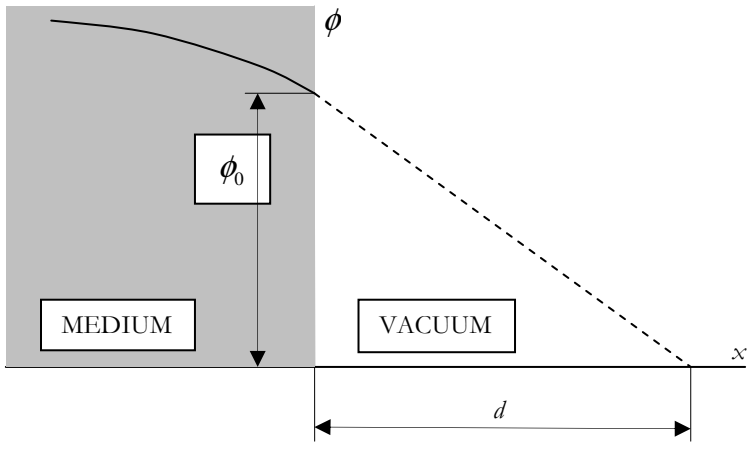

FIGURE 3-2: Extrapolation length.

More detailed transport theory studies indicate that taking,

(3-17) $$d \cong 0.7104\lambda_{tr},$$

will result in good prediction of the neutron flux in the medium by the diffusion theory. Thus the boundary condition for the diffusion equation can be written as,

(3-18) $$\phi(\tilde{\mathbf{r}}_s, t) = 0.$$

where $\tilde{\mathbf{r}}_s \equiv \mathbf{r}_s + \mathbf{d}$ is the **extrapolated boundary**.

The source term S in the neutron diffusion equation is the rate of neutron production per unit volume by fission. One can introduce here a definition of the infinite multiplication factor (a factor that will be described in more detail later),

$$k_\infty = \frac{Rate\ of\ neutron\ production}{Rate\ of\ neutron\ absorption},$$

which states that the rate of neutron production is equal to infinite multiplication factor times the rate of neutron absorption. Since the latter is equal to $\Sigma_a \cdot \phi$, the source S is obtained as,

(3-19) $$S = k_\infty \cdot \Sigma_a \cdot \phi.$$

For a critical reactor the neutron diffusion equation becomes,

(3-20) $$D\nabla^2\phi - \Sigma_a\phi + k_\infty\Sigma_a\phi = 0,$$

or

(3-21) $$\nabla^2\phi + \left[\frac{(k_\infty - 1)\Sigma_a}{D}\right]\phi = 0.$$

Using the definition of the diffusion length L, the equation reads,

(3-22) $$\nabla^2\phi + \frac{(k_\infty - 1)}{L^2}\phi = 0.$$

Introducing another important parameter called **material buckling** B_m, and defined as,

(3-23) $$B_m^2 = \frac{k_\infty - 1}{L^2},$$

Eq. (3-22) becomes,

(3-24) $$\nabla^2\phi + B_m^2\phi = 0.$$

3.1.4 Theory of a Homogeneous Critical Reactor

In a homogeneous reactor nuclear fuel and other materials form a homogeneous mixture. It is a convenient approximation of nuclear reactors, which allows for a simplified analysis of processes that take place in real, heterogeneous reactors. As an example, a homogeneous spherical reactor will be considered.

As derived in the previous subsection, the neutron source is set as $S = k_\infty \Sigma_a \phi(\mathbf{r},t)$. Assuming that this is the only source of neutrons in the reactor, the one-group diffusion approximation equation for the reactor becomes,

(3-25) $$\frac{1}{v}\frac{\partial \phi}{\partial t} = D\nabla^2\phi - \Sigma_a\phi + k_\infty\Sigma_a\phi,$$

with the initial condition given by Eq. (3-14) and the boundary condition given by Eq. (3-18). For a spherical homogeneous reactor with the extrapolated radius $\tilde{R}$, the equations become,

(3-26) $$\frac{1}{v}\frac{\partial \phi}{\partial t} = D\left(\frac{\partial^2\phi}{\partial r^2} + \frac{2}{r}\frac{\partial \phi}{\partial r}\right) - \Sigma_a\phi + k_\infty\Sigma_a\phi,$$

(3-27) $$\phi(r,0) = \phi_0(r),$$

(3-28) $$\phi(\tilde{R},t) = 0.$$

Equation (3-26) can be rewritten as follows,

(3-29) $$\frac{1}{vD}\frac{\partial \phi}{\partial t} = \frac{\partial^2\phi}{\partial r^2} + \frac{2}{r}\frac{\partial \phi}{\partial r} + \frac{k_\infty - 1}{D/\Sigma_a}\phi = \frac{\partial^2\phi}{\partial r^2} + \frac{2}{r}\frac{\partial \phi}{\partial r} + \frac{k_\infty - 1}{L^2}\phi$$

To solve the above equation, it is assumed that the solution can be expressed as,

(3-30) $$\phi(r,t) = R(r)T(t).$$

Substituting Eq. (3-30) into (3-29) yields,

$$\frac{1}{vD}R\frac{dT}{dt} = T\left(\frac{d^2R}{dr^2} + \frac{2}{r}\frac{dR}{dr}\right) + \frac{k_\infty - 1}{L^2}RT,$$

and dividing both sides with RT yields,

$$\frac{1}{vD}\frac{1}{T}\frac{dT}{dt} = \frac{1}{R}\left(\frac{d^2R}{dr^2} + \frac{2}{r}\frac{dR}{dr}\right) + \frac{k_\infty - 1}{L^2}$$

or

(3-31) $$\frac{1}{vD}\frac{1}{T}\frac{dT}{dt} - \frac{1}{L^2}(k_\infty - 1) = \frac{1}{R}\left(\frac{d^2R}{dr^2} + \frac{2}{r}\frac{dR}{dr}\right).$$

Since the left-hand-side of Eq. (3-31) is a function of *t* only, and the right-hand side is a function of *r*, the equation can be satisfied if both sides are equal to the same constant, say $-B^2$. Thus two ordinary differential equations are obtained,

(3-32) $$\frac{1}{T}\frac{dT}{dt} = vD\left[\frac{1}{L^2}(k_\infty - 1) - B^2\right],$$

(3-33) $$\frac{d^2R}{dr^2} + \frac{2}{r}\frac{dR}{dr} + B^2R = 0.$$

The solution of Eq. (3-32) is as follows,

(3-34) $$T = C \cdot \exp\left\{vD\left[\frac{1}{L^2}(k_\infty - 1) - B^2\right]t\right\},$$

where *C* is a constant.

Applying substitution $R(r) = u(r)/r$ in Eq. (3-33) yields,

$$\frac{d^2u}{dr^2} + B^2u = 0.$$

A general solution of this equation is as follows,

(3-35) $$u(r) = E_1 \sin Br + E_2 \cos Br,$$

thus the solution of Eq. (3-33) is as follows,

(3-36) $$R(r) = E_1\frac{\sin Br}{r} + E_2\frac{\cos Br}{r}.$$

Since *R(r)* can not be infinity when $r = 0$, then E_2 must be equal to zero, and the solution becomes,

(3-37) $$R(r) = E_1\frac{\sin Br}{r}.$$

This equation must satisfy the boundary condition given by Eq. (3-28), which now takes the form,

(3-38) $$\phi(\tilde{R}, t) = R(\tilde{R}) \cdot T(t) = 0 \quad \Rightarrow \quad R(\tilde{R}) = 0$$

for any value of *t*, thus,

(3-39) $$R(\tilde{R}) = E_1\frac{\sin B\tilde{R}}{\tilde{R}} = 0 \Rightarrow \sin B\tilde{R} = 0 \Rightarrow B_n\tilde{R} = n\pi,\ n = 1,2,\ldots.$$

As can be seen, Eq. (3-37) is satisfied by all functions of the form,

(3-40) $$R_n(r) = E_n \frac{\sin B_n r}{r}, \quad B_n = \frac{n\pi}{\tilde{R}}.$$

Numbers B_n are called **eigenvalues** and functions R_n **eigenfunctions** of the **boundary value problem** given by Eq. (3-33) together with the boundary condition given by Eq. (3-38).

Combining Eq. (3-30) with Eq. (3-34) and Eq. (3-40) yields a solution of Eq. (3-26) as follows,

(3-41) $$\phi(r,t) = \sum_{n=1}^{\infty} C_n \cdot \exp\left\{ vD\left[\frac{1}{L^2}(k_\infty - 1) - B_n^2 \right] t \right\} \frac{\sin B_n r}{r}.$$

Coefficients C_n can be found from the initial condition given by Eq. (3-27).

Equation (3-41) can be transformed as follows,

(3-42) $$\phi(r,t) = \sum_{n=1}^{\infty} C_n \cdot \exp\left\{ \frac{k_n - 1}{l_n} t \right\} \frac{\sin B_n r}{r},$$

where

(3-43) $$k_n = \frac{k_\infty}{1 + B_n^2 L^2},$$

(3-44) $$l_n = \frac{l_0}{1 + B_n^2 L^2},$$

(3-45) $$l_0 = \frac{1}{v\Sigma_a} = \frac{\lambda_a}{v}.$$

Parameter l_0 is the mean life-time of neutrons in an infinite media. Since eigenvalues B_n are increasing with increasing n, values of k_n, according to Eq. (3-43), must decrease. It means that if $k_1 = 1$, then all other values for higher n are less than one. This allows the following formulation of Eq. (3-42) for $k_1 = 1$,

(3-46) $$\phi(r,t) = C_1 \frac{\sin B_1 r}{r} + \sum_{n=2}^{\infty} C_n \cdot \exp\left\{ \frac{k_n - 1}{l_n} t \right\} \frac{\sin B_n r}{r}.$$

Now it can be seen that if $t \to \infty$, then, $\phi(r,t) \to \phi(r) = C_1 \sin B_1 r / r$. The conclusion is that if $k_1 = 1$ then the reactor attains steady-state, in which the source of neutrons comes from the fission of nuclei of the nuclear fuel. This is the condition when a self-sustained chain reaction exists in the reactor. This is the so-called critical condition of the reactor.

Taking in the following $k_1 = k$ and $B_1 = B$, the **criticality condition of a reactor** reads as follows,

(3-47) $$k = \frac{k_\infty}{1 + B^2 L^2} = 1,$$

where

(3-48) $$B^2 = \left(\frac{\pi}{\tilde{R}} \right)^2,$$

and the neutron flux distribution is given by the following equation,

(3-49) $$\phi(r,t) = C_1 \frac{\sin Br}{r}.$$

The criticality condition given by Eq. (3-47) can be derived in another way, by solving the steady-state diffusion equation (that is Eq. (3-11)) and seeking a positive solution that satisfies given boundary conditions. This approach will be demonstrated in the next sections using a cylindrical geometry of the reactor under consideration.

Equation (3-47) can be transformed as,

(3-50) $$B^2 = \frac{k_\infty - 1}{L^2}.$$

The parameter B^2 as given in Eq. (3-50) is a function of material property only and is called the **material buckling**. This is to distinguish from the parameter given by Eq. (3-48) which is called the **geometric buckling**. As can be seen, for critical reactor the material and the geometric buckling are equal to each other, that is,

(3-51) $$B_m^2 = B_g^2.$$

This equation plays a central role in the nuclear reactor design. Typically a nuclear reactor designer starts from evaluation of the geometric buckling to satisfy the requirements like the required reactor power and the maximum allowed fuel temperature. The geometric buckling can be found if the shape and the size of the reactor is known. Eq. (3-51) is then use to evaluate material properties that are required to make the reactor critical.

For a reactor with known material properties Eqs. (3-48) and (3-50) can be used to determine the critical size of the reactor. For a reactor with the spherical shape, one can find its size as follows,

(3-52) $$\tilde{R} = \frac{L\pi}{\sqrt{k_\infty - 1}}.$$

3.2 Neutron Flux in Critical Reactors

Distributions of neutron flux can be found by solving Eq. (3-10) (or (3-11) for steady-state situations) with proper boundary (Eq. (3-15) or (3-16)) and, if needed, initial (3-14) conditions. The most typical geometry - which is a finite cylinder - will be studied in this section. First a bare reactor, that is a reactor without a reflector will be

discussed. Next the influence of the reflector on the neutron distribution will be shown.

3.2.1 Finite-Cylinder Bare Reactor

As already mentioned, to find the criticality condition in a nuclear reactor one can seek positive solutions of a steady-state diffusion equation that satisfy proper boundary conditions.

In the method of variable separation it is assumed that the neutron flux in the finite cylinder is a function of two variables (r,z) and can be expressed as follows,

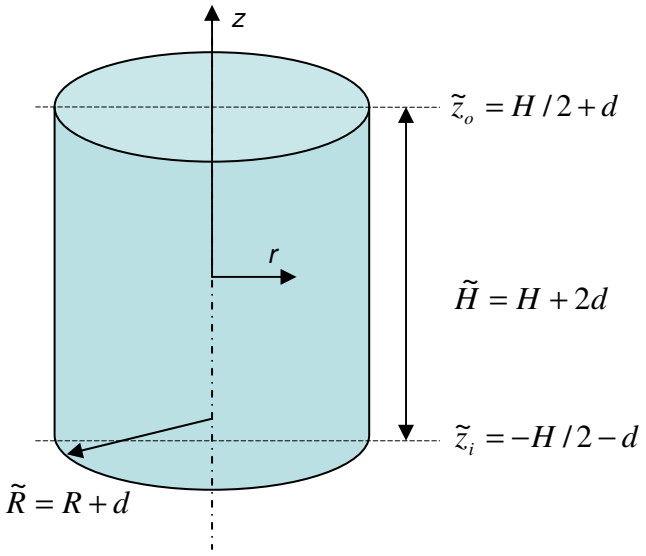

FIGURE 3-3: A finite-cylinder bare reactor with physical dimensions *R* and *H*.

(3-53) $$\phi(r,z) = R(r)\cdot Z(z).$$

In the cylindrical coordinate system, the Laplacian is as follows,

(3-54) $$\nabla^2\phi(r,z) = \frac{1}{r}\frac{\partial}{\partial r}\left(r\frac{\partial\phi}{\partial r}\right) + \frac{\partial^2\phi}{\partial z^2}.$$

Substituting Eqs. (3-53) and (3-54) into (3-24) yields,

(3-55) $$\frac{1}{r}\frac{d}{dr}\left(r\frac{dR(r)}{dr}\right)Z(z) + \frac{d^2Z(r)}{dz^2}R(z) + B_m^2R(r)Z(z) = 0.$$

Dividing both sides of Eq. (3-55) by product *R(r)Z(z)* gives,

(3-56) $$\frac{1}{r}\frac{d}{dr}\left(r\frac{dR(r)}{dr}\right)\frac{1}{R(r)} + \frac{d^2Z(z)}{dz^2}\frac{1}{Z(z)} + B_m^2 = 0.$$

Since the first term is a function of *r* only and the second term a function of *z* only, to satisfy the equation, each of them must be equal to a constant,

(3-57) $$\frac{d^2Z(z)}{dz^2}\frac{1}{Z(z)} = -k^2 \Rightarrow \frac{d^2Z(z)}{dz^2} + k^2 Z(z) = 0.$$

A general solution of the above equation is as follows,

(3-58) $$Z(z) = A_1 \sin(kz) + A_2 \cos(kz).$$

The equation for the radial part reads,

(3-59) $$\frac{d^2R(r)}{dr^2} + \frac{1}{r}\frac{dR(r)}{dr} + \alpha^2 R(r) = 0 \ ,$$

where,

(3-60) $$\alpha^2 = B_m^2 - k^2$$

With a general solution as follows,

(3-61) $$R(r) = C \cdot J_0(\alpha \cdot r) + D \cdot N_0(\alpha \cdot r).$$

Here J_0 is the Bessel function of the first kind and order 0 and N_0 is the Bessel function of the second kind and order 0. Noting that N_0 becomes infinite for $r = 0$, the constant D in Eq. (3-61) must be equal to zero: $D = 0$.

At the extrapolated radius of the cylinder the neutron flux will vanish,

(3-62) $$\phi(\tilde{R}, z) = 0, \qquad C \cdot J_0(\alpha \cdot \tilde{R}) = 0.$$

The above equation will be satisfied for,

(3-63) $$\alpha_n \tilde{R} = \xi_n, n = 1,2,... \ ; \ \alpha_n = \frac{\xi_n}{\tilde{R}},$$

where ξ_n is n-th root of the Bessel function $J_0(x)$. Equation (3-59) and corresponding boundary conditions will be satisfied by the following functions,

(3-64) $$R_n(r) = C_n J_0\left(\frac{\xi_n r}{\tilde{R}}\right), \quad n = 1,2,...$$

It can be easily checked that only for $n = 1$ ($\xi_1 \cong 2.405$) solution given by Eq. (3-64) is positive in the whole reactor domain. From Eq. (3-58) and boundary conditions at $\tilde{z}_i$ and $\tilde{z}_o$ results the following solution,

(3-65) $$Z_m(z) = A_{2,m} \cos\left(\frac{m\pi z}{\tilde{H}}\right),$$

where again only Z_1 is positive in the whole reactor domain. Thus the only positive solution satisfying the boundary conditions has the following form,

(3-66) $$\phi(r,z) = AJ_0\left(\frac{2.405r}{\tilde{R}}\right)\cos\left(\frac{\pi z}{\tilde{H}}\right).$$

From Eq. (3-60) one gets,

(3-67) $$B_m^2 = \left(\frac{2.405}{\tilde{R}}\right)^2 + \left(\frac{\pi}{\tilde{H}}\right)^2,$$

and constant A can be found from the total power of the reactor.

Equation (3-67) expresses the equality of the material buckling with a geometric parameter, described by the right-hand-side of the equation. This parameter is called, as already mentioned, the geometric buckling characterizing the considered geometry, and its values for various shapes (which can be obtained in the same manner as for the finite cylinder) are shown in TABLE 3.1. The table also shows the critical flux profile that corresponds to each reactor shape.

TABLE 3.1. Geometric buckling and critical flux profiles for selected geometries.

Shape	Geometric buckling	Flux profile
Slab of thickness a	$\left(\frac{\pi}{\tilde{a}}\right)^2$	$\cos\frac{\pi x}{\tilde{a}}$
Sphere with radius R	$\left(\frac{\pi}{\tilde{R}}\right)^2$	$\sin\left(\frac{\pi r}{\tilde{R}}\right)\Big/ r$
Rectangular parallelepiped with sides a, b, c	$\left(\frac{\pi}{\tilde{a}}\right)^2 + \left(\frac{\pi}{\tilde{b}}\right)^2 + \left(\frac{\pi}{\tilde{c}}\right)^2$	$\cos\left(\frac{\pi x}{\tilde{a}}\right)\cos\left(\frac{\pi y}{\tilde{b}}\right)\cos\left(\frac{\pi z}{\tilde{c}}\right)$
Finite cylinder with radius R and height H	$\left(\frac{2.405}{\tilde{R}}\right)^2 + \left(\frac{\pi}{\tilde{H}}\right)^2$	$J_0\left(\frac{2.405r}{\tilde{R}}\right)\cos\left(\frac{\pi z}{\tilde{H}}\right)$

Equation (3-67) can be rewritten as,

(3-68) $$B_m^2 = B_g^2,$$

where B_g^2 is the geometric buckling. Depending on the reactor shape it will be equal to one of the expressions in TABLE 3.1. Equation (3-68) states the criticality condition for a reactor. In other words, for given material with given B_m and given reactor shape with certain B_g, Eq. (3-68) must hold for the reactor to be critical.

Nuclear reactor designers are usually given B_g^2 (rather than B_m^2) since the core dimensions are determined from the thermal-hydraulic core design, which takes into

account the thermal limitations in the core. The core must be built large enough and provide enough heat transfer area to avoid excessively high temperatures for a desired power output. Once the core size is established, the nuclear designer must determine the fuel concentration or loading (that corresponds to obtaining a required B_m^2) that enable the core to operate at given power for a given period of time.

3.2.2 A Spherical Reactor with Reflector

A bare reactor has several drawbacks which cause that almost no reactors of this type exists in reality. These drawbacks are as follows:

- Relatively large amount of neutrons is lost due to leakage from a bare reactor. As a result, such reactors have large critical size and large critical mass, and utilization of the nuclear fuel is quite poor.

- The neutron flux distribution in a bare reactor, and consequently the distribution of heat sources are very uneven. Even that is causing uneconomical utilization of the nuclear fuel.

The two drawbacks cause that almost all reactors operating in the world are using reflectors. As the name indicates, the purpose of a reflector is to reflect back neutrons to the reactor. The reflector usually is surrounding the reactor core and contains the same material that is used for moderation (that is a material with large cross section for scattering and small cross section for absorption).

The one-group diffusion equations for a reactor with reflector are as follows,

(3-69) $$D_c \nabla^2 \phi_c - \Sigma_{a,c} \phi_c + k_\infty \Sigma_{a,c} \phi_c = 0,$$

(3-70) $$D_r \nabla^2 \phi_r - \Sigma_{a,r} \phi_r = 0,$$

where indices *c* and *r* indicate core and reflector, respectively.

The boundary conditions on the core-reflector boundary are as follows,

(3-71) $$\phi_c = \phi_r,$$

(3-72) $$D_c \frac{\partial \phi_c}{\partial n} = D_r \frac{\partial \phi_r}{\partial n},$$

and on the extrapolated boundary of the reflector,

(3-73) $$\phi_r = 0.$$

Solution of the boundary value problem given by Eqs. (3-69) through (3-73) determines the critical size of the reactor and the distribution of the neutron flux (power) in the critical reactor.

As an example, a spherical reactor with reflector is considered. For such reactor with core radius *R* and reflector thickness *T*, the boundary value problem is as follows,

(3-74) $$\frac{d^2\phi_c}{dr^2}+\frac{2}{r}\frac{d\phi_c}{dr}+B_c^2\phi_c=0,$$

(3-75) $$\frac{d^2\phi_r}{dr^2}+\frac{2}{r}\frac{d\phi_r}{dr}-\kappa_r^2\phi_r=0,$$

(3-76) $$\phi_c(R)=\phi_r(R),$$

(3-77) $$D_c\left.\frac{d\phi_c}{dr}\right|_R=D_r\left.\frac{d\phi_r}{dr}\right|_R,$$

(3-78) $$\phi_r\left(R+\tilde{T}\right)=0.$$

Here,

(3-79) $$B_c^2=\frac{k_\infty-1}{L_c^2},\quad L_c=\sqrt{D_c/\Sigma_{a,c}},$$

(3-80) $$\kappa_r^2=\frac{\Sigma_{a,r}}{D_r}=\frac{1}{L_r^2}.$$

A general solution of Eq. (3-74) is as follows,

$$\phi_c(r)=A_1\frac{\sin B_c r}{r}+A_2\frac{\cos B_c r}{r}.$$

Since the neutron flux is finite at $r=0$, A_2 must be equal to zero, and,

(3-81) $$\phi_c(r)=A\frac{\sin B_c r}{r},$$

where A is an arbitrary constant. A general solution of Eq. (3-75) is obtained as,

(3-82) $$\phi_r(r)=C_1\frac{\sinh \kappa_r r}{r}+C_2\frac{\cosh \kappa_r r}{r}.$$

From the boundary condition given by Eq. (3-78) results,

$$\phi_r\left(R+\tilde{T}\right)=C_1\frac{\sinh\left[\kappa_r\left(R+\tilde{T}\right)\right]}{R+\tilde{T}}+C_2\frac{\cosh\left[\kappa_r\left(R+\tilde{T}\right)\right]}{R+\tilde{T}}=0,$$

(3-83) $$C_2=-C_1\tanh\left[\kappa_r\left(R+\tilde{T}\right)\right]$$

Using Eq. (3-83) in (3-82) yields,

(3-84) $$\phi_r(r)=C\frac{\sinh\left[\kappa_r\left(R+\tilde{T}-r\right)\right]}{r}$$

where C is an arbitrary constant.

Substituting Eq. (3-81) and (3-84) into (3-76) yields,

$$A\frac{\sin B_c R}{R} = C\frac{\sinh\left[\kappa_r\left(R+\tilde{T}-R\right)\right]}{R} \Rightarrow A\sin\left(B_c R\right) = C\sinh\left(\kappa_r \tilde{T}\right) \tag{3-85}$$

Similarly, substituting the equations to the condition given by Eq. (3-77) yields,

$$D_c A\left(B_c R\cos B_c R - \sin B_c R\right) = -D_r C\left(\kappa_r R\cosh\kappa_r \tilde{T} + \sinh\kappa_r \tilde{T}\right) \tag{3-86}$$

Combining Eqs. (3-85) and (3-86) yields,

$$\cot B_c R = \frac{1}{B_c R}\left(1-\frac{D_r}{D_c}\right) - \frac{D_r \kappa_r}{B_c D_c}\coth\kappa_r \tilde{T}\,. \tag{3-87}$$

Having a given thickness of the reflector T and a given material buckling B_m (= B_c), Eq. (3-87) can be solved for the critical radius of the reactor core R. As can be seen, the radius is smaller than the corresponding critical radius of a reactor core without reflector, $R_c = \tilde{R}_c - d = \pi/B_c - d$. The difference,

$$\delta = R_c - R \tag{3-88}$$

is introduced as a measure of the **reflector savings**.

The reflector savings increase with the reflector thickness but it is not larger than L_r. It can be shown that the reflector thickness should be at most equal to 2 till 3 diffusion lengths L_r, since thicker reflectors do not improve the savings significantly.

It should be noted that reflected reactors have more uniform distribution of the neutron flux, and thus the power, which is advantageous from the point of view of heat transfer in the reactor core and the utilization of the nuclear fuel. The reflector savings can be calculated in the same manner for other reactor shapes and the conclusions are identical with those obtained for the spherical reactor.

3.3 Neutron Life Cycle

Not all neutrons produced by fission will cause new fission, since some of them:

1. Will be absorbed by non-fissionable material
2. Will be absorbed parasitically in fissionable material
3. Will leak out of the reactor

For the maintenance of a self-sustaining chain reaction it is enough that – on the average – at least one neutron produced in fission that causes fission of another nucleus.

The condition of a self-sustained chain reaction is conveniently expressed in terms of a multiplication factor. The number of neutrons absorbed or leaking out of the reactor will determine the value of this multiplication factor, and will also determine whether a new generation of neutrons is larger, smaller or the same size as the preceding generation.

Any reactor of a finite size will have neutrons leaking out of it. In general, the larger the reactor the lower the fraction of the neutron leakage. In particular, if the reactor is infinitely large there will be no leakage.

3.3.1 Four-Factor Formula

The measure of the increase or decrease in neutron flux in an infinite reactor is the **infinite multiplication factor**, k_∞. This factor is defined as a ratio of the neutrons produced by fission ion one generation to the number of neutrons lost through absorption in the preceding generation.

$$k_\infty = \frac{Neutron\ \ production\ from\ fission\ in\ one\ generation}{Neutron\ absorption\ in\ the\ preceding\ generation} \tag{3-89}$$

or

$$k_\infty = \frac{Rate\ of\ neutron\ \ production}{Rate\ of\ neutron\ absorption}. \tag{3-90}$$

The condition for criticality, i.e. for a self-sustaining fission chain to be possible, in the infinite system is that the rate of neutron production should be equal to the rate of absorption in the absence of extraneous sources. In other words, requirement for criticality is,

$$k_\infty = 1. \tag{3-91}$$

For some thermal reactors the infinite multiplication factor can be evaluated with a fair degree of accuracy by means of the **four factor formula**.

The basis of this formula is the assumed division of the neutrons into three categories:

1. Fission neutrons with energies in excess of about 1 MeV which can cause fission in uranium-238 as well as in uranium-235

2. Neutrons in the resonance regions which may be captured by uranium-238

3. Thermal neutrons which cause nearly all the fission in uranium-235 and thereby generate fission neutrons

The four factors formula is as follows,

$$k_\infty = \varepsilon \cdot p \cdot f \cdot \eta \tag{3-92}$$

where: ε = *Fast fission factor*

p = *Resonance escape probability*

f = *Thermal utilization factor*

η = *Reproduction factor*

The **fast fission factor** describes the process where fission is caused by fast neutrons. In thermal reactors using slightly enriched or natural uranium fuel, some neutrons, before they have been slowed down appreciably, will cause fission of both uranium-235 and uranium-238 nuclei.

At neutron energies greater than about 1 MeV, most of the fast neutron fissions will be of uranium-238, because of its larger proportions in the fuel. Fast fission results in the net increase in the fast neutron population of the reactor core. The fast neutron population in one generation is thus increased by the fast fission factor**.**

The fast fission factor is defined as the ratio of the net number of fast neutrons produced by all fissions to the number of fast neutrons produced by thermal fissions:

$$\varepsilon = \frac{\textit{Number of fast neutrons produced by all fissions}}{\textit{Number of fast neutrons produced by thermal fissions}} \tag{3-93}$$

In order for a neutron to be absorbed by a fuel nucleus as a fast neutron, it must pass close to a fuel nucleus while it is a fast neutron. The value of ε will be affected by the arrangement and concentration of the fuel and the moderator. It will be essentially equal to one for a homogeneous reactor where the fuel atoms are surrounded by moderator atoms. However, in a heterogeneous reactor all the fuel atoms are packed closely together in elements such as pins, rods or pellets. Thus neutron emitted from a single fission can pass close to another fuel nucleus. Various arrangements in heterogeneous reactor result in $\varepsilon \sim 1.02 \div 1.08$.

After fission neutrons diffuse through the reactor and collide with nuclei of fuel and non-fuel material loosing part of their energy. While neutrons are slowing down there is a chance that some of them will be captured by uranium-238 nuclei. Absorption cross-section of uranium-238 has several resonance peaks for neutron energies between 6 to 200 eV. The peak values can be as high as 10000 barns, whereas below 6 eV the absorption cross-section is as low as 10 barns. The probability that the neutron will not be absorbed by a resonance peak is called the **resonance escape probability**, *p*. the resonance escape probability, p is defined as the ratio of the number of neutrons that reach thermal energies to the number of fast neutrons that start to slow down:

$$p = \frac{\textit{Number of neutrons that reach thermal energy}}{\textit{Number of fast neutrons that start to slow down}}. \tag{3-94}$$

The value of resonance escape probability is determined largely by the fuel-moderator arrangement and the amount of enrichment of uranium-235. In a homogeneous reactor the neutrons slow down in a region close to fuel nuclei and thus the probability of being absorbed by uranium-238 is high. In the heterogeneous reactor neutrons slow down in the moderator where there are no atoms of uranium-238 and the probability of undergoing resonance absorption is low. The value of the resonance escape probability is not significantly affected by pressure or poison concentration. In water

moderated, low uranium-235 enrichment reactors, raising the temperature of the fuel will raise the resonance absorption in uranium-238 due to the **Doppler effect** (i.e. an apparent broadening of normally narrow resonance peaks due to thermal motion of nuclei). The increase in resonance absorption lowers the resonance escape probability. The resonance escape probability can be found from the following formula:

$$p(E) \approx \exp\left[-\frac{N_F \cdot I}{\bar{\xi} \cdot \Sigma_s}\right], \tag{3-95}$$

where $\bar{\xi}$ is the weighted average logarithmic energy decrement for both moderator and absorber, N_F is the number of fuel nuclei per unit volume of the system, I is the **effective resonance integral** and Σ_s is the total macroscopic cross section for scattering in the system.

Experimental measurements of the resonance integral for a system of isolated rods give the following formula:

$$I = a + b\sqrt{\frac{A}{M}}, \tag{3-96}$$

where a and b are constants for a given fuel material (equal to 2.95 and 81.5, respectively, for uranium and 4.45 and 84.5 for uranium dioxide, such that I will be in barns), A is the surface area (in m^2) and M is the mass (in kg) of a fuel rod:

$$I_U = 2.95 + 81.5\sqrt{\frac{A}{M}}\ [b]; \quad I_{UO_2} = 4.45 + 84.5\sqrt{\frac{A}{M}}\ [b] \tag{3-97}$$

The integral I depends on temperature as follows,

$$I(T) = I(300\ K)\left[1 + \beta\left(\sqrt{T} - \sqrt{300}\right)\right] \tag{3-98}$$

Here I(300 K) is the value of the integral at T = 300 K and β is a constant which depends on the nature of the fuel and the radius of fuel rods in heterogeneous systems. For UO_2 and typical fuel rods used in LWRs $\beta = 6\text{x}10^{-3}$.

Since neutrons absorbed by resonance capture in uranium-238 are lost and unable to take part in sustaining the fission chain, most thermal reactors are design to maximize the resonance escape probability as far as possible. In a homogeneous mixture of natural uranium fuel and carbon graphite moderator the highest value of k_∞ is 0.855 – hence a fission chain can not possibly be sustained. Heterogeneous arrangement of the same materials can lead to k_∞ as high as 1.08 due to the increase in the resonance escape probability.

Once thermalized, the neutrons continue to diffuse throughout the reactor and are subject to absorption by other materials in the reactor as well as the fuel. The **thermal utilization factor** f is defined as the ratio of the number of thermal neutrons absorbed in the fuel to the number of thermal neutrons absorbed in all reactor material.

$$f = \frac{\textit{Number of thermal neutrons absorbed in the fuel}}{\textit{Number of thermal neutrons absorbed in all reactor materials}}. \tag{3-99}$$

The thermal utilization factor can be expressed as follows:

$$f = \frac{\Sigma_{a,F} \cdot \phi_F \cdot V_F}{\Sigma_{a,F} \cdot \phi_F \cdot V_F + \Sigma_{a,M} \cdot \phi_M \cdot V_M + \Sigma_{a,C} \cdot \phi_C \cdot V_C + \Sigma_{a,P} \cdot \phi_P \cdot V_P}, \tag{3-100}$$

where subscripts *F*, *M, P* and *C* refer to uranium, moderator, poison and construction material (clad, spacers, etc), respectively. In a heterogeneous reactor the flux will be different in the fuel region than in the moderator region due to the high absorption rate by the fuel. In the homogenous reactor the neutron flux seen by the fuel, moderator, poisons and the construction material will be the same and the equation for f can be rewritten as,

$$f = \frac{\Sigma_{a,F}}{\Sigma_{a,F} + \Sigma_{a,M} + \Sigma_{a,P} + \Sigma_{a,C}}. \tag{3-101}$$

The coefficient f will not in general depend on the temperature. However, in heterogeneous water moderated reactors the moderator (water) expands with temperature and number of moderator atoms will decrease – and that results in increase of thermal utilization. Because of this effect the temperature coefficient for the thermal utilization factor is positive.

Most of the neutrons absorbed in the fuel cause fission, but some do not. The **reproduction factor** is defined as the ratio of the fast neutrons produced by thermal fission to the number of thermal neutrons absorbed in the fuel.

$$\eta = \frac{\textit{Number of fast neutrons produced by thermal fission}}{\textit{Number of thermal neutrons absorbed in the fuel}}. \tag{3-102}$$

The reproduction factor can also be stated as a ratio of rates as shown below. The rate of production of fast neutrons by thermal fission is equal to fission reaction rate ($\Sigma_{f,F} \cdot \phi_F$) *times* the average number of neutrons produced per fission (ν). The rate of absorption is $\Sigma_{a,F} \cdot \phi_F$ and thus the reproduction factor becomes,

$$\eta = \frac{\Sigma_{f,F} \cdot \phi_F \cdot \nu}{\Sigma_{a,F} \cdot \phi_F} = \nu \frac{\Sigma_{f,F}}{\Sigma_{a,F}}. \tag{3-103}$$

When fuel contains several fissionable materials and other materials, it is necessary to account for each material, e.g.

$$\eta = \frac{\sum_i \left(\nu_i \Sigma_{f,i}\right)}{\sum_j \left(\Sigma_{a,j}\right)}, \tag{3-104}$$

where the numerator is the sum of the $\nu\Sigma_f$ terms for all the fissile nuclides and the denominator is the total absorption cross section for all the species present in the fuel.

3.3.2 Six-Factor Formula

The infinite multiplication factor can fully represent only a reactor that is infinitely large. To completely describe the neutron life cycle in a real, finite reactor, it is necessary to account for neutrons that leak out. The multiplication factor that takes leakage into account is the **effective multiplication factor** k_{eff}. This coefficient is defined as follows,

$$k_{eff} = \frac{Rate\ of\ neutron\ \ production}{Rate\ of\ neutron\ absorption + rate\ of\ leakage}. \tag{3-105}$$

For critical reactor the neutron population is neither increasing nor decreasing and $k_{eff} = 1$. If the neutron production is grater than the absorption and leakage, the reactor is called supercritical; $k_{eff} > 1$. If the neutron production is less than the absorption and leakage, the reactor is called subcritical; $k_{eff} < 1$. The effective and the infinite multiplication factors are related to each other as follows,

$$k_{eff} = k_\infty P_{FNL} P_{TNL}, \tag{3-106}$$

where P_{FNL} is the **fast non-leakage probability** and P_{TNL} is the **thermal non-leakage probability**. Equation (3-106) represents the so-called **six-factor formula**.

Comparing Eq. (3-47) with (3-106) and noting that $k = k_{eff}$, one can conclude that in one-group treatment, the non-leakage probability of neutrons of a specific energy from a critical system can be calculated as,

$$P_{NL} = P_{FNL} P_{TNL} = \frac{1}{1 + L^2 B^2}. \tag{3-107}$$

FIGURE 3-4 illustrates the six-factor formula on a generation of 1000 neutrons. Due to fast fission, the number of neutrons is increased to 1040 (since the fast fission factor is assumed to be 1.04). Assuming next that the probability of fast non-leakage is equal to 0.865, the remaining number of fast neutrons is 900. That corresponds to the loss of 140 fast neutrons from the system. In addition, 180 neutrons is absorbed during moderation (resonance absorption), 100 neutrons escape after moderation (leakage of thermal neutrons) and 125 thermal neutrons are absorbed in non-fuel material. Finally the remaining 495 thermal neutrons are participating in fissions, which bring about 1000 fast neutrons of new generation. In that way the chain reaction is sustained at a constant level of neutrons from generation to generation.

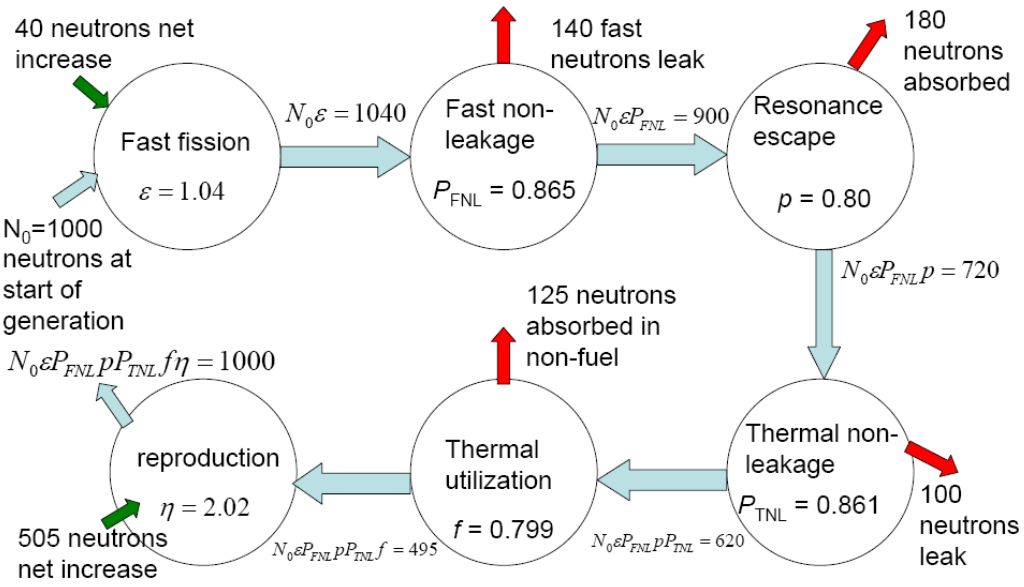

FIGURE 3-4: Illustration of six-factor formula.

3.4 Nuclear Reactor Transients

A nuclear reactor is a time dependent system, even if it operates at apparently steady conditions. This is due to persistent changes in fuel composition resulting from the fuel burn-up. The time changes of reactor properties due to fuel depletion are very slow ones and are typically investigated at time scales comparable to the length of the fuel cycle. This type of behavior is typically treated as a sequence of steady-state conditions. There are, however, reactor transient occurrences in which the core properties significantly change over time periods which are much shorter; with order of magnitude of hours, minutes or even seconds. Depending of the length of the characteristic time scale, the nuclear reactor transients can be roughly divided into three basic groups:

- Slow transients, in which the characteristic time scale is of order of weeks or months (for example fuel depletion)
- Moderate transients, in which the characteristic time scale is of order of hours (for example fuel poisoning with xenon-135 and samarium-149)
- Fast transients, in which the characteristic time scale is of order of seconds (for example control rod insertion)

The three types of transients are discussed below in more detail.

3.4.1 Nuclear Fuel Depletion

Analysis of nuclear fuel depletion is concerned with an analysis of the neutron flux variation over a long time period, comparable to the length of the fuel cycle. Since the transient is very slow, it is typically analyzed as a sequence of stationary states. Thus, for each such state, the neutron flux distribution is obtained from a pertinent set of steady-state equations. If the diffusion approximation is employed, the following equation is solved,

(3-108) $D_n \nabla^2 \phi_n - \Sigma_{a,n} \phi_n = \lambda_n \nu \Sigma_{f,n} \phi_n$, $n = 1, 2, \ldots$ (state index),

where λ_n is an eigenvalue of the problem at state *n*, which for a steady-state solution should be equal to 1. Thus, one of the design problems over a fuel cycle is to obtain the eigenvalues equal to unity.

Burnup calculations constitute other essential parts of the analysis of changing reactor properties over a fuel cycle. Typically the calculations take into account the following property changes (assuming enriched uranium as the fuel),

- consumption of the fissile material, uranium-235
- transmutation of uranium-238 into plutonium
- buildup of the fission products that have a significant cross-section for absorption (poisons)

The above-mentioned analysis open paths to optimization of the in-core fuel design, with the over-all goal to maximize the fuel burnup (or the efficiency of the fuel utilization).

3.4.2 Fuel Poisoning

During operation of a reactor the amount of fuel contained in the core constantly decreases. If the reactor is to operate during long periods, fuel in excess of that needed for exact criticality must be added. The positive reactivity due to the excess fuel must be balanced with negative reactivity from neutron-absorbing material.

Moveable control rods containing neutron-absorbing materials are one method used to offset the excess fuel. However, using control rods alone may be impractical, e.g. there is physically insufficient room for the control rods and their large mechanisms. To control large amounts of excess fuel **burnable poisons** are used. Burnable poisons are materials that have a high neutron absorption cross section that are converted into materials of relatively low absorption cross section as a result of neutron absorption.

Due to the burnup of the poison material, the negative reactivity of the poison decreases over core life. Ideally, these poisons should decrease their negative reactivity at the same rate the fuel's excess positive reactivity is depleted. Fixed burnable poisons are usually used in the form of compounds of boron or gadolinium that are shaped into separate lattice pins or plates, or introduced as additives to the fuel.

Soluble poisons, also called **chemical shim**, produce spatially uniform neutron absorption when dissolved in the water coolant. The most common soluble poison in PWRs is boric acid (**soluble boron** or **solbor**). The boric acid in the coolant decreases the thermal utilization factor, causing the decrease in reactivity.

By varying the concentration of boric acid in the coolant (a process referred to as **boration** and **dilution**) the reactivity of the core can be easily varied. If the boron concentration is increased (boration), the coolant/ moderator absorbs more neutrons, adding negative reactivity. If the boron concentration is reduced (dilution), positive reactivity is added.

Non-burnable poison is one that maintains a constant negative reactivity worth over the life of the core. While no neutron poison is strictly non-burnable, certain materials

can be treated as non-burnable poisons under certain conditions – for example hafnium. The removal – by absorption of neutrons – of one isotope of hafnium leads to the production of another neutron absorber, and continues through a chain of 5 absorbers – resulting in a long-lived burnable poison.

It is possible to make the reactivity of a poison material that is usually a burnable poison more uniform over core life through the use of self-shielding. In self-shielding the poison material is thick enough that only the outer layer of the poison is exposed to the neutron flux. The absorptions that take place in the outer layers reduce the number of neutrons that penetrate to the inner material. As the outer layers of poison absorb neutrons and are converted to non-poison materials, the inner layers begin absorbing more neutrons, and the negative reactivity of the poison is fairly uniform

Fission fragments generated at the time of fission decay to produce a variety of fission products. Fission products are of concern because:

- they become parasitic absorbers of neutrons
- Result in long term source of heat

Xenon-135 and samarium-149 have the most substantial impact on reactor design and operation. Both these poisons have impact on the thermal utilization factor and thus k_{eff} and reactivity.

The neutron absorption cross section of xenon-135 is equal to 2.6 x 10^6 barns. It is produced directly by some fissions, but it is more commonly a product of the tellurium-135 decay chain:

$$\begin{array}{l} \overset{\beta^-}{\underset{19\ s}{\rightarrow}}\ {}^{135}_{52}\mathrm{Te}\ \overset{\beta^-}{\underset{6.57\ hr}{\rightarrow}}\ {}^{135}_{53}\mathrm{I}\ \overset{\beta^-}{\underset{9.10\ hr}{\rightarrow}}\ {}^{135}_{54}\mathrm{Xe} \\ \rightarrow {}^{135}_{55}\mathrm{Cs}\ \overset{\beta^-}{\underset{2.3\cdot 10^6\ yr}{\rightarrow}}\ {}^{135}_{56}\mathrm{Ba}\quad \text{(stable)} \end{array} \tag{3-109}$$

The half-life of Te-135 is so short that it can be assumed that iodine-135 is produced directly from fission. Iodine-135 is not a strong neutron absorber, but decays to form the neutron poison xenon-135. 95% of all the xenon-135 comes from the decay of iodine-135. Therefore, the half-life of iodine-135 plays an important role in the amount of xenon-135 present.

The rate of change of iodine (dI/dt; I is the concentration of iodine-135) is equal to the rate of production minus the rate of removal. The rate of production is just equal to yield from fission = $\gamma_I \Sigma_f \varphi$, here $\gamma_I = 0.061$ is the fission yield. The rate of removal is equal to the decay rate ($\lambda_I I$; λ_I is the decay constant) plus the burnup rate ($\sigma_{a,I} I \varphi$),

$$\frac{dI}{dt} = \gamma_I \Sigma_f \phi - \lambda_I I - \sigma_{a,I} I \phi \tag{3-110}$$

Since the microscopic absorption cross section σ_I is quite small, the equation for the iodine-135 concentration can be written as follows,

(3-111) $$\frac{dI}{dt} = \gamma_I \Sigma_f \phi - \lambda_I I$$

When the rate of production of iodine equals the rate of removal, equilibrium exists – the iodine concentration remains then constant and equal to I_0,

(3-112) $$0 = \gamma_I \Sigma_f \phi - \lambda_I I_0 \Rightarrow I_0 = \frac{\gamma_I \Sigma_f \phi}{\lambda_I}.$$

Since the equilibrium iodine concentration is proportional to the neutron flux, ϕ, it is also proportional to reactor power level.

The rate of change of the xenon-135 concentration (dX/dt) is equal to:

- (+) Xenon-135 production from fission
- (+) iodine-135 decay
- (-) xenon-135 decay
- (-) xenon-135 burnup

(3-113) $$\frac{dX}{dt} = \gamma_X \Sigma_f \phi + \lambda_I I - \lambda_X X - \sigma_{a,X} \phi X .$$

The xenon burnup term $\sigma_{a,X} \phi X$ refers to neutron absorption by xenon-135 by the following reaction,

(3-114) $$^{135}_{54}Xe + ^{1}_{0}n \rightarrow ^{136}_{54}Xe + \gamma .$$

Xenon-136 is not a significant neutron absorber – therefore neutron absorption by xenon-135 constitutes removal of poison from the reactor. At equilibrium,

(3-115) $$0 = \gamma_X \Sigma_f \phi + \lambda_I I_0 - \lambda_X X_0 - \sigma_{a,X} \phi X_0 \Rightarrow X_0 = \frac{\gamma_X \Sigma_f \phi + \lambda_I I_0}{\lambda_X + \sigma_{a,X} \phi}.$$

Since,

(3-116) $$I_0 = \frac{\gamma_I \Sigma_f \phi}{\lambda_I},$$

the equilibrium concentration of xenon-135 is,

(3-117) $$X_0 = \frac{(\gamma_I + \gamma_X) \Sigma_f \phi}{\lambda_X + \sigma_{a,X} \phi}.$$

Comparing the equilibrium concentrations of iodine-135 and xenon-135 reveals that iodine concentration at equilibrium is linearly proportional to the neutron flux, and thus to the reactor power. Xenon-135 concentration increases with a lower rate than linear when reactor power increases.

When a reactor is shutdown, the neutron flux is reduced essentially to zero. Therefore, after shutdown, xenon-135 is no longer produced by fission and is no longer removed by burnup. The only remaining production mechanism is the decay of the iodine-135 which was in the core at the time of shutdown, and the only removal mechanism for xenon-135 is decay. Because the decay rate of iodine-135 is faster than the decay rate of xenon-135, the xenon concentration builds to a peak. Subsequently, the production from iodine decay is less than the removal of xenon by decay, and the concentration of xenon-135 decreases. The greater the flux level prior to shutdown, the greater the concentration of iodine-135 at shutdown; therefore, the greater the peak in xenon-135 concentration after shutdown.

During periods of steady state operation at a constant neutron flux level, the xenon-135 concentration builds up to its equilibrium value for that reactor power in about 40 to 50 hours.

After reactor shutdown, the differential equations for the concentration of iodine-135 and xenon-135 are as follows,

$$\frac{dI}{dt} = -\lambda_I I \,, \tag{3-118}$$

$$\frac{dX}{dt} = \lambda_I I - \lambda_X X \,. \tag{3-119}$$

The solution of Eq. (3-118) can be readily obtained as,

$$I = I_0 e^{-\lambda_I t} \,. \tag{3-120}$$

To solve Eq. (3-119), the iodine concentration given by Eq. (3-120) is used in Eq. (3-119) as follows,

$$\frac{dX}{dt} = \lambda_I I_0 e^{-\lambda_I t} - \lambda_X X \,, \tag{3-121}$$

and, after integration, the xenon-135 concentration is found as,

$$X(t) = \frac{\lambda_I}{\lambda_I - \lambda_X} I_0 \left(e^{-\lambda_X t} - e^{-\lambda_I t} \right) + X_0 e^{-\lambda_X t} \,. \tag{3-122}$$

One can calculate a dimensionless relative change of the xenon-125 concentration as follows,

$$\xi(t) = \frac{X(t)}{X_0} = \frac{\gamma_I}{\gamma_I + \gamma_X} \frac{\lambda_X + \sigma_{a,I}\phi_0}{\lambda_I - \lambda_X} \left(e^{-\lambda_X t} - e^{-\lambda_I t} \right) + e^{-\lambda_X t} \,. \tag{3-123}$$

Here ϕ_0 is the neutron flux in the reactor just before shutdown. The function expressed by Eq. (3-124) is plotted in FIGURE 3-5 for various values of the neutron flux just before the shutdown. As can be seen, the concentration increases when the shutdown neutron flux is high enough, and gets a maximum value after approximately 10 hours after the shutdown.

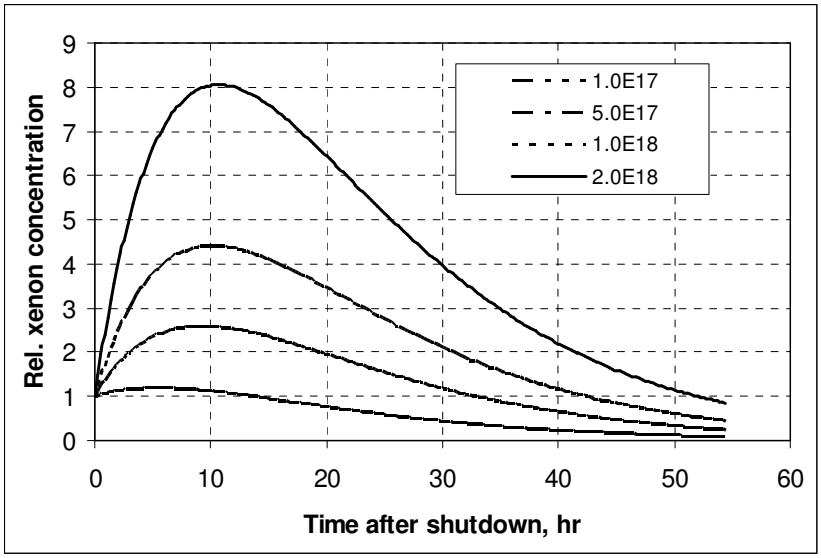

FIGURE 3-5: Relative xenon-135 concentration after shutdown of a reactor for neutron flux in range from 10^{17} to $2x10^{18}$ neutrons m^{-2} s^{-1}.

Assuming equilibrium concentrations of iodine and xenon before the reactor shutdown given by Eqs. (3-116) and (3-117), the xenon-135 concentration after the reactor shutdown is given by the following expression,

$$X(t) = \frac{\gamma_I \Sigma_f \phi_0}{\lambda_X - \lambda_I}\left(e^{-\lambda_I t} - e^{-\lambda_X t}\right) + \frac{(\gamma_I + \gamma_X)\Sigma_f \phi_0}{\lambda_X + \sigma_{a,X}\phi_0} e^{-\lambda_X t}. \tag{3-125}$$

Large thermal reactors with little flux coupling between regions may experience spatial power oscillations because of the non-uniform presence of xenon-135. The mechanism of **xenon oscillations** is described in the following four steps:

1. An initial lack of symmetry in the core power distribution (for example, individual control rod movement or misalignment) causes an imbalance in fission rates within the reactor core, and therefore, in the iodine-135 buildup and the xenon-135 absorption

2. In the high-flux region, xenon-135 burnout allows the flux to increase further, while in the low-flux region, the increase in xenon-135 causes a further reduction in flux. The iodine concentration increases where the flux is high and decreases where the flux is low

3. As soon as the iodine-135 levels build up sufficiently, decay to xenon reverses the initial situation. Flux decreases in this area, and the former low-flux region increases in power

4. Repetition of these patterns can lead to xenon oscillations moving about the core with periods on the order of about 15 hours

With little change in overall power level, these oscillations can change the local power levels by a factor of three or more. In a reactor system with strongly negative temperature coefficients, the xenon-135 oscillations are damped quite readily. This is one reason for designing reactors to have negative moderator-temperature coefficients.

Samarium-149 is the second most important fission-product poison because of its high thermal neutron absorption cross section of 4.1 x 10^4 barns. Samarium-149 is produced from the decay of the neodymium-149 fission fragment as shown in the decay chain below,

$$(3\text{-}126)\quad {}^{149}_{60}\mathrm{Nd} \xrightarrow[1.72\ hr]{\beta^-} {}^{149}_{61}\mathrm{Pm} \xrightarrow[53.1\ hr]{\beta^-} {}^{149}_{62}\mathrm{Sm\ (stable)}$$

For the purpose of examining the behavior of samarium-149, the 1.73 hour half-life of neodymium-149 is sufficiently shorter than the 53.1 hour value for promethium-149 that the promethium-149 may be considered as if it were formed directly from fission. This assumption, and neglecting the small amount of promethium burnup, allows the situation to be described as follows:

Rate of change of ^{149}Pm = yield from fission – decay of ^{149}Pm. Therefore:

$$(3\text{-}127)\quad \frac{dP}{dt} = \gamma_P \Sigma_f \phi - \lambda_P P$$

At equilibrium,

$$(3\text{-}128)\quad 0 = \gamma_P \Sigma_f \phi - \lambda_P P_0 \Rightarrow P_0 = \frac{\gamma_P \Sigma_f \phi}{\lambda_P}.$$

As can be seen, the equilibrium concentration of promethium-149 is linearly increasing with the neutron flux and thus with the reactor power.

The rate of samarium-149 formation is described as follows:

$$(3\text{-}129)\quad \frac{dS}{dt} = \gamma_S \Sigma_f \phi + \lambda_P P - \sigma_{a,S} \phi S\,.$$

Since the fission yield of samarium-149 is nearly zero, therefore the equation becomes:

$$(3\text{-}130)\quad \frac{dS}{dt} = \lambda_P P - \sigma_{a,S} \phi S\,,$$

and at equilibrium,

(3-131) $$0 = \lambda_P P_0 - \sigma_{a,S}\phi S_0 \Rightarrow S_0 = \frac{\lambda_P P_0}{\sigma_{a,S}\phi} = \frac{\gamma_P \Sigma_f}{\sigma_{a,S}}.$$

After reactor shut-down, the neutron flux drops to essentially zero, and the rate of samarium-149 production becomes as follows,

(3-132) $$\frac{dS}{dt} = \lambda_P P .$$

Because samarium-149 is not radioactive and is not removed by decay, it presents problems somewhat different from those encountered with xenon-135. The equilibrium concentration and the poisoning effect build to an equilibrium value during reactor operation. This equilibrium is reached in approximately 20 days (500 hours), and since samarium-149 is stable, the concentration remains essentially constant during reactor operation. When the reactor is shutdown, the samarium-149 concentration builds up as a result of the decay of the accumulated promethium-149.

The buildup of samarium-149 after shutdown depends upon the power level before shutdown. Samarium-149 does not peak as xenon-135 does, but increases slowly to a maximum value. After shutdown, if the reactor is then operated at power, samarium-149 is burned up and its concentration returns to the equilibrium value. Samarium poisoning is minor when compared to xenon poisoning. Although samarium-149 has a constant poisoning effect during long-term sustained operation, its behavior during initial startup and during post-shutdown and restart periods requires special considerations in reactor design.

There are numerous other fission products that, as a result of their concentration and thermal neutron absorption cross section, have a poisoning effect on reactor operation. Individually, they are of little consequence, but lumped together they have a significant impact. These are often characterized as **lumped fission product poisons** and accumulate at an average rate of 50 barns per fission event in the reactor.

In addition to fission product poisons, other materials in the reactor decay to materials that act as neutron poisons. An example of this is the decay of tritium to helium-3. Since tritium has a half-life of 12.3 years, normally this decay does not significantly affect reactor operations because the rate of decay of tritium is so slow. However, if tritium is produced in a reactor and then allowed to remain in the reactor during a prolonged shutdown of several months, a sufficient amount of tritium may decay to helium-3 to add a significant amount of negative reactivity. Any helium-3 produced in the reactor during a shutdown period will be removed during subsequent operation by a neutron-proton reaction.

3.4.3 Nuclear Reactor Kinetics

The objective of reactor kinetics is to investigate the fast transient behavior of a reactor subject to external perturbations. A point-kinetics model is obtained when the spatial distribution of the neutron flux is neglected and only the time behavior of the amplitude is concerned. The point-kinetics model can be derived for any number of delayed neutrons. Typically the models with one and six groups of delayed neutrons are considered. The six-group point kinetics model is summarized in TABLE 3.2.

TABLE 3.2. Point reactor kinetics model.

Neutron flux equation	$\frac{dn}{dt} = \frac{\rho - \beta}{\Lambda} n + \sum_{i=1}^{6} \lambda_i C_i + S$
Equations for concentration of precursors of delayed neutron: i = 1,…,6	$\frac{dC_i}{dt} = \frac{\beta_i}{\Lambda} n - \lambda_i C_i, \quad i = 1, \ldots, 6$

The values of decay constants and yields of delayed-neutron precursors are given in TABLE 3.3.

TABLE 3.3. Decay constants and yields of delayed-neutron precursors in thermal fission of uranium-235.

Decay constants and yields of delayed-neutron precursors in thermal fission of uranium-235			
$t_{1/2}$, [s]	λ_i, [s^{-1}]	β_i	β_i / λ_i
55.7	0.0124	0.000215	0.0173
22.7	0.0305	0.00142	0.0466
6.22	0.111	0.00127	0.0114
2.30	0.301	0.00257	0.0085
0.61	1.1	0.00075	0.0007
0.23	3.0	0.00027	0.0001
Total		**0.0065**	**0.084**

Some properties of the point kinetics model can be investigated using a one-group approximation. The total yield of the one group of delayed neutrons is obtained as a sum of yields in all groups. For uranium-235 this value is shown in TABLE 3.3 and is equal to $\beta = 0.0065$. The decay constant can be obtained from a proper averaging, e.g.,

$$\frac{\beta}{\lambda} = \sum_{i=1}^{6} \frac{\beta_i}{\lambda_i} \Rightarrow \lambda = \frac{\beta}{\sum_{i=1}^{6} \frac{\beta_i}{\lambda_i}}. \tag{3-133}$$

Using data from TABLE 3.3, the equivalent decay constant for one-group assumption for uranium-235 is obtained as $\lambda = 0.0065/0.084 \cong 0.08$ s^{-1}.

The equations in one group approximation of point kinetic equations are as follows,

$$\frac{dn}{dt} = \left(\frac{\rho - \beta}{\Lambda} \right) n + \lambda C + S, \tag{3-134}$$

$$\frac{dC}{dt} = \frac{\beta}{\Lambda} n - \lambda C. \tag{3-135}$$

Here C represents the concentration of precursors of all groups of delayed neutrons.

In the next section special cases of the point kinetic model will be considered and their solutions will be found.

The average **neutron generation time** Λ can be written in various forms as follows,

$$\Lambda = \frac{1}{\mathrm{v}\nu\Sigma_f} = \frac{l}{k} = \frac{l_\infty}{k_\infty} = \frac{1}{k_\infty \mathrm{v}\Sigma_a}. \tag{3-136}$$

Here l is the average neutron lifetime and k is the effective multiplication factor. The name "generation time" has been chosen since Λ represents the average time between two birth events in successive neutron generations. Firstly, $1/\Sigma_f$ is the mean free path for fission, that is, it is the average distance a neutron travels from its birth to a fission event. Then, $\left(1/\Sigma_f\right)/\mathrm{v} = \Delta t_f$ is the average time between the birth of a neutron and a fission event it may cause. Since ν-neutrons is released per fission, the averaged time between the birth of a neutron and the birth of new generation is as follows,

$$\frac{\Delta t_f}{\nu} = \frac{1}{\mathrm{v}\nu\Sigma_f} = \Lambda. \tag{3-137}$$

In a similar manner, the average traveling distance of a neutron between the birth and the death (absorption or leakage) is $1/\left(\Sigma_a + DB_g^2\right)$ and the average **neutron lifetime** can be obtained as,

$$l = \frac{1}{\mathrm{v}}\frac{1}{\Sigma_a + DB_g^2} = \frac{1}{\mathrm{v}\Sigma_a}\frac{1}{1+L^2B_g^2}, \tag{3-138}$$

since the one-group diffusion length is given as $L = \sqrt{D/\Sigma_a}$.

Eq. (3-138) yields,

$$l = \frac{1}{\mathrm{v}\Sigma_a k_\infty}\frac{k_\infty}{1+L^2B_g^2} = \frac{k}{\mathrm{v}\Sigma_a k_\infty} = k\cdot\Lambda. \tag{3-139}$$

Equation (3-139) indicates that the lifetime and the generation time are equal for a critical reactor. For subcritical reactor ($k < 1$) the neutron lifetime is shorter than the generation time and as a consequence, the neutron population will decrease. For supercritical reactor the lifetime will be longer and the neutron population will increase, whereas for a critical reactor the population remains constant.

3.4.4 Nuclear Reactor Dynamics

When power changes in a nuclear reactor are large enough to influence the value of the reactivity, the transient behavior of the reactor is termed as the nuclear reactor dynamics. As can be expected, the influence of power on the reactivity has to be quantified in order to properly describe the dynamic behaviour of the nuclear reactor.

During operation of a nuclear reactor the energy released due to nuclear fission is deposited to the coolant. The resulting temperature distribution in the fuel and coolant (in BWRs even the void fraction distribution) is a subject of the thermal-hydraulic analysis of the nuclear reactor. The temperature distribution, which in a general case is a function of both the time and the location, is influencing the values of microscopic cross-sections for various nuclear reactions caused by neutrons. As a result the reactivity will depend on the temperature changes.

From a practical point of view it is important to know what the influence of temperature on reactivity is and how it will influence the operation of the nuclear reactor. In general the following two cases can be considered:

- Reactivity increases with the temperature: in this case the increasing reactivity will cause the increase of the reactor power, which, in turn, will cause the increase of temperature, etc. That means in this case the reactor will be inherently unstable.

- Reactivity decreases with temperature: in this case the decreasing reactivity will cause the decrease of the reactor power which will be followed by the decrease of the temperature, and so on. Clearly the reactor will be inherently stable in such a case.

The conclusion is that reactors should be constructed in such a way which assures the decreasing reactivity in function of temperature. This can be achieved by using proper materials and a proper nuclear reactor configuration.

The reactivity changes with temperature because the reactivity depends on macroscopic cross sections, which themselves involve the atomic number densities of materials in the core,

(3-140) $$\Sigma(\mathbf{r},t) = N(\mathbf{r},t)\sigma(\mathbf{r},t)\,.$$

The atomic density $N(\mathbf{r},t)$ depends on the reactor power level because:

a) material densities depend on temperature T,

b) the concentration of certain nuclei is constantly changing due to neutron interactions (poisons and fuel burnup).

The microscopic cross section is written in Eq. (3-140) as an explicit function of the spatial location $\mathbf{r}$ and the time t. This must be done since the cross sections that appear in one-speed diffusion model are actually averaged over energy spectrum of neutrons that appear in the reactor core. Since this spectrum is itself dependent on the temperature distribution in the core and hence the reactor power level, this dependence must be taken into account in Eq. (3-140).

Such reactivity variation with the temperature is the principal feedback mechanisms determining the inherent stability of a nuclear reactor with respect to short-term fluctuations in power level. In principle, the reactivity feedback could be evaluated by solving heat transfer equations, both in fuel and coolant regions and predicting the temperature distribution in the reactor core for a given reactor power. However, such approach would end up with a very complex system of partial nonlinear differential equations. Typical simplification is based on the so-called "lumped-parameter" model in which the major parts of the reactor core are represented by a single averaged value of temperature, such as an average fuel temperature, moderator temperature and coolant temperature.

The subject of reactor dynamics analysis is to accommodate the core average temperatures such as T_F (fuel) and T_M (moderator) in suitable models of reactivity

feedback. To this end one can write the reactivity change as a sum of two contributions,

(3-141) $$\rho(t) = \delta\rho_{ext}(t) + \delta\rho_f(P).$$

The reactivity in Eq. (3-141) is measured with respect to the equilibrium power level P_0 (for which the reactivity is just equal to zero) and is a superposition of the "externally" controlled reactivity insertion (such as by the control rod movement) and "internal" reactivity change due to inherent feedback mechanisms, indicated here as a function of the power level.

For steady-state power level P_0, Eq. (3-141) becomes,

(3-142) $$0 = \rho_0 + \rho_f(P_0),$$

which merely states that to sustain the criticality of the system one has to supply external reactivity ρ_0 to counteract the negative feedback reactivity $\rho_f(P_0)$. The incremental reactivities appearing in Eq. (3-141) are then defined as,

(3-143) $$\delta\rho_{ext}(t) = \rho_{ext}(t) - \rho_0,$$

(3-144) $$\delta\rho_f(P) = \rho_f(P) - \rho_f(P_0).$$

The feedback mechanism in reactivity is schematically shown in FIGURE 3-6.

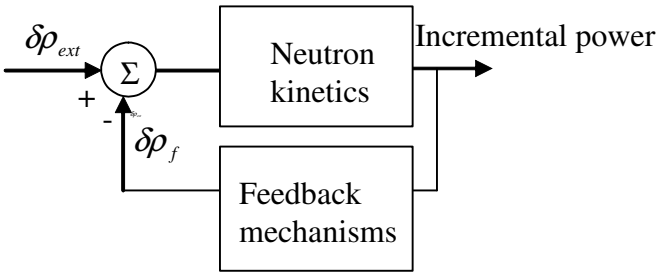

FIGURE 3-6: Reactivity feedback mechanisms.

With increasing material temperature, the nuclei will move with increasing speed. Since the nuclei move in a chaotic manner, their relative velocity against a monoenergetic neutron flux will no longer be constant and will have some distribution. This is equivalent to a situation in which neutrons would have a certain energy distribution when approaching stationary nuclei. This is the so-called **Doppler effect**, in analogy to a similar phenomenon known in acoustics and optics.

Due to the Doppler effect, the number of nuclear reactions caused by monoenergetic neutrons will depend on the temperature of the material. Without going into details it can be mentioned that with the increasing material temperature the microscopic absorption cross section will increase (e.g. of U-238) resulting in decreasing reactivity. Also the microscopic fission cross-section will decrease with the temperature leading to additional reduction of the reactivity.

One can estimate the Doppler effect on reactivity using the expression for the resonance escape probability as,

$$p = \exp\left[-\frac{N_F \cdot I}{\bar{\xi} \cdot \Sigma_s}\right], \tag{3-145}$$

where for metallic uranium and uranium dioxide fuel at 300K temperature, the effective resonance integral I is given as,

$$I_{uranium} = 2.95 + 81.5\sqrt{\frac{A}{M}}\ [b]; \quad I_{UO_2} = 4.45 + 84.5\sqrt{\frac{A}{M}}\ [b]. \tag{3-146}$$

The temperature dependence of the integral I is described by the following correlation obtained from experimental data,

$$I(T) = I(300\ K)\left[1 + \beta\left(\sqrt{T} - \sqrt{300}\right)\right], \tag{3-147}$$

where, for $^{238}UO_2$:

$$\beta = 6.1\times10^{-3} + 4.7\times10^{-3}\left(\frac{A}{M}\right). \tag{3-148}$$

A and M in Eqs. (3-146) and (3-148) are area (in m^2) and mass (in kg), respectively, of a fuel rod.

When k_{eff} remains constant from one generation of neutrons to another, it is possible to determine the number of neutrons at any particular generation by knowing the number of neutrons at "zero" generation, N_0, and the value of k_{eff}. Thus, after n generations the number of neutrons is equal to $N = N_0\left(k_{eff}\right)^n$.

In particular, if in the preceding generation there are N_0 neutrons, then there are $N_0 k_{eff}$ neutrons in the present generation. The change of the number of neutrons expressed as a fraction of the present number of neutrons is referred to as reactivity and is expressed as,

$$\rho = \frac{N_0 k_{eff} - N_0}{N_0 k_{eff}} = \frac{k_{eff} - 1}{k_{eff}}. \tag{3-149}$$

As can be seen, reactivity is a dimensionless number; however, since its value is often rather small, artificial units are defined. From the definition given by Eq. (3-149), the value of reactivity is in units of $\Delta k/k$. Alternative units are % $\Delta k/k$ and **pcm** (percent milli-rho). The conversions between these units are as follows,

$$1\,\Delta k/k = 100\%\,\Delta k/k = 10^5\,\text{pcm}, \tag{3-150}$$

$$1\%\,\Delta k/k = 0.01\,\Delta k/k = 10^3\,\text{pcm}, \tag{3-151}$$

(3-152) $1\text{pcm} = 10^{-5}\,\Delta k/k = 10^{-3}\%\,\Delta k/k$.

EXAMPLE 3-1. Calculate the reactivity in a reactor core when k_{eff} is equal to 1.002 and 0.998. SOLUTION: The reactivity is as follows: for k_{eff} = 1.002, ϱ = (1.002-1/1.002 = 0.001996 $\Delta k/k$ = 0.1996 % $\Delta k/k$ = 199.6 pcm. For k_{eff} = 0.998: ρ = (0.998-1/0.998 = 0.002 $\Delta k/k$ = 0.2 % $\Delta k/k$ = 200 pcm.

Other units often used in reactor analysis are dollars (\$) and cents. By definition, 1\$ is reactivity which is equivalent to the effective delayed neutron fraction, β, and, as can be expected, one cent (1c) reactivity is equal to one-hundreth of a dollar.

As already mentioned, the dependence of the reactivity on temperature has an important influence on the reactor dynamics and stability. In particular, a reactor will be stable when the reactivity is a decreasing function of temperature. Needless to say that the dependence of the reactivity on various parameters should be known. However, it is not possible (and not necessary for most practical purposes) to estimate such functions with all details. Instead a linearized form of the function is applied to evaluate the reactivity change due to various parameter changes, that is,

$$\begin{aligned}(3\text{-}153)\qquad \delta\rho(T_C, T_F, T_M, \ldots) &\cong \frac{\partial\rho}{\partial T_C}\delta T_C + \frac{\partial\rho}{\partial T_F}\delta T_F + \frac{\partial\rho}{\partial T_M}\delta T_M + \ldots \\ &= \alpha_T^C \delta T_C + \alpha_T^F \delta T_F + \alpha_T^M \delta T_M + \ldots\end{aligned},$$

where α_T^C, α_T^F, α_T^M are the coolant, fuel and moderator temperature coefficient of reactivity, respectively. These coefficients play important role in safe operation of nuclear reactors.

A single temperature coefficient of reactivity can be defined as a derivative of the core reactivity with respect to temperature,

$$(3\text{-}154)\qquad \alpha_T \equiv \frac{\partial\rho}{\partial T} \to \sum_j \frac{\partial\rho}{\partial T_j} = \sum_j \alpha_T^{(j)}.$$

Here j indicates that separate temperatures in the reactor ($j = C$ for coolant, $j = F$ for fuel, etc.) are taken into account.

The two dominant temperature effects in most reactors are the change in resonance absorption (Doppler effect) due to fuel temperature change and the change in the neutron energy spectrum due to changing moderator or coolant density (due to temperature, pressure or void fraction changes).

Noting that,

$$(3\text{-}155)\qquad \alpha_T \equiv \frac{\partial\rho}{\partial T} = \frac{1}{k_{eff}^2}\frac{\partial k_{eff}}{\partial T} \cong \frac{1}{k_{eff}}\frac{\partial k_{eff}}{\partial T},$$

one obtains,

$$\alpha_T = \frac{1}{k_{eff}}\frac{\partial k_{eff}}{\partial T_F} + \frac{1}{k_{eff}}\frac{\partial k_{eff}}{\partial T_M} = \alpha_T^F + \alpha_T^M \,. \tag{3-156}$$

Now changes in fuel temperature T_F do not affect the shape of the thermal neutron energy spectrum. It should be mentioned, however, that fuel and moderator temperature effects can not always be separated. In LWRs a change in moderator temperature will change the moderator density significantly, thereby influencing slowing down and hence resonance absorption. In spite of such interference, it is customary to analyze both coefficients separately.

The **fuel temperature coefficient** has an important influence on reactor safety in case of a large positive reactivity insertion. A negative fuel temperature coefficient is generally considered more important than a negative moderator temperature coefficient. The reason is that the negative fuel coefficient starts adding negative reactivity immediately, whereas the moderator temperature cannot turn the power rise for several seconds.

This coefficient is also called the **prompt reactivity coefficient** or the **fuel Doppler reactivity coefficient**. Its value can be readily obtained from Eq. (3-145) as,

$$\alpha_T^F = \frac{1}{k_{eff}}\frac{dk_{eff}}{dT_F} = \frac{1}{p}\frac{dp}{dT_F} = \ln p \frac{1}{I}\frac{dI}{dT_F} \,. \tag{3-157}$$

Using Eq. (3-147) in (3-157) yields,

$$\alpha_T^F = -\ln\left[\frac{1}{p(300K)}\right]\frac{\beta}{2\sqrt{T_F}} \quad . \tag{3-158}$$

When the moderator is at the same time used as a coolant (this is the case in LWRs), the moderator coefficient of reactivity will in principle reflect the influence of the coolant density changes on the reactivity.

The dominant reactivity effect in water-moderated reactors arises from changes in moderator density, due to the thermal expansion of the coolant fluid or due to the void formation. The principal effect is usually the loss of moderation that accompanies a decrease in moderator density and causes a corresponding increase in resonance absorption. It can be calculated as follows,

$$\alpha_T^M = \frac{1}{k_{eff}}\frac{dk_{eff}}{dT_M} = \frac{1}{p}\frac{dp}{dT_M} = \frac{1}{p}\frac{d}{dT_M}\left[\exp\left(-\frac{N_F}{\bar{\xi}N_M\sigma_s}I\right)\right] = \ln\left(\frac{1}{p}\right)\frac{dN_M}{dT_M} \,. \tag{3-159}$$

Since dN_M/dT_M is negative and may be quite large, particularly if the coolant temperature is close to the saturation temperature, the reactivity coefficient can also be large. Typical values of reactivity coefficients are given in TABLE 3.4.

TABLE 3.4. Reactivity coefficients.

Type of coefficient	BWR	PWR	HTGR	LMFBR
Fuel Doppler (pcm/K)	-4 to -1	-4 to -1	-7	-0.6 to -2.5
Coolant void (pcm/%void)	-200 to -100	0	-	-12 to +20
Moderator (pcm/K)	-50 to -8	-50 to -8	+1.0	-
Expansion (pcm/K)	~0	~0	~0	-0.92

3.4.5 Nuclear Reactor Instabilities

Important aspect of safe reactor operation is the stability of the nuclear reactor in an equilibrium state (either operating or shut-down reactor). Strictly speaking, at this point it is necessary to specify what is meant by the stability. Without going into mathematical details, it is assumed that the stability is defined in the Lapunov sense. It is assumed that a system is stable in the Lapunov sense if after a small perturbation from equilibrium the system will move to new conditions which are close to the initial equilibrium conditions.

There are several different methods to evaluate reactor stability at equilibrium. One method, which will be discussed in more detail, is based on the linearization of the system of differential equations and application of the Laplace transform.

The Laplace transform representation is particularly useful in the development of the important property of a system called the transfer function. In a general sense, the transfer function is a mathematical expression which describes the effect of a physical system on the signal transferred through it. For a system shown in FIGURE 3-7, the transfer function $G(s)$ is defined as a ratio of the Laplace transform of the output signal, $Y(s)$ to the Laplace transform of the input signal, $U(s)$; $G(s) = Y(s)/U(s)$.

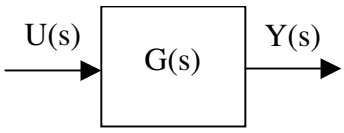

FIGURE 3-7: Open loop system.

The system represents a so-called open-loop system, that is, a system without feedback. A system with feedback, also called a closed loop system, is shown in FIGURE 3-8.

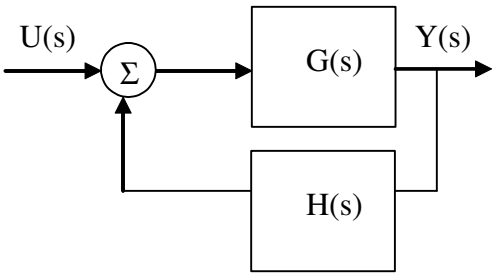

FIGURE 3-8: System with feedback.

G(s) represents the system (forward) transfer function and *H(s)* is the feedback transfer function. Performing a summation of signals at the input to the system yields,

(3-160) $$[U(s)+H(s)\cdot Y(s)]G(s)=Y(s).$$

Thus, the transfer function for the system with feedback (closed loop transfer function) becomes,

(3-161) $$G_T(s)\equiv\frac{Y(s)}{U(s)}=\frac{G(s)}{1-H(s)\cdot G(s)}.$$

Both the forward and multiple feedback reactor transfer functions have been derived in previous sections.

Reactor kinetics equations represent a typical example of an open-loop system. The input signal is then the reactivity and the output signal is the neutron flux. The transfer function, referred usually as a zero-power reactor transfer function, is defined as,

(3-162) $$G(s)=\frac{\hat{x}(s)}{\hat{\rho}(s)}.$$

Using the linearized reactor point kinetics equations (with dropped non-linear terms, which holds for small perturbations and $|\rho|<0.1\beta$), the transfer function of the zero power reactor is obtained as,

(3-163) $$G(s)=\frac{\hat{x}(s)}{\hat{\rho}(s)}=\frac{1}{\Lambda}\cdot\frac{1}{s\left(1+\frac{1}{\Lambda}\sum_{i=1}^{6}\frac{\beta_i}{s+\lambda_i}\right)}.$$

The gain $|G(j\omega)|$ and the phase angle $\arg(G(j\omega))$ of the transfer function are shown in FIGURE 3-9 and FIGURE 3-10, respectively.

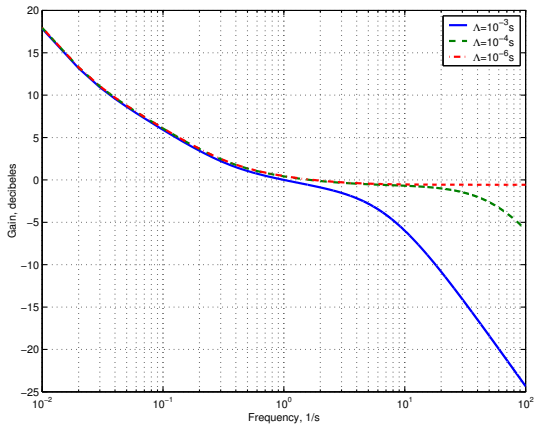

FIGURE 3-9: Gain plot for various neutron generation time values.

The gain plot shown in FIGURE 3-9 (often called the Bode diagram) indicates that an open-loop reactor system tends to be unstable as frequency becomes small, since the gain becomes infinite when frequency approaches zero. Thus, a reactor without feedback is expected to be intrinsically unstable.

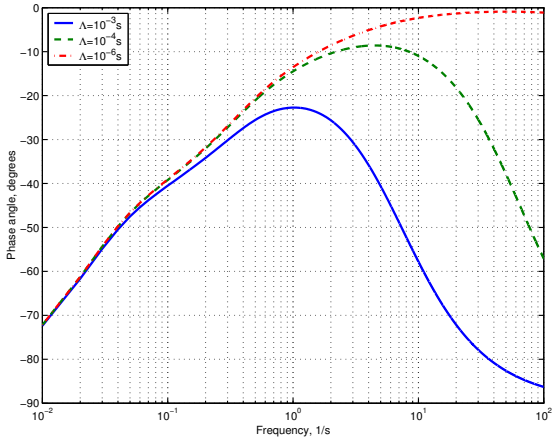

FIGURE 3-10: Phase plot for various neutron generation time values.

Reactor dynamics equations represent a typical example of a closed loop system. This is due to the presence of multiple feedbacks which exist in this case, as discussed in previous sections.

It is interesting to consider a special case of the open loop in which,

(3-164) $$U(s)\cdot G(s)\cdot H(s)=U(s)\,.$$

In this case the system will be self-excited if the feedback loop is closed. There will be no need for any external input signal since the feedback signal is in-phase with the external input. Equation (3-164) can be written as,

(3-165) $$\left[1-H(s)\cdot G(s)\right]U(s)=0\,.$$

Since the input perturbation is arbitrary, the condition for the instability is,

(3-166) $$1-H(s)\cdot G(s)=0\,.$$

Equation (3-166) is called the characteristic equation of the system and is the same as the denominator of the closed loop transfer function, given by Eq. (3-161).

One can observe that the roots of the characteristic function will be poles of the closed loop transfer function. If the closed loop transfer function has the form,

(3-167) $$F(s)=\frac{1}{s-a}\,,$$

the original *f(t)* of the transfer function *F(s)* is,

(3-168) $$f(t)=L^{-1}\{F(s)\}=e^{at}\,.$$

Transfer function $F(s)$ has a pole at $s = a$, which corresponds to the zero value of its denominator $s - a$. If now $Re(a) > 0$ the function $f(t)$ will diverge with time which indicates unstable system. In other words, roots of the characteristic equation may imply exponential divergence in the time domain. The limiting case when $Re(a) = 0$ is the marginal stability case in which a perturbation causes the system to oscillate sinusoidally, but not diverge with time. Naturally system is stable when $Re(a) < 0$, since then any perturbation will damp out with time.

One can formulate the following stability criterion for a closed loop system:

"*The necessary and sufficient condition for the closed loop system to be stable to small perturbations is that all the roots of the characteristic equation have negative real parts*".

If one can factor the closed loop transfer function using partial fraction expansion, the roots can be easily determined. This is the case when the closed loop transfer function has a form of a rational polynomial. In the case of complicated transcendental algebraic equations direct evaluation of roots is not trivial, however, and an approach using the Nyquist Criterion has proven to be an efficient way of investigation of the system stability.

An important parameter used in the evaluation of BWR stability is the **decay ratio**, which is defined as the ratio of two consecutive amplitudes in a given signal, as shown in FIGURE 3-11. The decay ratio can be calculated from the analytical solution as a ratio of the system response at time $t_0 + T$ to the value at t_0, where T is the period of oscillations. More information about reactor dynamics and stability can be found in [3-1].

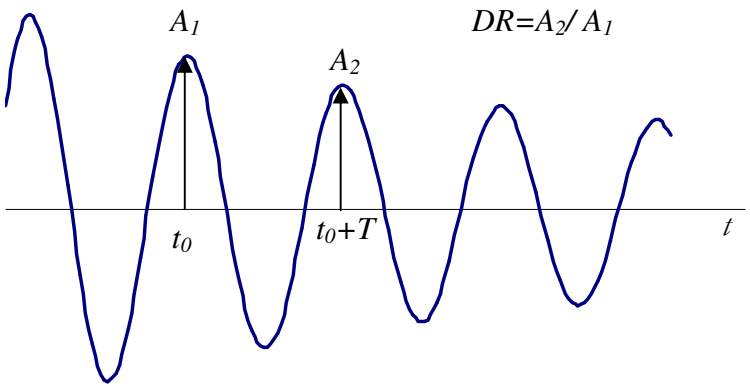

FIGURE 3-11: Definition of the decay ratio.

3.4.6 Control Rod Analysis

A control rod, with a cylindrical shape and a radius a (see FIGURE 3-12), inserted partly into a bare cylindrical reactor, will be considered. From the perturbation theory[3-4] it is obtained that the reactivity change caused by a perturbation in a reactor can be calculated as,

$$\Delta\rho = \frac{\int \phi\left(-\nabla\delta D\nabla + \delta\Sigma_a - \frac{1}{k}\nu\delta\Sigma_f\right)\phi dV}{\int \nu\Sigma_f\phi^2 dV}, \tag{3-169}$$

where the integration is over the whole volume of the reactor. Here δD, $\delta\Sigma_a$ and $\delta\Sigma_f$ are perturbations of the diffusion coefficient, the macroscopic cross section for absorption and the macroscopic cross section for fission, respectively. For control rods insertion only the macroscopic cross section for absorption is perturbed, thus,

$$\Delta\rho = \frac{\int \delta\Sigma_a\phi^2 dV}{\int \nu\Sigma_f\phi^2 dV}. \tag{3-170}$$

In Eq. (3-170) ϕ is the neutron flux in a not-perturbed critical reactor; that is in a reactor without the control rod. For finite-cylinder reactor (and using coordinate system as shown in FIGURE 3-12) the neutron flux is given as,

$$\phi(r,z) = AJ_0\left(\frac{2.405r}{\tilde{R}}\right)\sin\frac{\pi z}{\tilde{H}}. \tag{3-171}$$

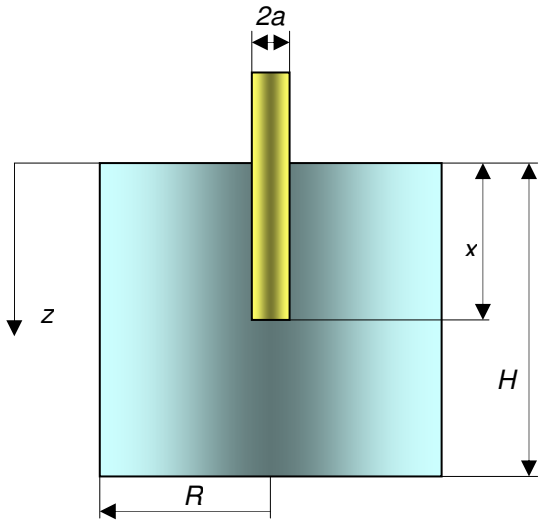

FIGURE 3-12: Partly inserted control rod.

For a control rod inserted in the core with a distance x, the perturbation of the macroscopic cross section for absorption can be expressed as,

$$\delta\Sigma_a = \begin{cases} \Sigma_{a,cr} - \Sigma_{a,c} & \text{for} \quad 0 \le z \le x, \quad 0 \le r \le a \\ 0 & \text{otherwise} \end{cases}, \tag{3-172}$$

where $\Sigma_{a,cr}$ and $\Sigma_{a,c}$ are the macroscopic cross sections for absorption for the control rod and the core, respectively.

Substituting Eqs. (3-171) and (3-172) into (3-170) yields,

$$\Delta\rho(x)=\frac{\int_0^a\int_0^x\left(\Sigma_{a,cr}-\Sigma_{a,c}\right)A^2J_0^2\left(\frac{2.405r}{\tilde{R}}\right)\sin^2\left(\frac{\pi z}{\tilde{H}}\right)2\pi r dr dz}{\int\nu\Sigma_f\phi^2dV}, \tag{3-173}$$

and for fully inserted control rod,

$$\Delta\rho(\tilde{H})=\frac{\int_0^a\int_0^{\tilde{H}}\left(\Sigma_{a,cr}-\Sigma_{a,c}\right)A^2J_0^2\left(\frac{2.405r}{\tilde{R}}\right)\sin^2\left(\frac{\pi z}{\tilde{H}}\right)2\pi r dr dz}{\int\nu\Sigma_f\phi^2dV}. \tag{3-174}$$

Dividing Eqs. (3-173) and (3-174) with each other yields,

$$\frac{\Delta\rho(x)}{\Delta\rho(\tilde{H})}=\frac{\int_0^x\sin^2\frac{\pi z}{\tilde{H}}dz}{\int_0^{\tilde{H}}\sin^2\frac{\pi z}{\tilde{H}}dz}=\frac{x}{\tilde{H}}-\frac{1}{2\pi}\sin\frac{2\pi x}{\tilde{H}}, \tag{3-175}$$

and finally,

$$\Delta\rho(x)=\Delta\rho(\tilde{H})\left(\frac{x}{\tilde{H}}-\frac{1}{2\pi}\sin\frac{2\pi x}{\tilde{H}}\right). \tag{3-176}$$

The above equation is graphically illustrated in FIGURE 3-13. As can be seen, for small changes of x around $x = 0.5$ the relative change of the reactivity is almost a linear function of x. This observation is used when performing calibration of control rods.

Applying similar as above approach based on the perturbation theory, it can be shown that if the control rod is placed at a distance r_0 from the core centerline (see FIGURE 3-14), then the reactivity change can be calculated as,

$$\Delta\rho(r_0)=J_0^2\left(\frac{2.405r_0}{\tilde{R}}\right)\Delta\rho(0). \tag{3-177}$$

Here: $\Delta\rho(r_0), \Delta\rho(0)$ - changes of the reactivity for a control rod located at a distance r_0 from the centerline and a control rod placed centrally, respectively.

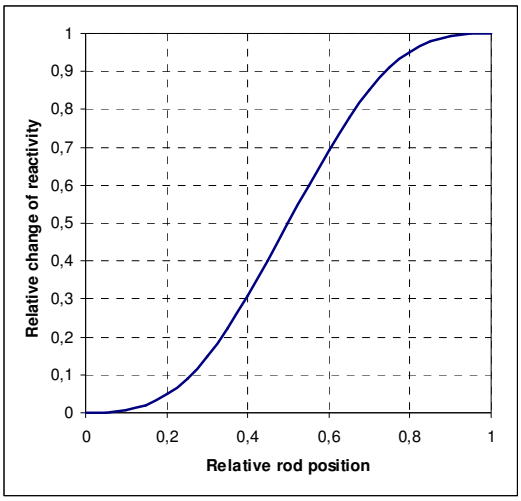

FIGURE 3-13: Relative reactivity change as a function of insertion distance of a centrally placed control rod.

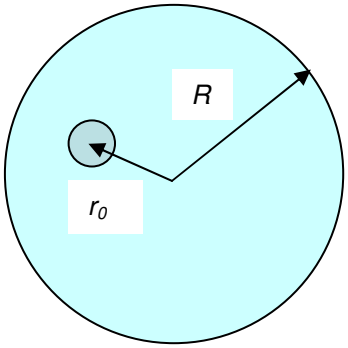

FIGURE 3-14: Control rod located at a distance r_0 from the centerline.

REFERENCES

[3-1] Anglart, H., *Nuclear Reactor Dynamics and Stability*, Compendium, KTH, 2009.

[3-2] Beckjord, E. Ex. Dir. et al., *The Future of Nuclear Power. An Interdisciplinary MIT Study*, MIT 2003, ISBN 0-615-12420-8

[3-3] Glasstone, S. and Sesonske, A., *Nuclear Reactor Engineering*, Van Nostrand Reinhold Compant, 1981, ISBN 0-442-20057-9.

[3-4] Duderstadt, J.J. and Hamilton, L.J., Nuclear Reactor Analysis, John Wiley & Sons, Inc.

[3-5] Stacey, W.M., *Nuclear Reactor Physics*, Wiley-VCH, 2004

EXERCISES

EXERCISE 3-1: Calculate the thermal utilization factor for a homogenized core composed of (in % by volume): UO_2 35% and H_2O 65%. The enrichment of the fuel is 3.2% (by weight). Microscopic cross sections [b] for absorption are as follows: water 0.66 [b], oxygen O: $2x10^{-4}$ [b], U-235: 681 [b], U-238: 2.7 [b]. Density of UO_2: 10200 kg/m^3, density of water: 800 kg/m^3.

EXERCISE 3-2: Calculate the resonance escape probability for a reactor as in the previous exercise assuming the fuel temperature T = 1500 K and the effective resonance integral for fuel at T = 300 K equal to 25 [b]. Microscopic cross sections for scattering are as follows: water 103 [b], oxygen O: 6 [b], U-235: 8 [b], U-238: 8.3 [b].

EXERCISE 3-3: Determine the effective multiplication factor and the neutron flux distribution in a homogeneous spherical reactor with radius R and with a reflector with the extrapolated thickness $\tilde{T}$ using the one-group diffusion approximation.

EXERCISE 3-4: Determine the effective multiplication factor and the neutron flux distribution in a homogeneous spherical bare reactor with:

$$\lambda_{tr,c} = 5 \cdot 10^{-3} m, \Sigma_{a,c} = 4m^{-1}, \Sigma_{f,c} = 3.4m^{-1}, \nu = 2.47, R = 0.2m \text{ and } k_\infty = 2.1.$$

How the effective multiplication factor will change if the reactor will be surrounded with a graphite reflector, with the following data:

$$\lambda_{tr,r} = 2.75 \cdot 10^{-2} m, \Sigma_{a,r} = 3.4 \cdot 10^{-2} m^{-1}, T = 0.6m \cdot$$

EXERCISE 3-5: Reactor as in EXERCISE 4 is surrounded with a graphite reflector. Investigate how the reflector thickness influences the effective multiplication factor. Is it possible to suggest an optimal thickness of the reflector?

EXERCISE 3-6: A homogeneous reactor with a finite-cylinder shape has a radius R and the extrapolated height $\tilde{H}$. The reactor is surrounded with a radial reflector with the extrapolated thickness $\tilde{T}$ and extrapolated height $\tilde{H}$. Determine the effective multiplication factor and the distribution of the neutron flux for a critical reactor using the one-group diffusion approximation.

EXERCISE 3-7: Investigate a possibility to construct a homogeneous reactor which would use the natural uranium as the fuel and graphite as the moderator. For that purpose it is necessary to calculate the infinite multiplication factor k_∞ as a function of the ratio N_M/N_F, where N_M and N_F are concentration of nuclei of moderator and fuel, respectively. It can be assumed that $\eta = 1.33$ and $\varepsilon = 1$. Use reasonable approximations.

EXERCISE 3-8: A cylindrical reactor core with dimensions H = 3.7 m and R = 2.2 m has a centrally inserted control rod to a certain unknown position x_0. The operator decided to measure the control rod worth and removed the rod from the core with dx = 2 cm. The measured increase of reactivity was 11.2 pcm. After the measurement, the control rod was moved back to the initial position x_0 and next inserted into the reactor core with dx = 2cm. The measured decrease of reactivity was 11.7 pcm. All reactivity changes are given in relation to the insertion length x_0. Calculate the initial insertion length of the control rod x_0 and the worth of the rod in the full-inserted position.

EXERCISE 3-9: LWR reactor core with UO_2 fuel contains 5.6×10^{27} nuclei of U-235 and the average thermal fission microscopic cross-section of the fuel is $\sigma_f = 344 \times 10^{-28}$ m^2. Assuming that the reactor operates with constant thermal power equal to 3000 MW, calculate: (a) average neutron flux in the core, (b) equilibrium number of iodine nuclei in the core, (c) equilibrium number of xenon nuclei in the core, (d) the time after shutdown when the number of xenon nuclei will have maximum. Given: iodine half-life 6.7 h, xenon half-life 9.2 h, iodine effective fractional yield from fission 0.061, xenon effective fractional yield from fission 0.003, microscopic absorption cross-section for xenon 2.6×10^6 barn.

Chapter

4

4 Heat Generation and Removal

This chapter presents methods to determine the distribution of heat sources and temperatures in various components of nuclear reactor. In safety analyses of nuclear power plants the amount of heat generated in the reactor core must be known in order to be able to calculate the temperature distributions and thus, to determine the safety margins. Such analyses have to be performed for all imaginable conditions, including nominal operation conditions, reactor startup and shutdown, as well as for removal of the decay heat after reactor shutdown. The first section presents the methods to predict the heat sources in nuclear reactors at various conditions. The following sections discuss the prediction of such parameters as coolant enthalpy, fuel element temperature, void fraction, pressure drop and the occurrence of the Critical Heat Flux (CHF) in nuclear fuel assemblies.

4.1 Energy from Nuclear Fission

4.1.1 Thermal Power of Nuclear Reactor

Consider a monoenergetic neutron beam in which n is the neutron density (number of neutrons per m^3). If v is neutron speed then nv is the number of neutron falling on 1 m^2 of target material per second. Since σ is the effective area per single nucleus, for a given reaction and neutron energy, then Σ is the effective area of all the nuclei per m^3 of target. Hence the product Σnv gives the number of interactions of nuclei and neutrons per m^3 of target material per second.

In particular, the fission rate is found as: $\Sigma_f nv = \Sigma_f \phi$, where $\phi = nv$ is the neutron flux (to be discussed later) and $\Sigma_f = N\sigma_f$, N being the number of fissile nuclei/m^3 and σ_f m^2/nucleus the fission cross section. In a reactor the neutrons are not monoenergetic and cover a wide range of energies, with different flux and corresponding cross section.

In thermal reactor with volume V there will occur $V\bar{\Sigma}_f\bar{\phi}$ fissions, where $\bar{\Sigma}_f$ and $\bar{\phi}$ are the average values of the macroscopic fissions cross section and the neutron flux, respectively.

To evaluate the reactor power it is necessary to know the average amount of energy which is released in a single fission. The table below shows typical values for uranium-235.

TABLE 4.1. Approximate distribution of energy per fission of uranium-235

	10^{-12} J = 1 pJ	MeV
Kinetic energy of fission products	26.9	168
Instantaneous gamma-ray energy	1.1	7
Kinetic energy of fission neutrons	0.8	5
Beta particles from fission products	1.1	7
Gamma rays from fission products	1.0	6
Neutrinos	1.6	10
Total fission energy	32	200

As can be seen, the total fission energy is equal to 32 pJ. It means that it is required ~3.1 10^{10} fissions per second to generate 1 W of the thermal power. Thus, the **thermal power of a reactor** can be evaluated as,

$$P = \frac{V\bar{\Sigma}_f\bar{\phi}}{3.1\cdot 10^{10}}\,(\mathrm{W})\,. \tag{4-1}$$

Thus, the thermal power of a nuclear reactor is proportional to the number of fissile nuclei, *N*, and the neutron flux $\bar{\phi}$. Both these parameters vary in a nuclear reactor and their correct computation is necessary to be able to accurately calculate the reactor power.

Power density (which is the total power divided by the volume) in nuclear reactors is much higher than in conventional power plants. Its typical value for PWRs is 75 MW/m^3, whereas for a fast breeder reactor cooled with sodium it can be as high as 530 MW/m^3.

4.1.2 Fission Yield

Fissions of uranium-235 nucleus can end up with 80 different primary fission products. The range of mass numbers of products is from 72 (isotope of zinc) to 161 (possibly an isotope of terbium). The yields of the products of thermal fission of uranium-233, uranium-235, plutonium-239 and a mixture of uranium and plutonium are shown in FIGURE 4-1.

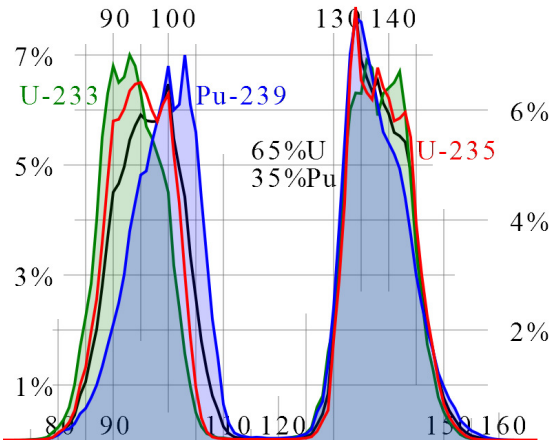

FIGURE 4-1: Fission yield as a function of mass number of the fission product (from Wikimedia Commons).

As can be seen in all cases there are two groups of fission products: a "light" group with mass number between 80 and 110 and a "heavy" group with mass numbers between 125 and 155.

4.1.3 Decay Heat

A large portion of the radioactive fission products emit gamma rays, in addition to beta particles. The amount and activity of individual fission products and the total fission product inventory in the reactor fuel during operation and after shut-down are important for several reasons: namely to evaluate the radiation hazard, and to determine the decrease of the fission product radioactivity in the spent fuel elements after removal from the reactor. This information is required to evaluate the length of the cooling period before the fuel can be reprocessed.

Right after the insertion of a large negative reactivity to the reactor core (for example, due to an injection of control rods), the neutron flux rapidly decreases according to the following equation,

$$\phi(t) = \phi_0 \left\{ \frac{\beta}{\beta - \rho} e^{\frac{\lambda\rho}{\beta-\rho}t} - \frac{\rho}{\beta - \rho} e^{-\frac{(\beta-\rho)t}{l}} \right\}. \tag{4-2}$$

Here $\phi(t)$ is the neutron flux at time t after reactor shut-down, ϕ_0 is the neutron flux during reactor operation at full power, ρ is the step change of reactivity, β is the fraction of delayed neutrons, l is the prompt neutron lifetime and λ is the mean decay constant of precursors of delayed neutrons. For LWR with uranium-235 as the fissile material, typical values are as follows: λ = 0.08 s^{-1}, β = 0.0065 and l = 10^{-3} s. Assuming the negative step-change of reactivity ρ = -0.09, the relative neutron flux change is given as,

$$\frac{\phi(t)}{\phi_0} = 0.067e^{-0.075t} + 0.933e^{-96.5t}. \tag{4-3}$$

The second term in Eq. (4-3) is negligible already after t = 0.01s and only the first term has to be taken into account in calculations. As can be seen, the neutron flux (and thus

the generated power) immediately jumps to ~6.7% of its initial value and then it is reduced e-fold during period of time $T = 1/0.075 = 13.3$ s.

After a reactor is shut down and the neutron flux falls to such a small value that it may be neglected, substantial amounts of heat continue to be generated due to the beta particles and the gamma rays emitted by the fission products. FIGURE 4-2 shows the fission product **decay heat** versus the time after shut down. The curve, which covers a time range from 1 to 10^6 years after shut down, refers to a hypothetical pressurized water-cooled reactor that has operated at a constant power for a period of time during which the fuel (with initial enrichment 4.5%) has reached 50 GWd/tU burnup and is then shut down instantaneously. Contributions from various species which are present in the spent fuel are indicated.

The power density change due to beta and gamma radiation can be calculated from the following approximate correlation[4-2],

$$\frac{q'''}{q'''_0} \cong 0.065\left[\left(t - t_{op}\right)^{-0.2} - t^{-0.2}\right], \tag{4-4}$$

Here q'''_0 is the power density in the reactor at steady state operation before shut down, q''' is the decay power density, t is the time after reactor shut down [s] and t_{op} is the time of reactor operation before shut down [s]. Equation (4-4) is applicable regardless of whether the fuel containing the fission products remains in the reactor core or it is removed from it. However, the equation accuracy and applicability is limited and can be used for cooling periods from approximately 10 s to less than 100 days.

Equation (4-4) can be transformed as follows,

$$\frac{q'''}{q'''_0} \cong \frac{0.065}{t_{op}^{0.2}}\left[\frac{1}{\left(\dfrac{t - t_{op}}{t_{op}}\right)^{0.2}} - \frac{1}{\left(\dfrac{t}{t_{op}}\right)^{0.2}}\right] = \frac{0.065}{t_{op}^{0.2}}\left[\frac{1}{\theta^{0.2}} - \frac{1}{(\theta+1)^{0.2}}\right]. \tag{4-5}$$

Here $\theta = \left(t - t_{op}\right)/t_{op}$ is the relative time after reactor shut down. Equation (4-5) is shown in FIGURE 4-3 for the reactor operation time t_{op} from 1 month to 1 year.

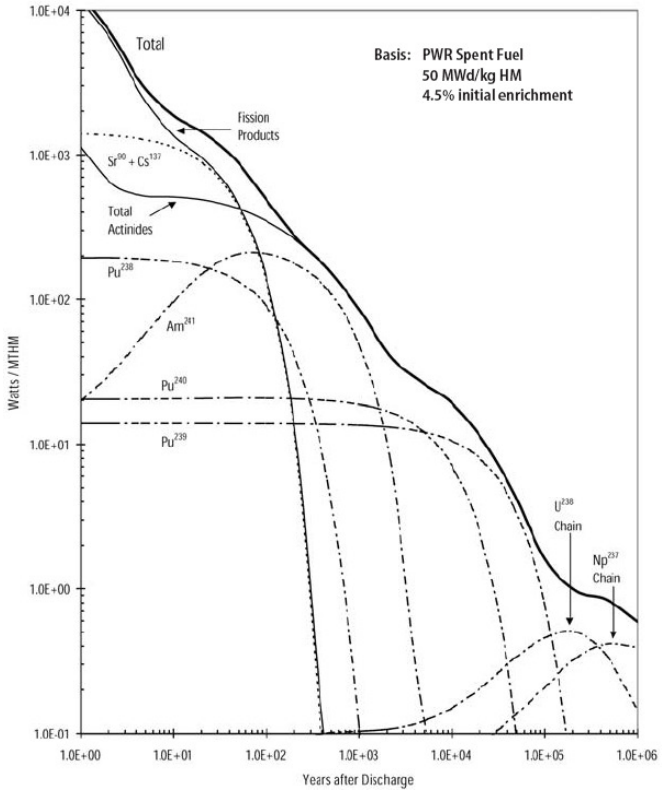

FIGURE 4-2: Fission-product decay heat power (in Watts per metric ton of heavy metal) versus time after shutdown in years, [3-2].

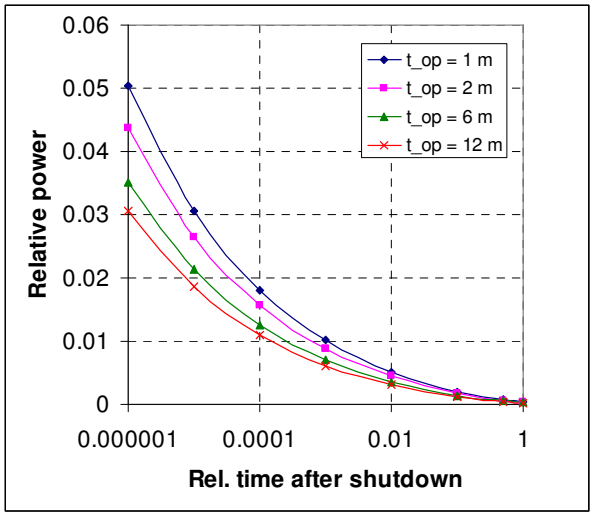

FIGURE 4-3: Relative decay power versus relative time after reactor shutdown for various operation periods from 1 month to 1 year.

4.1.4 Spatial Distribution of Heat Sources

The energy released in nuclear fission reaction is distributed among a variety of reaction products characterized by different range and time delays. Once performing the thermal design of a reactor core, the energy deposition distributed over the coolant and structural materials is frequently reassigned to the fuel in order to simplify the thermal analysis of the core. The volumetric fission heat source in the core can be found in general case as,

$$q'''(\mathbf{r}) = \sum_i w_f^{(i)} N_i(\mathbf{r}) \int_0^\infty dE \sigma_f^{(i)}(E) \phi(\mathbf{r}, E). \quad (4\text{-}6)$$

Here $w_f^{(i)}$ is the recoverable energy released per fission event of *i*-th fissile material, $N_i(\mathbf{r})$ is the number density of *i*-th fissile material at location $\mathbf{r}$ and $\sigma_f^i(E)$ is its microscopic fission cross section for neutrons with energy *E*. Since the neutron flux and the number density of the fuel vary across the reactor core, there will be a corresponding variation in the fission heat source.

The simplest model of fission heat distribution would correspond to a bare, homogeneous core. One should recall here the one-group flux distribution for such geometry given as,

$$\phi(r, z) = \phi_0 J_0\left(\frac{2.405r}{\tilde{R}}\right)\cos\left(\frac{\pi z}{\tilde{H}}\right). \quad (4\text{-}7)$$

Here ϕ_0 is the flux at the center of the core and $\tilde{R}$ and $\tilde{H}$ are effective (extrapolated) core dimensions that include extrapolation lengths as well as an adjustment to account for a reflected core.

Having a fuel rod located at $r = r_f$ distance from the centerline of the core, the volumetric fission heat source becomes a function of the axial coordinate, *z*, only,

$$q'''(z) = w_f \Sigma_f \phi_0 J_0\left(\frac{2.405r_f}{\tilde{R}}\right)\cos\left(\frac{\pi z}{\tilde{H}}\right). \quad (4\text{-}8)$$

There are numerous factors that perturb the power distribution of the reactor core, and the above equation will not be valid. For example fuel is usually not loaded with uniform enrichment. At the beginning of core life, higher enrichment fuel is loaded toward the edge of the core in order to flatten the power distribution. Other factors include the influence of the control rods and variation of the coolant density.

All these power perturbations will cause a corresponding variation of temperature distribution in the core. A usual technique to take care of these variations is to estimate the local working conditions (power level, coolant flow, etc) which are the closest to the thermal limitations. Such part of the core is called hot channel and the working conditions are related with so-called hot channel factors.

One common approach to define hot channel is to choose the channel where the core heat flux and the coolant enthalpy rise is a maximum. Working conditions in the hot channel are defined by several ratios of local conditions to core-averaged conditions. These ratios, termed the hot channel factors or power peaking factors will be considered in more detail in coming Chapters. However, it can be mentioned already here that the basic initial plant thermal design relay on these factors.

In thermal reactors it is assumed that 90% of the fission total energy is liberated in fuel elements, whereas the remaining 10% is equally distributed between moderator and reflector/shields.

4.2 Coolant Flow and Heat Transfer in Rod Bundles

Rod bundles in nuclear reactors have usually very complex geometry. Due to that a thorough thermal-hydraulic analysis in rod bundles requires quite sophisticated computational tools. In general, several levels of approximations can be employed to perform the analysis,

- simple one-dimensional analysis of a single subchannel or bundle,
- analysis of a whole rod bundle applying the subchannel-analysis code,
- complex three-dimensional analysis using Computational Fluid Dynamics (CFD) cods.

In this book only the simples approach is considered. In this approach, the single subchannel or rod bundle is treated as a one-dimensional pipe with a diameter equal to the hydraulic (equivalent) diameter of the subchannel or bundle. The hydraulic diameter of a channel of arbitrary shape is defined as,

$$D_h = \frac{4A}{P_w}, \tag{4-9}$$

where A is the channel cross-section area and P_w is the channel wetted perimeter. FIGURE 4-4 shows typical coolant subchannels in infinite rod lattices.

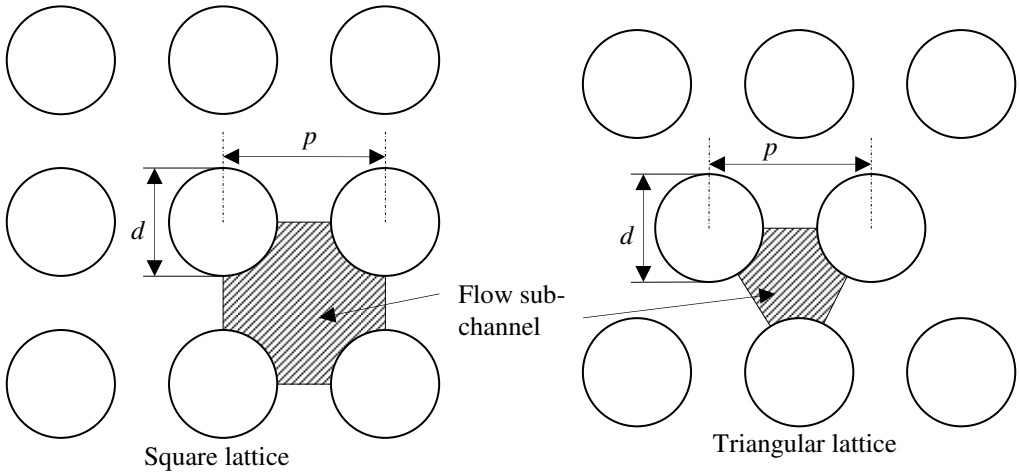

FIGURE 4-4: Typical coolant subchannels in rod bundles.

The hydraulic diameter for the square and triangular lattice can be calculated from Eq. (4-9) and from principles shown in FIGURE 4-4 as follows. The subchannel flow area is given as,

$$A = \begin{cases} p^2 - \dfrac{\pi d^2}{4} & \textit{for square lattice} \\ \dfrac{\sqrt{3}}{4} p^2 - \dfrac{\pi d^2}{8} & \textit{for triangular lattice} \end{cases},$$

and the wetted perimeter (part of the perimeter filled with walls) is given as,

$$P_w = \begin{cases} \pi d & \textit{for square lattice} \\ \frac{1}{2}\pi d & \textit{for triangular lattice} \end{cases}.$$

Here p is the lattice pitch and d is the diameter of fuel rods. The hydraulic diameter is obtained as:

$$D_h = \begin{cases} d\left[\frac{4}{\pi}\left(\frac{p}{d}\right)^2 - 1\right] & \textit{for square lattice} \\ d\left[\frac{2\sqrt{3}}{\pi}\left(\frac{p}{d}\right)^2 - 1\right] & \textit{for triangular lattice} \end{cases} \tag{4-10}$$

In case of fuel assemblies in Boiling Water Reactors (BWR), the hydraulic diameter should be based on the total wetted perimeter and the total cross-section area of the fuel assembly. Assuming fuel assembly as shown in FIGURE 4-5, the hydraulic diameter is as follows,

$$D_h \equiv \frac{4A}{P_w} = \frac{4w^2 - N\pi d^2}{4w + N\pi d} \tag{4-11}$$

Here N is the number of rods in the assembly, w is the width of the box [m] and d is the diameter of fuel rods [m].

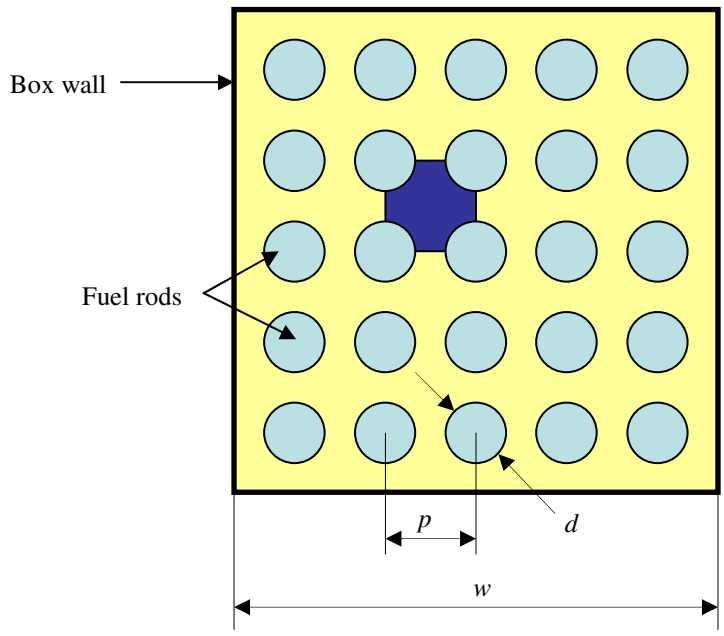

FIGURE 4-5: Cross-section of a BWR fuel assembly.

4.2.1 Enthalpy Distribution in Heated Channels

Assume a heated channel with an arbitrary axial distribution of the heat flux, *q''(z)*, and an arbitrary, axially-dependent geometry, as shown in FIGURE 4-6. The coolant flowing in the channel has a constant mass flow rate *W*.

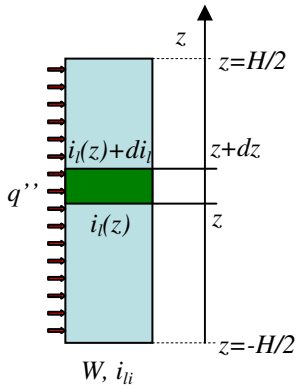

FIGURE 4-6: A heated channel.

Energy balance for a differential channel length between *z* and *z+dz* is as follows,

$$W \cdot i_l(z) + q''(z) \cdot P_H(z) \cdot dz = W \cdot \left[i_l(z) + di_l \right], \tag{4-12}$$

which leads to the following differential equation for the coolant enthalpy,

$$\frac{di_l(z)}{dz} = \frac{q''(z) \cdot P_H(z)}{W}. \tag{4-13}$$

Here $P_H(z)$ is the heated perimeter of the channel. Integration of Eq. (4-13) from the channel inlet to a certain location *z* yields,

$$i_l(z) = i_{li} + \frac{1}{W} \int_{-H/2}^{z} q''(z) \cdot P_H(z) dz \tag{4-14}$$

where $i_l(z)$ is the coolant enthalpy at location *z* and i_{li} is the coolant enthalpy at the inlet to the channel ($z = -H/2$).

4.2.2 Temperature Distribution in Channels with Single Phase Flow

For small temperature and pressure changes the enthalpy of a single-phase (non-boiling) coolant can be expressed as a linear function of the temperature. Assuming a uniform axial distribution of heat sources and a constant heated perimeter, Eq. (4-14) yields,

$$T_{lb}(z) = T_{lbi} + \frac{q'' P_H \left(z + H/2 \right)}{c_p W} \tag{4-15}$$

Here $T_{lb}(z)$ is the coolant **bulk temperature** at location *z*. The bulk temperature in a channel cross section is defined in such a way that it can be obtained from the energy balance over a portion of the channel. For an arbitrary velocity, temperature and fluid

property distribution across the channel cross section, the bulk temperature is found as,

$$T_{lb} = \frac{\int_A \rho_l c_{pl} v_l T_l dA}{\int_A \rho_l c_{pl} v_l dA}$$

Note that Eq. (4-15) is only valid for coolant without phase change, whereas Eq. (4-14) is applicable for both single-phase and two-phase flows.

As can be seen, the coolant temperature is a linear function of the distance from the inlet to the channel. Assuming that the total length of the channel is equal to H, the exit temperature is as follows,

$$T_{lbex} = T_{lbi} + \frac{q'' P_H H}{c_p W}. \quad (4\text{-}16)$$

The temperature distribution along the channel is shown in FIGURE 4-7.

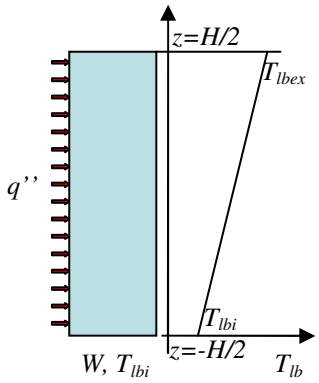

FIGURE 4-7: Bulk temperature distribution in a uniformly heated channel with a constant heated perimeter.

In nuclear reactor cores the axial power distribution may have various shapes. The cosine-shaped power distribution is obtained in cylindrical homogeneous reactors, as previously derived using the diffusion approximation for the neutron distribution calculation.

Using Eq. (4-8) and the coordinate system as indicated in FIGURE 4-8, the power distribution may be expressed as,

$$q''(z) = q_0'' \cdot \cos\left(\frac{\pi z}{\tilde{H}}\right). \quad (4\text{-}17)$$

Eq. (4-13) then becomes,

$$\frac{di_l(z)}{dz} = \frac{q_0'' \cdot P_H(z)}{W} \cos\left(\frac{\pi z}{\tilde{H}}\right), \quad \text{or} \quad \frac{dT_{lb}(z)}{dz} = \frac{q_0'' \cdot P_H(z)}{W \cdot c_p} \cos\left(\frac{\pi z}{\tilde{H}}\right). \quad (4\text{-}18)$$

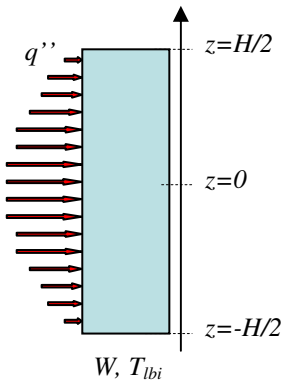

FIGURE 4-8: Heated channel with cosine power shape.

After integration, the coolant enthalpy and temperature distributions are as follows,

$$i_l(z) = \frac{q_0'' \cdot P_H}{W} \cdot \frac{\tilde{H}}{\pi}\left[\sin\left(\frac{\pi z}{\tilde{H}}\right) + \sin\left(\frac{\pi H}{2\tilde{H}}\right)\right] + i_{li}, \quad or$$

$$T_{lb}(z) = \frac{q_0'' \cdot P_H}{W \cdot c_p} \cdot \frac{\tilde{H}}{\pi}\left[\sin\left(\frac{\pi z}{\tilde{H}}\right) + \sin\left(\frac{\pi H}{2\tilde{H}}\right)\right] + T_{lbi} \tag{4-19}$$

The channel exit temperature and enthalpy can be found substituting $z = H/2$ into Eq. (4-19) as follows,

$$i_{lex} = i_l(H/2) = \frac{2q_0'' \cdot P_H \cdot \tilde{H}}{\pi \cdot W}\sin\left(\frac{\pi H}{2\tilde{H}}\right) + i_{li}, \quad \text{or}$$

$$T_{lbex} = T_{lb}(H/2) = \frac{2q_0'' \cdot P_H \cdot \tilde{H}}{\pi \cdot W \cdot c_p}\sin\left(\frac{\pi H}{2\tilde{H}}\right) + T_{lbi} \tag{4-20}$$

The axial distribution of the coolant temperature is shown in FIGURE 4-9.

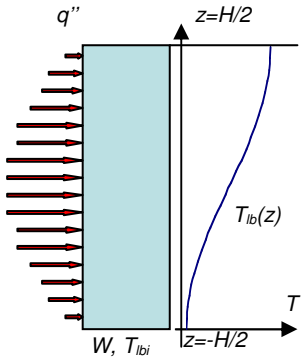

FIGURE 4-9: Distribution of coolant bulk temperature along channel with the cosine heat flux distribution.

4.2.3 Heat Conduction in Fuel Elements

Modern nuclear power reactors contain cylindrical fuel elements that are composed of ceramic fuel pellets located in metallic tubes (so-called cladding). A cross-section over a square lattice of fuel rods is shown in FIGURE 4-10. For thermal analyses it is convenient to subdivide the fuel rod assembly into subchannels. The division can be performed in several ways; however, most obvious choices are so-called coolant-centered subchannels and rod-centered subchannels. Both types of subchannels are equivalent in terms of major parameters such as the flow cross-section area, the hydraulic diameter, the wetted perimenter and the heated perimeter. In continuation, the thermal analysis will be performed for a single subchannel.

The stationary (time independent) heat conduction equation for an infinite cylindrical fuel pin, in which the axial heat conduction can be ignored is as follows:

$$-\frac{1}{r}\frac{d}{dr}\left(\lambda_F r \frac{dT_F}{dr}\right) = q''' , \qquad (4\text{-}21)$$

where T_F is the fuel temperature, [K], λ_F is the thermal conductivity of the fuel material, [W m^{-1} K^{-1}], q''' is the density of heat sources, [W m^{-3}] and r is the radial distance. Here the angular dependence of the temperature is omitted due to the assumed axial symmetry of the temperature distribution.

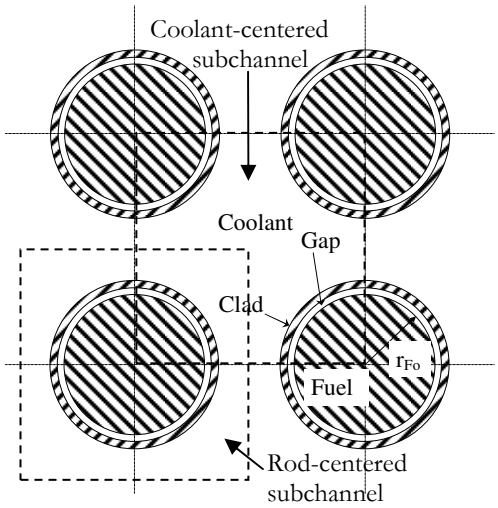

FIGURE 4-10: Cross-section of a square fuel lattice. Equivalent subchannels (coolant-centered and rod centerd) suitable for thermal analyses.

Assuming further that q''' is constant in a cross-section, Eq. (4-21) can be integrated to obtain:

$$\lambda_F r \frac{dT_F}{dr} = -\frac{r^2}{2} q''' \qquad (4\text{-}22)$$

If the fuel conductivity was constant, Eq. (4-22) could be integrated and the temperature distribution would be obtained. However in typical fuel materials the fuel thermal conductivity strongly depends on the temperature and this is the reason why the temperature distribution can not be found from Eq. (4-22) in a general analytical form. Instead, Eq. (4-22) is transformed and integrated as follows:

(4-23) $$\lambda_F dT_F = -\frac{r}{2} q''' dr \Rightarrow \int_{T_{Fc}}^{T_{Fo}} \lambda_F dT_F = -\frac{q'''}{2} \int_0^{r_{Fo}} r dr = -\frac{r_{Fo}^2}{4} q''',$$

where the integration on the left-hand-side is carried out from the temperature at the centerline, T_{Fc}, to the temperature on the fuel pellet surface $T_{Fo}=T_F(r_{Fo})$. Defining the average fuel conductivity as,

(4-24) $$\langle \lambda_F \rangle = \frac{1}{T_{Fc} - T_{Fo}} \int_{T_{Fo}}^{T_{Fc}} \lambda_F dT_F ,$$

the temperature drop across the fuel pellet can be found as,

(4-25) $$\Delta T_F \equiv T_{F_c} - T_{Fo} = \frac{q''' r_{Fo}^2}{4\langle \lambda_F \rangle}.$$

In the thermal analysis of reactor cores, the power is often expressed in terms of the linear power density, that is, the power generated per unit length of the fuel element,

(4-26) $$q' \equiv \pi r_{Fo}^2 q'''.$$

Combining Eqs.(4-25) and (4-26) yields,

(4-27) $$\Delta T_F = \frac{q'}{4\pi \langle \lambda_F \rangle}.$$

Equation (4-27) reveals that the fuel temperature drop is a function of the linear power density and the averaged fuel thermal conductivity.

In a similar manner the temperature drop across the gas gap can be obtained. In particular, Eq. (4-21) can be used to describe the temperature distribution in the gas gap, however, unlike for the fuel pellet, the heat source term is equal to zero and the gas thermal conductivity can be assumed constant, thus,

(4-28) $$-\frac{1}{r}\frac{d}{dr}\lambda_G r \frac{dT_G}{dr} = 0 \Rightarrow \lambda_G r \frac{dT_G}{dr} = C_1 \Rightarrow T_G(r) = \frac{C_1}{\lambda_G} \ln r + C_2 .$$

The integration constant C_1 can be found from the condition of the heat flux continuity at $r = r_{Fo}$,

(4-29) $$-\lambda_G \left.\frac{dT_G}{dr}\right|_{r=r_{Fo}} = -\frac{C_1}{r_{Fo}} = \frac{q'}{2\pi r_{Fo}} \Rightarrow C_1 = -\frac{q'}{2\pi},$$

and the temperature drop in the gap is found as,

(4-30) $$\Delta T_G = T_G(r_{Gi}) - T_G(r_{Go}) = \frac{q'}{2\pi\lambda_G} \ln \frac{r_{Go}}{r_{Gi}}.$$

Equation (4-30) is applicable to the clad material as well, since the assumptions on the heat generation and the thermal conductance are valid in this case as well. Substituting the proper dimensions and property data yields,

$$\Delta T_C = T_C(r_{Ci}) - T_C(r_{Co}) = \frac{q'}{2\pi\lambda_C}\ln\frac{r_{Co}}{r_{Ci}}, \tag{4-31}$$

where r_{Co} is the outer clad radius and λ_C is the clad thermal conductivity.

Heat transfer from the clad surface to the coolant is described by the following equation,

$$q'' = h(T_{Co} - T_{lb}), \tag{4-32}$$

where h is the convective heat-transfer coefficient. Taking into account that $q'' = q'/(2\pi r_{Co})$, the temperature drop in the coolant boundary layer is found as,

$$\Delta T_l \equiv T_{Co} - T_{lb} = \frac{q'}{2\pi r_{Co} h}. \tag{4-33}$$

The total temperature drop from the fuel centerline to the coolant is now obtained as,

$$\Delta T = \Delta T_F + \Delta T_G + \Delta T_C + \Delta T_l =$$
$$\frac{q'}{2\pi}\left(\frac{1}{2\langle\lambda_F\rangle} + \frac{1}{\lambda_G}\ln\frac{r_{Go}}{r_{Gi}} + \frac{1}{\lambda_C}\ln\frac{r_{Co}}{r_{Ci}} + \frac{1}{r_{Co}h}\right). \tag{4-34}$$

The total temperature drop in a fuel rod cross-section is illustrated in FIGURE 4-11.

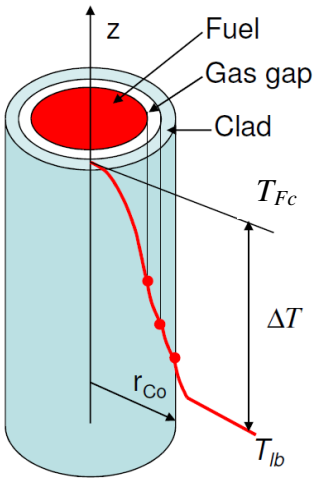

FIGURE 4-11. Temperature drops in a fuel rod.

EXAMPLE 4-1: During normal operation of a nuclear reactor, the highest power density in fuel pellets is equal to 900 MW m^{-3}. Find an increase of the maximum fuel and clad temperature if suddenly the heat transfer coefficient at the clad surface drops due to CHF from 50000 to 2000 W m^{-2} K^{-1}. The fuel rod geometry is shown in FIGURE 4-12. SOLUTION: From Eq. (4-34) it is clear that the only temperature drop that is affected by a change in the heat transfer coefficient is given by Eq. (4-33). The temperature drops in the gas gap, as well as in the fuel pellet and in the clad wall will remain the same, since the power density, and thus the linear power, as well as material properties and dimensions remain the same. Thus the temperature increase will be the same in all parts of the fuel rod and will be equal to $\Delta T = \Delta T_{l1} - \Delta T_{l1} = q'/(2\pi r_{Co} h_1) - q'/(2\pi r_{Co} h_2)$, where h_1 is the heat transfer coefficient before the occurrence of CHF and h_2 is the heat transfer coefficient after the occurrence of CHF. From Eq. (4-26) the linear power density is found as $q' = \pi r_{Fo}^2 q''' \cong 49.876$ kW/m. Thus $\Delta T = q'/(2\pi r_{Co})(1/h_1 - 1/h_2) \cong 793.8$ K. It can be seen that with this increase of the clad temperature the safety limit value (which is typically about 900 K) will be exceeded and the clad damage may occur.

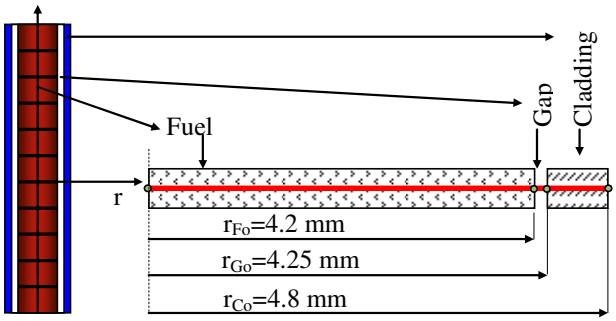

FIGURE 4-12: Fuel element used for calculations in EXAMPLE 4-1.

EXAMPLE 4-2: Calculate temperature drops in a fuel pellet, gas gap, clad and the thermal boundary layer using the following typical data for PWR: dimensions – pellet outer diameter d_{Fo} = 8.25 mm, gas gap outer diameter d_{Go} = 8.43 mm, clad outer diameter d_{Go} = 9.70 mm; thermal conductivity – clad λ_C = 11 W/m.K, gas gap λ_G = 0.6 W/m.K, fuel (UO_2) λ_F = 2.5 W/m.K; heat transfer coefficient h = 45000 W/m^2.K and linear power density q' = 41 kW/m. Calculate the maximum allowed linear power density if the fuel temperature shouldn't exceed the melting temperature (3073 K) and the coolant temperature is 600 K. SOLUTION: The temperature drops are obtained as follows,

$$\Delta T_F = \frac{q'}{4\pi\langle\lambda_F\rangle} = \frac{41000}{4\pi \cdot 2.5} = 1305.07 \text{ K}$$

$$\Delta T_G = \frac{q''' r_{Fo}^2}{2\lambda_G} \ln\left(\frac{r_{Go}}{r_{Fo}}\right) = \frac{q'}{2\pi\lambda_G} \ln\left(\frac{r_{Go}}{r_{Fo}}\right) = \frac{41000}{2\pi \cdot 0.6} \ln\left(\frac{8.43}{8.25}\right) = 234.73 \text{ K}$$

$$\Delta T_C = \frac{q'}{2\pi\lambda_C} \ln\left(\frac{r_{Co}}{r_{Go}}\right) = \frac{41000}{2\pi \cdot 11} \ln\left(\frac{9.7}{8.43}\right) = 83.25 \text{ K}$$

$$\Delta T_l = \frac{q''' r_{Fo}^2}{2 r_{Co} h} = \frac{q'}{2\pi r_{Co} h} = \frac{41000}{\pi 0.0097 \cdot 45000} = 29.9 \text{ K}$$

Thus the total temperature drop from the pellet center to the fluid bulk is as follows,

$$\Delta T = \Delta T_F + \Delta T_G + \Delta T_C + \Delta T_l = 1652.95 \text{ K} \cdot$$

The maximum allowed linear power can be found from the expression for the total temperature drop in a fuel element,

$$\Delta T = \frac{q'}{4\pi}\left[\frac{1}{\lambda_F}+\frac{2}{\lambda_G}\ln\left(\frac{r_{Go}}{r_{Fo}}\right)+\frac{2}{\lambda_C}\ln\left(\frac{r_{Co}}{r_{Go}}\right)+\frac{2}{r_{Co}h}\right].$$

Thus, the maximum linear power is obtained as,

$$q'_{\max} = \frac{4\pi(T_{melt}-T_{cool})}{\left[\frac{1}{\lambda_F}+\frac{2}{\lambda_G}\ln\left(\frac{r_{Go}}{r_{Fo}}\right)+\frac{2}{\lambda_C}\ln\left(\frac{r_{Co}}{r_{Go}}\right)+\frac{2}{r_{Co}h}\right]} = 61340.7\,\frac{\mathrm{W}}{\mathrm{m}}$$

4.2.4 Axial Temperature Distribution in Fuel Rods

In the previous section expressions for the axial distribution of coolant temperature have been derived. It has been shown that the axial distribution of coolant temperature varies with the shape of the axial heat flux distribution.

In particular, substituting Eqs. (4-17) and (4-19) into (4-32) yields the following expression for the temperature of the clad outer surface,

$$T_{Co}(z) = \frac{q''_0 \cdot P_H \cdot \tilde{H}}{\pi \cdot W \cdot c_p}\cdot\left[\sin\left(\frac{\pi z}{\tilde{H}}\right)+\sin\left(\frac{\pi H}{2\tilde{H}}\right)\right]+\frac{q''_0}{h}\cdot\cos\left(\frac{\pi z}{\tilde{H}}\right)+T_{lbi}\,. \tag{4-35}$$

FIGURE 4-13 shows the temperature of the clad outer surface as a function of the axial distance.

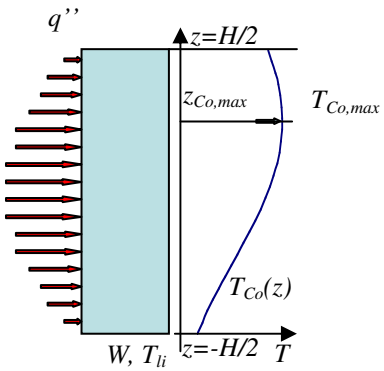

FIGURE 4-13: Axial distribution of the temperature of the clad outer surface with cosine axial power distribution in a channel.

It should be noted that the temperature of the clad outer surface gets its maximum value $T_{Co,max}$ at a certain location $z_{Co,max}$. This location can be found from Eq. (4-35) using the following condition,

$$\left.\frac{dT_{Co}(z)}{dz}\right|_{z=z_{Co,\max}} = 0\,. \tag{4-36}$$

It is convenient to represent the clad outer temperature as,

(4-37) $$T_{Co}(z) = A + B\sin\left(\frac{\pi z}{\tilde{H}}\right) + C_{Co}\cdot\cos\left(\frac{\pi z}{\tilde{H}}\right),$$

where,

(4-38) $$A = B\cdot\sin\left(\frac{\pi H}{2\tilde{H}}\right) + T_{lbi},\ B = \frac{q_0''\cdot P_H\cdot\tilde{H}}{\pi\cdot W\cdot c_p},\ C_{Co} = \frac{q_0''}{h}.$$

Using Eq. (4-37) in Eq. (4-36) yields,

$$B\cos\left(\frac{\pi z_{Co,\max}}{\tilde{H}}\right) - C_{Co}\sin\left(\frac{\pi z_{Co,\max}}{\tilde{H}}\right) = 0,$$

which is equivalent to the following equation,

$$\tan\left(\frac{\pi z_{Co,\max}}{\tilde{H}}\right) = \frac{B}{C_{Co}}.$$

Thus,

(4-39) $$z_{Co,\max} = \frac{\tilde{H}}{\pi}\arctan\left(\frac{B}{C_{Co}}\right).$$

It should be noted that a physically meaningful solution of the above equation should be positive and less than H.

Noting that,

$$\sin\left(\frac{\pi z_{Co,\max}}{\tilde{H}}\right) = \pm\frac{\tan\left(\frac{\pi z_{Co,\max}}{\tilde{H}}\right)}{\sqrt{1+\tan^2\left(\frac{\pi z_{Co,\max}}{\tilde{H}}\right)}} = \pm\frac{\frac{B}{C_{Co}}}{\sqrt{1+\left(\frac{B}{C_{Co}}\right)^2}},$$

and

$$\cos\left(\frac{\pi z_{Co,\max}}{\tilde{H}}\right) = \pm\frac{1}{\sqrt{1+\tan^2\left(\frac{\pi z_{Co,\max}}{\tilde{H}}\right)}} = \pm\frac{1}{\sqrt{1+\left(\frac{B}{C_{Co}}\right)^2}},$$

the maximum temperature of the clad outer surface becomes (taking only + sign),

(4-40) $$T_{Co,\max} = A + \sqrt{B^2 + C_{Co}^2}.$$

Using constants A, B and C_{Co} given by Eq. (4-38), the maximum clad outer temperature is obtained as,

$$T_{Co,\max} = \frac{q_0'' \cdot P_H \cdot \tilde{H}}{\pi \cdot W \cdot c_p} \cdot \sin\left(\frac{\pi H}{2\tilde{H}}\right) + T_{lbi} + \sqrt{\left(\frac{q_0'' \cdot P_H \cdot \tilde{H}}{\pi \cdot W \cdot c_p}\right)^2 + \left(\frac{q_0''}{h}\right)^2}, \tag{4-41}$$

or,

$$\frac{\pi \cdot W \cdot c_p \left(T_{Co,\max} - T_{lbi}\right)}{q_0'' \cdot P_H \cdot \tilde{H}} = \sin\left(\frac{\pi H}{2\tilde{H}}\right) + \sqrt{1 + \left(\frac{\pi \cdot W \cdot c_p}{P_H \cdot \tilde{H} \cdot h}\right)^2}. \tag{4-42}$$

Since the clad maximum temperature is located on the inner surface, it is of interest to find it as well. The axial distribution of the clad inner temperature can be obtained from Eqs. (4-31) and (4-35) as,

$$\begin{aligned} T_{Ci}(z) &= \Delta T_C + T_{Co}(z) = \\ &\frac{q'}{2\pi\lambda_C} \ln\frac{r_{Co}}{r_{Ci}} + \frac{q_0'' \cdot P_H \cdot \tilde{H}}{\pi \cdot W \cdot c_p} \cdot \left[\sin\left(\frac{\pi z}{\tilde{H}}\right) + \sin\left(\frac{\pi H}{2\tilde{H}}\right)\right] + \frac{q_0''}{h} \cdot \cos\left(\frac{\pi z}{\tilde{H}}\right) + T_{lbi} = \\ &\frac{q_0'' \cdot P_H \cdot \tilde{H}}{\pi \cdot W \cdot c_p} \cdot \left[\sin\left(\frac{\pi z}{\tilde{H}}\right) + \sin\left(\frac{\pi H}{2\tilde{H}}\right)\right] + q_0''\left(\frac{r_{Co}}{\lambda_C} \ln\frac{r_{Co}}{r_{Ci}} + \frac{1}{h}\right)\cos\left(\frac{\pi z}{\tilde{H}}\right) + T_{lbi} \end{aligned} \tag{4-43}$$

Equation (4-43) can be expressed in a short form as,

$$T_{Ci}(z) = A + B\sin\left(\frac{\pi z}{\tilde{H}}\right) + C_{Ci}\cos\left(\frac{\pi z}{\tilde{H}}\right). \tag{4-44}$$

Here A and B are given by Eq. (4-38) and,

$$C_{Ci} = q_0''\left(\frac{r_{Co}}{\lambda_C} \ln\frac{r_{Co}}{r_{Ci}} + \frac{1}{h}\right). \tag{4-45}$$

Using the same approach as in the case of the clad outer temperature, the location of the maximum temperature on the clad inner surface is found as,

$$z_{Ci,\max} = \frac{\tilde{H}}{\pi}\arctan\left(\frac{B}{C_{Ci}}\right), \tag{4-46}$$

and the corresponding maximum temperature is,

$$\begin{aligned} T_{Ci,\max} &= \frac{q_0'' \cdot P_H \cdot \tilde{H}}{\pi \cdot W \cdot c_p} \cdot \sin\left(\frac{\pi H}{2\tilde{H}}\right) + T_{lbi} + \\ &\sqrt{\left(\frac{q_0'' \cdot P_H \cdot \tilde{H}}{\pi \cdot W \cdot c_p}\right)^2 + \left[q_0''\left(\frac{r_{Co}}{\lambda_C} \ln\frac{r_{Co}}{r_{Ci}} + \frac{1}{h}\right)\right]^2} \end{aligned} \tag{4-47}$$

In a similar manner the fuel maximum temperature at the centerline can be found as,

$$T_{Fc}(z) = A + B\sin\left(\frac{\pi z}{\tilde{H}}\right) + C_{Fc}\cos\left(\frac{\pi z}{\tilde{H}}\right) \tag{4-48}$$

where

$$C_{Fc} = q_0''\left(\frac{r_{Co}}{\lambda_C}\ln\frac{r_{Co}}{r_{Ci}} + \frac{r_{Co}}{\lambda_G}\ln\frac{r_{Go}}{r_{Gi}} + \frac{r_{Co}}{2\langle\lambda_F\rangle} + \frac{1}{h}\right) \tag{4-49}$$

The maximum fuel temperature is located at,

$$z_{Fc,\max} = \frac{\tilde{H}}{\pi}\arctan\frac{B}{C_{Fc}}, \tag{4-50}$$

and its value is found as,

$$T_{Fc,\max} = \frac{q_0''\cdot P_H\cdot\tilde{H}}{\pi\cdot W\cdot c_p}\cdot\sin\left(\frac{\pi H}{2\tilde{H}}\right) + T_{lbi} + \sqrt{\left(\frac{q_0''\cdot P_H\cdot\tilde{H}}{\pi\cdot W\cdot c_p}\right)^2 + \left[q_0''\left(\frac{r_{Co}}{\lambda_C}\ln\frac{r_{Co}}{r_{Ci}} + \frac{r_{Co}}{\lambda_G}\ln\frac{r_{Go}}{r_{Gi}} + \frac{r_{Co}}{2\langle\lambda_F\rangle} + \frac{1}{h}\right)\right]^2}. \tag{4-51}$$

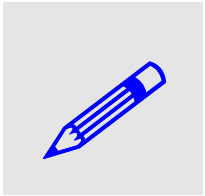

EXAMPLE 4-3. Calculate the axial temperature distribution of coolant, clad and fuel in a subchannel of a PWR fuel assembly. The fuel pellets with 8.2 mm diameter are clad with zircaloy 0.56 mm thick. The outer diameter of the clad rod is 9.6 mm. The coolant bulk inlet temperature is 588 K, mass flow rate per unit subchannel is 0.4 kg/s, the pressure is 155 bar, and the axial heat flux distribution on the clad outer surface is $q''(z) = 2\cdot10^5\cos(\pi z/\tilde{H})$ [W], where H = 3.7 m and the extrapolation length is 0.1 m. Use the same material properties as given in EXAMPLE 4-2 and assume lattice pitch-to-diameter ratio equal to 1.2. Calculate the heat transfer coefficient from the Dittus-Boelter correlation, using fluid properties at inlet temperature and pressure. SOLUTION: The flow cross-section of the subchannel is obtained as A_{xs} = 6.03x10^{-5} m^2 and the mass flux is obtained as $G = W/A_{xs}$ = 6630 kg/m^2.s. Using the Dittue-Boelter correlation, the heat transfer coefficient is obtained as h = 65347 W/m^2.K. Now the constants A, B and C_{Co} can be found as

$$B = \frac{q_0''\cdot P_H\cdot\tilde{H}}{\pi\cdot W\cdot c_p} \cong 3.159\ \text{K}$$

$$A = B\cdot\sin\left(\frac{\pi H}{2\tilde{H}}\right) + T_{lbi} \cong 591.149\ \text{K}$$

$$C_{Co} = \frac{q_0''}{h} \cong 3.061\ \text{K}$$

Thus, the clad outer temperature is given as,

$$T_{Co}(z) = A + B\cdot\sin\left(\frac{\pi z}{\tilde{H}}\right) + C_{Co}\cdot\cos\left(\frac{\pi z}{\tilde{H}}\right) = 591.149 + 3.159\cdot\sin(0.8055z) + 3.061\cdot\cos(0.8055z)$$

The maximum temperature of the clad outer surface is found as,

$$T_{Co,\max} = A + \sqrt{B^2 + C_{Co}^2} \cong 595.6\ \text{K}$$

and it is located at

$$z_{Co,\max} = \frac{\tilde{H}}{\pi}\arctan\left(\frac{B}{C_{Co}}\right) \cong 0.995\ \text{m}$$

Similar calculations are performed for the clad inner surface and for the fuel centerline. The calculated temperature distributions are shown in FIGURE 4-14.

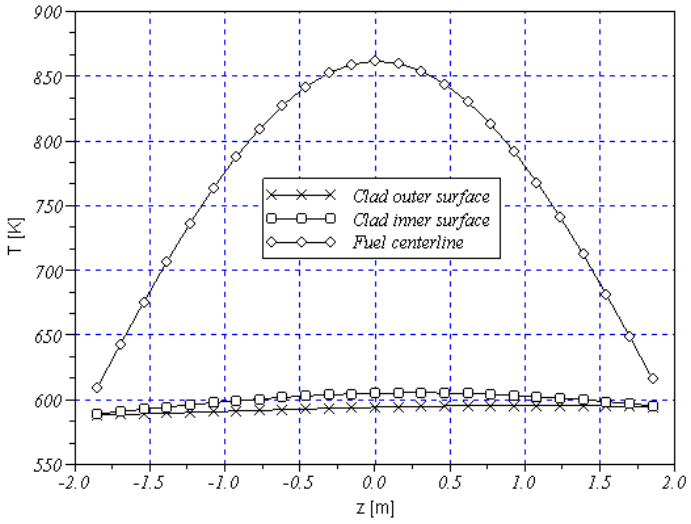

FIGURE 4-14: Axial distribution of temperature in fuel rod described in EXAMPLE 4-3.

4.3 Void Fraction in Boiling Channels

The characteristic feature of boiling channels is the presence of two phases: the liquid and the vapor phase. Clearly, the presence of two phases changes the fluid flow and heat transfer processes as compared to the non-boiling channels. In addition, the density changes of coolant are more significant in boiling channels due to the dramatic change of density once liquid transforms into vapor. Thus, to be able to predict the local value of the coolant density it is required to determine the local volume fraction of both phases. Typically, the void fraction (that is the volume fraction of the vapor phase) is determined using various models, as described below.

The various two-phase flow and heat transfer regimes in a boiling channel, such as BWR fuel assembly, is shown in FIGURE 4-15.

In the simplest two-phase flow model it is assumed that both phases are in the thermodynamic equilibrium and that they move with the same velocity. These assumptions are the basis of the **Homogeneous Equilibrium Model** (HEM), in which the local, channel-average void fraction is determined from the corresponding local value of the equilibrium thermodynamic quality.

4.3.1 Homogeneous Equilibrium Model

The HEM expression for the void fraction takes the following form,

$$\alpha = \begin{cases} 0 & \text{for} \quad x_e \le 0 \\ \dfrac{1}{1+\dfrac{\rho_g}{\rho_f}\cdot\left(\dfrac{1-x_e}{x_e}\right)} & \text{for} \quad 0 < x_e < 1 \\ 1 & \text{for} \quad x_e \ge 1 \end{cases} . \tag{4-52}$$

Here x_e is the equilibrium thermodynamic quality, which is determined from the energy balance of the coolant in the heated channel.

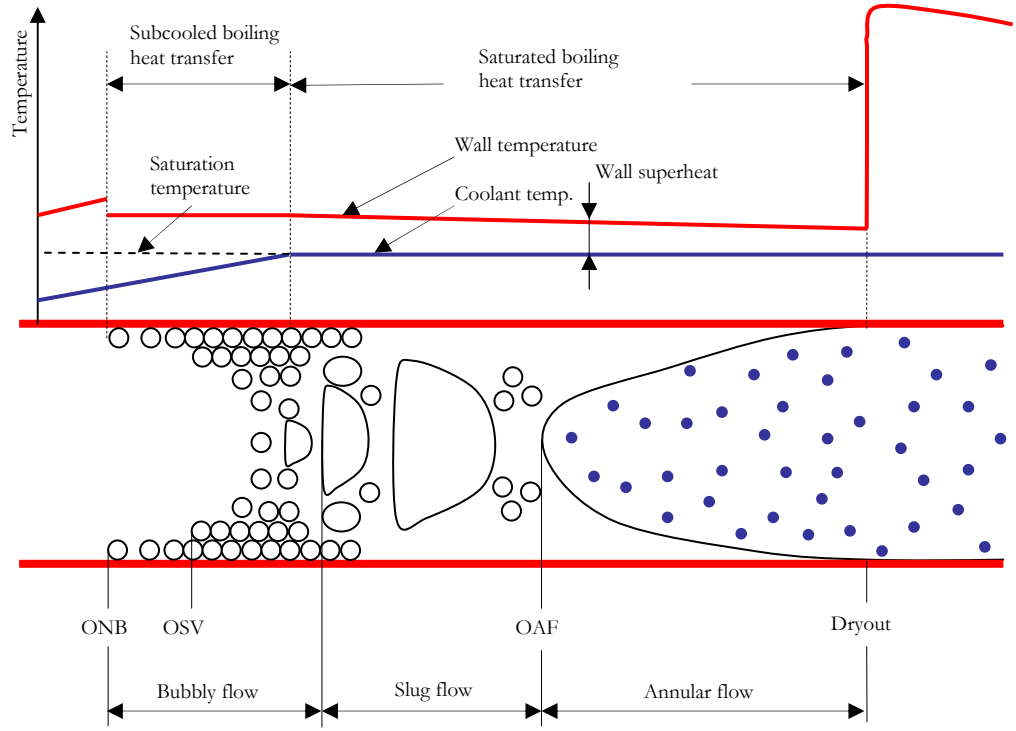

FIGURE 4-15: Two-phase flow and heat transfer regimes in a boiling channel: ONB – Onset of Boiling, OSV – Onset of Significant Void, OAF – Onset of Annular Flow.

Equation (4-52) strongly over-predicts the coolant density (that is it gives a higher value than the actual one) in the region of sub-cooled boiling, since it assumes only liquid, whereas in reality both the liquid and the vapor co-exist in that region.

4.3.2 Drift-Flux Model

Once applying the **Drift-Flux Model**, the void fraction is found as,

$$\alpha = \frac{J_v}{C_0 J + U_{vj}} \tag{4-53}$$

Equation (4-53) expresses the cross-section mean void fraction α in terms of channel mean superficial velocity of gas, J_v, total superficial velocity, J, and two parameters, C_0 and U_{vj}. The first parameter is the so-called **drift-flux distribution parameter** and is simply a covariance coefficient for cross-section distributions of void fraction and total superficial velocity. The second coefficient is the so-called **drift velocity** and can be interpreted as cross-section-averaged difference between the gas velocity and the superficial velocity, using local the void fraction as a weighting function. The drift-flux parameters are not constant and depend on flow conditions. TABLE 4.2 gives expressions for drift-flux parameters, which are valid in a wide range of flow conditions.

TABLE 4.2. Distribution parameter and drift velocity used drift-flux model.

Flow pattern	Distribution parameter	Drift velocity
Bubbly $0 < \alpha \le 0.25$	$C_0 = \begin{cases} 1 - 0.5\,p/p_{cr} & D_h \ge 0.05 \text{ m} \\ 1.2 \quad p/p_{cr} < 0.5 & D_h < 0.05 \text{ m} \\ 1.4 - 0.4\,p/p_{cr} \quad p/p_{cr} \ge 0.5 & \end{cases}$ [1]	$U_{vj} = 1.41\left(\frac{\sigma g(\rho_l - \rho_v)}{\rho_l^2}\right)^{0.25}$ [2]
Slug/churn $0.25 < \alpha \le 0.75$	$C_0 = 1.15$	$U_{vj} = 0.35\left(\frac{gD_h(\rho_l - \rho_v)}{\rho_l}\right)^{0.5}$
Annular $0.75 < \alpha \le 0.95$	$C_0 = 1.05$	$U_{vj} = 23\left(\frac{\mu_l j_l}{\rho_v D_h}\right)^{0.5}\frac{(\rho_l - \rho_v)}{\rho_l}$
Mist $0.95 < \alpha < 1$	$C_0 = 1.0$	$U_{vj} = 1.53\left(\frac{\sigma g(\rho_l - \rho_v)}{\rho_v^2}\right)^{0.25}$ [2]

[1] p_{cr} – critical pressure, [2] σ - surface tension

4.3.3 Subcooled Boiling Region

It is commonly accepted that a significant void fraction in a boiling channel appears at locations where bubbles depart from heated walls. The void fraction between that point, referred often as the **Onset of Significant Void fraction** (OSV) point, and the Onset of Nucleate Boiling (ONB) point is very small and can be neglected.

To establish the location of the OSV point it is recommended to use a correlation proposed by Saha and Zuber (1974), which states that OSV point is located at such position in a channel, where the local equilibrium quality is as follows,

$$x_{e,OSV} = \begin{cases} -0.0022\dfrac{q'' \cdot D_h \cdot c_{pf}}{i_{fg} \cdot \lambda_f} & \text{for} \quad \text{Pe} < 70000 \\ -154\dfrac{q''}{G \cdot i_{fg}} & \text{for} \quad \text{Pe} \ge 70000 \end{cases} \tag{4-54}$$

Here Pe is the Peclet number defined as,

$$\text{Pe} = \frac{G \cdot D_h \cdot c_{pf}}{\lambda_f}. \tag{4-55}$$

For a uniform heat flux distribution, the location of the OSV point is found from the energy balance as,

$$z_{OSV} = (x_{e,OSV} - x_{ei})\frac{W \cdot i_{fg}}{q'' \cdot P_H}. \tag{4-56}$$

Several models have been proposed to predict the flow quality downstream of the OSV point. Levy (1966) proposed a fitting relationship, which satisfy a condition at $z = z_{NVG}$, where $x = 0$ and also which will predict the flow quality to approach the equilibrium quality when z is increasing downstream of the OSV point. The Levy's relationship is as follows,

(4-57) $$x_a(z) = x_e(z) - x_e(z_{OSV}) \cdot e^{\frac{x_e(z)}{x_e(z_{OSV})}-1}.$$

Having the flow quality given by Eq. (4-57), one can apply the general drift flux model to calculate the void fraction distribution. The recommended expression for the distribution parameter for subcooled boiling is as follows,

(4-58) $$C_0 = \beta\left[1+\left(\frac{1}{\beta}\right)^b\right],$$

where,

(4-59) $$\beta = \frac{1}{1+\frac{\rho_g}{\rho_f}\frac{1-x_a(z)}{x_a(z)}},$$

(4-60) $$b = \left(\frac{\rho_g}{\rho_f}\right)^{0.1}.$$

The recommended by Lahey and Moody (1977) drift velocity is as follows,

(4-61) $$U_{vj} = 2.9\left(\frac{\sigma g(\rho_f - \rho_g)}{\rho_f^2}\right)^{0.25}.$$

This is similar to the expression recommended for bubbly flow (see TABLE 4.2) but a different constant should be used.

4.4 Heat Transfer to Coolants

4.4.1 Single-phase flow

The heat transfer coefficient h for coolant flow in a rod bundle is calculated from the Nusselt number Nu as follows,

(4-62) $$h = \frac{\mathrm{Nu}\cdot\lambda}{D_h},$$

where λ is the fluid thermal conductivity and D_h is the bundle hydraulic diameter.

For laminar flow far from the inlet to a channel, the Nusselt number is as follows,

(4-63) $$Nu = 4.364.$$

In the inlet region of the channel the following expression is valid,

(4-64) $$Nu = 1.31\frac{(1+2\varsigma)}{\sqrt[3]{\varsigma}}, \quad (0 < \varsigma < 0.04)$$

where

(4-65) $$\varsigma = \frac{z}{D_h} Pe$$

and Pe is the Peclet dimensionless number given as,

(4-66) $$\mathrm{Pe} = \frac{UD_h}{a}.$$

For turbulent flow in a pipe the Nusselt number can be calculated from the **Dittus-Boelter correlation**,

(4-67) $$\mathrm{Nu} = 0.023\,\mathrm{Re}^{0.8}\,\mathrm{Pr}^{n}.$$

Here Pr is the Prandtl number; Pr = *v*/*a*, and *v* is the kinematic viscosity of liquid. The formula is valid for Re > 10^4 and 0.7 < Pr < 100, n = 0.4 for fluid heating and n = 0.3 for fluid cooling.

Petukhov [4-6] proposed the following semi-empirical expression for the Nusselt number for turbulent flow in pipes,

(4-68) $$\mathrm{Nu} = \frac{(C_{f,p}/2)\mathrm{Re}\,\mathrm{Pr}}{1+13.6C_{f,p}+\left(11.7+1.8\,\mathrm{Pr}^{-1/3}\right)\sqrt{C_{f,p}/2}\left(\mathrm{Pr}^{2/3}-1\right)},$$

where C_{fp} is given by Eq. (4-92).

For rod bundles with triangular lattice and with 1.1 < *p*/*d* < 1.8 Ushakov (presented in [4-7]) proposed the following correlation,

(4-69) $$\mathrm{Nu} = \left\{0.0165+0.02\left[1-\frac{0.91}{(p/d)^2}\right]\left(\frac{p}{d}\right)^{0.15}\right\}\cdot \mathrm{Re}^{0.8}\,\mathrm{Pr}^{0.4},$$

where the correlation is valid for $5\cdot10^3$ < Re < $5\cdot10^5$ and 0.7 < Pr < 20.

Similar correlation was derived by Weissman[4-14],

(4-70) $$\mathrm{Nu} = C\,\mathrm{Re}^{0.8}\,\mathrm{Pr}^{1/3},$$

where:

$C = 0.026(p/d) - 0.024$ for triangular lattices with $1.1 < p/d < 1.5$,

$C = 0.042(p/d) - 0.024$ for square lattices with $1.1 < p/d < 1.3$.

Subbotin et al. recommended for heat transfer to liquids flowing in a bundle with triangular lattice the following correlation,

(4-71) $$\mathrm{Nu} = A\,\mathrm{Re}^{0.8}\,\mathrm{Pr}^{0.4},$$

where,

$$A = 0.0165 + 0.02\left[1 - \frac{0.91}{(p/d)^2}\right]\left(\frac{p}{d}\right)^{0.15}. \tag{4-72}$$

The correlation is valid for $1.1 < p/d < 1.8$, $1.0 < \mathrm{Pr} < 20$ and $5.10^3 < \mathrm{Re} < 5.10^5$.

For gas flow in tight rod bundles Ajn and Putjkov give,

$$\frac{\mathrm{Nu}_{\mathrm{bundle}}}{\mathrm{Nu}_{\mathrm{DB}}} = 1.184 + 0.351 \cdot \lg(p/d - 1). \tag{4-73}$$

The correlation is valid for $1.03 < p/d < 2.4$ and $\mathrm{Nu}_{\mathrm{DB}}$ is found from the Dittus-Boelter correlation given by Eq. (4-67).

Markoczy performed a study of experimental data obtained in 63 rod bundles with different geometry details and proposed the following relationship,

$$\frac{\mathrm{Nu}_{\mathrm{bundle}}}{\mathrm{Nu}_{\mathrm{DB}}} = 1 + 0.91\mathrm{Re}^{-0.1}\,\mathrm{Pr}^{0.4}\left(1 - 2e^{-B}\right), \tag{4-74}$$

where,

$$B = \begin{cases} \dfrac{2\sqrt{3}}{\pi}\left(\dfrac{p}{d}\right)^2 & \text{triangular lattice} \\ \dfrac{4}{\pi}\left(\dfrac{p}{d}\right)^2 - 1 & \text{square lattice} \end{cases}. \tag{4-75}$$

Here again $\mathrm{Nu}_{\mathrm{DB}}$ is found from the Dittus-Boelter correlation given by Eq. (4-67). The correlation is applicable in the following range of parameters:

$3 \cdot 10^3 < \mathrm{Re} < 10^6$

$0.66 < \mathrm{Pr} < 5$

$1.02 < p/d < 2.5$.

Another approach was proposed by Osmachkin [4-4], who recommended to calculate the Nusselt number from correlations which are valid for pipes, replacing however the hydraulic diameter with the "effective" one given by Eq. (4-90).

4.4.2 Two-phase boiling flow

Heat transfer coefficient for two-phase boiling flow can be predicted from various correlations, for example from the Jens Lottes (subcooled boiling) and the Chen (saturated boiling) correlations, described in [4-1].

A simple estimation of the boiling heat transfer coefficient can be obtained from a correlation proposed by Rasohin [4-8],

(4-76) $$h = \begin{cases} 5.5\,p^{0.25}(q'')^{2/3} & for \quad 0.1 < p \le 8 \\ 0.577\,p^{1.33}(q'')^{2/3} & for \quad 8 < p < 20 \end{cases},$$

where h is heat transfer coefficient [W/m^{2}K], p is pressure [MPa] and q'' is heat flux [W/m^2].

4.4.3 Liquid metal flow

Due to high thermal conductivity of liquid metals, the correlations for heat transfer coefficients differ from those for water and gases.

Comprehensive studies have been made on heat transfer to various liquid metals (Hg, Na, NaK, PbBi, Li, etc). Experiments performed in tubes indicate that a purity of the liquid metal is of importance. In highly pure liquid metals heat transfer is more intensive and can be described with the following correlation,

(4-77) $$\mathrm{Nu} = 5.0 + 0.025 \cdot \mathrm{Pe}^{0.8},$$

where Pe is the Peclet number defined as,

(4-78) $$\mathrm{Pe} = \mathrm{Re} \cdot \mathrm{Pr} = \frac{D_h U \rho c_p}{\lambda}.$$

If no special measures are undertaken to purify the liquid metal, the heat transfer is slightly deteriorated due to a deposition of oxide layer on the solid surface. Heat transfer coefficient is then obtained from the following equation,

(4-79) $$\mathrm{Nu} = 3.3 + 0.014 \cdot \mathrm{Pe}^{0.8}.$$

There are several correlations which are applicable to fuel rod bundles. The following correlation has been proposed by Dwyer,

(4-80) $$\mathrm{Nu} = 6.66 + 3.126s + 1.184s^2 + 0.0155(\Psi \cdot \mathrm{Pe})^{0.86},$$

where,

$$\Psi = 1 - \frac{0.942 s^{1.4}}{\mathrm{Pr}\left(\mathrm{Re}/10^3\right)^{1.281}},$$

and $s = p/d$. Here Nu is the Nusselt number, p and d are lattice pitch and rod diameter, respectively; Pr is the Prandtl number and Pe is the Peclet number defined by Eq. (4-78). Equation (4-80) is valid for $s > 1.35$.

For tightly packed square lattices, the following correlation is applicable,

(4-81) $$\mathrm{Nu} = 0.48 + 0.0133\mathrm{Pe}^{0.70}.$$

For triangular lattice, the following correlations have been proposed:

Borishanski et al.:

(4-82) $$\mathrm{Nu} = 24.151 \cdot \lg\left[-8.12 + 12.76s - 3.65s^2\right] + 0.0174\left[1 - e^{-6(s-1)}\right](\mathrm{Pe} - 200)^{0.9},$$

Graber:

(4-83) $$\mathrm{Nu} = 0.25 + 6.2s + (0.32s - 0.07) \cdot \mathrm{Pe}^{(0.8\text{-}0.024s)},$$

Calamai et al.:

(4-84) $$\mathrm{Nu} = 4 + 0.16s^5 + 0.33s^{3.8} \cdot \left(\frac{\mathrm{Pe}}{100}\right)^{0.86}.$$

For square lattice, the following correlation has been proposed by Zhukov:

(4-85) $$\mathrm{Nu} = 7.55s - 14s^{-5} + A \cdot \mathrm{Pe}^{(0.64+0.264s)},$$

where A = 0.09 for rod bundles with spacers and A = 0.07 for rod bundles without spacers.

It has been demonstrated that the Nusselt number for the square lattice is lower than that for triangular lattice bundles, assuming that all other parameters are the same.

4.4.4 Supercritical water flow

Supercritical water is used as the working fluid in conventional coal-fired power plants and is considered as coolant in one of the six reactor system concepts envisaged to deployment after year 2025 (so-called Generation IV reactors). Supercritical water is an attractive coolant, since the occurrence of the boiling crisis is eliminated. However, under certain conditions so-called heat transfer deterioration may occur, which require application of proper correlations to correctly predict temperatures of heated walls.

Critical parameters for water are 22.1 MPa and 374.1 °C. Typical parameters considered for reactors cooled with critical water are 25 MPa and temperature in a range from 280 to 580 °C. In this range of parameters, the water property exhibit anomaly at the pseudo-critical temperature (which for pressure 25 MPa is 384.86 °C). FIGURE 4-16 shows the temperature dependence of selected properties.

The significant change of physical properties around the pseudo-critical point is accompanied with anomalous heat transfer results observed in experiments, e.g. [4-10] and [4-11]. The current understanding of the governing phenomena indicates that the change of properties is not enough to explain the heat transfer anomalies. It is believed that the onset of the heat transfer anomaly depends both on fluid property variation as well as on the flow acceleration and buoyancy effects. However, the mechanism is still not fully understood.

The heat transfer anomaly manifests itself as either enhancement or deterioration of heat transfer coefficient. The latter is of particular interest, since it brings about an increase of the heated wall temperature.

Unlike the Critical Heat Flux (CHF), which occurs only for sub-critical pressures and which brings about a violent increase of the wall temperature, the **Heat Transfer Deterioration** (HTD) is connected to a rather mild wall temperature increase. Such

behavior creates a difficulty once trying to set a criterion for the onset of the HTD occurrence.

Definitions for HTD used in the literature are quite ambiguous, resulting probably from the mild character of the governing phenomena. Yamagata *et al.* **Error! Reference source not found.**] define the HTD condition as such, when the measured heat transfer coefficient is 'significantly' lower than that predicted from their own correlation, valid for low heat flux conditions. Based on that criterion, they proposed that the limit heat flux for the onset of HTD is as follows

$$q_c'' = 0.2 \cdot G^{1.2}, \quad (4\text{-}86)$$

where q_c'' is heat flux in [kW/m^2] and G is mass flux in [kg/m^2.s].

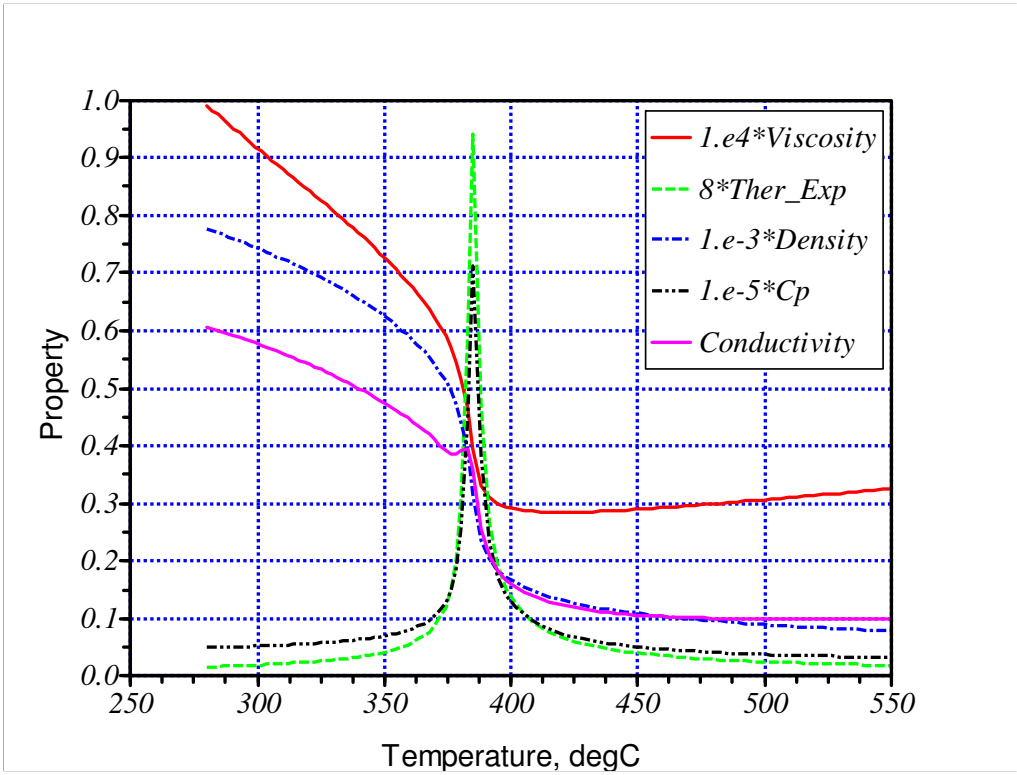

FIGURE 4-16: Property variation of supercritical water at 25 MPa pressure.

There are many correlations proposed for prediction of the heat transfer coefficient under deterioration conditions. One of the correlations that shows probably the best agreement with experiments was proposed by Jackson [4-12] and is as follows,

$$\mathrm{Nu_b} = 0.0183 \cdot \mathrm{Re}_b^{0.82}\, \mathrm{Pr}_b^{0.5} \left(\frac{\rho_w}{\rho_b}\right)^{0.3} \left(\frac{\overline{c_p}}{c_{pb}}\right)^n, \quad (4\text{-}87)$$

where the exponent n is given as:

For $T_b < T_w < T_{pc}$ and $1.2T_{pc} < T_b < T_w$, $n = 0.4$.

For $T_b < T_{pc} < T_w$, $n = 0.4 + 0.2\left(\frac{T_w}{T_{pc}} - 1\right)$.

For $T_{pc} < T_b < 1.2T_{pc}$ and $T_b < T_w$, $n = 0.4 + 0.2\left(\frac{T_w}{T_{pc}} - 1\right)\left[1 - 5\left(\frac{T_b}{T_{pc}} - 1\right)\right]$.

Here T is temperature in Kelvin, ρ is density and c_p is the specific heat. Indices b, pc and w in Eq. (4-87) refer to the bulk, pseudo-critical and wall temperature, respectively. The equation contains a modified specific heat calculated as,

$$\overline{c_p} = \frac{i_w - i}{T_w - T_b}.$$

It should be noted that the application of the correlation requires iterations, since in order to calculate the Nusselt number, the wall temperature has to be known.

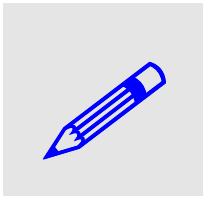

EXAMPLE 4-4. Calculate the wall temperature at the exit from a pipe with length L = 4.2 m and internal diameter D = 10 mm. The pipe is uniformly heated with total heat q = 150 kW and cooled with supercritical water at pressure p = 250 bars, inlet temperature 280 °C and inlet mass flux G = 450 kg/m^2.s. Apply both the Dittus-Boelter and the Jackson correlation and compare the results. SOLUTION: the inlet enthalpy is found from property functions for given pressure and temperature and is equal to i_{in} = 1.23 MJ/kg. The outlet enthalpy is found from the energy balance as follows: $i_{out} = i_{in} + 4q/(G \cdot \pi \cdot D^2)$ = 2.291 MJ/kg. From tables, the corresponding water temperature is found to be equal to 387.2 °C. This is the bulk temperature of the supercritical water at the outlet from the pipe. The dynamic viscosity of the water at the exit is found from tables as 3.42x10^{-5} Pa.s and the Prandtl number is 5.815. The heat transfer coefficient is found from the Dittus-Boelter correlation as h_{DB} = 16199.3 W/m^2.K. Since the heat flux is $q'' = q/(L \cdot \pi \cdot D)$ = 1136.8 kW/m^2, the wall temperature is found as $T_w = T_b + q''/h_{DB}$ = 457.4 °C. Similar calculations performed with the Jackson correlation (note that iterations are needed to find the modified specific heat) give the following heat transfer coefficient: h_J = 4587 W/m^2.K. This gives the wall temperature equal to $T_w = T_b + q''/h_J$ = 635 °C. As can be seen much higher wall temperature is obtained as compared to the temperature calculated with the Dittus-Boelter correlation.

4.5 Pressure Drops

Calculation of pressure drops in a reactor core is important since they influence the flow distribution in subchannels and thus affect the local thermal margins. In addition, the total pressure drop over the coolant circulation loop has to be known in order to determine the needed pumping power.

4.5.1 Single-phase flows

One can identify several mechanisms that will cause a pressure drop along the fuel assembly:

1. Friction losses from the fuel rod bundle
2. Local loses from the spacer grids
3. Local loses at the core inlet and exit (contraction and expansion)
4. Elevation pressure drop

The total pressure drop in a channel with a constant cross-section area can be calculated from the following equation:

$$-\Delta p_{tot} = -\Delta p_{fric} - \Delta p_{loc} - \Delta p_{elev} = \left(\frac{4C_f L}{D_h} + \sum_i \xi_i \right) \frac{G^2}{2\rho} + L\rho g \sin\varphi \,. \tag{4-88}$$

Here C_f is the Fanning friction coefficient, L is the length of the channel, G is the mass flux, D_h is the channel hydraulic diameter and ρ is the coolant density.

The friction coefficient for laminar flow can be written in a general form as,

$$C_f = a \cdot \mathrm{Re}^{-b} \,, \tag{4-89}$$

where a and b are constants, which for the laminar flow in a pipe are equal to 16 and -1, respectively. For laminar flow in rod bundles, Osmachkin proposed to use Eqs. (4-88) and (4-89), where hydraulic diameter D_h is replaced with an "effective" diameter given as,

$$D_{eff} = \frac{2\varepsilon}{(1-\varepsilon)^2} \left(\frac{\varepsilon}{2} - \frac{3}{2} - \frac{\ln\varepsilon}{1-\varepsilon} \right) D_h \,, \tag{4-90}$$

where ε is the fraction of the cross-section of the bundle which is occupied by rods. The formula is applicable for rod bundles with triangular lattice and for $p/d > 1.3$.

For turbulent flow the coefficients in Eq. (4-89) are obtained experimentally. For flow in a rod bundle with triangular lattice (see FIGURE 4-4) and $1.0 < p/d < 1.5$, the Fanning friction coefficient can be calculated as,

$$C_{f,b} = \left(0.96 \frac{p}{d} + 0.63 \right) C_{f,p} \,, \tag{4-91}$$

where $C_{f,p}$ is the friction factor proposed by Filonenko [4-7], which is valid for tubes and annuli for $\mathrm{Re} > 4000$:

$$C_{f,p} = 0.25 \left(1.82 \lg_{10} \mathrm{Re} - 1.64 \right)^{-2} \,. \tag{4-92}$$

For rod assemblies Aljoshin et al. [4-5] proposed a general correlation as follows,

$$C_f = A \frac{P_{w,ch}}{P_{w,r}} \left(\frac{A_{ch}}{A_r} \right)^m \mathrm{Re}^{-0.25} \,, \tag{4-93}$$

where $P_{w,ch}$ and $P_{w,r}$ – are the wetted perimeters of the channel and rods, respectively; A_{ch} and A_r – are the cross-section areas of the channel and rods, respectively. The formula is valid for rod bundles with triangular lattice, for which $A = 0.47$, $m = 0.35$ and $4 \cdot 10^3 < \mathrm{Re} < 10^5$, and for rectangular lattice, for which $A = 0.38$, $m = 0.45$ and $10^3 < \mathrm{Re} < 5 \cdot 10^5$.

Additional pressure losses are associated with spacer grids, the coolant inlet and exit of the bundle as well as the sudden area changes of the bundle cross-section area. Such losses are classified as the local pressure losses and are calculated according to the following general expression,

$$\Delta p_{loc} = \xi_{loc} \frac{G^2}{2\rho}, \tag{4-94}$$

where ξ_{loc} is the local pressure loss coefficient.

The local loss coefficient for grid spacers is in general dependent on the spacer geometry and is usually determined in an experimental way. Typical spacer loss coefficient is expressed as,

$$\xi_{spac} = a + b \cdot \mathrm{Re}^{-c}, \tag{4-95}$$

where a, b and c a are constants determined experimentally.

For sudden enlargement and contraction of the channel, the local pressure losses can be calculated according procedures described in [4-1].

4.5.2 Two-phase flows

Pressure drop in fuel assemblies with two-phase flow can be calculated according to the procedures described in [4-1], using the hydraulic diameter as described by Eqs. (4-9) and (4-10) with some modifications appropriate to the fuel assembly design. As shown in [4-1], the total two-phase flow pressure drop in a channel with a constant cross-section area can be calculated as,

$$-\Delta p = r_3 C_{f,lo} \frac{4L}{D_h} \frac{G^2}{2\rho_l} + r_4 L \rho_l g \sin\varphi + r_2 \frac{G^2}{\rho_l} + \left(\sum_{i=1}^{N} \phi_{lo,i}^2 \xi_i \right) \frac{G^2}{2\rho_l}. \tag{4-96}$$

Here r_2, r_3 and r_4 are two-phase pressure drop multipliers (acceleration, friction and gravitation, respectively) and $\phi_{lo,i}^2$, ξ_i are local loss multiplier and local pressure loss coefficient, respectively, at location i in the channel.

4.6 Critical Heat Flux

The conditions at which the wall temperature rises and the heat transfer decreases sharply due to a change in the heat transfer mechanism are termed as the **Critical Heat Flux** (CHF) conditions. The nature of CHF, and thus the change of heat transfer mechanism, varies with the enthalpy of the flow. At subcooled conditions and low qualities this transition corresponds to a change in boiling mechanism from nucleate to film boiling. For this reason the CHF condition for these circumstances is usually referred to as the **Departure from Nucleate Boiling** (DNB).

At saturated conditions, with moderate and high qualities, the flow pattern is almost invariably in an annular configuration. In these conditions the change of the heat transfer mechanism is associated with the evaporation and disappearance of the liquid film and the transition mechanism is termed as **dryout**. Once dryout occurs, the flow pattern changes to the liquid-deficient region, with a mixture of vapor and entrained

droplets. It is worth noting that due to high vapor velocity the heat transport from heated wall to vapor and droplets is quite efficient, and the associated increase of wall temperature is not as dramatic as in the case of DNB.

The mechanisms responsible for the occurrence of CHF (DNB- and dryout-type) are not fully understood, even though a lot of effort has been devoted to this topic. Since no consistent theory of CHF is available, the predictions of CHF occurrence relay on correlations obtained from specific experimental data. LWR fuel vendors perform their own measurements of CHF in full-scale mock-ups of fuel assemblies. Based on the measured data, proprietary CHF correlations are developed. As a rule, such correlations are limited to the same geometry and the same working conditions as used in experiments.

Most research on CHF published in the open literature has been performed for upward flow boiling of water in uniformly heated tubes. The overall experimental effort in obtaining CHF data is enormous. It is estimated that several hundred thousand CHF data points have been obtained in different labs around the world. More that 200 correlations have been developed in order to correlate the data. Discussion of all such correlations is not possible; however, some examples will be described in this section.

4.6.1 Departure from Nucleate Boiling

The usual form of a **DNB correlation** is as follows,

$$q''_{cr} = q''_{cr}(G, p, D_h, L, \ldots), \tag{4-97}$$

which means that the main parameters that influence the occurrence of DNB are mass flux, G, pressure, p, as well as the hydraulic diameter, D_h and length L of the heated channel.

For upflow boiling of water in vertical 8-mm tubes with constant heat flux, Levitan and Lantsman recommended the following correlation for DNB:

$$q''_{cr}\big|_{8mm} = \left[10.3 - 7.8\frac{p}{98} + 1.6\left(\frac{p}{98}\right)^2\right]\left(\frac{G}{1000}\right)^{1.2\{[0.25(p-98)/98]-x_e\}} e^{-1.5x_e}. \tag{4-98}$$

Here q''_{cr} is the critical heat flux [MW m^{-2}], p is the pressure in [bar], G is the mass flux in [kg m^{-2} s^{-1}]. The correlation is valid in ranges $29.4 < p < 196$ [bar] and $750 < G < 5000$ [kg m^{-2} s^{-1}] and is accurate to ±15%.

The correlation can be applied to channels with arbitrary diameters if the following correction factor is applied,

$$q''_{cr} = q''_{cr}\big|_{8mm} \cdot \left(\frac{8}{D}\right)^{0.5}, \tag{4-99}$$

where D is the tube diameter in [mm] and $q''_{cr}\big|_{8mm}$ is the critical heat flux obtained from Eq. (4-98).

One of the earliest correlations for DNB applicable to fuel rod bundles was given by Bowring, who proposed the following expression,

$$q''_{cr} = \frac{A + D \cdot G\Delta i_{subi} / 4}{C + L}, \tag{4-100}$$

where,

$$A = \frac{0.579 F_{B1} D \cdot G \cdot i_{fg}}{1 + 0.0143 F_{B2} D^{1/2} G}, \tag{4-101}$$

$$C = \frac{0.077 F_{B3} D \cdot G}{1 + 0.347 F_{B4} (G/1356)^{n}}, \tag{4-102}$$

Here D is the hydraulic diameter in [m], G is the mass flux in [kg m^{-2} s^{-1}], i_{fg} is the latent heat in [J kg^{-1}], p is the pressure in [Pa], Δi_{subi} is the inlet subcooling [J kg^{-1}] and L is the tube length [m]. The correlation parameters n, F_{B1}, F_{B2}, F_{B3} and F_{B4} are functions of pressure and are as follows,

$$n = 2.0 - 0.5 p_R, \tag{4-103}$$

$$p_R = \frac{p}{6.895 \cdot 10^{6}}, \tag{4-104}$$

$$F_{B1} = \begin{cases} \dfrac{p_R^{18.942} \exp[20.8(1 - p_R)] + 0.917}{1.917} & p_R \le 1 \\ p_R^{-0.368} \exp[0.648(1 - p_R)] & p_R > 1 \end{cases}, \tag{4-105}$$

$$\frac{F_{B1}}{F_{B2}} = \begin{cases} \dfrac{p_R^{1.316} \exp[2.444(1 - p_R)] + 0.309}{1.309} & p_R \le 1 \\ p_R^{-0.448} \exp[0.245(1 - p_R)] & p_R > 1 \end{cases}, \tag{4-106}$$

$$F_{B3} = \begin{cases} \dfrac{p_R^{17.023} \exp[16.658(1 - p_R)] + 0.667}{1.667} & p_R \le 1 \\ p_R^{-0.219} & p_R > 1 \end{cases}, \tag{4-107}$$

$$\frac{F_{B4}}{F_{B3}} = p_R^{1.649}. \tag{4-108}$$

The correlation is based on a fit to data in the ranges $136 < G < 18600$ [kg m^{-2} s^{-1}], $2 < p < 190$ [bar], $2 < D < 45$ [mm] and $0.15 < L < 3.7$ [m].

For PWR conditions, when heat flux is uniformly distributed along the channel, the General Electric Company (GE) correlation is widely applied (Jansen and Levy, [4-13]),

(4-109) $$q''_{cr} = q''_{cr70} + 6.2\cdot 10^{3}(70 - p),$$

where,

(4-110) $$q''_{cr70} = \begin{cases} 10^{6}\left(2.24 + 0.55\cdot 10^{-3} G\right) & if \quad x < x_1 \\ 10^{6}\left(5.16 - 0.63\cdot 10^{-3} G - 14.85x\right) & if \quad x_1 \le x < x_2 \\ 10^{6}\left(1.91 - 0.383\cdot 10^{-3} G - 2.06x\right) & if \quad x_2 \le x \end{cases}.$$

Here,

$$x_1 = 0.197 - 0.08\cdot 10^{-3} G,\ x_2 = 0.254 - 0.019\cdot 10^{-3} G,$$

q''_{cr} - critical heat flux, [W/m^2]

x - equilibrium quality,

G - mass flux, [kg/m^2.s],

p - pressure, [bar].

The correlation is applicable in the following range of parameters: pressure p = 42÷102 bars, mass flux G = 540÷8100 kg/m^2.s, quality x = 0.0÷0.45, hydraulic diameter D_h = 6.2÷32 mm, channel length L = 0.74÷2.8 m.

Westinghouse Company developed similar correlation for uniformly heated bundles, W-3 (Tong et al.),

(4-111)
$$\begin{aligned} q''_{cr,U} = A\{&2.022 - 0.0004302\,p_R + (0.1722 - 0.0000984\,p_R)e^{[(18.177 - 0.004129\,p_R)x]}\}\cdot \\ &\left[(0.1484 - 1.596x + 0.1729x|x|)G_R + 1.037\right](1.157 - 0.869x)\cdot \\ &\left(0.2664 + 0.8357e^{-3.151 D_E}\right)(0.8258 + 0.000784\Delta i_R) \end{aligned}$$

where,

$$p_R = \frac{p}{6.8947\cdot 10^{3}},\ p - \text{pressure [Pa]}$$

$$G_R = \frac{G}{1.3562\cdot 10^{-3}},\ G - \text{mass flux [kg/m}^2\text{.s]}$$

$$A = 3.1695\cdot 10^{5}$$

x - quality

$\Delta i_R = \dfrac{i_f - i_{li}}{2326}$, i_f, i_{li} – saturated and inlet enthalpy, respectively [J/kg].

For non-uniform power distributions, the following correction factor has to be used,

(4-112) $$F_c \equiv \frac{q''_{cr,U}(z_{cr})}{q''_{cr,NU}(z_{cr})} = \frac{C}{1-e^{-C\cdot z_{cr}}} \int_0^{z_{cr}} \frac{q''(z)}{q''(z_{cr})} e^{-C(z_{cr}-z)} dz ,$$

where $q''_{cr,U}(z_{cr})$ is the value of the critical heat flux calculated from Eq. (4-109), z_{cr} is the axial coordinate of DNB point, *q''(z)* is the axial distribution of the heat flux and *C* is an empirical constant.

4.6.2 Dryout

The usual form of a **dryout correlation** is as follows,

(4-113) $$x_{cr} = x_{cr}(G, p, D_h, L_B, ...),$$

which means that the main parameters that influence the occurrence of dryout are mass flux, *G*, pressure, *p*, hydraulic diameter D_h, **boiling length** (that it the distance from the beginning of saturated flow to the dryout point), L_B, and possibly other.

For dryout predictios in 8-mm pipes Levitan and Lantsman recommended the following expression:

(4-114) $$x_{cr}\big|_{8mm} = \left[0.39 + 1.57\frac{p}{98} - 2.04\left(\frac{p}{98}\right)^2 + 0.68\left(\frac{p}{98}\right)^3\right]\left(\frac{G}{1000}\right)^{-0.5} .$$

Here x_{cr} is the critical quality, *p* is the pressure in [bar] and *G* is the mass flux in [kg m^{-2} s^{-1}]. The application region of the correlation is $9.8 < p < 166.6$ [bar] and $750 < G < 3000$ [kg m^{-2} s^{-1}] and the accuracy of x_{cr} is ±0.05.

The critical quality given by Eq. (4-114) can be used for other tube diameters with the following correction factor:

(4-115) $$x_{cr} = x_{cr}\big|_{8mm} \cdot \left(\frac{8}{D}\right)^{0.15} .$$

Here $x_{cr}\big|_{8mm}$ is the critical quality obtained from Eq. (4-114) and *D* is the tube diameter in [mm].

For fuel rod bundles the following correlation was proposed by General Electric:

(4-116) $$x_{cr} = \frac{A \cdot L_B^*}{B + L_B^*}\left(\frac{1.24}{R_f}\right),$$

where,

$L_B^* = L_B / 0.0254$, L_B - boiling length in [m],

R_f - radial peaking factor,

$$A = 1.055 - 0.013\left(\frac{p_R - 600}{400}\right)^2 - 1.233G_R + 0.907G_R^2 - 0.285G_R^3$$

$$B = 17.98 + 78.873G_R - 35.464G_R^2,$$

$G_R = G/1356.23$, G – mass flux in [kg m^{-2} s^{-1}],

$p_R = p/6894.757$, p – pressure in [Pa].

The correlation is valid for 7x7 bundles. It can also be applied to 8x8 bundles once replacing B with $B/1.12$.

REFERENCES

[4-1] Anglart, H., *Thermal-Hydraulics in Nuclear Systems*, Compendium KTH, 2010.

[4-2] Glasstone, S. and Sesonske, A., *Nuclear Reactor Engineering*, Van Nostrand Reinhold Compant, 1981, ISBN 0-442-20057-9.

[4-3] Idelchik, Handbook of flow pressure losses

[4-4] Osmachkin, V.S., Investigation of the thermal-hydraulic characteristics of mockups of fuel rod assemblies in Kurchatov Institute (Russian), 1974.

[4-5] Aljoshin, V.S., Kuznetsov, N.M., Sarkisov, A.A., Submarine nuclear reactors (Russian), 1968.

[4-6] Petukhov, B.S., Genin, L.G., Kovalev, S.A., Heat transfer in nuclear power plants (Russian), Atomizdat, 1974.

[4-7] Subbotin, V.I., et al, Hydrodynamics and heat transfer in nuclear power plants (principles of analysis) (Russian), Atomizdat, 1975.

[4-8] Rasohin, N.G. et al., 'Prediction of boiling heat transfer,' *Teploenergetika*, **9**, 1970.

[4-9] Tong, L., Boiling crisis and critical heat flux, 1969.

[4-10] Shitsman, M.E., "Impairment of the heat transmission at supercritical pressures," *High Temperatures*, **1**, *2*, 237-244 (1963).

[4-11] Yamagata, K, Nishikawa, K., Hasegawa, S., Fujii, T. and Yoshida, S., "Forced Convective Heat Transfer to Supercritical Water Flowing in Tubes," *Int. J. Heat Mass Transfer*, **15**, 2575-2593 (1972).

[4-12] Jackson, J.D., "Consideration of the Heat Transfer Properties of Supercritical Pressure Water in Connection of with the Cooling of Advanced Nuclear Reactors," *Proc. 13th Pacific Basin Nuclear Conference, Shenzen City, China*, 21-25 (2002).

[4-13] Janssen, E. and Levy, S., General Electric Company Report APED-3892, 1962.

[4-14] Weissman, J. "Heat Transfer to Water Flowing Parallel to Tube Bundles," Nucl. Sci. and Eng., **6**:78, 1978.

EXERCISES

EXERCISE 4-1: A nuclear power plant operated during 11 month with constant power 1200 MWe and with thermal efficiency 34% before the reactor was shutdown for refueling. Calculate the decay power of the reactor at time equal to 24 hours after the shutdown. Calculate the total decay heat (in MWh) generated by the core during the refueling outage assuming that it started 1 day after the reactor shutdown and it lasted for 5 days

EXERCISE 4-2: BWR fuel assembly has 24 rods with diameter d_r = 9.63 mm and heated length L = 3.77 m. The cross-section area of the fuel assembly is A = 2.35 10^{-3} m^2, and the hydraulic diameter d_h = 9.6 mm. The axial distribution of heat flux is described with the following function: $q''(z) = q_0''\left(\frac{1}{2} + \frac{\pi}{4}\sin\frac{\pi z}{L}\right)$. The bundle is electrically heated and cooled with water flowing vertically upward. The power is distributed uniformly between the rods. The bundle is tested in a thermal-hydraulic laboratory under the following conditions: inlet mass flux G = 1200 kg/m^2.s, inlet water temperature T_{li} = 483 K, system pressure p = 7 MPa and the total power applied to the bundle q = 900 kW. Calculate: (a) total enthalpy increase in the bundle, (b) the maximum value of the heat flux in the bundle, (c) the maximum clad outer temperature and its axial location (d) the total pressure drop in the rod bundle.

EXERCISE 4-3: Fuel rod, with heat density in fuel pellet q''' = 950 MW/m3, has the following radial dimensions: fuel pellet outer radius: r_F = 4.2 mm, gas gap outer radius: r_G = 4.25 mm, clad outer radius r_C = 4.82 mm. Calculate: (a) temperature rise in fuel, gas gap and cladding if the thermal conductivities are 4.82 W/m.K, 0.28 W/m.K, and 12 W/m.K, respectively; (b) temperature rise in fuel if the fuel conductivity is given as the following function of temperature: $\lambda_F = \frac{4000}{130+T} + 0.34\cdot 10^{-12}T^4$ (T in K), assuming that the maximum fuel temperature is equal to 2000 K.

EXERCISE 4-4: A vertical BWR fuel assembly has 100 uniformly heated rods with linear power q' = 25 kW m^{-1} in each rod. The bundle is cooled with water flowing upward at pressure 7.0 MPa, inlet subcooling 10 K and inlet mass flux 1500 kg m^{-2} s^{-1}. The assembly is 3.65 m long, has a quadratic cross-section with box width equal to 140 mm and the rod outer diameter equal to 10 mm. Given: saturation temperature: 559 K, latent heat: 1505 kJ kg^{-1}, liquid specific heat: 5205 J kg^{-1} K^{-1} , liquid saturation enthalpy: 1268 kJ kg^{-1} , density: liquid 740 kg m^{-3}, vapor 35 kg m^{-3} , liquid thermal conductivity: 0.57 W m^{-1} K^{-1} , liquid dynamic viscosity: 9.12x10^{-5} Pa s. Using the Levitan and Lantsman correlation for dryout, calculate the critical power of the fuel assembly and using HEM, find the total pressure drop.

Chapter

5

5 Materials and Mechanics of Structures

The choice of materials for nuclear applications has to be based on consideration of such properties as the cross-section for neutron absorption, the resistance to corrosion, the resistance to radiation damages and the resistance to high temperatures and mechanical loads. Clearly, the prevailing conditions during the life-time of the nuclear power plant will determine which materials are suitable for the desired purposes. Consequently, materials which are acceptable in thermal reactors are not necessarily the best choice for the fast reactors and better alternatives should be always sought. This chapter contains the general aspects of material properties and the analyses of their behavior in nuclear applications.

5.1 Structural Materials

Structural materials are such materials that should withstand the desing loads during the operation of the nuclear power plant. Due to that, the materials should demonstrate a high enough strength to prevent any kind of failure that would jeopardize the system integrity and/or safety.

5.1.1 Stainless Steels

Stainless steel is a steel alloy with a minimum of 11% of chromium content by mass. Due to this content of chromium stainless steels have a higher resistance to corrosion, but in general, are not stain-proof.

Austenitic stainless steels have austenite (also known as the gamma phase of iron) as their primary phase. These alloys contain mainly chromium and nickel, but sometime also other elements. Austenitic stainless steels are corrosion resistant and have good mechanical properties, but they suffer some degradation as a result of exposure to fast neutrons. Selected austenitic stainless steels used in reactor applications are listed in TABLE 5.1.

TABLE 5.1. Composition of selected austenitic stainless steels for reactor applications.

SS, Swedish	AISI (USA)	Carbon, %	Chromium, %	Nickel, %	Other Elements
2333	304	0.08	18 to 20	8 to 11	-
2352	304L	0.03	18 to 20	8 to 11	-
2343	316	0.10	16 to 18	10 to 14	Mo (2-3%)

2352	316L	0.03	16 to 18	10 to 14	Mo (1.75-2.5%)

5.1.2 Low-alloy Carbon Steels

Low-allow carbon steels are steels in which the main alloying constituent is carbon, with additional alloying elements such as manganese, nickel, chromium, molybdenum and others, which are added to improve the alloy mechanical properties. Thees steels are mainly used in pressure vessels and other components where the corrosion resistance is not required but the ability to withstand thermal stresses is desirable. Such steel is used for PWR pressure vessel, where the inside of the vessel is usually clad with a thin layer of stainless steel or Inconel to provide the corrosion resistance.

5.1.3 Properties of Selected Steel Materials

The physical properties of selected steel materials are given in TABLE 5.2.

TABLE 5.2. Physical properties of selected steel materials

Material	Temperature, K	Density, kg/m^3	Young's Modulus, GPa	Poisson's Ratio	Yield Strength, MPa
Carbon steel (A 533-B)	300	7860	207	0.28	340
	600	-	182	-	280
	750	-	172	-	240
	800	-	169	-	200
Stainless steel (type 347)	300	7950	193	0.27	205
	500	7860	173	0.30	-
	700	7710	166	0.31	150
	800	-	157	0.32	-
Zircaloy-2	300	6560	95	0.43	300
	500	-	90	0.38	170
	600	-	78	-	117

Austenitic steel (type 304 & 316)	300	8000	193	0.27 - 0.30	205 *)

*) 0.2% offset yield point

5.2 Cladding Materials

Cladding materials should be resistant to corrosion and they should have good mechanical properties at high temperatures. Fuel cladding shouldn't in addition interact with neutrons.

5.2.1 Zirconium

Zirconium has a small capture cross section for thermal neutrons and furthermore it is resistant to corrosion by water at the operating temperature of water-cooled reactors. Due to that, zirconium alloys have found extensive use in the fuel cladding for such reactors.

Zirconium ores contain 0.5 to 3% of hafnium, which has a large cross section for thermal neutron capture. This puts high requirements on removal of hafnium from zirconium to make it suitable for reactor applications. Two alloys are used as cladding materials: zircaloy-2 (1.5% Zn, 0.15% Fe, 0.1% Cr and 0.05% Ni) and zircaloy-4 (1.5% Zn, 0.2% Fe, 0.1% Cr and 0.007% Ni).

5.2.2 Nickel Alloys

Nickel alloys demonstrate a resistance to corrosion at high temperatures. Inconels (containing about 15% chromium, 7% iron and smaller amounts of other elements) are sometimes used instead of stainless steel because they are less subject to stress-corrosion cracking. However the alloy should not be used inside the reactor core due to the presence of cobalt. Instead it can be used as pressure-vessel lining or in steam generators.

5.3 Coolant, Moderator and Reflector Materials

Coolant, moderator and reflector materials used in nuclear applications have to possess low cross section for absorption of neutrons in order to improve the neutron economy in the nuclear reactors. In addition, coolants should have good thermal-hydraulic properties to effectively cool the nuclear fuel elements.

5.3.1 Coolant Materials

Various coolant materials have been applied in nuclear reactors. Most thermal reactors are cooled with ordinary water. This type of coolant has several advantages such as low price, good thermal-hydraulic properties and reasonably good nuclear properties (such as low cross section for neutron absorption). Heavy water is used when the nuclear fuel has low enrichment and improved neutron economy is needed. In fast reactors various gas or liquid metal coolants are employed such as helium, CO_2, sodium, lead and lead-bismuth eutectic. The main properties of selected coolants are given in TABLE 5.3.

TABLE 5.3. Properties of selected reactor coolants

Fluid	Temerature K	Density Kg/m^3	Specific heat J/kg/K	Viscosity, $Pa.s \cdot 10^5$	Thermal conductivity W/m/K	Prandtl number
Helium	293	0.178	5200	1.86	0.141	0.68
p =	500	0.0973	5200	2.80	0.211	0.69
10^5 Pa	700	0.0703	5200	3.48	0.278	0.65
	900	0.0529	5200	4.14	0.335	0.64
	1100	0.0432	5200	4.6	0.389	0.61
Steam	558.83	36.524	5354	1.896	0.0643	1.577
p =	600	30.487	3436	2.099	0.0592	1.219
7 MPa	700	23.655	2570	2.559	0.0646	1.018
	800	19.913	2403	2.989	0.0755	0.952
	900	17.356	2375	3.400	0.0879	0.919
Water	300	999.63	4162	85.27	0.6140	5.780
p =	400	940.91	4241	22.04	0.6886	1.357
7 MPa	450	894.27	4368	15.45	0.6806	0.991
	500	835.35	4622	11.88	0.6467	0.849
	558.83	739.72	5400	9.125	0.5687	0.866
Sodium	373	925	1382.3	68.19	84.92	0.0111
p =	473	904	1343.3	45.24	81.02	0.0075
10^5 Pa	573	881	1309.4	34.16	77.12	0.0058
	673	856	1282.6	27.96	73.19	0.0049
	773	832	1263.9	23.57	69.28	0.0043
	873	808	1253.5	20.86	65.37	0.0040
Lead,	603	10670	147.30	254.7	15.83	0.0237

$p = 10^5$ Pa [5-2]	673	10580	147.30	213.86	16.58	0.0190
	773	10460	147.30	184.63	17.66	0.0154
	873	10340	147.30	156.48	18.74	0.0123
	973	10210	147.30	139.94	19.82	0.0104
	1073	10090	147.30	131.96	20.90	0.0093

5.3.2 Moderator and Reflector Materials

The moderator and reflector materials should have small absorption cross section and possibly large scattering cross section. Several low mass number materials such as ordinary water, heavy water, beryllium, carbon (graphite) and zirconium hydride possess these types of properties. Nuclear properties of typical moderator materials are given in TABLE 5.4.

TABLE 5.4. Properties of selected moderator materials at 293 K.

Material	Ordinary water	Heavy water	Beryllium	Graphite
Atomic or molecular weight	18	20	9	12
Density, kg/m^3	1000	1100	1850	1700
Nr atoms or molecules/m^3 x 10^{-28}	3.34	3.32	12.4	8.55
σ_a, barns	0.66	0.003	0.0092	0.0034
σ_s, barns	103	13.6	6.1	4.8
Σ_a, 1/m	2.2	0.0085	0.114	0.029
Σ_s, 1/m	345	45	76	41

5.3.3 Selection of Materials

The main criteria for material selection in nuclear power plants are safety, reliability, life-length and economy. One of the important aspects in selection of materials is the previous experience in using a certain material in equivalent conditions.

To satisfy the criteria the following principles are followed:

- these parts that are not affected by corrosion should be made of carbon steels or low alloy steels,

- other primary reactor systems should be made of stainless steels or nickel alloys.

TABLE 5.5 contains a list of materials that are typically selected for various primary components in nuclear power plants.

TABLE 5.5. Typical material selection for various components in nuclear power plants.

Component	Function	Material requirement	Material used
Reactor pressure vessel	To contain and support the reactor core and reactor internal parts	High strength material with as little as possible deterioration with time. Due to neutrons, low contents of cobalt, copper and phosphor is required.	Carbon steel A 533-B
Reactor inner parts	To support, form and contain the core; to direct coolant (water and steam) flow; to control reactor power and to separate steam and water.	Materials for inner parts must be resistant to corrosion. Materials should not contain cobolt-60 isotop and should be resistant to high neutron fluxes.	Austenitic stainless steels (SS 2333 or AISI 304) or Inconel-600. If high strength is required: SS2570 (A286)
Steam generator	To transfer the heat from the primary circuit and to generate steam.	Materials must be resistant to corrosion.	Carbon steel A 533-B for pressure vessel. Heat exchanger tubes are made of Inconel-600 or Incoloy-800.
Turbine set	To transfer the thermal energy of steam into a mechanical energy of rotation. To condens steam after leaving the turbine.	In nuclear power plants with secondary circuits there are no additional requirements as compared with fossil-powered plants. In BWR materials should not contain cobolt-60 isotopes.	Turbine rotor is made of ASTM A-470 cl. 5. Condenser tubes are made of Titanium. Pipes and

			valves are made of carbon steels.

5.4 Mechanical Properies of Materials

5.4.1 Hooke's Law

Hooke's law is the constitutive equation for the linear elastic and one-dimensional systems is as follows,

$$\varepsilon = \frac{\sigma}{E}, \tag{5-1}$$

where $\varepsilon = \Delta l / l$ is the strain, defined as a ratio of the length increase to the initial length of a material sample, $\sigma = F/A$ is the stress, defined as a ratio of the normal force F to the sample cross section area A, and E is the Young's modulus (know also as modulus of elasticity). Elongation of a material sample into one direction, in which the load is acting, causes a contraction of the sample in the normal direction. The contraction is given as,

$$\varepsilon_n = -\nu \frac{\sigma}{E}, \tag{5-2}$$

where ν is the Poisson's ratio.

Both the Young's modulus and the Poisson's ratio are material properties.

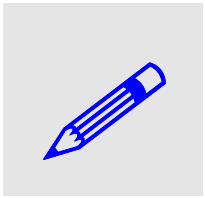

EXAMPLE 5-1. Consider a simple bar (shown in FIGURE 5-1) fixed at one end, at x = 0 and subject to a concentrated force at the other end (x = 2 m). Calculate the displacement and stress distribution in the bar. SOLUTION: The stress distribution in the bar can be calculated as: $\sigma = F/A = 1000/1e-4 = 10$ MPa. The corresponding strain is found as $\varepsilon = \sigma/E = 10^7/2.1\cdot 10^{11} = 4.76\cdot 10^{-5}$. The displacement will depend on the distance from the fixed wall and in general can be given as $u = \varepsilon \cdot x$. For x = 2 m (whole length of the bar), the displacement is found as u = $4.76\cdot 10^{-5}$ x $2\cdot 10^3$ mm = 0.0952 mm.

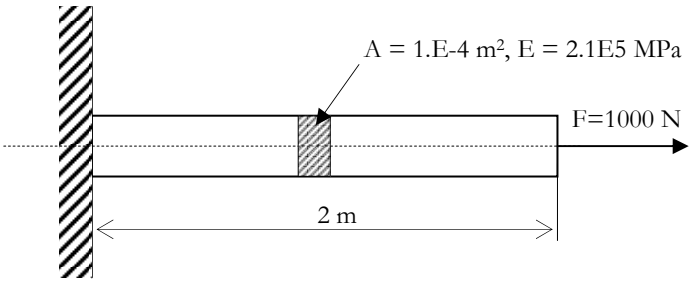

FIGURE 5-1. Bar subjected to a concentrated end load.

In the three dimensional state of stress, the Hooke's law for isotropic materials is as follows,

$$\varepsilon_x = \frac{1}{E}\left[\sigma_x - \nu\left(\sigma_y + \sigma_z\right)\right]$$
$$\varepsilon_y = \frac{1}{E}\left[\sigma_y - \nu\left(\sigma_x + \sigma_z\right)\right]$$
$$\varepsilon_z = \frac{1}{E}\left[\sigma_z - \nu\left(\sigma_x + \sigma_y\right)\right]$$
(5-3)
$$\varepsilon_{xy} = \frac{\sigma_{xy}}{2G}$$
$$\varepsilon_{xz} = \frac{\sigma_{xz}}{2G}$$
$$\varepsilon_{yz} = \frac{\sigma_{yz}}{2G}$$

where *x, y* and *z* are Cartesian coordinates, σ_x, σ_y and σ_z are normal stresses acting along these coordinates, σ_{xy}, σ_{xz} and σ_{yz} are shear stresses and *G* is the shear modulus.

For isotropic materials, the relation between the shear modulus *G* and the Young's modulus *E* is as follows,

(5-4) $$G = \frac{E}{2(1+\nu)}.$$

In a two-dimensional state of stress, it can be easily demonstrated that there are two orthogonal planes in which the shear stress vanishes and only normal stresses are present. These planes are called the principal planes and the stresses the principal stresses. There is a graphical representation of the two-dimensional stress state and the relation between local stresses and the principle stresses known as the Mohr's circle. The principle stresses can be also derived for a general three-dimensional stress state, however, the derivation is more complex. In this case the principle stresses are found as roots of the following characteristic equation,

(5-5) $$\sigma^3 - I_1\sigma^2 + I_2\sigma - I_3 = 0,$$

where,

(5-6) $$I_1 = \sigma_x + \sigma_y + \sigma_z$$

(5-7) $$I_2 = \sigma_x\sigma_y + \sigma_y\sigma_z + \sigma_z\sigma_x - \sigma_{xy}^2 - \sigma_{yz}^2 - \sigma_{xz}^2$$

(5-8) $$I_3 = \sigma_x\sigma_y\sigma_z + 2\sigma_{xy}\sigma_{yz}\sigma_{xz} - \sigma_x\sigma_{xy}^2 - \sigma_y\sigma_{yz}^2 - \sigma_z\sigma_{xz}^2$$

are three invariants of the three dimensional stress tensor.

5.4.2 Stress-Strain Relationships

A typical stress-strain graph for low-carbon steel is shown in FIGURE 5-2. Initially the stress increases linearly with the strain and the Hooke's law prevails. At point 2 the curve levels off and plastic deformation occurs. This point on the stress-strain curve is called the yield point and the corresponding stress value the **yield stress**.

The yield point is not always as easily defined as shown in FIGURE 5-2. For example, for high strength steels and aluminium alloys an arbitrary **offset yield point** is defined. The value of this is usually defined at 0.2% of the strain.

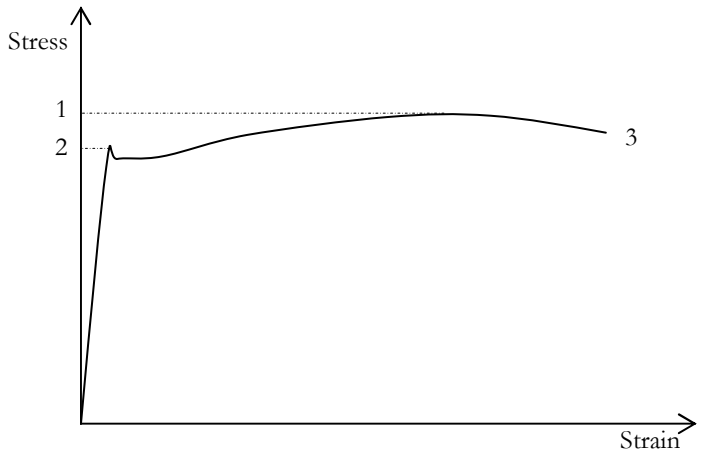

FIGURE 5-2. Stress versus strain curve: 1 – ultimate strength point, 2 – yield strength point, 3- rupture point.

The peak stress on the strain-stress curve is known as the **ultimate tensile strength** (point 1 in FIGURE 5-2). The region between the yield strength and the ultimate tensile strength is termed as the strain hardening region. Brittle materials (for example concrete) do not have a yield point and do not strain-harden which means that the ultimate strength and breaking strength are the same.

5.4.3 Ductile and Brittle Behaviour

Ductility is a property of a material that describes to what extend the material can be plastically deformed without fracture. FIGURE 5-3 shows typical examples of the ductile and brittle fracture.

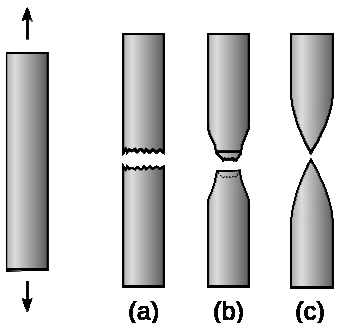

FIGURE 5-3. Ductile versus brittle of round metal bars after tensile testing; (a) brittle fracture, (b) ductile fracture, (c) purely ductile fracture.

5.4.4 Creep

Creep is a tendency of a material to the slow plastic deformation under a constant mechanical and/or thermal load. Generally the creep exhibits three stages: (1) primary creep with a high rate of the strain increase with time, (2) secondary creep, in which the strain stays constant or only slightly increases with time, (3) accelerating creep, in which the strain increases rapidely and becomes so large as to produce failure.

Creep is important in nuclear applications, but its effect may be two-fold:

- creep can be advantageous as to relief the stresses,
- creep can be disadvantageous due to significant shape changes of a structure; for example excessive creep of cladding may lead to fuel damage.

5.5 Strength of Materials and Stress Analysis

The purpose of the strength of materials and stress analysis is to estimate the over-all resistance of given structure to external loads.

Stress analysis is a discipline which has as a goal to evaluate stresses in a given structure due to applied loads. The most common way to perform a stress analysis of any system is to employ computer codes that calculate the distribution of stresses and strains due to given external or internal loads. Such codes are based on the Finite Element Methods (FEM), which employ a division of the computational domain into small objects connected through nodes. The unknown parameters, such as strains and stresses are determined at nodes, whereas their values inside finite elements are computed from so called shape functions.

In a simplified analysis the stresses are determined from known dimensions and applied loads to a specific structure. In many cases known analytical solutions for stress distributions can be employed.

To evaluate the mechanical integrity of a structure and to provide a proper margin to failure, the maximum stresses must be limited by certain pre-determined criteria. Typical approach is to compare the maximum stress with the allowable stress obtained from a proper yield criterion.

5.5.1 Yield Criteria

One of the objectives of the stress analysis is to determine the conditions when plastic deformation, or yielding, is initiated in the body under consideration. For that purpose a special scalar function of the stress tensor is derived. Several such functions have been proposed, but the most widely used is the von Mises yield criterion based on the Maxwell-Huber-Hencky-von-Mises maximum strain energy theory. In three-dimensional stress state, the Mises stress can be expressed as,

$$\sigma_v = \sqrt{\frac{(\sigma_1 - \sigma_2)^2 + (\sigma_2 - \sigma_3)^2 + (\sigma_3 - \sigma_1)^2}{2}}. \quad (5\text{-}9)$$

Von Mises yield criterion states that yielding in 3-D occurs when the distortion strain energy reaches that required for uniaxial loading. Thus, it can be written as,

(5-10) $$2\sigma_{\max}^2 \geq (\sigma_1 - \sigma_2)^2 + (\sigma_2 - \sigma_3)^2 + (\sigma_3 - \sigma_1)^2 .$$

Another failure criterion used in practical application is due to Tresca. The criterion specifies that a material would flow plastically if,

(5-11) $$\sigma_{tresca} = \sigma_1 - \sigma_3 \geq \sigma_{\max} .$$

5.5.2 Stress Analysis in Pipes and Pressure Vessels

For a pipe or elongated vessel with inside (or outside) pressure p, inner diameter D (radius R) and wall thickness h, the stresses are calculated as,

(5-12) $$\sigma_1 = \frac{pD}{2h} = \frac{pR}{h},$$

(5-13) $$\sigma_2 = \frac{1}{2}\sigma_1 = \frac{pR}{2h},$$

where σ_1 is the circumferential stress and σ_2 is the longitudinal stress.

The corresponding strain rates are as follows,

(5-14) $$\varepsilon_1 = \frac{1}{E}(\sigma_1 - \nu\sigma_2) = \frac{pR}{2Eh}(2-\nu),$$

(5-15) $$\varepsilon_2 = \frac{1}{E}(\sigma_2 - \nu\sigma_1) = \frac{pR}{2Eh}(1-2\nu).$$

The enlargement of the vessel radius is given as,

(5-16) $$\Delta R = R\varepsilon_1 = \frac{pR^2}{2Eh}(2-\nu),$$

and the elongation of the vessel is,

(5-17) $$\Delta l = l\varepsilon_2 = \frac{pRl}{2Eh}(1-2\nu).$$

Here R and l are the internal radius and the length of the vessel, respectively.

For pipes and pressure vessels with thick walls, the tangential (hoop) stress is given as,

(5-18) $$\sigma_t = -\frac{p_a - p_b}{a^2 - b^2}\frac{a^2 b^2}{r^2} - \frac{p_a a^2 - p_b b^2}{a^2 - b^2},$$

and the radial stresses as,

(5-19) $$\sigma_r = \frac{p_a - p_b}{a^2 - b^2}\frac{a^2 b^2}{r^2} - \frac{p_a a^2 - p_b b^2}{a^2 - b^2}.$$

Here p_a and p_b are the external and internal pressure, respectively, a and b are the external and internal radii of the vessel, and r is the radial coordinate.

In case when only the internal pressure is acting, the stresses are the highest on the internal surface of the wall and become,

(5-20) $$\sigma_t = \frac{p_b\left(a^2 + b^2\right)}{a^2 - b^2},$$

(5-21) $$\sigma_r = -p_b .$$

EXAMPLE 5-2. The design internal pressure in a pipe is 17.5 MPa and its outer diameter is 0.5 m. The pipe is made of steel with allowable stress 190 MPa at the design temperature. Evaluate the minimum permissible thickness of the pipe wall assuming that the circumferential stress should be lower than the allowable stress and that a thin wall model can be applied. SOLUTION: from Eq. (5-12) the circumferential stress is obtained as $\sigma_1 = p(D_o - 2h)/2h$ where D_o is the outer pipe diameter. The pipe thickness can be found as $h = pD_o/[2(\sigma_1 + p)] = 0.5 \cdot 17.5 \cdot 10^6 \cdot 0.5/\left(190 \cdot 10^6 + 17.5 \cdot 10^6\right) \cong 0.021\ \mathrm{m}$.

5.5.3 Thermal Stresses

The stresses in construction materials are not only created by mechanical loads, but may result from temperature differences. Typically various systems in nuclear power plant are assembled at the ambient temperature. During the plant operation, the temperature is elevated to a new value which corresponds to the local conditions. Due to that the elements are elongated as a result of the termal dilatation. Thermal stresses will be developed if the element is not allowed to freely move. Another type of thermal stresses will develop in solid materials in which exists a strong temperature gradient. In such case the stresses will depend on the material property (the termal expansion coefficient) and the temperature gradient. Both types of thermal stresses should be analysed on the design stage and proper design solutions should be adopted to keep the stresses below the safety limits.

5.6 Material Deterioration, Fatigue and Ageing

During a nuclear power plant operation, construction materials are constantly changing their properties. Taking into account the long life-time of a plant, these changes can be very significant and their over-all influence on the plant components safety and their integrity must be taken into consideration.

5.6.1 Radiation Effects in Materials

One of the specific conditions that need to be considered for nuclear power plants is the presence of radiation. There are four types radiation. Alpha and beta radiation is short-range and typically not influencing the choice of material. Neutron and gamma radiation, however, have significant range and is therefore influencing the behavior of construction materials.

Neutrons that participate in the chain reaction in the reactor core have a wide range of energy: from thermal (~0.025 eV) to fast fission neutrons (~10^6 – 10^7 eV). In the central part of the core the neutron flux can be as high as 10^{18} n/m^2.s. There are no materials that are not affected (sooner or later) by this high radiation. Typically what

happens is that atoms are displaced from their positions due to elastic collisions with neutrons. The total number of atom displacements is a measure of the radiation damage of a material.

The rate of production of displacements by neutrons may be expressed as,

$$\dot{n} = N\sigma_d(E)\phi(E),$$

where $\dot{n}$ is the rate of displacements, N is the atom density of the target material, $\sigma_d(E)$ is the microscopic cross section for displacement and $\phi(E)$ is the flux of neutrons. In general, both the microscopic cross section for displacement and the neutron flux are functions of the energy of neutrons, E. It can be shown that,

$$\sigma_d(E) \approx \sigma_s(E)\frac{E}{AE_d}.$$

Here $\sigma_s(E)$ is the total elastic scattering cross section of the target material for neutrons of energy E, E_d is the displacement energy (typically its value is equal to 25 to 30 eV for metals) and A is the mass number of the target nucleus. The fraction of displaced atoms during a period of time Δt, assuming a constant neutron flux, may be found as,

$$\int_{\Delta t} \frac{\dot{n}}{N} dt \equiv \frac{n(E)}{N} = \phi(E)\Delta t \frac{\sigma_s(E)E}{AE_d}. \quad (5\text{-}22)$$

The product $\phi(E)\Delta t$ is expressed in units of neutrons/m^2 and is called the **fluence**. The fraction $n(E)/N$ is known as the **displacements per atom** (**dpa**).

In boiling water reactors only the components inside the reactor core (fuel assemblies, control rods, etc) and limited parts of the reactor pressure vessel receive high enough radiation to be affected. The effect of radiation on reactor pressure vessel is larger in the pressurized water reactors since the vessel is smaller and thus the distance between the vessel wall and the reactor core is smaller as well.

The changes of material properties due to radiation are monitored through placement of material samples at various selected places in the nuclear reactor core. The samples are investigated on a regular basis and in this way it is possible to predict the expected changes of material properties during the lifetime of the reactor.

Certain atoms may absorb neutrons. Obviously, construction materials should not contain these types of atoms, since such materials should have the lowest possible cross-section for absorption. The absorption of neutrons in construction materials influences the required enrichment of fuel and is thus of highest economic importance.

Finally, neutrons can activate the construction material through creation of radiactive isotopes. For example Zr-94 after activation by a neutron becomes Zr-95 with half-time equal to 65 days. It is clear that if a construction material contains isotopes that are activated by neutrons, it will introduce severe limitations on the material

management and possibility to repair the damaged parts. In that respect coblt-59 is particularly undesirable insertion into a construction material, since, when activated by neutrons, it creates cobolt-60 which has half-time as long as 5.3 years. Thus construction materials for nuclear applications have to be carefully analyzed as far as the component isotopes are concerned and particularly undesirable isotopes (such as cobolt-60) must be kept at as low level as possible.

EXAMPLE 5-3. Calculate the fraction of iron atoms that are displaced in a sample of steel, which is exposed to a fluence of 10^{24} neutrons/m^2 with an average energy of 0.11 MeV. Assume E_d = 25 eV. SOLUTION: The fraction of displayed atoms is obtained from Eq. (5-22), where for iron A = 56 and the macroscopic cross section for scattering is obtained from Eq. (1-20) as

$\sigma_s \approx 4\pi R^2 \approx 4\pi\left(1.3\cdot 10^{-15} A^{1/3}\right)^2 \approx 3.1\cdot 10^{-28}$ m^2. Thus

$n(E)/N \approx 10^{24}\cdot 3.1\cdot 10^{-28}\cdot 1.1\cdot 10^{5}/56/25 \cong 0.0244\cdot$

5.6.2 Corrosion of Metals

Corrosion is the disintegration of a material into its constituent atoms due to chemical reactions with its surroundings. Most often it means electrochemical oxidation of metals in reaction with oxidants, such as oxygen. Corrosion of metals in aqueous media generally results from heterogeneities encountered in the solid material. Such heterogeneities may exist due to impurity inclusions, differences in grain sizes and composition and differences in stresses. The corrosion might then occur at anodic regions, where the metal dissolves. At cathodic regions hydrogen is liberated or oxidized to water.

Intergranular corrosion (IGC) occurs at grain boundaries, which are anodic with respect to the grains themselves. Intergranular corrosion can occur in certain stainless steels (e.g. type 304) which have been improperly heat treated. It is sometime observed on each side of heat-affected zone of a weld in stainless steel.

Corrosion of metals is significantly influenced by the chemical environment that the materials are interfacing with. Corrosion may also interfere with other phenomena such as mechanical or thermal stresses. This may lead to certain undesirable effects such as the stress corrosion or environmentally accelerated fatigue.

Stress corrosion cracking (SCC) is a sudden failure of normally ductile metal subjected to a tensile stress in a corrosive environment. For example, austenitic steels may crack in the presence of chlorides. This type of failure is particularly dangerous in nuclear applications because it is difficult to detect and it usually progresses very fast. There are three basic factors that influence the stress corrosion cracking: (1) a susceptible material, (2) a corrosive environment, and (3) tensile stresses above a threshold. To prevent the occurrence of the stress corrosion cracking is is necessary to remove at least on of these three factors.

5.6.3 Chemical Environment

In BWRs the reference pressure and the temperature are equal to 7 MPa and 559 K (saturation temperature of water at the reference pressure), respectively. The core inlet parts are typically affected by 10-15 K lower temperature, whereas the coolant temperature at the inlet to the reactor pressure vessel is about 100 K below the saturation temperature. The concentration of oxygen and hydrogen in the reactor coolant is strictly controlled. The standard concentrations have been 200-400 ppb

(part-per-bilion, 10^{-9}) O_2 and about 10 ppb H_2. In the alternative water chemistry (AWC) approach, the concentrations are 5-10 ppb O_2 and 50-150 ppb H_2. To reduce the corrosion, the water electrical conductivity must be kept as low as possible. This is achieved by continuous water cleaning. Typical conductivity of water in BWR is about 10 –20 μS/m (at 298 K).

In PWRs the reference pressure and the temperature are equal to 15.5 MPa and 593 K, respectively. The main difference of water chemistry in PWRs and BWRs is presence of the boric acid (H_3BO_3) in the former. The concentration of the boron in water varies during the fuel cycle. Typical values are 1800 ppm (part-per-milion, 10^{-6}) B at the beginning of cycle and 10 ppm B at the end of cycle. To mitigate the pH-lowering effect of the boric acid, various forms of alkali have to be added. In western PWRs ^{7}LiOH is used, whereas in VVERs KOH/NH_3 is employed. The concentration of alkali is such as to yield pH at the level from 7.5 to 8.5. The water conductivity in the primary loop depends on the concentrations of the boron and alkali. Typical value for PWRs is 2000 μS/m (at 298 K).

5.6.4 Material Fatigue

In case of cyclic loads a progressive and localized failure of material may occur even though the nominal maximum stress values are less than the ultimate tensile stress limit or even less than the yield stress limit of the material. The starting point of any fatigue analysis is the Wöhler (or *S-N*) curve, in which the magnitude of a cyclic stress, *S*, is plotted against the logarithmic scale of cycles to failure, *N*. Typical Wöhler curves for steels and aluminium alloys are shown in FIGURE 5-4. As can be seen, the peak stresss decreases with increasing number of cycles. For mild steels the cycles can be continued indefinitely provided the peak stress is below the endurance (fatigue strength) limit value.

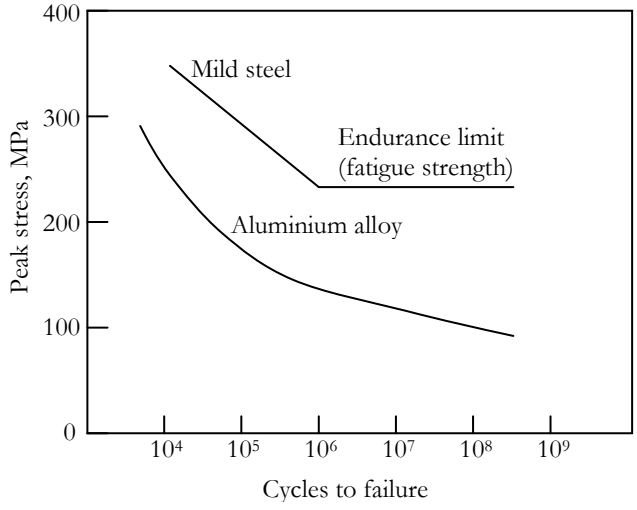

FIGURE 5-4. Typical Wöhler curves for steels and aluminium alloys.

For aluminium alloys the Wöhler curve monotonically decreases in the whole range of cycles and there is no clear endurance limit value for peak stresses. In this case the endurance limit is taken to be the stress when the number of cycles to failure is 10^7 or 10^8.

5.6.5 Thermal Fatigue

Thermal fatigue arises when cyclic stresses result from cyclic temperature changes in a solid material. Temperature changes may occur in various places in nuclear power plants. For example in PWRs the temperature will vary in the pressurizer due to pressure controlling by both water heating and steam spray cooling. Temperature changes are expected to occur in the whole primary system (reactor pressure vessel, piping, etc) due to power changes, reactor shutdown and startup. These types of temperature fluctuations can be forseen on the design stage of the plant and the safe peak stresses can be evaluated for expected number of cycles. Typically the peak stresses in the affected areas should be below the endurance limit to withstand unlimited number of cycles.

Thermal fatigue may lead to severe damages if it occurs in unexpected places. A typical unfavorable situation can arise if a valve, which is normally closed during standard plant operation and separates waters at different temperatures, starts to leak. The mixing of water streams with different temperatures may lead to oscillation of wall temperature, which may lead to failure due to the thermal fatigue. This process can be additionally accelerated due to a presence of welds or discontinuity stresses.

5.6.6 Ageing

Managing ageing of structures, system and components of nuclear power plants is important from the safety point of view. In general, this term is used both to take into account the physical process of material degradadation that takes place due to the plant operation, and to express the obsolescence of particular systems as compared to current standards. The aging process of a nuclear power plant should be monitored and adequate precautions should be taken as described in Safety Guides (e.g. IAEA Safety Standard on "Ageing Management for Nuclear Power Plants").

REFERENCES

[5-1] ASME Pressure Vessel Code, Part III.

[5-2] IAEA Safety Standard: Aeging Management for Nuclear Power Plants.

EXERCISES

EXERCISE 5-1: Calculate the minimum thickness of a pipe with external diameter equal to 550 mm carrying water at pressure 7 MPa and temperature 300 K. The pipe is made of stainless steel type 347.

EXERCISE 5-2: The design internal pressure in the PWR pressure vessel is 17.5 MPa and the outer radius is 2.5 m. The vessel is made of carbon steel with allowable stress 190 MPa at the design temperature. Evaluate the minimum permissible thickness of the reactor pressure vessel wall.

Chapter

6

6 Principles of Reactor Design

The design of nuclear reactors includes several aspects. Firstly, the design must reflect the purpose for which the reactor is to be used. Clearly, different design criteria will be applied for submarine propulsion reactors and for commercial power reactors. Irrespective of the reactor type, the initial design is typically based on the previous experience in the field. For example, very little has been changed in the design of nuclear fuel assemblies starting from generation I through generation IV of nuclear reactors. The evolutionary – rather than revolutionary – changes in reactor designs stems from the fact that reactor design is a very costly process and all possible design flaws must be avoided at earliest possible stage.

This chapter provides principles of the nuclear reactor design. The goal is to indicate the necessary steps that have to be followed during the design process, however, without providing in-depth description of the involved methods.

The first section contains a short description of the nuclear design process, in which the spatial power distribution in a reactor core is evaluated. It also contains such topics as the enrichment, burnable absorbers and refueling design. The second section is dealing with the thermal-hydraulic design in which the distribution of temperature in the reactor core is derermined. Finally, the third section contains a description of the principles of the mechanical design of nuclear power systems.

6.1 Nuclear Design

A nuclear design of a reactor core is performed at various stages of nuclear power plant design, construction and operation. Such designs usually have different levels of accuracy and may be performed as an evaluation, a variant study, or as a verification calculation. An evaluation design employs simplified methods and is based on various simplifying assumptions. A variant study has as a goal to demonstrate the advantages and disadvantages of various design options. Such study is usually performed to support a choice of the optimal reactor design. Finally, the verification calculation has as an objective to perform the nuclear design with the highest possible accuracy.

The main goals of the nuclear desing are to determine:

- the excess reactivity and its effects at any operation condition of the reactor,
- the composition of the nuclear fuel as a function of burnup,
- efficiency of control rods and of safety systems,

- power density distribution as a function of space coordinates and time.

A nuclear design is a computation-intensive process and usually engages several computational programs. Such programs are improved on a regular basis as new methods, which are both faster and more accurate, are developed.

In general the most optimal reactor design is such that has the minimum capital and fuel cost components. The fuel cost depends mainly on the initial enrichment and on the fuel burnup. With increasing fuel enrichment, the fuel burnup increases, but so does the cost of the fuel loaded into the core.

Another parameter that influences the fuel burnup is the ratio of the moderator to the fuel. This ratio, however, is not a free parameter and is typically determined based on safety considerations as to provide a negative moderator reactivity coefficient.

There are various algorithms that may be applied to the nuclear desing of a reactor. Here a simplified approach is shown in order to make the whole process more transparent. In real applications the design process might be much more complex.

It is assumed that the reactor has a cylindrical shape and is divided into L axial zones. Often two zones ($L = 2$) are assumed. In this case the zones are big enough and their mutual influence on each other can be neglected while deriving the constants for analysis of the reactor as a whole. In the same manner the reflector is divided into several radial zones to include not only water, but also construction materials. In calculations it is assumed that the reflector consists of a homogeneous mixture of water and steel.

Nuclear calculations are performed in a equivalent homogeneous cell containing fuel, moderator and construction material. In calculations only few groups of neutrons are considered. More detailed analyses indicate that the best results are obtained with four groups, as shown in TABLE 6.1.

TABLE 6.1. Four-group model for cell calculations.

Group	High Energy	Low Energy	Comment
1	10 MeV	0.821 MeV	The low energy limit corresponds to the threshold energy for fission of ^{238}U
2	821 keV	5.53 keV	The low energy limit corresponds to the lowest energy of fission neutrons
3	5530 eV	0.625 eV	Neutrons in the resonance region
4	0.625 eV	0	Thermal neutrons

The calculation algorithm is as follows:

1. Determine constants for a unit cell. Perform homogenization of the equivalent cell.

2. Determine the neutron spectrum and calculate the constants for one- or two-group diffusion approximation of the whole reactor with the reflector.

3. For given reactor dimensions (they are usually determined on other bases) calculate the effective multiplication factor, k_{eff}.

4. Repeat calculations for various conditions such as: cold reactor, hot reactor, hot reactor with poisons, etc.

5. Evaluate the effect of the control rods.

6. Calculate the power density distribution.

7. In coupled thermal-hydraulic calculations, determine temperature and density distributions of all materials in the reactor. If new values significantly differ from the previous values, repeat calculations from Step 1.

8. Calculate the fuel burnup and the fuel isotopic composition.

6.1.1 Enrichment design

In LWRs light water (H_2O) is used as moderator (and coolant). Since H_2O is not as good moderator as e.g. heavy water (D_2O), the fuel must be enriched in U-235. The required enrichment depends on whether the fuel will be used as initial fuel or as replacement fuel, and also on the required burnup and the length of the fuel cycle.

For initial fuel (first loaded to reactor) the required enrichment is about 2% of U-235. For replacement fuel (used for refueling) the enrichment should increase to 2.5 – 3.5% of U-235. The required enrichment will increase with the length of the fuel cycle and 3.5% is a typical value for a 2-year-long fuel cycle.

The neutron flux over a single fuel assembly is not evenly distributed, which is caused by the non-uniform distribution of the coolant in the assembly. To obtain as flat as possible neutron flux distribution in a fuel assembly, the enrichment is varied in different fuel rods. Thus, in rods close to water volumes is the enrichment reduced. Nearer the bundle center the enrichment is increased, since less moderator is present there compared to the periphery.

The main principle is that the optimal design of fuel assembly yields as uniform power distribution as possible, keeping as high reactivity as possible.

The quality of the power distribution is expressed with the internal power distribution factor, popularly called F_{int}. The parameter is defined as a ratio of maximum rod power to mean in the assembly. Normally it should be from 1.06 to 1.16, depending on the fuel assembly design.

6.1.2 Burnable absorbers

The purpose of burnable absorbers is to reduce the excess reactivity at the beginning of a cycle. The burnable absorbers (called also burnable poisons) are mixed with fuel, in that way their influence on the neutron flux can be easily controlled in space, since they are located in such positions where they are needed. The usual material used for the burnable absorbers include Bor (B) and Gadolinium (Gd). The former one is used mainly in PWRs, whereas the latter one is used in BWRs.

6.1.3 Refueling

During operation of a nuclear reactor the excess reactivity must be large enough to allow for the reactor operation at full power. Since this excess reactivity decreases during reactor operation, it is necessary to refuel the reactor core on regular basis. Fuel is used in a best way when it is replaced successively, with 20 to 40% at each refueling.

The placement of fresh fuel in a reactor core is governed by requirement of maximum fuel utilization and preservation of the required thermal margins. It means that fuel assemblies are reshuffled during each refueling to optimally satisfy the above-mentioned requirements.

The length of a fuel cycle varies and can be from 12 to 20 months. The length of the fuel cycle depends on several factors, like the required fuel burnup at the following refueling. In some countries (e.g. Sweden) refueling is typically scheduled for the summer period when the demand on electricity (and thus the price of electricity) is low. This enforces a 12-month-long fuel cycle.

6.2 Thermal-Hydraulic Design

The primary goals of the thermal core design include achieving a high power density (to minimize core size), a high specific power (to minimize fuel inventory) and high coolant exit temperatures (to maximize thermodynamic efficiency). These goals should be achieved with preserved safety criteria that apply to the nuclear power plant systems and components.

The thermal-hydraulic design of a nuclear reactor consists typically of the following steps:

1. Determine the thermal power of individual fuel assemblies using as the starting point the spatial distribution of power in the reactor core, which is known from the nuclear core design.

2. Determine the total mass flow rate throough the core, W_c, resulting from the stationary momentum conservation in the primary loop.

3. Determine the distribution of coolant flow through the fuel assemblies in the reactor core that satisfy the required principle of the flow profiling.

4. Determine the actual distribution of coolant flow through fuel assemblies that satisfy the mass and momentum conservation over the reactor core.

5. Determine the pressure losses in fuel assemblies in the reactor core.

6. Determine the axial distribution of coolant enthalpy, temperature, pressure, quality and void fraction as well as the heat flux from the fuel elements to the coolant.

7. Determine the pressure loss coefficients.

8. Determine the critical values of heat flux or critical power of fuel assemblies with respect of the occurrence of the boiling crisis.

9. Determine heat transfer coefficients.

10. Determine the axial and radial temperature distribution in nuclear fuel rods.

Step 3 is required when a non-uniform distribution of coolant flow through the reactor core is to be achieved by introduction of the variable throttling at the inlets to fuel assemblies. The determined throttling distribution is then used in step 4 to calculate the actual flow distribution in the reactor core.

6.2.1 Thermal-Hydraulic Constraints

The goals of the core design are subject to several important constraints. The first important constraint is that the core temperatures remain below the melting points of core components. This is particularly important for the fuel and the clad materials.

There are also limits on heat transfer rate between the fuel elements and coolant, since if this heat transfer rate becomes too large, critical heat flux may be approached leading to boiling transition. This, in turn, will result in a rapid increase of the clad temperature.

The coolant pressure drop across the core must be kept low to minimize pumping requirements as well as hydraulic stresses on core components.

Above mentioned constraints must be analyzed over core live, since as the power distribution in the core changes due to fuel burnup or core reloading, the temperature distribution will similarly change.

Furthermore since the cross sections governing the neutronics of the core are strongly temperature- and density-dependent, there will be a strong coupling between the thermal-hydraulic and neutronic behavior of the reactor core.

6.2.2 Hot Channel Factors

One of the main goals of the thermal-hydraulic core analysis is to ensure that the thermal limitations on the core behavior are not exceeded. So far two such limitations have been discussed shortly:

To exclude melting of the fuel, the linear power density must be limited,

(6-1) $$q'(\mathbf{r}) < q'_{\max} .$$

Another limitation is dictated by the requirement that the surface heat flux always remains below the critical limit,

(6-2) $$q''(\mathbf{r}) < q''_{CHF} .$$

Here **r** is any location in the nuclear core.

In addition to the two limitations, other issues like thermal and fission gas stresses on the clad can limit the core performance and thus can limit power generation. Furthermore, the core stability consideration may be another limiting circumstance.

A thorough thermal-hydraulic analysis of the core requires a detailed, three-dimensional calculation of the core power distribution, including the effects of fuel burnup, fission product buildup, control distributions, and moderator density variations over core life. This information is next used to determine the coolant flow and temperature distribution throughout the core. Even though such types of calculations are performed nowadays, they are quite expensive and time consuming. Especially for fast transient applications they are prohibitively expensive and are avoided.

To make the thermal-hydraulic core analysis more practical, a common approach is to investigate how closely the **hot channel** in the core approaches the operating limitations. Then if one can ensure that the thermal conditions of this channel remain below the core limitations, the remaining channels will presumably fall within design limitations. One usually defines the hot channel in the core as that coolant channel in which the core heat flux and enthalpy rise is the largest. Associated with this channel are various hot channel or **hot spot** factors relating the performance of this channel to the average behavior of the core.

The fuel assembly having the maximum power output is defined as the **hot assembly**. The hot spot in the core is the point of maximum heat flux or linear power density, while the hot channel is defined as the coolant (sub-) channel in which the hot spot occurs or along which the maximum coolant enthalpy increase occurs.

The **nuclear hot channel** is defined to take into account the variation of the neutron flux and fuel distribution within the core.

The **radial nuclear hot channel factor** is defined as,

$$F_R^N = \frac{\textit{average heat flux of the hot channel}}{\textit{average heat flux of the channels in core}} = \frac{\int_{-H/2}^{H/2} q''(\mathbf{r}_{HC})dz}{\frac{1}{N_C}\sum_{i=1}^{N_C}\int_{-H/2}^{H/2} q''(\mathbf{r}_i)dz} \tag{6-3}$$

.

Here N_C is the total number of channels in core. In a similar manner, the **axial nuclear hot channel factor** is defined as,

$$F_Z^N = \frac{\textit{maximum heat flux of the hot channel}}{\textit{average heat flux of the hot channel}} = \frac{\max_z[q''(\mathbf{r}_{HC})]}{\frac{1}{H}\int_{-H/2}^{H/2} q''(\mathbf{r}_{HC})dz}. \tag{6-4}$$

The **total nuclear hot channel factor** or **nuclear heat flux factor** is then,

(6-5) $$F_q^N = \frac{maximum\ heat\ \ flux\ in\ the\ core}{average\ heat\ \ flux\ in\ the\ core} = F_R^N F_Z^N .$$

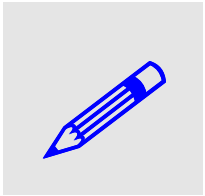

EXAMPLE 6-1: The power distribution in a homogeneous, bare cylindrical core is described by the following expression (assuming for simplicity $\tilde{R} \cong R$ and $\tilde{H} \cong H$,

$$q'''(z) = w_f \Sigma_f \phi_0 J_0\left(\frac{2.405 r_f}{R}\right)\cos\left(\frac{\pi z}{H}\right).$$

The radial factor is then

$$F_R^N = \frac{J_0(0)\int_{-H/2}^{H/2}\cos\left(\frac{\pi z}{H}\right)dz}{\frac{1}{\pi R^2}\int_0^R J_0\left(\frac{2.405 r}{R}\right)2\pi r dr \int_{-H/2}^{H/2}\cos\left(\frac{\pi z}{H}\right)dz} \approx 2.32$$

and the axial factor is,

$$F_Z^N = \frac{J_0(0)\cos(0)}{J_0(0)\frac{1}{H}\int_{-H/2}^{H/2}\cos\left(\frac{\pi z}{H}\right)dz} \approx 1.57$$

This implies the overall hot channel factor: $F_q^N \approx 2.32 \cdot 1.57 \approx 3.642$.

This is a quite conservative (e.g. high) estimation of the factor. A zone-loaded PWR will typically have a nuclear hot channel factor of $F_q^N \approx 2.6$.

The nuclear heat flux hot channel factor is defined assuming nominal fuel pellet and rod parameters. In reality, however, there will be local variation in fuel pellet density, enrichment and diameter, surface area of fuel rod and eccentricity of the fuel-clad gap due to manufacturing tolerances and operating conditions. The more general **heat flux hot channel factor** or **total power peaking factor** F_q is defined as the maximum heat flux in the hot channel divided by the average heat flux in the core (allowing for above-mentioned variability). F_q and F_q^N are related by defining an **engineering heat flux hot-channel factor** F_q^E.

(6-6) $$F_q^E = \frac{F_q}{F_q^N}.$$

Typically F_q^E is close to unity reflecting the fact that manufacturing tolerances are quite small (in modern PWRs, $F_q^E \approx 1.03$).

One can also define an **enthalpy-rise hot channel factor**,

(6-7) $$F_{\Delta H} = \frac{maximum\ coolant\ enthalpy\ rise}{average\ coolant\ enthalpy\ rise}.$$

This factor is a function of both variations in the power distribution and coolant flow. For example, some 3-10% of the coolant flow bypasses the fuel assemblies, due to leaks or the presence of other core components. This factor accounts for

manufacturing tolerances and also structure displacement (box bow, rod bow, etc) caused by the operation conditions.

6.2.3 Safety Margins

Practically all systems have some limits of safe operation. For example, elevators have a certain limit value of the load that they can carry. **Safety limit** for engineering systems can usually be determined with a reasonably good approximation, but never exactly. This is due to the fact that the limit value, when the system breaks, depends on many uncertain factors, such as the manufacturing tolerances, material properties, load characteristics, etc. Thus, for safety reasons the allowed value of the critical parameter of the considered system must be lower than the known limit value, when the system breaks. The difference between the actual and the limit value of the critical parameter is called the safety margin.

Safety margins are expressed in the same physical units as the critical parameters. For example, if the critical parameter is a load (as in case of elevators), the safety margin is expressed in Newtons (N).

Safety limits in nuclear power plants are provided in the technical specifications of the systems. In each country the safety limits are provided by a proper authority (SSM in Sweden). Such safety limits are called acceptance criteria and include such parameters as the reactor coolant system pressure, linear heat generation of fuel, fuel temperature, fuel clad temperature, percentage of fuel failure, departure from nuclear boiling ratio and critical power ratio. Thus safety margins can be express as differences between acceptance criteria and actual values of plant parameters. The various definitions given above are illustrated in FIGURE 6-1.

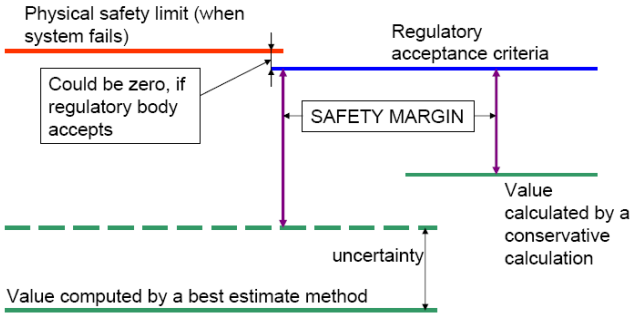

FIGURE 6-1: Relationship between the actual value, the safety limit and the safety margin.

The actual value of any parameter in nuclear power plant is not known exactly, since the calculation procedures are always connected to uncertainties. These uncertainties result from the modeling approximations, numerical errors and errors imbedded in correlations that are used in calculations.

There are two principle ways to predict the actual values of parameters:

- conservative predictions, in which all parameters are assumed to have the most unfavorable value that could be expected at any foreseen circumstances

- best-estimate predictions, in which all parameters are assumed to have statistically-mean value from the set of possible values at any foreseen circumstances

In the best-estimate approach it is necessary to evaluate the final uncertainty of the parameter under consideration.

Safety limits are set as international standards and are accepted by national regulatory bodies. Selected safety limits are as follows:

- **Peak Clad Temperature** (PCT) – 1478 K (1204 °C),
- maximum clad oxidation – 17% of clad thickness,
- maximum hydrogen generation – not to exceed deflagration or detonation limits for containment integrity.

One of the objectives of the thermal-hydraulic core design is to determine the thermal margins as accurately as possible. On one hand the margins should be large enough to ensure safe operation of the nuclear power plant. On the other hand the plant should operate at conditions that ensure high performance and efficiency. The safety margins in nuclear power plants contain several contributing factors, as indicated in FIGURE 6-2.

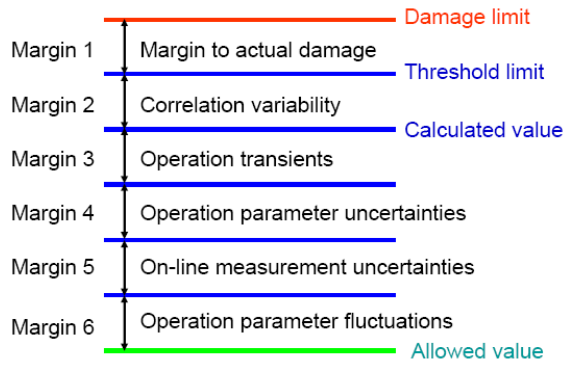

FIGURE 6-2: Various components of safety margins.

6.2.4 Heat Flux Limitations

If the limit of critical heat flux is exceeded in any place in nuclear reactor core, the clad and fuel temperature will significantly increased due to deteriorated heat transfer to coolant. The DNB-type limitation is particularly important in PWRs, however, it can not be ruled out even in BWR, in cases when the axial power distribution is inlet-skewed. The dryout-type limitation is a concern in BWR exclusively.

Typical way to express the heat flux limitation condition is by means of a ratio of the critical heat flux to the actual one. For PWR applications the following ratio is used,

$$DNBR(z) = \frac{q''_{DNB}(z)}{q''(z)}, \tag{6-8}$$

where:

$DNBR(z)$ - **Departure from Nucleate Boiling Ratio** at location z,

$q''_{DNB}(z)$ - value of the critical flux at location z,

$q''(z)$ - value of the actual heat flux at location z.

FIGURE 6-3 illustrates the typical distributions of DNBR, the critical heat flux and the actual heat flux in a heated channel.

For BWRs the following ratio is used,

(6-9) $$CPR = \frac{q_{cr}}{q_{ac}},$$

where,

CPR - **Critical Power Ratio**

q_{cr} - critical power in a fuel assembly (that is the power at which the dryout occurs),

q_{ac} - actual power of the fuel assembly.

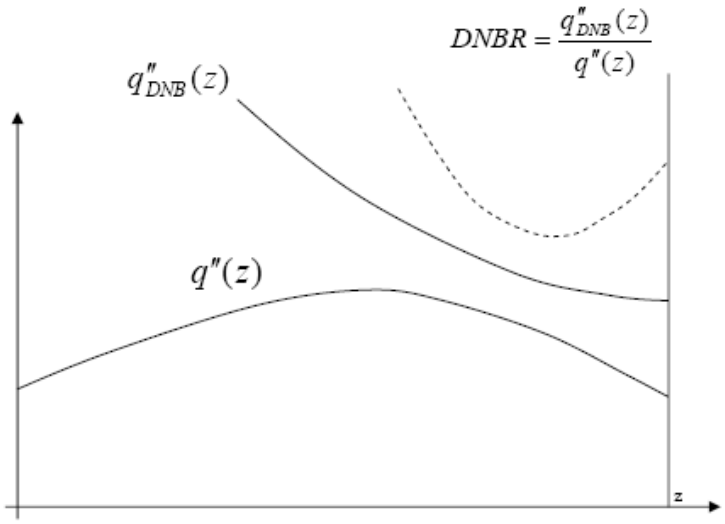

FIGURE 6-3: Distributions of DNBR, critical heat flux and actual heat flux in a heated channel.

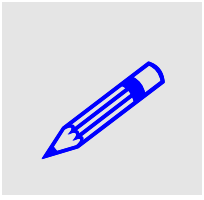

EXAMPLE 6-2: A vertical PWR fuel rod bundle with hydraulic diameter D_h = 10 mm and length H = 3.66 m is heated with non-uniform heat flux distribution given as $q''(z) = q''_0\{1+\cos[\pi(z/H-0.5)]\}$ and cooled with water coolant at 15.5 MPa pressure, 30 K inlet subcooling and mass flux G = 2000 kg/m².s. Use the Lntsman&Levitan DNB correlation and find the MDNBR (minimum DNBR) and its location in the channel. SOLUTION: the actual and the DNB heat flux distributions are plotted along the channel and shown in FIGURE 6-4. The MDNBR is found as z = 2.745 m from the inlet and its value is 1.393.

A script to perform calculations in EXAMPLE 6-2 and to plot the DNBR distribution along the heated channel is given below.

COMPUTER PROGRAM: Program to plot curves shown in FIGURE 6-4.

```
// Calculate MDNBR in a channel and plot
// axial distributions of quality, critical
// heat flux, actual heat flux and DNBR
//
//   Channel geometry
D    = 0.01;            // Hydraulic diameter
L    = 3.66;            // Heated length
//--------------------
// Working conditions
p = 155.;               // Pressure
dTsubi = 30;            // Inlet subcooling
G = 2000;               // Inlet mass flux
q2p0 = 0.54e6;          // Heat flux in the center
//--------------------
// properties
i_f = hlsat(p);   // Liquid saturation enthalpy
i_g = hvsat(p);   // Vapor saturation enthalpy
i_lin  = hliq(p, tsat(p)-dTsubi);  // Inlet liquid enthalpy
i_fg = i_g - i_f; // Latent heat
x_in = (i_lin-i_f)/i_fg;  // Inlet quality
//
qcon = (10.3 - 7.8*p/98. + 1.6*(p/98)^2);  // Quality-independent part
qcon = qcon*sqrt(0.008/D);                 // Diameter correction
//----------------------
// Calculations
z = linspace(0,L,25);
q2p = q2p0*(1+cos(%pi*(z/L-0.5)));
x = x_in + (4*q2p0/(G*D*i_fg)) * (z+L/%pi* (sin(%pi*(z/L-0.5)) +1));
q2pcr = 1.e6*qcon*(G/1000.).^(1.2*((0.25*(p-98)/98)-x)).*exp(-1.5*x);
dnbr = q2pcr./q2p;
[MDNBR,k] = min(dnbr);
// ---------------------
// Plot the axial distributions of heat flux, critical heat flux
// DNBR and quality
f1=scf(1);
af=get("current_axes");    // Get axes
af.font_size = 3;          // Axes font size
af.font_style = 3;         // Axes font style
af.x_label.font_size = 3;  // x-axis labels font size
af.y_label.font_size = 3;  // y-axis labels font size
tf=af.title;               // Titles
tf.font_size = 3;          // Title font size
xgrid(2);
xtitle(" ","Distance, [m]","Heat Flux, [MW/m^2], Quality [-]");
f=get("current_figure");
fignum=f.figure_id;
fignam="L9Ex2";
plot(z,q2p/1e6,'o-',z,q2pcr/1e6,'^-.',z,dnbr,'v--',z,x,'k*')
legend(['Heat Flux','CHF','DNBR','Quality'],a=1);
```

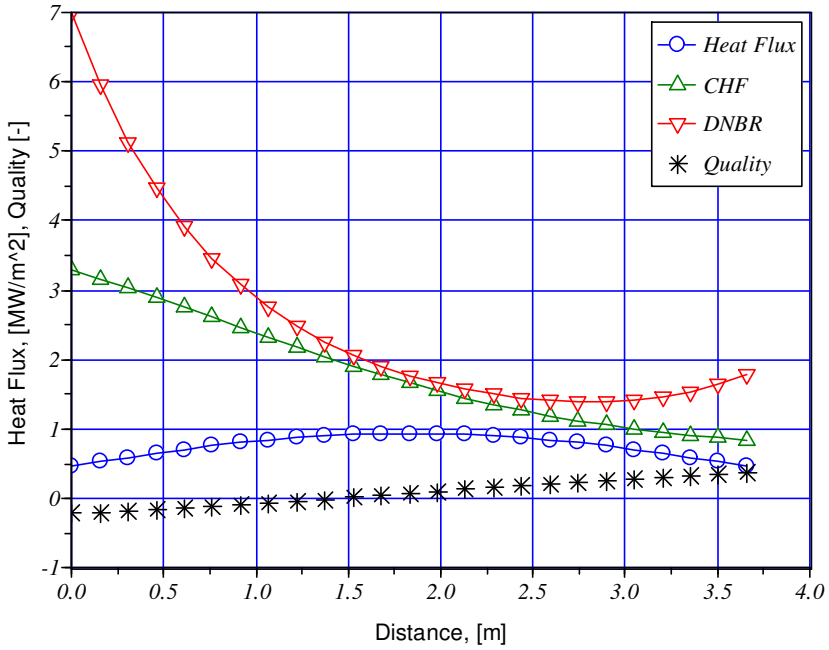

FIGURE 6-4: Distributions of the actual and DNB heat flux in a heated channel from EXAMPLE 6-2.

6.2.5 Core-Size to Power Relationship

The averaged linear power density in fuel rods is given as,

$$q'_{AVR} = \frac{C_1 q_R}{H \cdot N_R}, \tag{6-10}$$

where:

q'_{AVR} - core-averaged linear power density [W/m],

C_1 - fraction of the core power generated in the fuel (~0.95÷0.97),

q_R - total thermal reactor power [W],

H - core height [m],

N_R - number of fuel rods.

The average core power density is equal to the core power q_R divided by the core volume V_R, that is,

$$q'''_{AVR} \equiv \frac{q_R}{V_R} = \frac{\frac{HN_R q'_{AVR}}{C_1}}{\frac{\pi D_C^2}{4} H} = \frac{4 q'_{AVR} N_R}{C_1 \pi D_C^2}. \tag{6-11}$$

Here D_C is the core diameter. On a purely geometrical consideration, the relationship between the averaged linear and volumetric power densities for square rod lattices is as follows,

$$q'''_{AVR} = \frac{q'_{AVR}}{p^2}, \tag{6-12}$$

where p is the lattice pitch.

Combining Eqs. (6-10) through (6-12), the following expression for the required core diameter is obtained,

$$D_C = 2p\sqrt{\frac{q_R}{Hq'_{AVR}\pi}}. \tag{6-13}$$

For a target reactor height H and power q_R, the core diameter can be decreased by decreasing the lattice pitch or by increasing the linear power density. Obviously, the linear power density in the channel with the highest peaking factor has to be lower than the maximum limit value, that is,

$$q'(z) < q'_{MAX} = q'_{AVR} F_q^N, \tag{6-14}$$

and the required minimum core diameter is obtained as,

$$D_{C,MIN} = 2p\sqrt{\frac{q_R F_q^N}{Hq'_{MAX}\pi}}. \tag{6-15}$$

The maximum allowable linear heat density q'_{MAX} is obtained from a proper DNB or dryout correlation, assuming the required safety factor DNBR or CPR.

Equation (6-15) reveals the importance of the total nuclear heat flux factor F_q^N: keeping this factor low allows to reduce the minimum required core diameter.

6.2.6 Probabilistic Assessment of CHF

Once determining the local value of the critical heat flux, it may be calculated only with some limited accuracy. Correlation developers usually specify the correlation accuracy by giving the standard deviation of the predicted value. Typically it is assumed that CHF is a stochastic variable which has the normal distribution (also called the Gauss distribution). Such distribution is shown in FIGURE 6-5 (probabilistic density function) and FIGURE 6-6 (cumulative distribution function for the normal distribution.

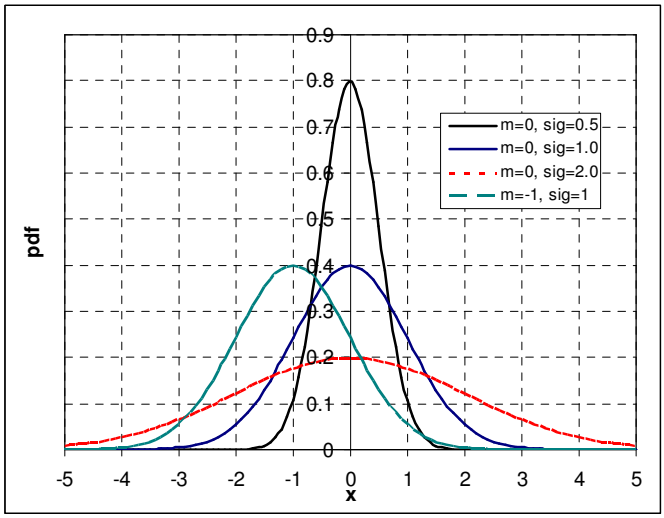

FIGURE 6-5: Probability density function (pdf) for the normal distribution.

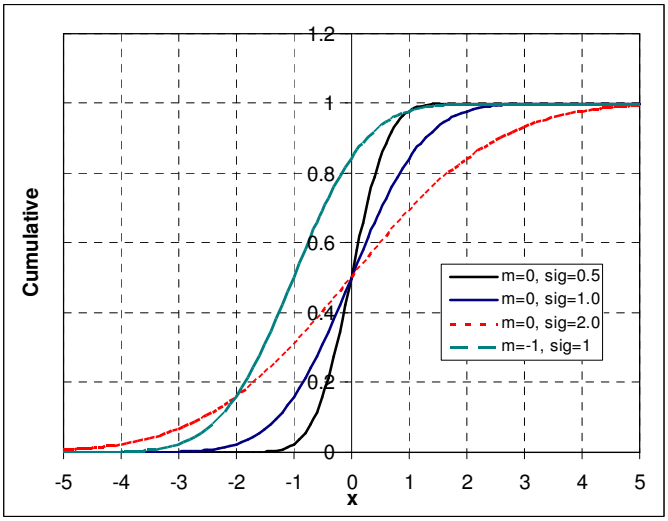

FIGURE 6-6: Cumulative distribution function for the normal distribution.

If the probability distribution function of CHF for a single rod is as shown in FIGURE 6-7 and the actual value of the heat flux is given by the vertical line AB, then the shaded area corresponds to the probability that the rod will experience CHF.

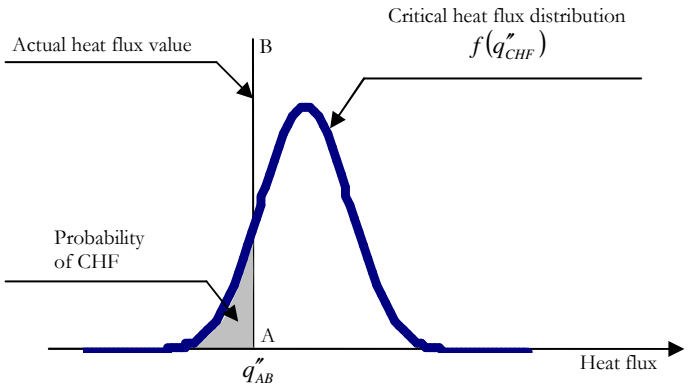

FIGURE 6-7: Graphical illustration of the probability of CHF with known value of the actual heat flux.

The probability of CHF with known actual value of heat flux, q''_{AB} can be calculated as,

$$p_{CHF} \equiv p(q''_{CHF} < q''_{AB}) = \frac{1}{\sigma\sqrt{2\pi}} \int_0^{q''_{AB}} e^{\frac{(q''_{CHF} - \overline{q''_{CHF}})^2}{2\sigma^2}} dq''_{CHF} \,. \tag{6-16}$$

Here $\overline{q''_{CHF}}$ is the mean value of the critical heat flux and σ is its standard deviation. Note that the integration is carried out from 0 rather than from $-\infty$ since the heat flux can not be negative. In practical calculations the cumulative distribution function of a standard normal variable is used. This function, defined as,

$$\Phi(z) = p(Z < z) = \frac{1}{\sqrt{2\pi}} \int_{-\infty}^{z} e^{\frac{-\xi^2}{2}} d\xi \,, \tag{6-17}$$

is given in table forms in handbooks dealing with statistics. The function is usually given for z-values between 0 and 5. To obtain its value for $-5 < z < 0$, the following relationship is used,

$$\Phi(-z) = 1 - \Phi(z) \,. \tag{6-18}$$

Thus, the CHF probability can be calculated using the standard function as follows,

$$p_{CHF} = 1 - \Phi\left(\frac{\overline{q''_{CHF}} - q''_{AB}}{\sigma}\right) \,. \tag{6-19}$$

APPENDIX C contains a table with values of the above function.

EXAMPLE 6-3: A single fuel rod operates at a constant and uniform heat flux equal to 1 MW/m². With the current cooling conditions, the calculated critical heat flux is 1.1 MW/m². The correlation developer specified that the standard deviation for the correlation is equal to 5%. Assuming the normal distribution of the CHF probability density function, calculate the probability of the CHF occurrence for the rod. SOLUTION: The CHF standard deviation is equal to 0.05*1.1 = 0.055 MW/m². The argument of the standard cumulative function is equal to (1.1-1)/0.055 = 1.81818… ~= 1.82. From the table in APPENDIX C, the probability of CHF is found equal to 0.03438.

In a similar way the probability of CHF can be calculated when both the CHF and the actual heat flux have known probabilistic density function distributions. In such cases, the probability of dryout is estimated as illustrated in FIGURE 6-8.

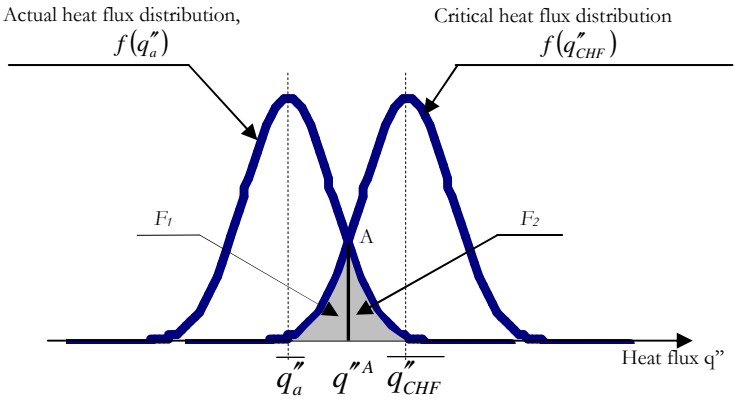

FIGURE 6-8: Graphical illustration of the probability of CHF when both the actual and the critical value of the heat flux are stochastic functions with known distributions.

The figure shows the probability density functions for the actual, q''_a, and the critical heat flux, q''_{CHF}. Both these functions have in general different shapes, but it is assumed that they follow the normal distribution. The curves cross each other at point *A*. The shaded areas are given as,

$$F_1 = \int_0^{q''^A_{CHF}} f(q''_{CHF})dq''_{CHF}\,, \tag{6-20}$$

$$F_2 = \int_{q''^A_a}^{\infty} f(q''_a)dq''_a\,. \tag{6-21}$$

F_1 is the probability that $q''_{CHF} < q''^A$, that is, the probability that the critical heat flux is less then the heat flux at point *A*. Similarly, F_2 is the probability that $q''_a > q''^A$, that is, the probability that the actual heat flux is larger than the heat flux at point *A*. Thus the product F_1F_2 is the probability that simultaneously $q''_{CHF} < q''^A$ and $q''_a > q''^A$, in which case the CHF will occur.

However, the product F_1F_2 is not equal to the probability of CHF occurrence, since such stochastic events corresponding to CHF as $q''_a > q''_{CHF} \cap q''_{CHF} > q''^{A}_{CHF}$ or $q''_a > q''_{CHF} \cap q''_a < q''^{A}_a$ are excluded. Thus, the product F_1F_2 is the lower estimate of the CHF probability, that is,

(6-22) $$p_{CHF} > F_1F_2,$$

for any values of $q''_a > q''_{CHF}$.

The probability that both $q''_a < q''^{A}_a$ and $q''_{CHF} > q''^{A}_{CHF}$ is given by the product $(1-F_1)(1-F_2)$ and corresponds to the situations when CHF will not occur. However, this product is not equal to the probability of the non-occurrence of CHF, since such stochastic events corresponding to non-CHF cases as $q''_a < q''_{CHF} \cap q''_{CHF} > q''^{A}_{CHF}$ are not included. Thus, the product $(1-F_1)(1-F_2)$ is the lower estimate of the no-CHF probability, that is,

(6-23) $$p_{no-CHF} > (1-F_1)(1-F_2).$$

Since,

$$p_{CHF} + p_{no-CHF} = 1,$$

then, the CHF probability is determined by the following interval,

(6-24) $$F_1F_2 < p_{CHF} < F_1 + F_2 - F_1F_2.$$

In the computational procedure, it is first necessary to find the heat flux at point A and next to find areas F_1 and F_2 using the standard cumulative function, as shown in the example above.

6.2.7 Profiling of Coolant Flow through Reactor Core

A nuclear reactor core consists of many parallel connected heated channels through which the total flow is distributed according to the distribution of local pressure losses. Since all channels have common inlet and outlet plena, the total pressure drop in each channel is the same and equal to the total pressure drop over the whole reactor core. In a design of nuclear reactor cores it has to be considered how to distribute the flow through the heated channels. Such process is called flow profiling through the reactor core.

The flow profiling is performed with two types of general assumptions:

- *profiling with constant distribution of heat sources*, in which it is assumed that during the whole period of the reactor operation the power distribution will have the same spatial shape,

- *profiling with variable distribution of heat sources,* in which a variation of the heat source distribution during the whole period of the reactor operation is taken into consideration.

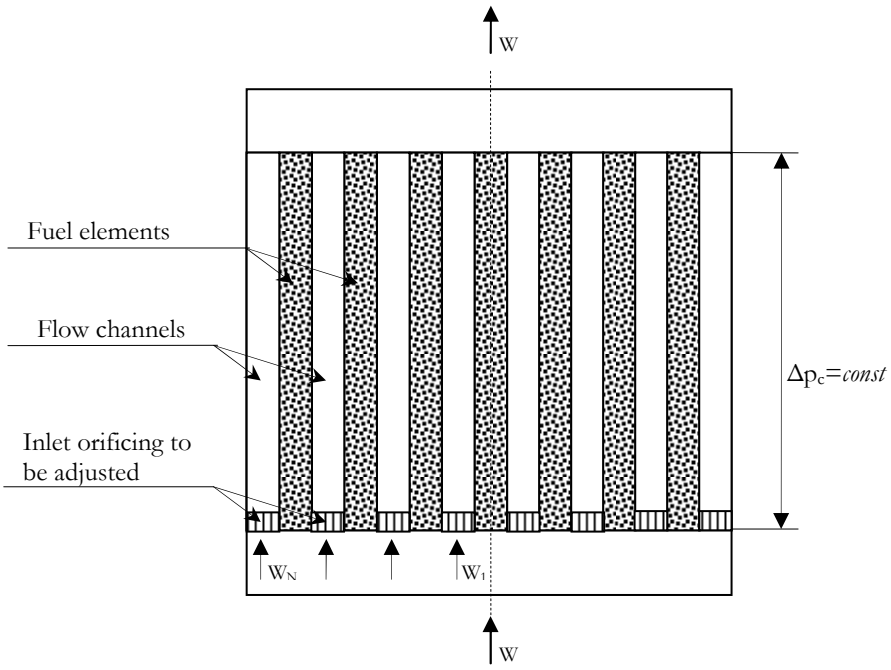

FIGURE 6-9: Flow distribution through parallel channels in a reactor core.

The following constraints have to be satisfied once performing the flow profiling:

(6-25) $$\sum_{i=1}^{N} W_i = W$$

(6-26) $$\Delta p_i = \Delta p_c = const\,,\ i = 1, \ldots, N$$

Using the above equations, the inlet orificing should be selected in such a way that:

- the total pressure drop over the reactor core is the lowest possible,
- the total reactor power is the highest possible with given limiting values and required safety margins for all safety parameters,
- coolant flow through the reactor core remains stable in all channels under all anticipated conditions.

A complete and thorough flow profiling that satisfies all three conditions is a complex process and its description is beyond the scope of the present book. Here a simple system (see EXAMPLE 6-4 and FIGURE 6-10), is analyzed to demonstrate some particular features of the flow profiling analysis.

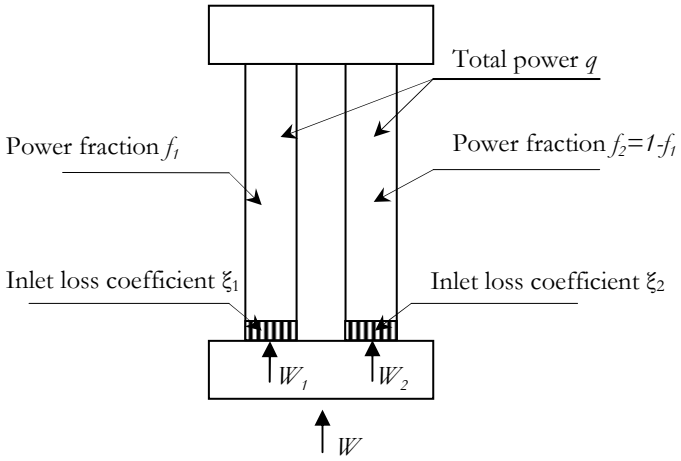

FIGURE 6-10: Flow profiling in a two-channel system with non-uniform power distribution.

EXAMPLE 6-4: Two identical heated channels have common inlet and outlet plena, as shown in FIGURE 6-10. Determine the required inlet loss coefficients to obtain the maximum total power of both channels q and the minimum required pumping power if the power fractions in channels are known and equal to f_1 and f_2. Neglect the hydrodynamic flow stability considerations. Assume that the limiting thermal parameter is the heat flux in the channels. Use the Levitan&Lantsman correlation to determine the DNB heat flux. SOLUTION: Clearly, the solution is trivial if both power fractions are equal to each other. In this situation the flows should be equal in both channels. To get the minimum required pumping power, the pressure losses should be as low as possible, thus no additional orificing should be introduced (the flow stability is not discussed in this example); this leads to the following solution: $W_1 = W_2 = W/2$ and $\xi_1 = \xi_1 = 0$. Thus, in the continuation it is assumed that f_1 and f_2 are not equal. The critical heat flux in each of the channels is obtained as (see Eqs. (4-98) and (4-99)),

$$q''_{cr,1}=\left(\frac{8}{D}\right)^{0.5}\left[10.3-7.8\frac{p}{98}+1.6\left(\frac{p}{98}\right)^2\right]\left(\frac{W_1/A}{1000}\right)^{1.2\{[0.25(p-98)/98]-x_{e,1}\}}e^{-1.5x_{e,1}}=\varphi_1(p,D,A)\cdot\varphi_2(x_{e,1})\cdot W_1^{\varphi_3(p,x_{e,1})}$$

Here φ_1, φ_2 and φ_3 denote functions of given parameters. Since the channels are identical and assuming that the reference pressure in the DNB correlation is the same for both channels, the critical heat flux in the second channel is given as,

$$q''_{cr,2}=\varphi_1(p,D,A)\cdot\varphi_2(x_{e,2})\cdot W_2^{\varphi_3(p,x_{e,2})}$$

The maximum power in the system will be obtained when the critical power ratio are equal in both channels. That is,

$$CPR_1=\frac{q''_{cr,1}}{q''f_1}=\frac{\varphi_1(p,D,A)\cdot\varphi_2(x_{e,1})\cdot W_1^{\varphi_3(p,x_{e,1})}}{q''f_1}=CPR_2=\frac{\varphi_1(p,D,A)\cdot\varphi_2(x_{e,2})\cdot W_2^{\varphi_3(p,x_{e,2})}}{q''(1-f_1)}$$

The above equation must be solved together with the mass conservation equation $W_1 + W_2 = W$ to obtain the required mass flow rate distribution, W_1 and W_2. In the next step, the pressure drop equations for both channels must be solved to obtain the required orificing to realize the required mass flux distribution.

6.3 Mechanical Design

The purpose of the mechanical design is to establish the construction details of plant components to withstand loads during the operation of the nuclear power plant.

6.3.1 Design Criteria and Definitions

Design criteria are specified in the boiler and pressure vessel codes such as the ASME Code section III[6-1].

The basic design criterion stipulates that the nuclear power plant design should be such that stress intensities will not exceed the specified limits.

The failure theory is based on the maximum shear stress theory. The maximum shear stress at a point is equal to one-half the difference between the algebraically largest and the algebraically smallest of the three principal stresses.

A **primary stress** is any normal stress or a shear stress developed by an imposed loading which is necessary to satisfy the laws of equilibrium of external and internal forces and moments. The main characteristic of a primary stress is that it is not self-limiting. Primary stresses that considerably exceed the yield strength will result in failure. A thermal stress is not classified as a primary stress. Example of primary stress is a general membrane stress in a circular cylindrical or a spherical shell due to internal pressure or to distributed live loads.

A **secondary stress** is a normal stress or a shear stress developed by the constraint of adjacent material or by self-constraint of the structure. A general thermal stress is an example of a secondary stress.

A **thermal stress** is a self-balancing stress produced by a nonuniform distribution of temperature or by differing thermal coefficients of expansion.

6.3.2 Stress Intensity

The algebraic difference between the largest and (algebraic) smallest of the principal stresses at a given location is called the *equivalent intensity of combined stresses*. This term is commonly abbreviated to **stress intensity** and is equivalent to twice the maximum shear stress.

Once determining stress intensities, the following steps should be followed:

1. At the point on the component which is being investigated, choose an orthogonal set of coordinates, such as tangential, radial and longitudinal, and designate them with subscripts t, r and l. The stress components in these directions are then designated σ_t, σ_r and σ_l for direct stresses and τ_{lt}, τ_{lr} and τ_{rt} for shearing stresses.

2. Calculate the stress components for each type of loading to which the part will be subjected and assign each set of stress to one or a group of the following categories:

    a. General primary-membrane stress, P_m,

    b. Local primary-membrane stress, P_L,

    c. Primary bending stress, P_b,

d. Expansion stress, P_e,

e. Secondary stress, Q,

f. Peak stress, F.

3. For each category, calculate the algebraic sum of the σ_t's that results from the different types of loadings and similary for the other five stress components. Certain combinations of these categories must also be considered.

4. Translate the stress components for the t, r and l directions into principal stresses, σ_1, σ_2 and σ_3.

5. Calculate the stress differences S_{12}, S_{23}, S_{31} from the relations, $S_{12} = \sigma_1 - \sigma_2$, $S_{23} = \sigma_2 - \sigma_3$, $S_{31} = \sigma_3 - \sigma_1$. The stress intensity S is found as the largest absolute value of S_{12}, S_{23}, S_{31}.

6.3.3 Piping Design

For a straight pipe under internal pressure, the minimum thickness of a pipe wall required for design pressure shall be determined from one of the following formulas[6-1],

$$t_m = \frac{pD_o}{2(S_m + y \cdot p)} + a \quad \text{or} \quad t_m = \frac{pD + 2a(S_m + y \cdot p)}{2(S_m + y \cdot p - p)}, \tag{6-27}$$

where,

t_m - the minimum required wall thickness, m

p - internal design pressure, MPa

S_m - maximum allowable stress at design temperature, MPa

D - inside pipe diameter, m

D_o - outside pipe diameter, m.

a - an additional thickness (due to corrosion, material removal, etc), m

$y = 0.4$.

Additional thickness should be added to pipe bends, pre-manufactured elbows, branch connections, openings, closures, etc. The required additional thickness is specified in more detailed pipe design codes.

6.3.4 Vessels Design

A tentative thickness of cylindrical shells and spherical shells can be found as[6-1],

(6-28) $$t_{CS} = \frac{pR}{S_m - 0.5p} \text{ or } t_{CS} = \frac{pR_o}{S_m + 0.5p},$$

(6-29) $$t_{SS} = \frac{pR}{2S_m - p} \text{ or } t_{SS} = \frac{pR_o}{2S_m}.$$

Here,

t_{CS} - thickness of cylindrical shell, m

t_{SS} - thickness of spherical shell, m

p - internal pressure, MPa

S_m - maximum allowable stress at design temperature, MPa

R - inside radius of shell, m

R_o - outside radius of shell, m.

Once a tentative wall thickness in a vessel is establish, additional calculations are needed to account for local stress values due to openings, nozzles, reinforcements and welding joints. The recommendations given in a pertinent pressure vessel code should be followed.

REFERENCES

[6-1] ASME Pressure Vessel Code. Part III.

EXERCISES

EXERCISE 6-1: A certain reactor contains 50000 identical fuel rods subject to exactly the same operating conditions. The safety authority requires that no single fuel rod should be under CHF during normal operating conditions. Assume a normal distribution of the probability of CHF: (a) What should be the limit probability of CHF for a single fuel rod to satisfy the requirement of the safety authority? (b) Find the minimum CPR to satisfy the requirement assuming that the operating conditions are known exactly and the standard deviation of the CHF correlation is 3.5%, (c) How the reactor power should change to satisfy the same requirement if the standard deviation of the CHF correlation was 7% instead of 3.5%?.

Chapter 7

7 Environmental and Economic Aspects of Nuclear Power

Energy in general can be considered in two categories – primary and secondary. Primary energy is energy in the form of natural resources, such as wood, coal, oil, natural gas, natural uranium, wind, hydro power and sunlight. Secondary energy is in the more usable forms which primary energy may be converted to, such as electricity, petrol and hydrogen. Primary energy can be either renewable (solar, wind, wave, biomass, geothermal energy and hydro power) or non-renewable (fossil fuels – coal, oil and natural gas – and uranium). Each kind of energy transformation from the primary to the secondary form has some environmental effects, as well as it is connected with specific costs.

Uranium is abundant in nature and technologies exist that can extend its use 60-fold if demand requires it. World mine production is about 35000 tons per year, but a lot of the market is being supplied from secondary sources such as stockpiles, including material from dismantled nuclear weapons. Practically all of it is used for electricity. Uranium has the highest heat value of all known fuels and that makes it a very attractive source of energy.

Due to fission processes that take place in nuclear reactors highly radioactive fission products are produced. These wastes must be carefully taken care of to not pollute the environment. All this basic aspects of nuclear fuel cycle are discussed in this Chapter.

7.1 Nuclear Fuel Resources and Demand

7.1.1 Uranium Resources

Identified resources of uranium consist of **Reasonably Assured Resources** (RAR) and **Inferred Resources** which are recoverable at a cost of less than $130/kgU. The identified resources increased significantly between 2003 and 2005 from 4588000 tU to 4743000 tU (increase with 155000 tU). Some of the increase is due to new discoveries resulting from increased exploration, but the major part of the increase result from higher prices of uranium[7-5].

Undiscovered Resources include Prognosticated Resources (PR) and Speculative Resources (SR). PR refers to uranium resources that are expected to occur in well defined geological trends of known deposits. SR refers to uranium resources that are thought to exist in geologically favourable, yet unexplored areas, thus they are assigned a lower degree of confidence than PR. In total PR are estimated to 2518800 tU and SR to 7535900 tU, with cost lower than $130/kgU[7-5].

Other resources include **unconventional uranium resources** (in which uranium exists at very low grades) and other potential nuclear fuel materials (e.g. thorium). Most of the unconventional uranium resources are associated with uranium in phosphates (about 22 million tons), but other potential sources exist, e.g. seawater and black shale. Thorium is abundant and widely dispersed, and its resources are estimated to more than 4.5 million tons. This estimate is considered conservative, since data from China, Central and Eastern Europe and the Former Soviet Union are not includes[7-5].

Uranium production increased from 36050 tU in 2002 to 40263 tU in 2004 and is estimated to 41250 tU in 2005. Uranium is mainly produced using open-cut (26.6%) and underground mining (40.1%) techniques followed by conventional uranium milling. Other mining methods include *in situ* leaching (ISL) (19.2%). Total potential production capability is predicted to rapidly increase to 83370 tU/year in 2010 and then increase gradually to 86900 tU/year in 2025[7-5].

There are several factors that affect nuclear power capacity and related uranium requirements. One of the factors is the nuclear energy availability. In 2004, the average world nuclear energy availability factor was 83.2% compared with 71% in 1990. In addition, many power plants are undergoing life extension and power uprates leading to even more increased capacities. All these factors make forecasts of the uranium requirements rather uncertain.

World annual uranium requirements were about 67320 tU in 2004 and 66840 tU in 2005[7-5]. Current (May 2008) number of operating nuclear reactors worldwide is 439. They have the total power output of 372.2 GWe and produced during year 2007 2617.9 billion kWh (TWh), which corresponds to 16% of the total electricity production world-wide. The required uranium to support the current production corresponds to 65500 tU.

The number of reactors (shown in TABLE 7.1) increases steadily, but not dramatically. At present there are 28 reactors under construction, with total planned power output of 22645 MWe; 62 reactors are planned, with total power output of 68021 MWe; and 161 reactors are proposed, with expected total power output of 120625 MWe[7-6]. The installed nuclear capacity is projected to grow to about 449 GWe net (low estimate – grow of 22%) or 533 GWe net (high estimate – grow of 44%) by the year 2025. World reactor-related uranium requirements by the year 2025 are projected to increase to between 82275 tU (low estimate) and 100760 tU (high estimate). The requirements in the North America and the Western Europe region are expected to either remain fairly constant or decline slightly, whereas they will increase in the rest of the World[7-5].

TABLE 7.1. World nuclear power generation and capacity (Source: IAEA and WNA)).

	As of May 2008		2007	
Country	Number of Nuclear Units	Nuclear Capacity (MW)	Nuclear Generation (BkWh)	Nuclear Fuel Share (Percent)
Argentina	2	935	6.7	.2
Armenia	1	376	2.4	

Belgium	7	5,824	45.9	3.5
Brazil	2	1,795	12.4	4.0
Bulgaria	2	1,906	13.7	.8
Canada	18	12,589	96.5	2.1
China	11	8,572	62.6	6.0
Czech RP	6	3,619	24.6	.9
Finland	4	2,696	22.5	0.2
France	59	63,260	418.6	8.9
Germany	17	20,470	133.2	6.8
Hungary	4	1,829	13.9	5.9
India	17	3,782	15.9	6.8
Japan	55	47,587	266.4	.5
Korea Rep.	20	17,451	136.6	7.5
Lithuania	1	1,185	9.1	5.3
Mexico	2	1,360	10.4	4.4
Netherlands	1	482	4.0	.6
Pakistan	2	425	2.3	.1
Romania	2	1,300	7.1	.3
Russia	31	21,743	147.8	3.0
Slovakia	5	2,034	14.2	6.0
Slovenia	1	666	5.4	4.3
South Africa	2	1,800	12.6	1.6
Spain	8	7,450	52.3	.5
Sweden	10	9,014	64.4	7.4
Switzerland	5	3,220	26.3	6.1

				0.0
Taiwan, China	6	4,921	39.0	9.3
U.K.	19	10,222	57.5	5.1
U.S.	104	100,582	806.5	9.4
Ukraine	15	13,107	87.2	8.1
Total	439	372,202	2,617.9	

7.1.2 Thorium Fuel

Thorium is much more abundant in nature than uranium. It is a naturally occurring, slightly radioactive metal discovered in 1828 by the Swedish chemist Jons Jakob Berzelius. Thorium occurs in several minerals, such as the rare-earth-thorium-phosphate mineral, monazite, which contains up to about 12% thorium oxide.

TABLE 7.2. Thorium reserves in the world.

Country	Reserves (tons)
Australia	300000
India	290000
Norway	170000
USA	160000
Canada	100000
South Africa	35000
Brazil	16000
Other countries	95000
World total	1200000

Thorium is not fissile itself, but Th-232 isotope, when absorbing slow neutrons, is producing uranium-233, which is fissile. U-233 has higher neutron yield per neutron absorbed than both U-235 and Pu-239. This make possible to use thorium in a breeding cycle.

7.1.3 Nuclear Fuel Demand

In current light water reactors only slightly above 0.5% of natural uranium is used for energy production. The uranium which is left after enrichment (so-called depleted

uranium) and in spent fuel is treated as wastes. Some part of uranium is converted in reactors into plutonium.

With the present fleet of nuclear reactors (439 units with total electricity generation 2.6×10^{12} kWh per year) would the currently known uranium resources suffice for about 85 years. The same uranium resources would suffice for over 5000 years if fuel breeding from uranium-238 is employed. Thus breeder reactors should be used if nuclear power is to play a major role in the energy production in the future.

Evaluation of nuclear fuel demand is difficult, because it depends on many factors which are changing with time. If the installed electric capacity of a nuclear power plant is P_e, [GWe] then the annual thermal energy output of the plant is given as,

$$Q = \frac{P_e C_F 365}{\eta_{th}}, \tag{7-1}$$

where Q is the annual thermal energy output [GWd], C_F is the capacity factor (which indicates the fraction of the capacity which is actually used. Typical values are 0.8 to 0.9) and η_{th} is the thermal efficiency of the power plant.

The mass of enriched fuel needed per year depends on the generated annual thermal energy Q and on the fuel burnup B_d, which indicates the amount of thermal energy obtained from a unit mass (usually metric ton) of enriched fuel. The required mass is thus obtained as,

$$M = \frac{Q}{B_d}, \tag{7-2}$$

where M is the mass of enriched fuel loaded per year [tU/year] and B_d is the fuel burnup [GWd/tU]. Substituting Eq. (7-1) into(7-2) gives,

$$M = \frac{P_e C_F 365}{\eta_{th} B_d}. \tag{7-3}$$

Equation (7-3) gives the required mass of enriched uranium for a given nuclear power plant. The required mass of the natural uranium depends on the enrichment of fuel and tails.

7.2 Fuel Cycles

The nuclear fuel cycle consists of the steps required to produce nuclear power, including the input of fissile material, the processes that convert raw material to useful forms, the output of energy, and the treatment and/or disposition of spent fuel and various waste streams. The steps are shown in FIGURE 7-1.

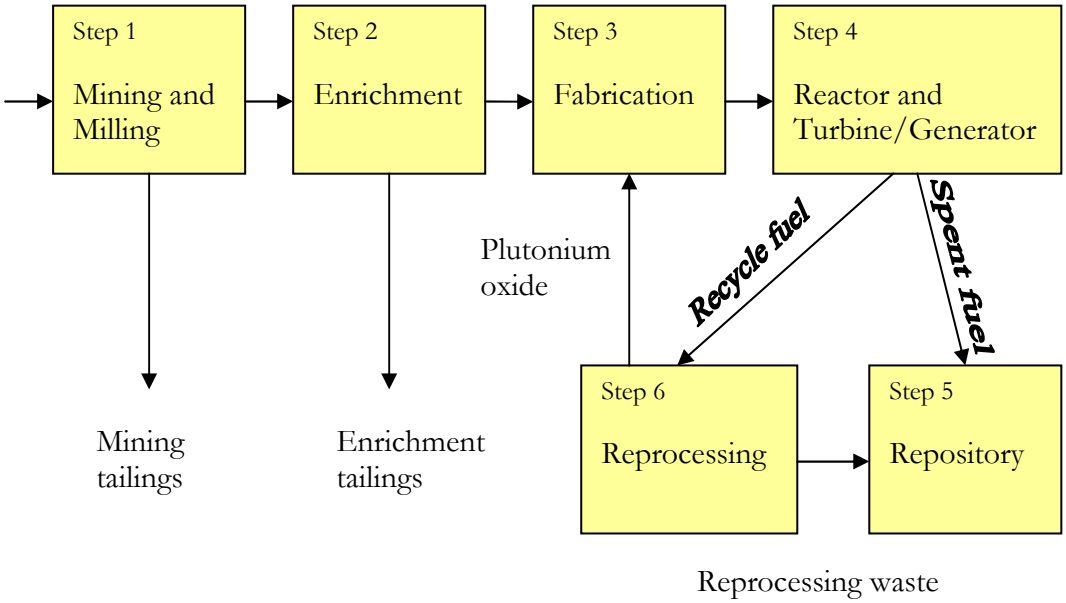

FIGURE 7-1: Nuclear fuel cycle diagram.

7.2.1 Open Fuel Cycle

In the **open fuel cycle** fuel is not reprocessed and after usage in reactor is placed in the repository. It appears as steps 1 through 5 in FIGURE 7-1. This is most often used system in most countries using the common kinds of reactors. It requires uranium ore as input, milling and purification of natural uranium, conversion of the uranium to a chemical form suitable for enrichment, enrichment of the U-235 isotope, fuel fabrication, loading of uranium fuel assemblies in a reactor and then the reactor operation. At the end of useful life, spent fuel is removed from the reactor, stored in a pool of water for cooling and shielding of radioactivity, then removed and placed in air-cooled casks at the reactor sites for interim storage, and finally removed to geologic waste storage.

7.2.2 Closed Fuel Cycle

Plutonium production in the open-fuel cycle represents a significant energy resource, but requires reprocessing of spent fuel to recover the plutonium and to fabricate new fuel. Recycling of fuel can be done in thermal reactors and in fast reactors.

Closed fuel cycle for thermal reactors is shown in FIGURE 7-1 as steps 1-2-3-4-6-3. As can be seen it adds another process in comparison with the open fuel cycle, i.e., fuel reprocessing. Several countries (France, Japan, Russia and the UK) have reprocessing plants in operation. Spent fuel reprocessing is very costly and, in some countries, thermal recycle is not considered as an economic choice.

Close fuel cycle for fast breeder reactors is similar to that of thermal reactors, however, with some important differences. A fast breeder reactor is capable by design of producing more fissile isotopes than it consumes, thus making it possible to provide a growing resource of energy that does not require a continuing supply of U-235 or Pu-239 after an initial investment of fissile fuel at the beginning of its life. Fuel enrichment for fast reactors is higher (15-20%) than it is in LWRs. Breeder reactor cores typically

have two regions: a "seed" region on the inside of the core, and a "blanket" region surrounding the "seed". **Seed fuel assemblies** consist of fissile fuel, 15%-20% fissile plutonium, and this region provides power and fission neutrons to maintain criticality, while **blanket assemblies** contain fertile fuel, U-238, for breeding of new plutonium.

7.3 Front-End of Nuclear Fuel Cycle

The "Front-End" of the nuclear fuel cycle consists of several processes which include mining, milling, conversion, enrichment and fabrication.

7.3.1 Mining and Milling of Uranium Ore

Uranium is usually mined by either surface (open cut) or underground mining techniques, depending on the depth at which the ore body is found. For example, in Australia the Ranger mine in the Northern Territory is open cut, while Olympic Dam in South Australia is an underground mine (which also produces copper, with some gold and silver). On the contrary, most Canadian uranium mines are underground. Ore grades vary at different places and are usually less than 0.5% U_3O_8.

The mined uranium ore (i.e. rock containing economically recoverable concentrations of uranium) is sent to a mill which is usually located close to the mine. At the mill the ore is crushed and ground to a fine slurry which is leached in sulfuric acid to allow the separation of uranium from the waste rock. It is then recovered from solution and precipitated as uranium oxide (U_3O_8) concentrate. (Sometimes this is known as **yellowcake**, though it is finally khaki in color.) After high-temperature drying, the uranium oxide, now khaki in color, is packed into 200-litre drums for shipment. The radiation level one meter from such a drum of freshly processed U_3O_8 is about half that (from cosmic rays) received by a person on a commercial jet flight. The solids remaining after the uranium is extracted are pumped as a slurry to the tailings dam, which is engineered to retain them securely. Tailings contain most of the radioactive material in the ore, such as radium.

Some new mines use *in situ* leaching (ISL) to extract the uranium from the ore body underground and bring it to the surface in solution. It is recovered in the same fashion.

Uranium minerals are always associated with other elements such as radium and radon in radioactive decay series. Therefore, although uranium itself is barely radioactive, the ore which is mined must be regarded as potentially hazardous, especially if it is high-grade ore. The radiation hazards involved, however, are virtually all due to the associated elements and are similar to those in many mineral sands operations. Any underground uranium mine is ventilated with powerful fans.

7.3.2 Uranium Separation and Enrichment

The vast majority of all nuclear power reactors in operation and under construction require 'enriched' uranium fuel in which the content of the U-235 isotope has been raised from the natural level of 0.72 atom percent (a/o) to about 3.5 weight percent (w/o) or slightly more. The enrichment process removes 85w/o of the U-238 by separating gaseous uranium hexafluoride (UF_6) into two streams: One stream is enriched to the required level and then passes to the next stage of the fuel cycle. The other stream is depleted in U-235 and is called 'tails'. It is mostly U-238.

So little U-235 remains in the tails (usually less than 0.3w/o) that it is of no further use for energy, though such 'depleted uranium' is used in metal form in yacht keels, as counterweights, and as radiation shielding, since it is 1.7 times denser than lead.

NOTE CORNER: It must be noted that although isotopic abundances are always given in atom percent (a/o), sometime it is preferred to specify enrichments in weight percent (w/o).

Separation of uranium isotopes is a very difficult task since the two isotopes, U-235 and U-238 have very nearly the same atomic weight. Chemically they can not be separated, of course, as they have exactly the same chemical properties. Separation is thus accomplished by physical means, such as either gaseous diffusion method or gas-centrifuge method.

Separation process is schematically shown in FIGURE 7-2, where the feed material with mass M_F and weight enrichment x_F is separated into the final product with mass M_P and the weight enrichment x_P, and the tails with mass M_T and enrichment x_T.

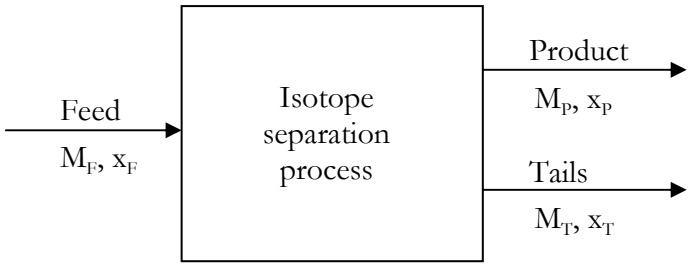

FIGURE 7-2: Schematics of a separation process.

Since there are virtually no losses of uranium, its total mass is conserved as follows,

$$M_F = M_P + M_T .$$

Similarly, the mass of U-235 is the same before and after enrichment,

$$x_F M_F = x_P M_P + x_T M_T .$$

Eliminating M_F from the last two equations yields,

(7-4) $$M_F = \frac{x_P - x_T}{x_F - x_T} M_P .$$

This equation gives the amount of feed material that is required to obtain a specified amount of enriched product.

Equation (7-4) indicates that the required mass of natural uranium increases with the product enrichment. For PWRs, the required enrichment for a given burnup can be approximated using the following correlation, valid for enrichments up to 20%, [7-1]:

$$x_p = 0.41201 + 0.11508\left(\frac{n+1}{2n}B_d\right) + .0.00023937\left(\frac{n+1}{2n}B_d\right)^2, \tag{7-5}$$

where n is the number of fuel batches, i.e. the fraction of the core refueled per cycle is $1/n$.

The isotope separation is a costly process that requires a considerable amount of work. A so-called value function has been developed on the basis of the theory of the gaseous diffusion cascade. It can be shown that the value of uranium as a function of its enrichment in weight percent, x, can be given as,

$$V(x) = (1-2x)\ln\frac{1-x}{x}. \tag{7-6}$$

The function is shown in FIGURE 7-3.

The separative work associated with the production of a given amount of enriched uranium is defined as the increase in total value of the uranium after separation process. This work is calculated as,

$$SWU = M_P V(x_P) + M_T V(x_T) - M_F V(x_F),$$

where SWU is the number of **separative work units**. Since,

$$M_T = M_F - M_P,$$

it can be expressed as,

$$SWU = M_P[V(x_P) - V(x_T)] - M_F[V(x_F) - V(x_T)]. \tag{7-7}$$

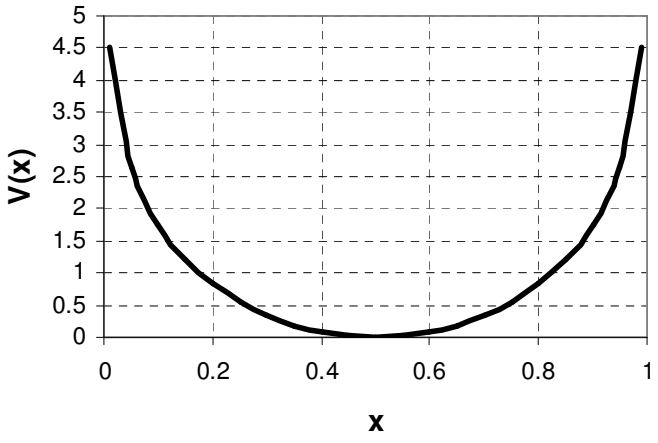

FIGURE 7-3: The separation value function versus enrichment x in weight percent.

The separative work can be expressed per unit mass of the product as,

$$\frac{SWU}{M_P} = V(x_P) - V(x_T) - \frac{M_F}{M_P}[V(x_F) - V(x_T)]. \quad (7\text{-}8)$$

It should be noted that *SWU* has the same units as mass, which is kg.

EXAMPLE 7-1. Calculate the amount of natural uranium and *SWU* that are needed to produce 100000 kg of 3.5w% enriched uranium, assuming tails with 0.2w%. SOLUTION: Note that for natural uranium x_F = 0.711w%. Eq. (7-6) yields: $V(x_P)$ = 3.085, $V(x_F)$ = 4.869, $V(x_T)$ = 6.188. For x_T = 0.002, Eq. (7-4) yields: M_F = (0.035-0.002)/(0.00711-0.002)*100000 = 6.458 10^5 kg. From Eq. (7-7) the number of separative work units is as follows: $SWU = 10^5*(3.085-6.188) - 6.458\ 10^5*(4.869-6.188) = 5.415\ 10^5$ kg.

The cost per separative work unit is determined from the enrichment plant operating costs and the cost of the capital invested in the plant. If C_S is the cost of a separative work unit (in €/kg or $/kg), then

$$M_P C_P = SWU \cdot C_S + M_F C_F - M_T C_T, \quad (7\text{-}9)$$

and

$$C_P = \frac{SWU}{M_P} \cdot C_S + \frac{M_F}{M_P} C_F - \frac{M_T}{M_P} C_T. \quad (7\text{-}10)$$

Here C_P, C_F and C_T are the costs per kg of product, feed and tails, respectively. According to Eq. (7-9) the cost of the product is equal to the cost of the enrichment operation plus the cost of the feed, less credit for the value of the tails (which is usually neglected).

Several methods for enrichment of uranium have been developed, of which two are of special interest, namely the gaseous-diffusion and gas-centrifuge methods.

The gaseous-diffusion method is based on the different rates at which gases of different molecular weights diffuse through a porous barrier. The only suitable compound of uranium for use in the gaseous-diffusion process is the hexafluoride. It is solid at room temperature but it sublimes above 56.4 ºC.

The basic principle of the separation of isotopes by gaseous diffusion is that, in a mixture of gases at a certain temperature, the average molecular kinetic energy is the same for each gas. As a consequence, the lighter molecules will have higher average speeds than the heavier molecules, with the velocity ratio,

$$\frac{v_L}{v_H} = \sqrt{\frac{M_H}{M_L}}.$$

This ratio is called the theoretical separation factor α^*:

$$\alpha^* = \sqrt{\frac{M_H}{M_L}} = \sqrt{\frac{352}{349}} \approx 1.0043 .$$

As can be seen this factor is very close to unity and thus, the degree of enrichment in uranium-235 as a result of diffusion through a single barrier is very small. A "cascade" of barriers must be employed in order to achieve substantial enrichment.

The stage separation factor α is defined as,

(7-11) $$\alpha = \frac{x_e/(1-x_e)}{x_d/(1-x_d)}$$

where x_e and x_d are the weight fractions of uranium-235 in the enriched and the depleted streams leaving the stage. α, which is the actual measure of the uranium-235 enrichment, is found to be less than the theoretical separation factor α^*, and approximately equal to 1.003 as compared to 1.0043.

It can be shown that to obtain the final product and the tails with weight fractions of uranium-235 x_P and x_T, respectively, the required number of stages in cascade, N_{s-c} is given as,

(7-12) $$N_{s-c} = \frac{2}{\alpha - 1} \ln \frac{x_P/(1-x_P)}{x_T/(1-x_T)} - 1.$$

For example, with $x_P = 0.03$, $x_T = 0.003$ and $\alpha = 1.003$, $N_{s-c} = 1553$.

The gas-centrifuge method is based on the principle that if a gas containing molecular species with different masses is centrifuged, the heavier molecules will move towards the periphery of the centrifuge whereas the lighter ones will remain in the center. It can be shown that the equilibrium stage separation factor is,

(7-13) $$\alpha = \exp\left[\frac{(M_L - M_H)v^2}{2RT}\right],$$

where M_L and M_H are the molecular weights (kg/mol) of the light and the heavy molecules, R is the universal gas constant (8.31 J/mol/K), T is the absolute temperature of the gas an v is the linear velocity of gas.

For example, if a cylindrical centrifugal bowl with diameter 0.2 m, rotating with 30000 rpm (500 rotations per second), contains UF_6 at temperature T = 330 K, the equilibrium separation factor is,

$$\alpha = \exp\left[\frac{(0.238 - 0.235)(2\pi \cdot 0.1 \cdot 500)^2}{2 \cdot 8.31 \cdot 330}\right] \approx 1.055 .$$

As can be seen the stage separation factor for the gas-centrifugal method is higher than for the gas diffusion method. The required number of stages is thus reduced. For example, with $x_P = 0.03$, $x_T = 0.003$ and $\alpha = 1.055$, Eq. (7-12) yields $N_{s-c} = 84$.

7.3.3 Fuel Fabrication

Enriched UF_6 is transported to a fuel fabrication plant where it is converted to uranium dioxide (UO_2) powder and pressed into small pellets. These pellets are inserted into thin tubes, usually of a zirconium alloy (zircalloy) or stainless steel, to form fuel rods. The rods are then sealed and assembled in clusters to form fuel elements or assemblies for use in the core of the nuclear reactor.

7.4 Back-End of Nuclear Fuel Cycle

The **Back-End of the nuclear fuel cycles** consists of several processes to handle wastes in environment-friendly way.

Despite its demonstrable safety record over half a century, one of the most controversial aspects of the nuclear fuel cycle today is the question of management and disposal of radioactive wastes. The most difficult of these are the high-level wastes, and there are two alternative strategies for managing them:

• reprocessing spent fuel to separate them (followed by vitrification and disposal),

• direct disposal of the fuel containing high levels of radioactivity as waste .

The principal nuclear wastes remain locked up securely in the ceramic reactor fuel. “Burning” the fuel of the reactor core produces fission products such as various isotopes of barium, strontium, cesium, iodine, krypton and xenon (Ba, Sr, Cs, I, Kr, and Xe). Many of the isotopes formed as fission products within the fuel are highly radioactive, and correspondingly short -lived.

As well as these smaller atoms formed from the fissile portion of the fuel, various transuranic isotopes are formed by neutron capture. These include Pu-239, Pu-240 and Pu-241, as well as others arising from some of the U-238 in the reactor core by neutron capture and subsequent beta decay. All are radioactive and apart from the fissile plutonium which is partly "burned", they remain within the spent fuel when it is removed from the reactor. The transuranic isotopes and other actinides form most of the long-lived portion of high-level waste.

While the civil nuclear fuel cycle generates various wastes, these do not become “pollution”, since virtually all are contained and managed, otherwise they would be dangerous. In fact, nuclear power is the only energy-producing industry which takes full responsibility for all its wastes and fully costs this into the product. Furthermore, the expertise developed in managing civil wastes is now starting.

7.4.1 Fuel Burnup

During fission process of uranium-235 in a reactor core, fission products are produced and accumulated. Some of the fission products have large absorption cross-sections for neutrons and significantly reduce the reactivity of the reactor. When the excess reactivity is too small to operate the reactor, a portion or whole fuel must be exchange in the core, even though there is still a large number of uranium-235 atoms that have not fissioned.

The period of reactor operation with the same fuel batch is called a fuel cycle. The length of a fuel cycle depends on the available excess reactivity and the increasing

probability of fuel damage. Some of the fission products are released from fuel pellets as gases and accumulate in the gas gap and plenum of a fuel rod, leading to an increased pressure inside the cladding.

The allowable fuel burnup determines the amount of fission products that can be produced without leading to fuel damages. Higher fuel burnup means longer fuel cycle. Fuel burnup is expressed in the amount of thermal energy (usually in GWd – giga-watt-days) that can be obtained from one ton of enriched uranium (1 tU). A typical value of burnup in current LWRs is 50 GWd/tU. Typical isotopic composition of PWR fuel with burnup equal to 33 GWd/tU is shown in FIGURE 7-4.

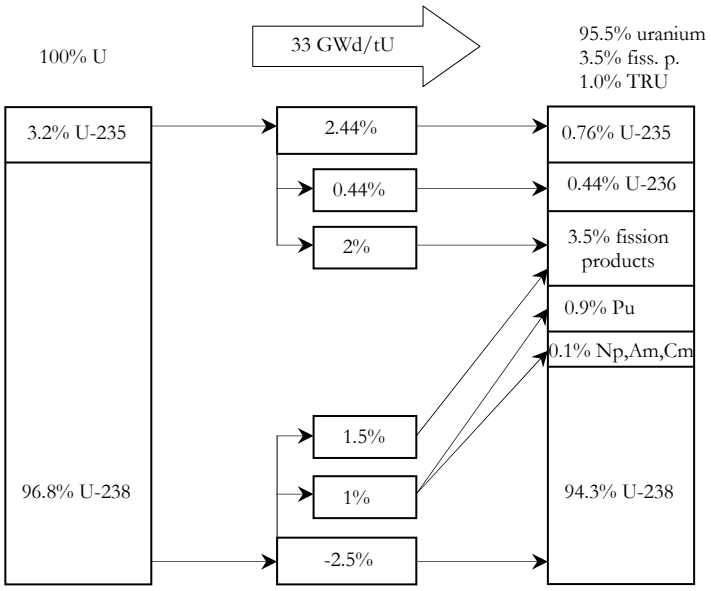

FIGURE 7-4: Change in isotope composition in nuclear fuel with burnup 33 GWd/tU.

As can be seen, uranium-238 (94.3%) remains the major component of the spent fuel. The new components are as follows: fission products (3.5%), plutonium (0.9%) and minor actinides (0.1%). Minor actinides are all elements created in reactor with atomic number higher than uranium, except for plutonium. Minor actinides together with plutonium are termed as transuranic (TRU) elements. The change in isotopic composition of spent fuel depends on burnup, as shown in table below.

TABLE 7.3. Isotopic composition of spent fuel, [7-1].

	33 GWd/tU	**50 GWd/tU**	**100 GWd/tU**
Uranium	95.5%	93.4%	87.43%
Fission products	3.5%	5.15%	10.30%
Plutonium	0.9%	1.33%	1.97%
Minor actinides	0.1%	0.12%	0.30%

Spent fuel remains radioactive during a long period of time, as shown in FIGURE 7-5. The curves shown in the figure have been obtained for PWR reactor, with 50 GWd/tU burnup and initial enrichment 4.5%.

Another measure of risks posed by the spent fuel is so called radiotoxicity. Strictly speaking, radiotoxicity R_T at a given time t is calculated as,

$$R_T(t) = \sum_{all\ radionuclides\ i} \left(\frac{\lambda_i N_i(t)}{MPC_i^{water}} \right), \tag{7-14}$$

where $\lambda_i N_i(t)$ is the quantity of radioisotope i present in 1 metric ton of waste at time t (in Bq/tU) and MPC_i^{water} is the maximum permissible concentration of isotope i in water (in Bq/m^3). The calculation of the maximum permissible concentration for each radionuclide is based on the assumption that an adult would ingest water containing the radionuclide at a constant rate of 2 liters per day during one year. The concentration limit is determined by imposing the requirement that the individual should receive a committed effective dose no greater than 50 millirems from this source. The calculated radiotoxicity for PWR spent fuel with 50 GWd/tU and initial enrichment 4.5% is shown in FIGURE 7-6.

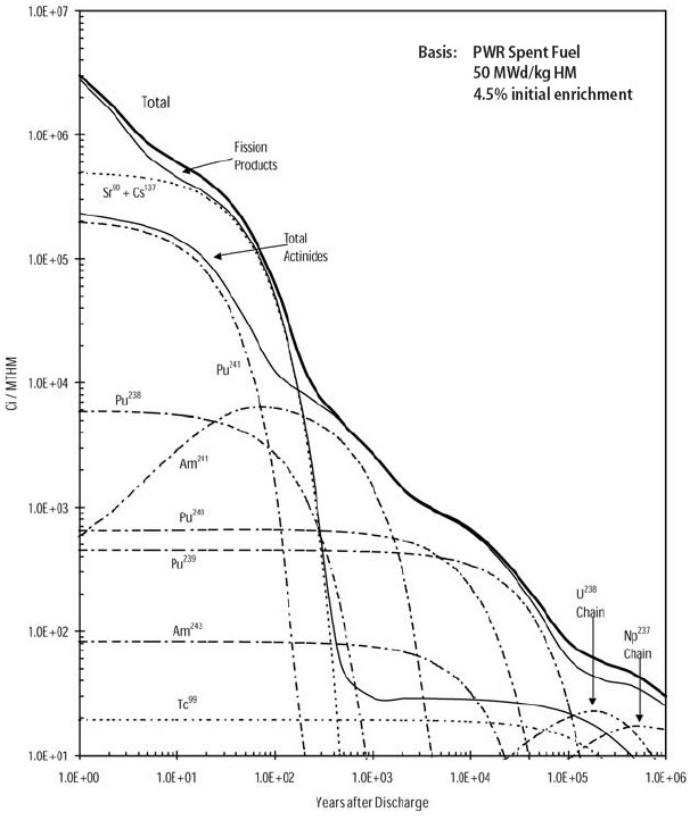

FIGURE 7-5: Radioactivity profile of spent fuel (curie/tU) as a function of time after discharge from reactor (years), [7-1].

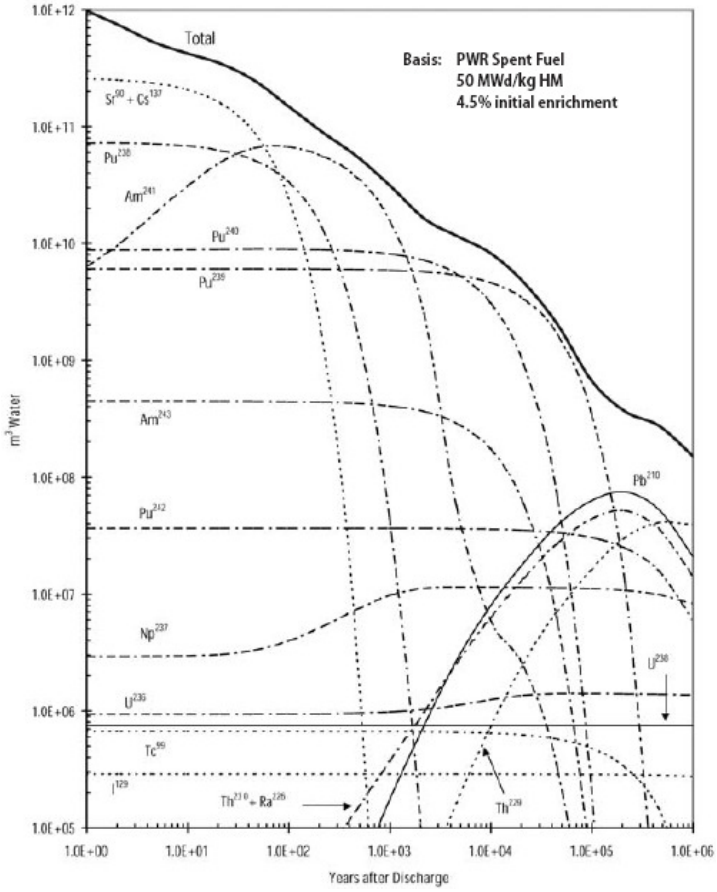

FIGURE 7-6: Radiotoxicity of PWR spent fuel (in m^3 of water) versus time after discharge (in years), [7-1].

7.4.2 Repository

Spent fuel assemblies taken from the reactor core are highly radioactive and give off a lot of heat. They are therefore stored in special ponds which are usually located at the reactor site, to allow both their heat and radioactivity to decrease. The water in the ponds serves the dual purpose of acting as a barrier against radiation and dispersing the heat from the spent fuel.

Spent fuel can be stored safely in these ponds for long periods. It can also be dry stored in engineered facilities. However, both kinds of storage are intended only as an interim step before the spent fuel is either reprocessed or sent to final disposal. The longer it is stored, the easier it is to handle, due to decay of radioactivity.

7.4.3 Reprocessing

Spent fuel still contains approximately 96% of its original uranium, of which the fissionable U-235 content has been reduced to less than 1%. About 3% of spent fuel comprises waste products and the remaining 1% is plutonium (Pu) produced while the fuel was in the reactor and not "burned" then.

Reprocessing separates uranium and plutonium from waste products (and from the fuel assembly cladding) by chopping up the fuel rods and dissolving them in acid to separate the various materials. Recovered uranium can be returned to the conversion plant for conversion to uranium hexafluoride and subsequent re-enrichment. The

reactor-grade plutonium can be blended with enriched uranium to produce a **mixed oxide (MOX) fuel**, in a fuel fabrication plant.

MOX fuel fabrication occurs at five facilities in Belgium, France, Germany and UK, with two more under construction. There have been 25 years of experience in this, and the first large-scale plant, Melox, commenced operation in France in 1995. Across Europe about 30 reactors are licensed to load 20-50% of their cores with MOX fuel, and Japan plans to have one third of its 53 reactors using MOX by 2010.

The remaining 3% of high-level radioactive wastes (some 750 kg per year from a 1000 MWe reactor) can be stored in liquid form and subsequently solidified.

Reprocessing of spent fuel occurs at seven facilities in Europe with a capacity of over 5000 tons per year and cumulative civilian experience of 55,000 tons over 35 years.

After reprocessing the liquid high-level waste can be calcined (heated strongly) to produce a dry powder which is incorporated into borosilicate (Pyrex) glass to immobilize the waste. The glass is then poured into stainless steel canisters, each holding 400 kg of glass. A year's waste from a 1000 MWe reactor is contained in 5 tons of such glass, or about 12 canisters 1.3 meters high and 0.4 meters in diameter. These can be readily transported and stored, with appropriate shielding.

This is as far as the nuclear fuel cycle goes at present. The final disposal of vitrified high-level wastes, or the final disposal of spent fuel which has not been reprocessed spent fuel, has not yet taken place. FIGURE 7-7 shows illustratively the amount of vitrified waste arising from nuclear electricity generation for one person through a lifetime.

The waste forms envisaged for disposal are vitrified high-level wastes sealed into stainless steel canisters, or spent fuel rods encapsulated in corrosion-resistant metals such as copper or stainless steel. The most widely accepted plans are for these to be buried in stable rock structures deep underground. Many geological formations such as granite, volcanic tuff, salt or shale will be suitable. The first permanent disposal is expected to occur about 2010.

Most countries intend to introduce final disposal sometime after about 2010, when the quantities to be disposed of will be sufficient to make it economically justifiable.

FIGURE 7-7: Borosilicate glass from the first waste vitrification plant in UK in the 1960s. This block contains material chemically identical to high-level waste from reprocessing spent fuel. A piece this size from modern vitrification plants would contain the total high-level waste arising from nuclear electricity generation for one person throughout a lifetime.

7.4.4 Partitioning and Transmutation of Nuclear Wastes

From FIGURE 7-5 and FIGURE 7-6 it is clear that various species have different properties in terms of radioactivity and radiotoxicity over time. One possible approach

to optimize the treatment of nuclear wastes would be thus to partition the wastes into different parts, each containing species with a similar properties. For example, fission products strontium-90 and cesium-137 with half-lives of about 30 years each, accounts for the bulk of radioactivity in spent fuel during first several decades. Extracting these fission products from the spent fuel and storing them separately would allow for reduction of the required repository space.

Another strategy would be to extract the uranium and TRU elements from the spent fuel. These would lead to increased storage capacity of a given repository as well.

An option which is thoroughly investigated includes both partitioning and transmutation of nuclear wastes. There are three principal motivations for this strategy:

- If the long-lived isotopes could be extracted and destroyed, many more locations would be considered suitable for hosting repositories, since the period of time during which the wastes would be dangerous would be shorten dramatically (from about 300000 years to about 1000 years).

- The thermal load would be reduced leading to an increased capacity of a given repository.

- It would eliminate the risk that plutonium could later be recovered from a repository and used for weapons.

7.4.5 Safeguards on Uranium Movement

Uranium may only be exported to countries which have bilateral safeguards agreements, in addition to their acceptance of International Atomic Energy Agency (IAEA) safeguards under the multilateral Nuclear Non-Proliferation Treaty (NPT). Australia, for instance, has a network of 19 such bilateral agreements covering almost 30 countries.

Safeguards apply to all exports and subsequent transfers of uranium and to its possible processing and subsequent re-use. They are based on customer countries being parties to the NPT.

No uranium can be exported without the government first approving the terms and conditions of the sale contract.

Since Canada and Australia are major uranium exporters, examples will be given how uranium movement is handled by these countries.

The Canadian federal nuclear regulatory agency is the Canadian Nuclear Safety Commission. The CNSC administers the agreement between Canada and the IAEA for the application of safeguards in Canada and it assists the IAEA by allowing access to Canadian nuclear facilities and arranging for the installation of safeguards equipment at Canadian sites. It also reports regularly to the IAEA on nuclear materials held in Canada.

The Australian Safeguards & Non-proliferation Office (ASNO), which is part of the Department of Foreign Affairs and Trade, administers Australia's bilateral safeguards agreements. In addition, ASNO keeps account of nuclear material and associated

items in Australia through its administration of the Nuclear Non-Proliferation (Safeguards) Act 1987. It provides information to the IAEA on all nuclear material in Australia which is subject to safeguards, as well as on uranium exports, as required by Australia's NPT agreement with the IAEA.

Both countries have in place an accounting system that follows uranium from the time it is produced and packed for export, to the time it is reprocessed or stored as nuclear waste, anywhere in the world. It also includes plutonium which is in the spent fuel.

For instance, all documentation relating to Australian-obligated nuclear material (AONM) is carefully monitored and any apparent discrepancies are taken up with the country concerned. There have been no unreconciled differences in accounting for AONM.

These systems operate in addition to safeguards applied by the IAEA which keep track of the movement of nuclear materials through overseas facilities and which verify inventories.

A typical contract for the sale of Australian or Canadian uranium oxide concentrate to an electricity generating utility in say Germany, could first entail shipment to the USA for conversion to uranium hexafluoride. The equivalent quantity of uranium hexafluoride might then be sent from USA to the UK for enrichment, and then on to a fuel fabrication plant in Germany to be turned into uranium dioxide, before going into the core of a reactor owned by the utility with whom the sale was originally contracted. Later, the spent fuel from the reactor may go to the UK or France for reprocessing.

When uranium goes through a continuous process such as conversion or enrichment, it is not possible to distinguish Australian- or Canadian-origin atoms of uranium from atoms of uranium supplied by other countries. The only way to track the quantity of uranium is to use accounting principles, so ensuring that there is no loss of nuclear material during transportation and processing.

In the 1990s uranium mines gained a competitor, in many ways very welcome, as military uranium came on to the civil market. Weapons-grade uranium has been enriched to more than 90% U-235 and must be diluted about 1:25 or 1:30 with depleted uranium (about 0.3% U-235). This means that progressively, Russian and other stockpiles of weapons material are used to produce electricity.

Weapons-grade plutonium may also be diluted and used to make mixed oxide (MOX) fuel for use in ordinary reactors or in special reactors designed to 'burn' it for electricity.

7.5 Fuel Utilization and Breeding

In thermal reactors not only uranium-235 is fissioned but also some fertile uranium-238 is converted into fissile plutonium-239, part of which is fissioned during operation. However, the total number of plutonium-239 nuclei is less than the number of uranium-235 nuclei consumed. The efficiency with which fuel is being utilized is expressed as,

$$CR = \frac{Number\ of\ \ fissile\ nuclei\ \ produced}{Number\ of\ \ fissile\ nuclei\ destroyed}.$$

The ratio CR is called the **conversion ratio**. If the ratio is larger than one, it is called the breeding ratio (BR).

Both CR and BR are space and time dependent and could be in principle calculated in the same manner as fuel burnup. In practice, however, some approximations are used and the ratio is determined at a specific time rather than the global or net value. Thus the ratio at a given time can be defined as,

$$CR\ (or\ BR) = \frac{Rate\ of\ \ formation\ of\ \ fissile\ nuclei}{Rate\ of\ \ destruction\ of\ \ fissile\ nuclei},$$

where the rates formation and destruction refer to a given time and CR (or BR) in general vary with time during reactor operation.

The conversion ratio applies to thermal reactors with natural or slightly enriched uranium as fuel. In such reactors plutonium -239 is produced as a result of the capture by uranium-238 of thermal and resonant neutrons. The rate of production of fission neutrons from a given fissile species in a thermal neutron flux ϕ is $\phi N\sigma_a\eta\varepsilon$, where N is the concentration of fissile nuclei, σ_a is the thermal-neutron absorption cross section, η is the reproduction factor (number of fast neutrons produced per neutron absorbed in fissile nuclei) and ε is the fast fission factor.

The rate of formation of plutonium-239 contains two terms:

- formation due to thermal neutron capture - $\phi N^{238}\sigma_c^{238}$,
- formation due to resonance neutron capture - $\phi\varepsilon P_{FNP}(1-p)\sum_{all\ fissile\ species}(N\sigma_a\eta)$.

Here P_{FNP} is the nonleakage probability in slowing down of fast neutrons into the resonance region; p is the resonance escape probability (thus 1-p is the fraction of the neutrons in the resonance region that is captured by uranium-238 to form plutonium-239).

Initially after reactor startup there is no plutonium-239 and uranium-235 is the only fissile material. For such conditions, the initial conversion ratio is found as,

(7-15) $$CR = \frac{N^{238}\sigma_c^{238} + \varepsilon P_{FNP}(1-p)N^{235}\sigma_a^{235}\eta^{235}}{N^{235}\sigma_a^{235}} = \frac{N^{238}\sigma_c^{238}}{N^{235}\sigma_a^{235}} + \varepsilon P_{FNP}(1-p)\eta^{235}.$$

During reactor operation plutonium-239 is produced which contributes in both capture and generation of neutrons. As a result the conversion ratio is decreasing. Nevertheless a large initial conversion ratio is desirable, since it extends fuel burnup. In commercial water-cooled reactors its value is approximately 0.6. However, only slightly

above 50% of the generated plutonium-239 is fissioned, one-sixth is lost by neutron capture and the rest remains in the spent fuel.

The breeding ratio, even though in principle equivalent to the conversion ratio, is calculated in a slightly different manner. This is due to the fact that a breeder usually consists of a core, containing both fissile and fertile species, surrounded by a blanket containing only the fertile species. Thus, the **breeding ratio** at a given time is given as,

$$BR = \frac{\int_{core} \phi \Sigma_c^{fertile} dV + \int_{blanket} \phi \Sigma_c^{fertile} dV}{\int_{core} \phi \left(\Sigma_f + \Sigma_c \right)^{fissile} dV} . \tag{7-16}$$

Here Σ_f and Σ_c are the macroscopic fission and capture cross sections, respectively.

The breeding ratio can be divided into two parts as follows.

The **external (or blanket) breeding ratio**,

$$EBR = \frac{core\ leakage}{\int_{core} \phi \left(\Sigma_f + \Sigma_c \right)^{fissile} dV} ,$$

which can be shown to approximately be equal to,

$$EBR \approx \frac{\Sigma_f^{core}}{\Sigma_f^{fissile}} (\eta - 1) . \tag{7-17}$$

The **internal (or core) breeding ratio**,

$$IBR = \frac{\int_{core} \phi \Sigma_c^{fertile} dV}{\int_{core} \phi \left(\Sigma_f + \Sigma_c \right)^{fissile} dV} \approx \frac{\Sigma_f^{core}}{\Sigma_f^{fissile}} \frac{\eta}{\nu} . \tag{7-18}$$

Clearly, the total (internal plus external) breeding ratio depends on the neutron spectrum (since e.g. η depends on the neutron energy) and macroscopic cross sections. For sodium-cooled fast reactors with dioxides of plutonium-239 (fissile species) and uranium-238 (fertile species) the total breeding ratio is estimated to be about 1.2. With carbide (UC and PuC) fuel and blanket material the breeding ratio should be even larger.

Another figure of merit used to describe the breeding potential is the doubling time, which is defined as the operating time of a breeder reactor required to produce excess fissile material equal to the initial quantity in the fuel cycle both inside and outside of the reactor. The doubling time can be calculated from the following expression[7-3]:

(7-19) $$T_d \approx \frac{10^3 M(1+\gamma)}{GP(1+\overline{\alpha})(1-F)}\, days\,,$$

where M is the initial mass of fissile material in the reactor, G is the breeding gain equal to BR -1, P is the thermal power of the breeder rector in megawatts, F is the fraction of fissions in fertile nuclides, $\overline{\alpha}$ is an appropriate average value of Σ_c/Σ_f for all the fissile species present in the reactor and γM is the mass of fissile material outside of the reactor during equilibrium operation. In the above formula it is assumed that fission of 1 kg of any fissile material generates approximately 10^3 MW of thermal power.

EXAMPLE 7-2. A 1000 MWe power fast breeder power station operates at a thermal efficiency of 40% and an average plant capacity factor of 0.75. The initial reactor inventory is 2600 kg of fissile plutonium and the outside inventory is half of this amount. Estimate the doubling time assuming BR = 1.2, $\overline{\alpha}$ = 0.25 and F = 0.2. SOLUTION: The average thermal power is found as P = 1000*0.75/0.4 = 1.9x10^3 MW. The doubling time is obtained as

$$T_d \approx \frac{10^3 2.6\cdot 10^3(1+0.5)}{0.2\cdot 1.9\cdot 10^3(1+0.25)(1-0.2)}\, days = 28\ years\cdot$$

Due to the desirable breeding potential of fast neutron reactors, a world-wide effort is undertaken to develop them for commercial use. Starting from 1950 until now about 20 fast neutron reactors have been operating and some have supplied electricity commercially. This corresponds to over 300 reactor-years of operating experience. Several fast reactors are in operation, including Phoenix in France (since 1973), FBTR in India (since 1985), Jojo in Japan (since 1978), BR5/10, BOR 60 and BN600 in Russia (the last one since 1980). The largest fast reactor for production of electricity - Superphenix 1 with 1240 MWe power - was build in France. It operated with major technical difficulties during 1985-98[7-7].

There are two major types of fast neutron reactors: "burners" – which are net consumers of plutonium and "breeders" – which produce more plutonium than they consume. Fast breeding reactors remain the main goal of fast reactor development to secure long term fuel supply. They can extend the world's uranium resources by factor of about 60. This fact makes it economically feasible to utilize ores with very low uranium concentrations and potentially even uranium found in the oceans[7-4].

Renewed interest in fast breeding reactors has several reasons. In the longer term, beyond 50 years, uranium resource availability will become a limiting factor unless breakthrough occurs in mining or extraction technologies. On the one hand the existing known and speculative economic uranium resources are sufficient to support thermal reactors with a once-through cycle only until mid-century. Additional limiting factor facing an essential role for nuclear energy based such reactors is the availability of the spent-fuel repository space worldwide. On the other hand in the most advanced fuel cycles using fast spectrum reactors and extensive recycling, it may be possible to reduce the radiotoxicity of all wastes such that the isolation requirement can be reduced by several orders of magnitude (e.g. from 300000 to 1000 years) after discharge from the reactor[7-8].

The above mentioned issues are addressed in the new development program of Generation IV reactors. Five out of six Generation IV systems have actinide management as a mission to address the issues of the deposition of spent nuclear fuel and high level wastes. These are: Gas-Cooled Fast Reactor (GFR), Lead-Cooled Fast Reactor (LFR), Molten Salt Reactor (MSR), Supercritical-Water-Cooled Reactor (SCWR) and Sodium-Cooled Fast Reactor (SFR). Very-High-Temperature Reactor (VHTR) uses thermal neutron spectrum and once-through system, and is designed for high-temperature process heat applications, such as the coal gasification and the thermo-chemical hydrogen production[7-8].

A standing working group within a framework of IAEA – Technical Working Group on Fast Reactors (TWG-FR) – provides a forum for non-commercial scientific and technical information and development programs on advances in fast neutron reactors, [7-9]. The fast reactor database is available on the IAEA website and is maintained by the International Working Group on Fast Reactors (WGFR)[7-10].

7.6 Environmental Effects of Nuclear Power

The heat values of various fuels are shown in the table below.

TABLE 7.4. Energy conversion: typical heat values of various fuels.

Type of fuel	Heat Value, MJ/kg
Firewood	16
Brown coal	9
Black coal (low quality)	13-20
Black coal	24-30
Natural gas	39
Crude oil	45-46
Natural uranium in light water reactor	500 000

The difference in the heat value of uranium compared with coal and other fuels is important since it directly affects the amount of wastes that each fuel produces. For instance, 1000 MWe power station consumes about 3.1 million tons of black coal each year and produces about 7 million tons of waste. A nuclear power plant of equal power uses 24 tons of uranium UO_2 enriched to 4% (this requires mining of over 200 tons of natural uranium or 25000-100000 tons uranium ore) and produces about 700 kg of high-level radioactive waste (after reprocessing of 97% of fuel).

Due to the low rate of wastes produced by nuclear power stations, nuclear industry is able to take care of all wastes resulting from the electricity production. Using uranium

as fuel helps to cope with one of the major environmental problems called greenhouse effect.

In recent years attention has been focused on the climate change effects of burning fossil fuels, especially coal, due to the carbon dioxide which this releases into the atmosphere.

Carbon dioxide contributes about half of the human-induced increase in the greenhouse effect. Electricity generation is one of the major sources of this carbon dioxide, giving rise to about one quarter of it, or some 9% of the human-induced greenhouse increase.

Coal-fired electricity generation gives rise to nearly twice as much carbon dioxide as natural gas per unit of power, but hydro and nuclear do not directly contribute any. If the entire world's nuclear power were replaced by coal-fired power, emissions from electricity generation would rise by a third; that is 2400 million tons of carbon dioxide would be released into the atmosphere. This can be compared with the target of a 5% reduction – or 600 million tons per year – in carbon dioxide by the year 2010, as agreed in 1997 at Kyoto just for the developed countries. FIGURE 7-8 shows greenhouse gas emissions for various fuel types used for the electricity production.

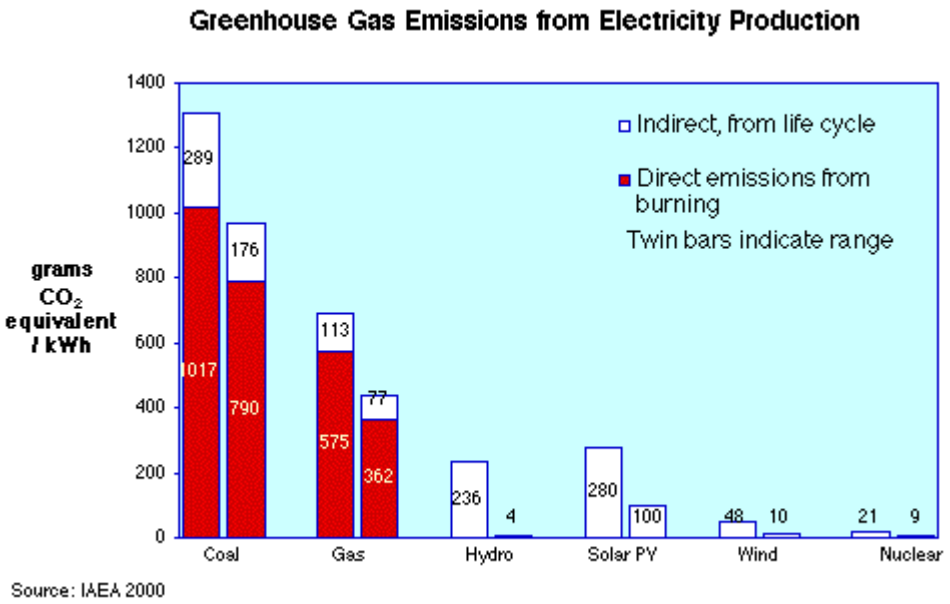

FIGURE 7-8: Greenhouse gas emissions from electricity production.

Conversely, there is scope for reducing coal's carbon dioxide contribution to the greenhouse effect by substituting natural gas or nuclear power, and by increasing the efficiency of coal-fired generation itself, a process which is well under way. Nuclear power is well suited to meeting the demand for continuous, reliable supply on a large scale (i.e. base-load electricity), the major part of demand.

7.7 Economic Aspects of Nuclear Power

Estimation of costs is one of the most important tasks while considering a construction of a new nuclear power plant. A legitimate question is if the electrical energy obtained from a nuclear power plant is cheaper than that obtained from other energy sources. The answer to this question is neither clear nor simple. One of the reasons for this difficulty is the fact that the costs of energy production vary from country to country and depend on many specific conditions. Due to that the above-posed question does not have a general answer and the costs of electricity must be estimated on the case-by-case basis.

In evaluation of total costs, the following part costs must be taken into account:

- investment cost (project and construction)
- operation and maintenance costs
- fuel costs
- plant decommissioning costs

For any country in the world, a construction of a nuclear power plant is a serious undertaking. This is particularly true for countries that invest into the first nuclear power plant. Typically such undertaking engages many parties: governments, authorities, industries, universities, research centers and – last but not least – the general public. To carry out such a complex process and evaluate their costs some standards must be followed. IAEA published a technical report on *Economic Evaluation of Bids for Nuclear Power Plants* (Technical Report Series No. 396, IAEA, Vienna, 2000). The purpose of this guidebook is to facilitate economic and financial bid evaluation. Thus, many economic aspects of nuclear power are treated there in a great detail.

When calculating costs of the electricity production, it is necessary to take into account the time aspect, since both the costs and the produced (and sold) electricity are distributed over time. Simplified cost estimation can be obtained from the following expression,

$$C = \frac{\sum_t \frac{I_t + M_t + F_t + D_t}{(1+d)^t}}{\sum_t \frac{E_t}{(1+d)^t}}, \qquad (7\text{-}20)$$

where:

C - discounted electricity costs in €/kWe

I_t - investment cost at time t in €

M_t - operation and maintenance cost at time t in €

F_t - fuel cost at time t in €

D_t - decommissioning cost at time t in €

E_t - energy production at time t in kWe

d - discount rate.

The costs obtained from Eq. (7-20) for various energy sources can be compared to each other. Usually the comparisons are performed with two reference values of the discount rate: 5 and 10%. Typical comparisons are done for nuclear power plants against coal and natural gas fired power plants. In general, the higher discount rate is in favor of fossil-fired power plants, since their investment costs are substantially lower than those of nuclear power plants. Nevertheless, the influence of local conditions (country) seems to be more significant than the influence of the discount rate. TABLE 7.5 shows the estimated cost ratio of electricity produced in nuclear power plant versus fossil-fired plants for various countries.

TABLE 7.5. Comparison of unit costs of electricity production in NPP compared with fossil-fired plants in selected countries.

Country / Region	**Electricity cost from NPP (100% - coal-fired plant)**		**Electricity cost from NPP (100% - natural gas-fired plant)**	
	d = 5%	d = 10%	d = 5%	d = 10%
Belgium	88%	110%	90%	118%
Czech Republic & Slovakia	88%	98%	79%	100%
Finland	80%	109%	80%	120%
France	60%	80%	60%	80%
Hungary	70%	85%	80%	110%
Japan	85%	95%	70%	95%
UK	100%	130%	110%	170%
Central Canada	85%	120%	60%	92%
Middle West USA	95%	100%	90%	120%

As can be seen, the cost of electricity from nuclear power plants varies from 60 to 170%. For some countries (France, Japan, Czech Republic and Slovakia) the nuclear power is the only economically motivated choice. Only for UK the fossil-fired plants can deliver cheaper electricity.

It should be mentioned that in the comparison presented in TABLE 7.5 the external costs of the production of electricity are not taken into account. Such costs (for example the cost of the emission of greenhouse gases) are significant and their inclusion into the comparison will make the nuclear power even more profitable source of electricity.

REFERENCES

[7-1] Beckjord, E. Ex. Dir. et al., *The Future of Nuclear Power. An Interdisciplinary MIT Study*, MIT 2003, ISBN 0-615-12420-8

[7-2] Duderstadt, J.J. and Hamilton, L.J., Nuclear Reactor Analysis, John Wiley & Sons, Inc.

[7-3] Glasstone, S. and Sesonske, A., *Nuclear Reactor Engineering*, Van Nostrand Reinhold Compant, 1981, ISBN 0-442-20057-9.

[7-4] Seko, N. "Aquaculture of Uranium in Seawater by a Fabric-Adsorbent Submerged System," Nuclear Technology, **144**, 274 (Nov. 2003).

[7-5] Uranium 2005: Resources, Production and Demand, A Joint Report by the OECD Nuclear Energy Agency and the International Atomic Energy Agency ("Red Book", 21st edition).

[7-6] http://www.world-nuclear.org/info/reactors.htm

[7-7] http://www.world-nuclear.org/info/inf98.htm

[7-8] http://gif.inel.gov/roadmap/pdfs/gen_iv_roadmap.pdf

[7-9] http://www.iaea.org/inis/aws/fnss/twgfr/index.html

[7-10] http://www-frdb.iaea.org/index.html

EXERCISES

EXERCISE 7-1: A core of a pressurized water reactor has a cylindrical shape with height H = 3.66 m and diameter D = 3.37 m. The mean neutron flux in the core is equal to 2.87×10^{17} neutron/m^2.s and the mean macroscopic cross section for fission is equal to 10.88 1/m. Calculate the required initial weight enrichment of the UO_2 fuel if the designed burnup is 33 GWd/tU and 1/3 of the core will be refueled each year.

EXERCISE 7-2: For the same reactor as described in previous exercise calculated the needed mass of the enriched and the natural uranium assuming that the plant capacity factor is 0.9.

EXERCISE 7-3: For the same reactor as described in EXERCISE 7-1 calculate SWU and the cost of enrichment assuming x_T = 0.3w/o and a unit cost of SWU equal to 45€.

Appendix

A

Appendix A - Bessel Functions

The Bessel differential equation is as follows:

$$x^2\frac{d^2y}{dx^2}+x\frac{dy}{dx}+\left(x^2-n^2\right)y=0\,,\quad \text{n>= 0.} \tag{A-1}$$

Its general solution can be found as,

$$y(x)=C_1J_n(x)+C_2N_n(x) \tag{A-2}$$

where $J_n(x)$: is known as the Bessel function of the first kind:

$$J_n(x)=\left(\frac{x}{2}\right)^n\sum_{k=1}^{\infty}\frac{(-1)^k\left(\frac{x}{2}\right)^{2k}}{k!(n+k)!} \tag{A-3}$$

and $N_n(x)$ is the Bessel function of the second kind (called also the Neumann function) given as,

$$N_n(x)=\frac{J_n(x)\cos n\pi-J_{-n}(x)}{\sin n\pi} \tag{A-4}$$

For small x, the functions have an asymptotic values described with:

$$J_n(x)\approx\frac{1}{2^n n!}x^n\,,\qquad N_n(x)\approx 2^{n-1}(n-1)!\,x^{-n}\,,\quad \text{n=/ 0} \tag{A-5}$$

For large x they are approximately described with:

$$J_n(x)\approx\sqrt{\frac{2}{\pi x}}\cos\left(x-\frac{\pi}{4}-\frac{n\pi}{2}\right),\quad N_n(x)=\sqrt{\frac{\pi}{2x}}e^{-x} \tag{A-6}$$

The plot of the Bessel function of the first kind and of the zero order ($n = 0$) is shown in the Figure below.

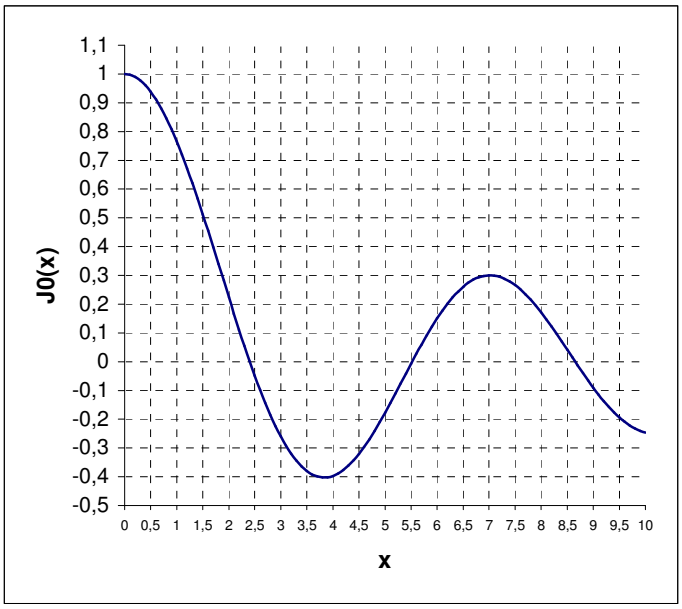

FIG. A-1. Plot of $J_0(x)$ function.

Derivatives of the Bessel functions are calculated as follows,

$$\frac{dZ_n(\alpha x)}{dx} = \alpha Z_{n-1}(\alpha x) - \frac{n}{x} Z_n(\alpha x), \quad Z = J, N \tag{A-7}$$

Selected useful integrals of the Bessel functions are as follows,

$$\int x Z_0(x) dx = x Z_1(x), \quad \int Z_1(x) dx = -Z_0(x). \tag{A-8}$$

Appendix

B

Appendix B - Selected Nuclear Data

Data for fissionable and fertile isotopes and for thermal neutrons with $v_0 = 2200$ m/s

Isotope	σ_a [b]	σ_f [b]	σ_s [b]	ν	α	η	$T_{1/2}$
^{233}U	581	527	10	2.492	0.0899	2.287	$1.6\ 10^5$ y
^{235}U	694	582	10	2.418	0.169	2.068	$7.1\ 10^8$ y
^{238}U	2.71	0.0005	10	-	-	-	$4.5\ 10^9$ y
^{239}U	-	15	-	-	-	-	23.5 m
U-nat	7.68	4.18	8.3	2.418	0.811	1.335	-
^{232}Th	7.65	0.0002	12.6	-	-	-	$1.45\ 10^{10}$ y
^{237}Np	170	0.020					$2.2\ 10^6$ y
^{239}Pu	1026	746	9.6	2.871	0.362	2.108	$2.44\ 10^4$ y
241Pu	1377	1009	-	2.927	0.365	2.145	13.2 y

Appendix

C

Appendix C – Cumulative Standard Normal Distribution

Values of $1-\Phi(z)$ where $\Phi(z)=p(Z\le z)=\frac{1}{\sqrt{2\pi}}\int_{-\infty}^{z} e^{\frac{-\xi^2}{2}}\,d\xi$

z	0	0.01	0.02	0.03	0.04	0.05	0.06	0.07	0.08	0.09
0.0	0.500000	0.496011	0.492022	0.488034	0.484047	0.480061	0.476078	0.472097	0.468119	0.464144
0.1	0.460172	0.456205	0.452242	0.448283	0.444330	0.440382	0.436441	0.432505	0.428576	0.424655
0.2	0.420740	0.416834	0.412936	0.409046	0.405165	0.401294	0.397432	0.393580	0.389739	0.385908
0.3	0.382089	0.378280	0.374484	0.370700	0.366928	0.363169	0.359424	0.355691	0.351973	0.348268
0.4	0.344578	0.340903	0.337243	0.333598	0.329969	0.326355	0.322758	0.319178	0.315614	0.312067
0.5	0.308538	0.305026	0.301532	0.298056	0.294599	0.291160	0.287740	0.284339	0.280957	0.277595
0.6	0.274253	0.270931	0.267629	0.264347	0.261086	0.257846	0.254627	0.251429	0.248252	0.245097
0.7	0.241964	0.238852	0.235762	0.232695	0.229650	0.226627	0.223627	0.220650	0.217695	0.214764
0.8	0.211855	0.208970	0.206108	0.203269	0.200454	0.197663	0.194895	0.192150	0.189430	0.186733
0.9	0.184060	0.181411	0.178786	0.176186	0.173609	0.171056	0.168528	0.166023	0.163543	0.161087
1.0	0.158655	0.156248	0.153864	0.151505	0.149170	0.146859	0.144572	0.142310	0.140071	0.137857
1.1	0.135666	0.133500	0.131357	0.129238	0.127143	0.125072	0.123024	0.121000	0.119000	0.117023
1.2	0.115070	0.113139	0.111232	0.109349	0.107488	0.105650	0.103835	0.102042	0.100273	0.098525
1.3	0.096800	0.095098	0.093418	0.091759	0.090123	0.088508	0.086915	0.085343	0.083793	0.082264
1.4	0.080757	0.079270	0.077804	0.076359	0.074934	0.073529	0.072145	0.070781	0.069437	0.068112
1.5	0.066807	0.065522	0.064255	0.063008	0.061780	0.060571	0.059380	0.058208	0.057053	0.055917
1.6	0.054799	0.053699	0.052616	0.051551	0.050503	0.049471	0.048457	0.047460	0.046479	0.045514
1.7	0.044565	0.043633	0.042716	0.041815	0.040930	0.040059	0.039204	0.038364	0.037538	0.036727
1.8	0.035930	0.035148	0.034380	0.033625	0.032884	0.032157	0.031443	0.030742	0.030054	0.029379
1.9	0.028717	0.028067	0.027429	0.026803	0.026190	0.025588	0.024998	0.024419	0.023852	0.023295
2.0	0.022750	0.022216	0.021692	0.021178	0.020675	0.020182	0.019699	0.019226	0.018763	0.018309
2.1	0.017864	0.017429	0.017003	0.016586	0.016177	0.015778	0.015386	0.015003	0.014629	0.014262
2.2	0.013903	0.013553	0.013209	0.012874	0.012545	0.012224	0.011911	0.011604	0.011304	0.011011
2.3	0.010724	0.010444	0.01017	0.009903	0.009642	0.009387	0.009137	0.008894	0.008656	0.008424
2.4	0.008198	0.007976	0.007760	0.007549	0.007344	0.007143	0.006947	0.006756	0.006569	0.006387
2.5	0.006210	0.006037	0.005868	0.005703	0.005543	0.005386	0.005234	0.005085	0.00494	0.004799
2.6	0.004661	0.004527	0.004396	0.004269	0.004145	0.004025	0.003907	0.003793	0.003681	0.003573
2.7	0.003467	0.003364	0.003264	0.003167	0.003072	0.002980	0.002890	0.002803	0.002718	0.002635
2.8	0.002555	0.002477	0.002401	0.002327	0.002256	0.002186	0.002118	0.002052	0.001988	0.001926
2.9	0.001866	0.001807	0.001750	0.001695	0.001641	0.001589	0.001538	0.001489	0.001441	0.001395
3.0	0.001350	0.001306	0.001264	0.001223	0.001183	0.001144	0.001107	0.00107	0.001035	0.001001
3.1	0.000968	0.000935	0.000904	0.000874	0.000845	0.000816	0.000789	0.000762	0.000736	0.000711

3.2	0.000687	0.000664	0.000641	0.000619	0.000598	0.000577	0.000557	0.000538	0.000519	0.000501
3.3	0.000483	0.000466	0.000450	0.000434	0.000419	0.000404	0.000390	0.000376	0.000362	0.000349
3.4	0.000337	0.000325	0.000313	0.000302	0.000291	0.000280	0.000270	0.000260	0.000251	0.000242
3.5	0.000233	0.000224	0.000216	0.000208	0.000200	0.000193	0.000185	0.000178	0.000172	0.000165
3.6	0.000159	0.000153	0.000147	0.000142	0.000136	0.000131	0.000126	0.000121	0.000117	0.000112
3.7	0.000108	0.000104	9.96E-05	9.57E-05	9.20E-05	8.84E-05	8.50E-05	8.16E-05	7.84E-05	7.53E-05
3.8	7.23E-05	6.95E-05	6.67E-05	6.41E-05	6.15E-05	5.91E-05	5.67E-05	5.44E-05	5.22E-05	5.01E-05
3.9	4.81E-05	4.61E-05	4.43E-05	4.25E-05	4.07E-05	3.91E-05	3.75E-05	3.59E-05	3.45E-05	3.30E-05
4.0	3.17E-05	3.04E-05	2.91E-05	2.79E-05	2.67E-05	2.56E-05	2.45E-05	2.35E-05	2.25E-05	2.16E-05
4.1	2.07E-05	1.98E-05	1.89E-05	1.81E-05	1.74E-05	1.66E-05	1.59E-05	1.52E-05	1.46E-05	1.39E-05
4.2	1.33E-05	1.28E-05	1.22E-05	1.17E-05	1.12E-05	1.07E-05	1.02E-05	9.77E-06	9.34E-06	8.93E-06
4.3	8.54E-06	8.16E-06	7.80E-06	7.46E-06	7.12E-06	6.81E-06	6.50E-06	6.21E-06	5.93E-06	5.67E-06
4.4	5.41E-06	5.17E-06	4.94E-06	4.71E-06	4.50E-06	4.29E-06	4.10E-06	3.91E-06	3.73E-06	3.56E-06
4.5	3.40E-06	3.24E-06	3.09E-06	2.95E-06	2.81E-06	2.68E-06	2.56E-06	2.44E-06	2.32E-06	2.22E-06
4.6	2.11E-06	2.01E-06	1.92E-06	1.83E-06	1.74E-06	1.66E-06	1.58E-06	1.51E-06	1.43E-06	1.37E-06
4.7	1.30E-06	1.24E-06	1.18E-06	1.12E-06	1.07E-06	1.02E-06	9.68E-07	9.21E-07	8.76E-07	8.34E-07
4.8	7.93E-07	7.55E-07	7.18E-07	6.83E-07	6.49E-07	6.17E-07	5.87E-07	5.58E-07	5.30E-07	5.04E-07
4.9	4.79E-07	4.55E-07	4.33E-07	4.11E-07	3.91E-07	3.71E-07	3.52E-07	3.35E-07	3.18E-07	3.02E-07

INDEX